DEPARTMENT OF FOOD TECHNOLOGY
MASSEY UNIVERSITY
PALMERSTON NORTH
NEW ZEALAND

HEAT TRANSFER AND FOULING IN FILM EVAPORATORS WITH ROTATING SURFACES

A THESIS PRESENTED IN PARTIAL FULFILMENT OF
THE REQUIREMENTS FOR THE DEGREE OF
DOCTOR OF PHILOSOPHY IN FOOD TECHNOLOGY
AT MASSEY UNIVERSITY

HONG CHEN
B.E., M.Tech. (Honours)
1997

ABSTRACT

A study was made on the heat transfer and fouling in thin film evaporators with rotating surfaces. Both theoretical and experimental studies were carried out, in order to gain a better understanding of these evaporators and their design principles, so that this type of evaporator could be effectively used in an on-farm milk evaporation system.

By using Nusselt-type assumptions, a theoretical model, which was used to predict the liquid film thickness and heat transfer coefficients on the rotating cone, was developed. The theoretical equations obtained revealed basic relationships between the variables and provided a fundamental knowledge of the liquid flow and heat transfer in the film evaporators with rotating surfaces.

The experimental studies on heat transfer were conducted on a Centritherm evaporator, which is available commercially (40° half cone angle), a specially made cone evaporator (10° half cone angle) and a falling film evaporator with a rotating tube. Variables evaluated were the rotating speed, the cone angle, the feed flow rate, the evaporating temperature, the temperature difference between the steam condensing and the liquid evaporating temperatures, and sugar concentration when sugar solution was used. The experimentally measured overall heat transfer coefficients were compared with the theoretical values.

It was found that the measured overall heat transfer coefficients increased with increase of the cone rotating speed, and with the rise of the liquid evaporating temperature. The feed flow rate was found to have a more significant effect on the measured overall heat transfer coefficients in the falling film evaporator with a rotating tube than that in the Centritherm and the cone evaporators. The overall heat transfer coefficients decreased with increase of the concentration of sugar solutions, mainly due to the increase of liquid viscosity. It was also found

that the measured overall heat transfer coefficients in the Centritherm evaporator increased with an increase in temperature difference up to 30K (for water, 10% sugar solution and skim milk) and then decreased (for water and 10% sugar solution). The formation of bubbles on the evaporating surface at high temperature differences was likely to be cause of this effect.

Increase of the cone angle resulted in thinner liquid films and higher heat transfer coefficients. This was reflected in the following experimental results: the measured overall heat transfer coefficients in the falling film evaporator with a rotating tube were slightly lower than those measured in the cone evaporator, but much lower than those obtained in the Centritherm evaporator.

The experimental results showed that rotating the tube of a falling film evaporator increased the overall heat transfer coefficient but the increase obtained was very dependent on feed flow rate, and was not sufficient to justify the use of this evaporator in the industry.

With the Centritherm evaporator, good agreement between theoretical and experimental overall heat transfer coefficients as a function of the cone rotating speed was obtained by using water. The theoretical model, however, does not adequately describe the whole evaporation process at conditions other than those assumed in the model, which are: laminar liquid film flow, and heat transfer by conduction through the liquid film. It is suggested that waves existing in the liquid film at high Reynolds numbers, and bubble formation on the heating surface at high temperature difference, are the major reasons for the discrepancy between theoretical and experimental results.

For the fouling study, the Centritherm evaporator was mainly employed, and three liquid systems: reconstituted skim milk, reconstituted whey solutions and sweet cheese whey solution, were selected. It was found that no fouling was detected after 6 hours' operation in the Centritherm evaporator when

reconstituted skim milk and reconstituted whey solutions were used. This indicates that the aggregated whey proteins, which are formed in the manufacture of skim milk powder and whey powder, are less active in inducing fouling. For this reason, only the sweet cheese whey solution was used in further studies.

It was confirmed that fouling is strongly linked with the liquid evaporating temperature and the temperature difference between steam condensing and liquid evaporating temperatures. In general, the higher the evaporating temperature and the temperature difference, the faster the deposition rate and the greater the fouling on the surface. It was found that 72% Bovine Serum Albumins (BSA) denatured after running the evaporator, at a evaporating temperature of 70°C and a temperature difference of 20K, for 6 hours. Though the content of BSA in whey solution is small, the denatured BSA could be easily attached to the surface. By association with other depositable materials existing in the whey solution, the thin layer of deposit could reduce the heat transfer coefficients significantly. This was attributed to the lower thermal conductivity of the deposited layer. Fouling was also found to be a function of the liquid velocity. This effect was more significant at lower evaporation temperatures. Increasing the rotating velocity would delay the formation of an initial layer and reduce the rate of fouling.

It was also found that there was an induction period in the fouling curves when the evaporating temperature was 60°C. The induction period was reduced when new whey solutions were introduced into the evaporator. It proved the fact that depositable materials are much more easily adsorbed on fouled or unclean surfaces than on clean surfaces. The increase of fouling rate when new whey solutions were introduced suggested that the concentration of activated molecules in the solutions strongly affected the fouling process. A possible mechanism of whey fouling on the rotating surface was proposed.

During this study, an attempt was made to develop a new type of evaporator in which a vapour compressor would be integrated with the rotating surface. This was unsuccessful due to the failure of compressing the vapour. Concerning the on-farm evaporation system, which requires an evaporator with high efficiency, compact, and minimum heat load to milk, it is suggested that a rotating surface evaporator with the top cone angle close to 90° (like a disk evaporator) would be optimum and worth to explore.

ACKNOWLEDGEMENTS

I wish to express my deepest appreciation and gratitude to my supervisor, Mr. Selwyn Jebson, for his supervision, guidance, encouragement, patience and friendship, and to my co-supervisor, Dr. Osvaldo Campanella, for his suggestions, valuable advice and encouragement throughout this study at Massey University.

I would like to extend my appreciation to Professor Peter Munro and Mr. Rod Bennett, for their help and care, to Dr. Tuoc Trinh for his stimulating discussions, to Mr. Byron Mckillop for his valuable assistance in setting up the experimental apparatus, to Mr. Palatasa Havea for his assistance in testing whey protein samples, to Mr. Mike Conlon, Mr. Alistar Young, Mr. Garry Radford, Ms. June Latham, Mr. Steve Glassgow, Mr. Hank van Til, Mr. Mark Dorsey for their help in providing technical assistance during the experimental work, to Dr. P.K. Samal and his colleagues at Longburn Cheese Factory of Tui Milk Products Company in Palmerston North for their efforts in arranging the whey solutions.

The staff of the Department of Food Technology were very helpful throughout the duration of my study.

I am also grateful to Professor Alan Williams and Mrs Beverley Williams, for their generous help, continuous care and friendship.

I would also like to mention the enjoyable company and moments provided by my friends, fellows at Massey University, and the members of New Zealand-China Friendship Society, who in many ways contributed to the completion of this work. Especially, I have to mention that when I was involved in an unfortunate car accident, many friends provided their help for my family to go

through a difficult time. Their invaluable assistance is very much appreciated and will be always remembered.

Finally, I would like to express my special thanks to my wife, Xinjun, for her love, encouragement, patience and typing. During this period, my son, John, and my daughter, Helen, came to this world and brought us a newly happy life. I also thank my father, mother, sister, grandmother, parents-in-law as well as the whole family for their understanding and constant support and helpfulness.

TABLE OF CONTENTS

LIST OF FIGURES

LIST OF TABLES

NOMENCLATURE

Roman letters

A	heat transfer area (m^2)
A_l	liquid side heat transfer area (m^2)
A_m	average heat transfer area (m^2), defined as: $(A_s-A_l)/\ln(A_s/A_l)$
A_s	steam side heat transfer area (m^2)
a	acceleration due to rotating (m/s^2)
C	constant
C_p	specific heat (kJ/kg.K)
d	inside tube diameter (m)
d_o	outside diameter on the top of cone (m)
D	outside tube diameter (m)
D_o	outside diameter at the bottom of cone (m)
Fr	Froude number, defined as: $[u^2/(g.d)]$
g	acceleration due to gravity (m/s^2)
g'	corrected gravitational acceleration, defined as $g.\cos\beta$ (m/s^2)
h_{fg}	latent heat of vapour condensation (kJ/kg)
h'_{fg}	effective latent heat of vapour condensation (kJ/kg), defined as: $h_{fg}[1+0.68C_p(T_s - T_{ws})/h_{fg}]$
h_s	steam side heat transfer coefficient ($kW/m^2.K$)
h_l	liquid side heat transfer coefficient ($kW/m^2.K$)
h_l'	corrected liquid side heat transfer coefficient ($kW/m^2.K$)
H_o	initial overall heat transfer coefficient ($kW/m^2.K$)
H_{cal}	calculated overall heat transfer coefficient ($kW/m^2.K$)
H_{exp}	measured overall heat transfer coefficient ($kW/m^2.K$)
$H(t)$	measured overall heat transfer coefficient at time t ($kW/m^2.K$)
Ja	Jacob number, defined as: $C_p(T_s-T_w)/h'_{fg}$
k	thermal conductivity of liquid (W/m.K)
k_d	thermal conductivity of fouling layer (W/m.K)
k_{ss}	thermal conductivity of sugar solution (W/m.K)

k_w	thermal conductivity of wall (W/m.K)
L	characteristic distance (m)
L_1	distance from the vertex to the apex of a truncated cone (m)
l	length of the cone (mm)
Nu	Nusselt number, defined as: h_iL/k
Nu'	modified Nusselt number, defined as eq (3-4)
Nu_{ro}	rotational Nusselt number, defined as eq (5-37)
Pr	Prandtl number, defined as: $C_p\mu/k$
Q	amount of heat (kW)
Q_f	feed flow (m^3/s)
q	heat flow (kW/m^2)
r	inner radius on the any position of cone (m)
r_i	inner radius on the top of cone (m)
R_f	fouling resistance ($m^2.K/kW$)
$R_f(t)$	fouling resistance at time t ($m^2.K/kW$)
Re_a	axial flow Reynolds number, defined as: Du/ν
Re_r	rotational flow Reynolds number, defined as: $D^2\Omega/\nu$
R_i	inner radius at the bottom of cone (m)
R_o	rotation parameter, defined by eq (5-19)
U_m	characteristic velocity (m/s)
U_x	component of liquid velocity in X direction (m/s)
U_y	component of liquid velocity in Y direction (m/s)
U_φ	component of liquid velocity in φ direction (m/s)
u	liquid flow velocity (m/s)
T	temperature (°C)
T_{evp}	evaporating temperature (°C)
T_l	liquid temperature (°C)
T_s	steam temperature (°C)
T_{sat}	saturation temperature (K)
T_w	wall temperature (°C)
T_{wl}	surface temperature of cone on liquid side (°C)

T_{ws}	surface temperature of cone on steam side (°C)
ΔT	temperature difference between the evaporating and the steam condensing temperatures (K)
ΔT_B	temperature difference between the wall and liquid saturation temperature (K)
W_{cal}	calculated flow rate of vapour condensate (kg/s)
W_{exp}	measured flow rate of vapour condensate (kg/s)
We	Weber number, defined as: $[(\rho.u^2.\delta\ /\sigma)^{1/2}]$
X	downward distance along cone surface (m)
Y	distance from surface (m)

Greek symbols

α	thermal diffusitivity (m^2/s)
β	half angle of the cone
δ	thickness of liquid film (mm)
δ_d	thickness of the fouling layer (mm)
δ_w	thickness of wall (mm)
μ	dynamic viscosity (Pa.s)
ν	kinematic viscosity (m^2/s)
ρ	density of liquid (kg/m^3)
ρ_v	density of vapour (kg/m^3)
ρ_{ss}	density of sugar solution (kg/m^3)
Ω	angular velocity (rad/s)
φ	angular co-ordinate
Γ	local mass flow rate in the film per unit width of surface (kg/m.s)
τ_{yx}	radial shear stress (N/m^2)
$\tau_{y\varphi}$	tangential shear stress (N/m^2)
σ	surface tension (N/m)

Superscripts

*	dimensionless quantity

Abbreviations

BPE	Boiling Point Elevation
CIP	Cleaning In Place
DM	Dry Matter
ET	Evaporation Temperature
FF	Feed Flow
FFE	Falling Film Evaporator
FT	Feed Temperature
PAGE	Polyacrylamide Gel Electrophoresis
RS	Rotating Speed
TS	Total Solids

LIST OF PUBLICATIONS

H.Chen, R.S.Jebson and O.H.Campanella, 1993, Factor Affecting Heat Transfer in the Centritherm Evaporator, *Proceedings, the APCChE/CHEMECA 1993 Conference*, Vol.3, pp 227-233, Melbourne, Australia.

H.Chen, R.S.Jebson & O.H.Campanella, 1994, Heat Transfer Coefficients for Evaporation from the Inner Surface of the Rotating Cone, *Proceedings, CHEMECA 1994 Conference*, Vol.2, pp 695-702, Perth, Australia.

H.Chen, R.S.Jebson & O.H.Campanella, 1994, Performance of the Centritherm Evaporator for Concentration of High Viscosity Solutions, *Proceedings of the Inaugural New Zealand Postgraduate Conference for Engineering and Technology Students*, Department of Production Technology, Massey University, pp 60-65.

R.S.Jebson, H.Chen, & O.H.Campanella, 1995, Heat Transfer Coefficients on the Inner Surface of the Rotating Cone, *Proceedings, 1995 Asian Pacific Confederation of Chemical Engineer*, Vol.2, pp 125-136, Taibei Taiwan.

H.Chen, R.S.Jebson & O.H.Campanella, 1996, Fouling in the Centritherm Evaporator with Whey Solutions, *Proceeding of IPENZ 1996 Conference*, Vol.2, Part 2, pp 308-313, Dunedin, New Zealand.

R.S.Jebson, H.Chen & O.H.Campanella, 1997, Study on a Rotating Tube Falling Film Evaporator, *Proceeding of IPENZ 1997 Conference*, Vol.2, pp 41-45, Wellington, New Zealand.

H.Chen, R.S.Jebson & O.H.Campanella, 1997, Determination of Heat Transfer Coefficients in Rotating Cone Evaporators Part I, *Food and Bioproducts Processing*, Trans IChemE, Vol. **75**, Part C, pp 17-22.

R.S.Jebson and H.Chen, 1997, Performances of Falling Film Evaporators on Whole Milk and a Comparison with Performance on Shim Milk, *Journal of Dairy Research*, **64**, pp 57-67.

H.Chen, R.S.Jebson & O.H.Campanella, 1997, Determination of Heat Transfer coefficients in Rotating Cone Evaporators Part II, a paper to be submitted to *Food and Bioproducts Processing*, Trans IChemE, Part C.

H.Chen, R.S.Jebson & O.H.Campanella, 1997, Fouling of Heat Transfer Surface by Whey Solution in Rotating Film Evaporators, a paper to be submitted to *International Journal of Food Science and Engineering.*

PART I

GENERAL INTRODUCTION

CHAPTER 1
INTRODUCTION

1.1 Evaporation

Evaporation is the process of conversion of a liquid into its vapour. It is also the name given to a widely used unit operation in which solutions are concentrated by evaporating a volatile solvent. It is one of the oldest means ever to have been adopted for separating liquid mixtures by heat on an industrial scale (Billet, 1989) and is still an important technique used for the removal of water and sometimes other liquids in industry.

Evaporation often encroaches upon the other unit operations known as distillation, drying and crystallisation. Evaporation is distinguished from distillation in that no attempt is made to separate the components of the vapours in evaporation. Evaporation differs from drying in that the residue is always a liquid, which means that the heat must be transferred in the evaporator to a solution, although the desired final products may be in a solid form. Evaporation is differentiated from crystallisation in that the former is concerned with concentrating a solution rather than producing or building crystals (Minton, 1986).

In an evaporator, heat must be supplied to the liquid through a heat exchange surface, and the vapour and liquid separated. An evaporation process is therefore both a heat exchange operation and a vapour-liquid separation. In industry, the heat is usually supplied by condensation of steam. In the food industry, the evaporated portion is usually pure water, although some other volatile components of the solutions are also partially or totally vaporized.

Evaporation is extensively used in the food industry for the following reasons:

(1) To reduce storage and shipping volumes of liquid foods, hence to reduce packaging, storage, transport and distribution costs;

(2) To pre-concentrate foods prior to drying, freezing or sterilisation and hence to save energy in subsequent operations;

(3) To increase the solids content of a food and hence to provide storage stability for it by reducing water activity;

(4) To provide concentrates that are convenient to use for consumer and for further processing.

Basically an evaporation system consists of:

(1) A heat exchanger to supply sensible heat to raise the liquid to its boiling point and provide the latent heat of vaporisation;

(2) A separator in which the vapour is separated from the concentrated liquid phase;

(3) A condenser to condense the vapour and remove the condensate from the system;

(4) A vacuum device to withdraw non-condensable gases and maintain a constant evaporating temperature.

There is not any single type of evaporator which could be satisfactory for all applications and different kinds of feed. In general, the different designs for the heat exchangers result in different types of the evaporators. Evaporators used for concentration of liquids in the industry are normally classified as follows (Billet, 1989):

(a) Natural circulation evaporator

(b) Forced circulation evaporator

(c) Climbing film evaporator

(d) Falling film evaporator

(e) Flash evaporator

(f) Horizontal heated tubes evaporator

(g) Thin film evaporator

Figure 1.1 shows schematic diagrams of these types of evaporators.

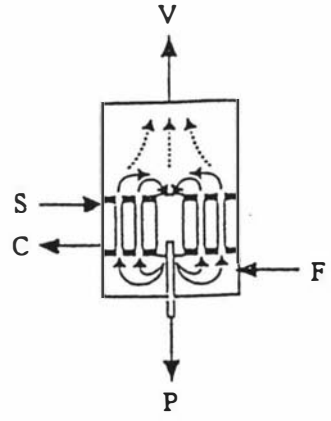

(a) Natural circulation evaporator

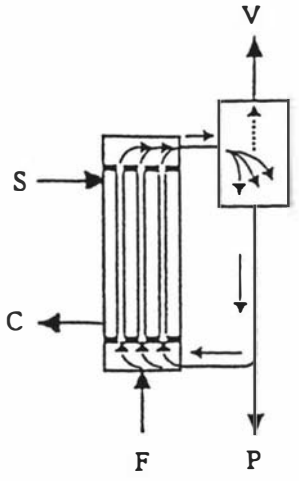

(b) Forced recirculation evaporator

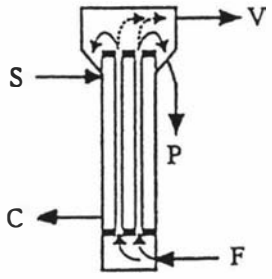

(c) Climbing film evaporator

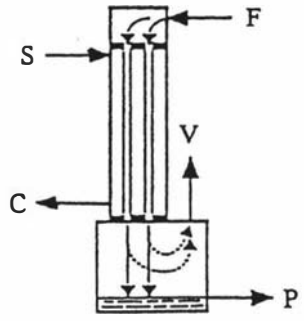

(d) Falling film evaporator

F – Feed
V – Vapour
S – Steam
P - Product (concentrate)
C - Condensate

Figure 1.1 The different types of evaporator (continued on the next page)

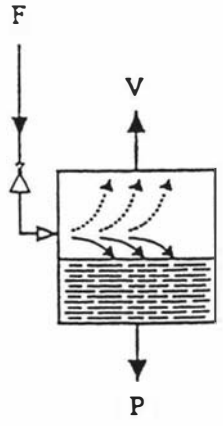

(e) Flash evaporator

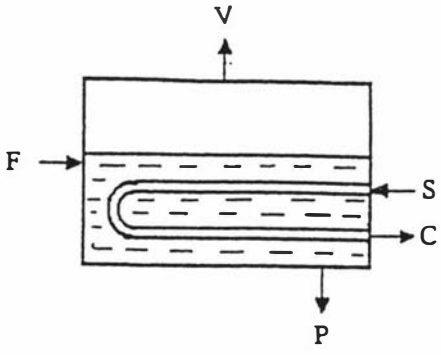

(f) Horizontal heated tubes evaporator

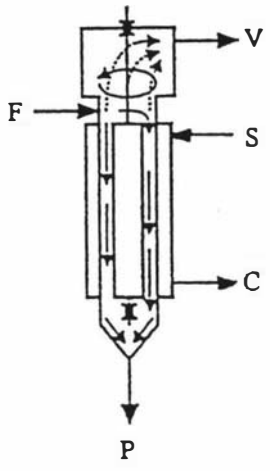

(g-1) Wipers thin film evaporator

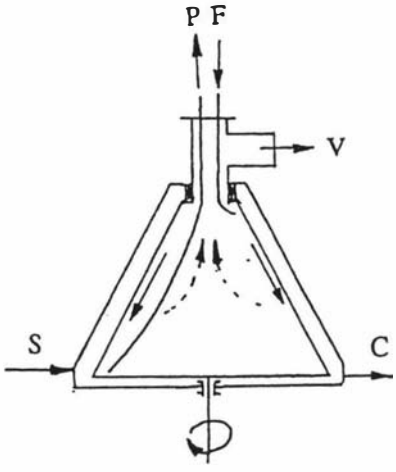

(g-2) Rotating surface thin film evaporator

F - Feed
V - Vapour
S - Steam
P - Product (concentrate)
C - Condensate

Figure 1.1 The different types of evaporator (continued)

The natural circulation evaporator (Fig. 1.1 a) was the first type of evaporator to receive wide acceptability for the industrial concentration of liquids. It became so common that this type was sometimes known as the standard evaporator (Minton, 1986). The vertical tube bundle with a central downtake is located inside a steam chest enclosed by a cylindrical shell. The circulation of liquid (natural convection) past the heating surface is induced by boiling, which improves the heat transfer.

The forced circulation evaporator (Fig. 1.1 b) was developed from the standard evaporator. It has a vertical heated tube bundle located in an external heater separated from the downtake, which made it possible to pump the liquid upwards through the tube bundle. The fast liquid velocities improve the heat transfer and reduce the degree of fouling. This evaporator can also be operated by natural circulation.

The climbing film evaporator (Fig. 1.1 c) has long heating tubes (up to 7 m) and the feed is pumped into the bottom of the vertical tubes. The production of vapour bubbles carries the liquid up the tubes, which results in an upwardly flowing film of liquid on the top of tube wall, with a high velocity vapour core. This evaporator has relatively high heat transfer coefficients and little or no re-circulation.

The falling film evaporator (Fig. 1.1 d) has vertical heating tubes and the feed is carefully distributed to the top of the tubes. The feed forms a thin film and flows down on the inner surfaces of the tubes. The vapour and the concentrate leaves at the bottom of the tubes. This evaporator works successfully with wall temperatures of 2-3°C above the feed boiling temperature and has a low residence time.

The flash evaporator (Fig. 1.1 e) is a low pressure chamber without heaters, in which a hot feed is introduced and flash evaporation of the liquid occurs. This type of evaporator is the most suitable for solutions which are prone to salting or scaling and are very corrosive. It has been successfully used for producing potable water from seawater (Al-Zubaidi, 1987).

The horizontal heated tube evaporator (Fig. 1.1 f) has heating tubes (within which steam condenses) immersed in the liquid to be evaporated. It is used in the production of potable water.

The thin film evaporators have been designed to deal with viscous solutions and have low residence times. There are two basic types: the one shown in Figure 1.1 g-1, in which wipers are mounted to scrape the liquid off the heating surface, the other one shown in Figure 1.1 g-2, in which a rotating heating surface is included. The later one is further detailed in section 1.3. The study carried out in this work was on the thin film evaporator with rotating surface as that illustrated in Figure 1.1 g-2.

Although the underlying principle of evaporation is simple, the detailed liquid flow patterns and the evaporation mechanisms on the heating surfaces are not very well understood. The complications in the evaporation process also arise as a result of the variety of products processed which have different properties. The behaviour of the liquid during evaporation introduces a number of aspects of which consideration must be given in designing and selecting evaporators. In other words, many parameters that depend on the characteristic properties of the evaporating liquid govern the choice of equipment and the operating conditions. They generally include: (a) the liquid's viscosity in relation to the degree of concentration required; (b) the tendency to salting, scaling and fouling; (c) the hold up time for thermally unstable products. These properties are also affected by the physical properties of the processing liquids, including thermal conductivity, density and thermal capacity. For dairy products, the particular parameters to be considered are creaming, souring, foaming, undesirable changes in viscosity and taste, discolouring, fouling and burn-on at the surface of the heaters.

1.2 Evaporation technology used in the dairy industry

Evaporation technology is intensively used in production of milk powder, condensed milk, lactose, whey protein concentrates. In the dairy industry, evaporators are often used in conjunction with spray drying units. In these cases the concentration process in the evaporator is very important because the specific energy consumption of the evaporator is much lower than that of the dryer. At the same time, by far the largest part of moisture (up to 90%) is removed in the evaporator (Grønlund, 1984, Fluck, 1988). Evaporation is also claimed to be a compulsory step in powder processing because milk powder produced from evaporated milk has longer shelf life and larger particles with a smaller amount of occluded air (Carić, 1994).

It has been calculated that in the manufacture of milk powder, 50% of the energy consumed is required at the evaporation stage. In New Zealand 1% of the total energy from fossil fuels is consumed in evaporation processes (Jebson, 1989). Therefore, the study of the evaporation process in order to obtain a better understanding of the heat transfer involved in it has an important industrial value.

Due to the heat-sensitive nature of milk and the energy costs rising, there are two aspects of the evaporation process which have received much attention during its development. One is to improve the quality of the finished product following an evaporation process, to enable a better price to be obtained from it. Another is to reduce the cost of removing water by this means.

Various types of evaporators have been used over the years in the dairy industry. The natural circulation evaporators (Fig. 1.1 a and b) were the standard plant for many years. These were superseded first by the climbing film evaporator (Fig. 1.1 c), and then by the falling film evaporator (Fig. 1.1 d), which gave rise to a much improved product quality due to considerably reduced residence times. Nowadays, the dominant evaporators used in New Zealand dairy industry are the falling film evaporators.

Although there are other concentration techniques (membrane technology and freeze concentration etc.) being developed, evaporation is, and no doubt will remain, a major technique used for the removal of water in the dairy industry (Fergusson, 1989). In New Zealand, evaporation is the only process used for the concentration of milk (Mackereth, 1995).

1.3 The thin film evaporator with rotating heating surface

Although evaporators are tending to become larger and despite the efforts to improve the efficiency of the process, the evaporation process is still costly. It is therefore believed that scope exists for the development of a compact, low cost, evaporator, linked to a cost-effective heat transfer surface (Reay, 1991).

Rotating the surface on which evaporation takes place appears to be a logical way of developing this type of evaporator. In fact, this type of evaporator has been used for decades. Thin-film evaporators with rotating heating surfaces provide an alternative of small to medium capacities in the food, chemical, and pharmaceutical industries.

This kind of evaporator has an externally heated rotor in the form of a truncated cone. The liquid to be evaporated is fed onto the inner surface of the cone, and the steam condenses on the outer surface. Under the centrifugal field, the liquid film on the inner surface moves very fast in a radial direction, consequently the liquid film becomes extremely thin. Therefore, the heat transfer resistance of liquid film is small. On the other hand, the condensate from the steam is impelled off from the outer surface of the cone by the action of the centrifugal force, which results in more areas being exposed for steam to be condensed. Therefore, the measured overall heat transfer coefficients on the rotating cone surface could be as high as 10 kW/m^2K (Chen *et al.*, 1993, Anon, 1990) compared to 2-3 kW/m^2K for a falling film evaporator (Chen, 1992).

This type of evaporator is especially suitable for heat sensitive biological materials. As the liquid film passes the heating surface rapidly, the liquid residence time in the actual evaporation zone may be only a fraction of a second (Billet 1989). This short time is sufficient to evaporate the liquid to required concentration and minimising deterioration of the product's characteristics, such as taste, colour, protein and vitamin content (Mannheim and Paasy, 1974).

This type of evaporator can be also used to concentrate viscous solutions, because the liquid can be distributed and moved along the heating surface with the assistance of centrifugal force generated in the rotating system. The viscosity of the final product produced in this type of evaporators could be up to 20 Pa.s (Mannheim and Paasy, 1974).

Applications of this type of evaporator have been found in many industries, but there is a lack of basic studies dealing with the operation and performance of this type of evaporator.

1.4 Fouling in evaporation

Fouling in food process plants is an example of an especially severe problem which affects most heat transfer equipment. Deposit material on the heat transfer surface acts as a barrier to heat transfer, decreases the overall heat transfer coefficient, increases the overall plant pressure drop and poses a threat to plant sterility. Fouling in heat transfer is still a major unresolved problem (Whalley, 1992). As the fouling process is extremely complex, any increased understanding of fouling would be of industrial value (Fryer *et al.*, 1995).

Fouling on the evaporator heat transfer surface is a major reason for frequent and expensive cleaning, which is required for efficient and safe operation (Fryer, 1989). Fouling in tubular and plate heat exchangers as well as ultra high temperature (UHT)

plants has been studied considerably during the last two decades (Burton, 1988); however, the study of fouling in evaporation process has not received much attention. This may be due to the extremely complex nature of the fouling process. The relatively low temperature range involved in the evaporation process also means that the process of deposit layer development on the surface is slow, therefore longer times should be needed to conduct experimental work. No study of fouling in thin film evaporators with rotating surface has been reported up to date.

1.5 On-farm evaporation system

The idea of milk pre-concentration in farms has attracted world-wide interest for many years. If milk can be pre-concentrated in the farm, the pre-concentrated milk clearly should be cheaper to transport to the processing plants than the normal milk. Similarly, all the other volume dependent handling and processing costs should be favourably affected by concentration. For example, pumps, milk storage capacities and refrigeration loads would be reduced proportionately, as well as cheese vat capacities or evaporator loads in milk powder plants. The dairy factory effluent would also be reduced.

There are three main concentration techniques which could be used in the dairy industry, evaporation, membrane technology and freeze concentration. The freeze concentration has not been considered for farm operation due to its high equipment costs and the difficulty of separation of the ice particles from viscous concentrate (Dickey and Craig, 1993). Membrane technologies, including reverse osmosis and ultra-filtration systems have the advantage of eliminating the heat effects on the milk, but require very pure water, which is not readily available on many farms, for cleaning. Therefore, evaporation technology is the only viable alternative for farm pre-concentration of milk. Robertson (1987) pointed out that on-farm milk concentration using either membrane processing or mini-evaporators may be a concept which will be of rapidly increasing importance in the decade ahead.

The ideal evaporator to be used in on-farm evaporation system should be highly-efficient and compact, and cause minimal damage to milk (i.e. once through evaporator). If a suitable design is used, taking into account the whole energy consumption on the farm, especially employing LPG fuel to drive the engine, an evaporation system would be an effective method of on-farm concentration (Jebson *et al.*, 1993).

It has been proposed to develop a new on-farm evaporation system at the Department of Food Technology, Massey University. The proposed system is shown in Figure 1.2.

This system is operated as follows: The fresh whole milk is first collected in the buffer tank and then heated and pumped into the evaporator. The concentrated milk from the evaporator is chilled in a plate heat exchanger and then passed to the storage tank. The storage temperature is about 5°C and the maximum storage time is about 3 days. Finally the concentrated milk is transported by tanker to the dairy factory for further processing and may be stored in the dairy factory for a while (maximum two days) before processing.

Research work on both chemical and microbiological qualities of pre-concentrated milk qualities has just been completed (Xu, 1996). The results showed that pre-concentrated milk had an acceptable quality to be used in the industry. From a microbiological point of view, it was found that the number of total bacteria were much less in the pre-concentrated milk than in the raw milk, therefore, the pre-concentrated milk can be stored safely for the proposed period of time at the farm and the dairy factory.

The research work carried out in this project intended to satisfy the requirement for the development of the on-farm evaporation system.

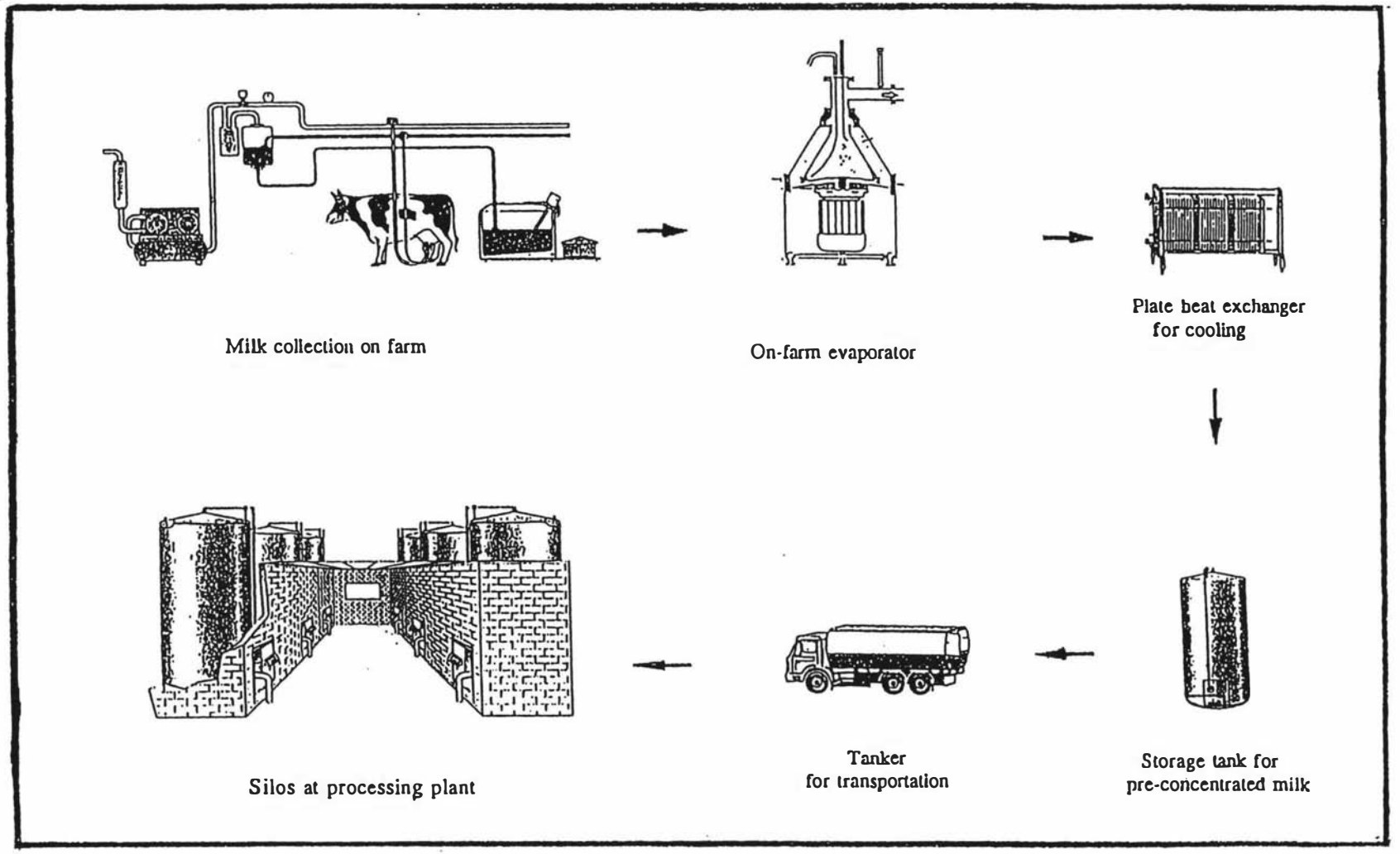

Figure 1.2 The proposed on-farm evaporation system

CHAPTER 2
OBJECTIVES

The thin film evaporator with rotating surface is a highly efficient and compact evaporator, which could be a good choice for the on-farm evaporation system. Although it has been used in producing many products, very few theoretical and systematic studies have been undertaken on the performance of this type of evaporator. To use this evaporator effectively and make further developments, it is necessary to understand the evaporation process and mechanism that occurs on the rotating surface as well as its fouling behaviour.

The objectives of this work were:

(1) To develop a theoretical model that can be used to calculate liquid film thickness and heat transfer coefficients in the rotating surface evaporator and to illustrate the relevant factors affecting the liquid film flow and the heat transfer.

(2) To increase the understanding of the factors controlling the heat transfer coefficients in rotating surface evaporator through an experimental study, in particular the effect of rotating speed, cone angle, feed flow, evaporating temperature and temperature differences on the heat transfer coefficient.

(3) To investigate the fouling behaviour on the rotating surface with changes of operational variables, namely running time, evaporating temperature, temperature differences, rotating speed and feed flow rate, using whey solutions as a model system.

The majority of experimental work was undertaken on the Centritherm evaporator. A cone evaporator with a 10° half cone angle and a single tube falling film evaporator with rotating surface were also built and used for the experimental approach.

PART II

HEAT TRANSFER IN EVAPORATORS WITH ROTATING SURFACES

CHAPTER 3
HEAT TRANSFER IN THIN FILM EVAPORATORS - LITERATURE REVIEW

Fluid flow and heat transfer processes associated with liquid-vapour phase changes phenomena are typically among the more complex transport circumstances encountered in engineering applications (Carey, 1992). The evaporation of a liquid film occurring in a rotating system is a very complex phenomena, in which the flow pattern of the film, the mechanisms of heat transfer and evaporation as well as the assistance of the centrifugal force are all involved. The available information on these specific aspects is incomplete. This literature review, therefore, focuses first on the flow of films and heat transfer associated to it, the boiling phenomena, and heat transfer enhancement by surface rotation. Then, some related aspects of heat transfer in the evaporation process, as well as the development of evaporation technology used in the dairy industry, are presented. Finally, the thin film evaporators with rotating surfaces are reviewed.

3.1 Liquid film flow

The flow of liquids in thin layers is often observed in our daily life, a common example is the flow of rain water on window. The occurrence and applications of film flow in modern technology are numerous and important. The falling liquid film under the action of gravity can be found in thin film evaporators, film condensers, irrigated cooling towers and falling film absorbers. The thin film flow, as the result of the application of a forced centrifugal field, can be found in the thin film evaporator with rotating surface and rotating disk atomizers (Blass, 1979). Extensive research work has been done to study the film flow on plates and tubes both theoretically and experimentally.

3.1.1 The flow regimes of the liquid film

It is well known in fluid mechanics that below a certain critical value of the Reynolds number (Re) the flow will be mainly laminar in nature, while above this value, turbulence plays an important part. The same is true for a film flow, though it must be remembered that in thin films a large part of the total film thickness continues to be occupied by the relatively non turbulent "laminar sublayer" even at large flow rates (Fulford, 1964).

The Reynolds number for a flowing liquid film is defined as:

$$Re = \frac{4\Gamma}{\mu} \tag{3-1}$$

Where: Γ is defined as the local mass flow rate in the film per unit width of surface (kg/m.s);
μ is the liquid viscosity (Pa.s).

Strictly speaking, the flow regime of a film cannot be defined uniquely as laminar or turbulent because of the presence of the free surface in film flow. Under suitable conditions, it is possible to have smooth laminar flow, wavy laminar or turbulent flow, where the wavy flows may be subdivided into gravity or capillary types.

In order to simplify the problem, three different flow regimes have been identified (Fulford, 1964; Hallström, 1985):

1) Smooth laminar;
2) Wavy laminar; and
3) Turbulent.

The transition from smooth to wavy laminar can occur for Reynolds numbers up to 30 (Benjamin, 1957). Based on experiments using liquids with different physical properties

falling in vertical tubes, it appears that wave formation will develop when the Froude number (defined as $u^2/[g.d]$) is greater than 1 (Jackson, 1955).

Hallström (1985) reported that for water, if the vapour shear is negligible, the smooth laminar regime takes place for Reynolds numbers below 20-30, and the wavy laminar regime starts at Reynolds numbers about 30-50.

It was found that turbulent motion first appears at Reynolds numbers between 250 and 500 (Fulford, 1962), 200 and 600 (Blass, 1979), or 1,080 (Dukler and Bergelin, 1952). The gradual transition to turbulent occurs with the increase of Reynolds number from 1,000 to 4,000 (Ueda and Tanaka, 1975) and Reynolds numbers from 1,500 to 1,800 (Levich, 1962). Fully turbulent flow exists at Reynolds numbers between 1,000 to 3,000 (Hallström, 1985); and Reynolds numbers greater than 10,000 (Gimbutis *et al.*, 1978).

Moresi (1985) suggested that although there was scatter in the published experimental data, most investigators seemed to support a Reynolds number lower limit for the laminar-turbulent transition between 1,000 to 1,600; with a less well-marked upper value of about 3,200.

Schwartzberg (1988) summarized work of several researchers (e.g. Yanniotis, 1983; Chavarria, 1983) and reported that at Reynolds number less than 500, the heat transfer coefficient of the evaporating fluid increased linearly as Reynolds number increased, at the range of 500 to 1,600, the heat transfer coefficient remained fairly constant or decreased slightly, at Reynolds number beyond 1,600; the heat transfer coefficient increased slightly as Reynolds number increased.

The correlations developed by Chun and Seban (1971) working with water and Wilke (1962) working with water and ethylene glycol show that the transition point (critical Reynolds number) from laminar to turbulent can be detected by the change in heat transfer rate. They, nevertheless, suggested that a Weber number (defined as $[\rho.u^2.\delta/\sigma]^{1/2}$) of the order of unity may be used as a transition criteria for falling films.

Dukler (1960) pointed out that the transition from laminar to turbulent flow in a thin film cannot be expected to be sharp, since due to the thinness of films, a large portion of the total film thickness is occupied by the laminar sublayer even at flow rates above the critical Reynolds number. The transition is likely to be a gradual process.

3.1.2 Flow features of the falling liquid films

Knowledge of falling film flow features is necessary for heat and mass-transfer theoretical analysis (Fulford, 1964). The pioneering work in this field was that of Nusselt (1916) on the theoretical determination of velocity fields, average velocities and film thicknesses for smooth laminar films falling at steady state on flat surfaces with zero free surface interfacial shear. Since then, quite a few papers have appeared in the literature, and most of work has been done only in the laminar flow regime, because beyond this regime the film flow is usually so complex that no satisfactory general theory has yet been possible (Blass, 1979). Dukler and Bergelin (1952) deduced the velocity profile and film thicknesses for a turbulent film flow based on the universal dimensionless velocity profile equations of Nikuradse (1933). Blass (1979) obtained the falling film thickness as a function of the Reynolds number graphically at Reynolds numbers between 10 to 5,000, as well as the equations to calculate the mean film thickness and the mean film velocity.

A stable film means that the film liquid completely wets the flow surface, however, even without heat or mass transfer, dry spots may be formed as the Reynolds number is reduced to a minimum value (a critical Reynolds number). Film surface instabilities are dampened by surface tension, as established in the work of Benjamin (1957), who also stated that total stability cannot be obtained by merely increasing surface tension and that vertically falling films are unstable at all flow rates. Brauer (1956) reported experimental values for the critical Reynolds number of films containing small quantities of surface-active materials in solution. In this case, the value of critical Reynolds numbers appeared to depend on the surface tension of the solution. This effect is probably due to the layer of surface-active material present at the interface.

If temperature or concentration gradients are present in the liquid film, the Marangoni effect should be included in the stability analysis (Blass, 1979). The Marangoni effect is the surface motion of the liquid as a results of local surface tension differences. If there is a somewhat thin section of film with a smaller surface tension than the neighbouring thick sections, then, on the basis of the tendency toward a minimum free surface energy, the liquid in the region close to the interface is drawn from the thin section of the film into the thicker zone. As a result, the film can be thinned so much that it ruptures and flows into separate rivulets. This effect would be likely to occur in highly concentrated solutions with some lower surface tension materials.

Two extensive reviews of film flow features have been given by Fulford (1964) and Blass (1979).

3.2 Liquid boiling phenomena

Boiling heat transfer studies are traditionally divided in two parts: pool boiling and flow boiling. Pool boiling represents the situation in which boiling occurs on a single heated surface in a large pool of quiescent liquid. The flow boiling refers to the situation in which there is bulk motion of the liquid past the heated surface, usually in tubes (Thome, 1990).

3.2.1 Pool boiling

Pool boiling by itself is of limited practical significance as a process, but it is studied extensively to gain insight into the more complex problem of flow boiling. An exhaustive review of pool boiling was given by Van Stralen and Cole (1979).

The nature of the pool boiling process varies considerably depending on the conditions at which boiling occurs.

The heating rate or the level of heat flux, the physical and thermophysical properties of the liquid and vapour, the surface material and finish, and the physical size of the heated surface all may have an effect on the boiling process.

Four regimes have been classically recognized for pool boiling, single-phase natural convection, nucleate boiling, transition boiling and film boiling. These regimes are most easily understood in terms of the so-called boiling curve: a plot of heat transfer coefficient (h_l) versus the wall superheat, given by the temperature difference between the wall temperature (T_w) and the ambient liquid temperature (T_l). The classical pool boiling curve was determined in an early investigation conducted by Nukiyama (1934). Figure 3.1 shows the boiling curve for water at atmospheric pressure.

It is clearly shown on the boiling curve that at very low wall superheat levels, the heat transfer coefficient is also low and increases slowly with wall superheat (section "a-b" in Figure 3.1). This indicates that no nucleation sites may be active and heat may be transferred from the surface to the ambient liquid by natural convection alone. The heat transfer coefficient associated with natural convection is relatively low.

As superheat becomes large enough, nucleation at some of the nucleate sites on the surface is initiated. This onset of nucleate boiling condition occurs at point "b" in Figure 3.1.

Once nucleate boiling is initiated, any further increase in wall temperature causes the heat transfer coefficients increase rapidly, which is shown as the section "b-d" of the curve and corresponds to the nucleate boiling regime. The active sites are few and widely separated at low wall superheat levels. This range of conditions, corresponding to segment "b-c" of the curve, is sometimes referred to as the isolated bubble regime or discrete nucleate boiling.

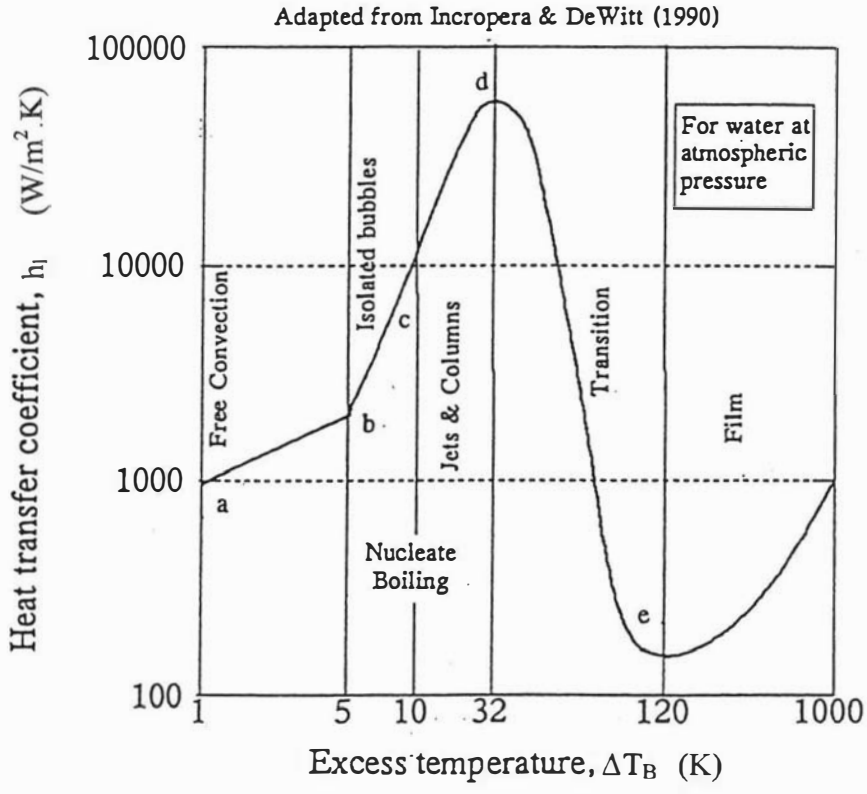

Figure 3.1 The boiling curve for water at atmospheric pressure.

With increasing surface superheat, more and more sites become active, and the bubble frequency at each site generally increases. Eventually, the active sites are spaced so closely that bubbles from adjacent sites merge together during the final stages of growth and release. Vapour is being produced so rapidly that bubbles merging together form columns of vapour slugs that rise upward in the liquid pool toward its free surface. This higher range of wall superheat, corresponding to segment "c-d" of the boiling curve, is referred to as the regime of slugs and columns or fully developed nucleate boiling.

The increasing of the wall temperature within the slugs and columns region ultimately results in a peaking of the heat transfer coefficient at point "d".

If the wall temperature is increased beyond this critical condition, a regime is encountered in which the heat transfer coefficient decreases as the wall superheat increases. This regime, which is usually referred to as the transition boiling regime corresponds to segment "d-e" on the boiling curve.

As the wall temperature is increased, eventually a point is reached at which the surface is hot enough to sustain a stable vapour film on the surface for an indefinite period of time. The entire surface then becomes blanketed with a vapour film, thus making the transition to the film boiling regime. This transition occurs at point "e" and the heat transfer coefficient increases again after this point.

3.2.2. Flow boiling

Due to the bulk liquid flowing over the heating surface, the interaction of the flow regime and the heat transfer mechanism make the flow boiling process become more complex.

Two arrangements are normally considered for flow boiling inside tubes; vertical tubes and horizonal tubes. The boiling characteristics of both orientations are significantly

different, so that different correlations are used for each of them. An extensive review of flow boiling inside tubes was given by Collier (1981a).

There are two important types of heat transfer mechanisms in flow boiling, nucleate boiling and convective interface boiling. However, the proportion of these two mechanisms varies over the length of the heating tubes.

In most (but not all) systems of practical interest, the onset of nucleate boiling is achieved at or just beyond the point where the bulk flow reaches the saturated liquid condition (boiling temperature) (Carey, 1992).

Thome (1990) pointed out that the wall superheat required to initiate boiling in flow boiling is not the same as that for nucleate pool boiling because the thermal boundary layers created by the respective processes are quite different.

Many correlations have been proposed to estimate the wall superheat required for the onset of nucleate boiling inside tubes (Bergles and Rohsenow, 1964; Sato and Matsullura, 1961; and Frost and Dzakowic, 1967). A widely quoted expression is that of Davis and Anderson (1966):

$$\Delta T_B = \left(\frac{8 \sigma T_{sat} q}{h_{fg} \rho_v k} \right)^{\frac{1}{2}} \qquad (3\text{-}2)$$

where: ΔT_B is the temperature difference between the wall and saturation temperature (K),

σ is the surface tension (N/m),

T_{sat} is the saturation temperature (K),

q is the heat flux(W/m^2),

h_{fg} is the latent heat of vaporization (J/kg),

ρ_v is the vapour density (kg/m^3),

k is the liquid thermal conductivity (W/m.K).

The physical properties are evaluated at the saturation conditions corresponding to the local pressure.

3.3 Heat transfer through a thin liquid film

In general, the heat transfer mechanisms through a thin liquid film could be conduction, convection or nucleate boiling, the proportions of each one are mainly dependent on the heating rate and the liquid flow pattern. The thermophysical properties of the liquid, namely thermal conductivity, viscosity, density, specific heat, latent heat, surface tension and boiling point elevation, and the conditions of the heating surface all may also have an effect on the heat transfer process. As a result of the heat transfer through the liquid film, part of liquid is evaporated. The vapour velocity over the vapour-liquid interface may also affect the liquid film flow pattern and consequently the heat transfer.

Four possible mechanisms for liquid film evaporation are discussed in the literature (Dengler and Addoms, 1956; Chun and Seban, 1971; Angeletti and Moresi 1983; and Thome, 1990). These include:

(1) Convective interface boiling, where heat transfer through the liquid film is by conduction and convection, the evaporation occurs only at the vapour-liquid interface of the film. The whole process is mainly governed by liquid flow conditions and thermophysical properties.

(2) Low rate nucleate boiling, where bubbles form and break but do not affect heat transfer greatly. Observations show that in this case bubbles move with the film without reaching the surface.

(3) High rate nucleate boiling, where the presence of the bubbles significantly affects liquid flow pattern and where the bubbles follow one another in channels across the film. The mixing of the liquid entails a significant improvement in heat transfer.

(4) Vapour film evaporation, where vapour film is evolved from bubbles produced at the tube surface.

The heating rate for a liquid film on the heating surface could be expressed as the heat flux, which is the heat transferred per specific area, or the wall superheat, which is the temperature difference between the wall and the liquid-vapour interface, similar to the wall superheat used in the pool boiling curve. From the pool boiling curve for water, it can be seen that, at atmospheric pressure, natural convection occurs when wall superheat is less than 5°C and isolated bubble nucleate boiling occurs when wall superheat is in the range 5 to 10°C. When a water film trickles down a tube under gravity, the critical degree of wall superheat required for vapour bubbles to be formed on the surface is up to 7°C, but if the heating rate is not very high, e.g. if heat flux is less than 30 kW/m^2, only convective interface boiling applies on the water film (Billet, 1989). Chun and Seban (1971) showed in their experimental results that a wall superheat of 3.7°C was required for nucleation in water at atmospheric pressure. According to Blass (1979), for water and aqueous solutions, transition from interface boiling to nucleate boiling in liquid films occurs at heat fluxes in the range of 40 to 60 kW/m^2, and at temperature differences in the range of 6 to 7.5°C. In his study of the effect of surface roughness on the boiling phenomena, Bell (1982) found that the ordinary engineering surfaces require surface superheats of the order of at least 3 to 5°C to initiate nucleation of a stable boiling phase.

Dengler and Addoms (1956) pointed out that in all cases an increase in liquid velocity past a surface was shown to raise the temperature difference required to initiate nucleate boiling at that surface. In other words it means that at a constant temperature difference the heat flux contribution by nucleate boiling decreases with increasing velocity until the boiling ceases entirely. It may be explained as that the greater velocity tends to prevent bubble formation at the wall (O'Connor and Russell, 1978). This effect of liquid velocity on nucleation, incidentally, can be observed by anyone stirring a pot of boiling water.

The wall superheat required for nucleate boiling also increases when the boiling temperature is reduced (Müller-Steinhagen, 1989). Thome (1990) argued that the formation of the vapour core in a tube may lead to a complete suppression of bubble growth in the liquid film at the tube wall.

In falling film evaporators, liquid distributed on the top of the tubes flows down on the inner surface as a thin film under the action of gravity and later accelerated by the vapour velocity. Several heat-transfer mechanisms may coexist depending on local conditions (O'Connor and Russell, 1978). Kroll and McCutchan (1968) found the interface evaporation plays the major role in the heat transfer at lower heat flux. But the low rate nucleate evaporating mechanism is regarded by Sinek and Young (1960) as the most probable mechanism in the falling film evaporators.

Billet (1989) thought that the flow pattern in the evaporator decidedly affects heat transfer on the liquid side of the heater, and that the amount of vapour in the liquid is a crucial factor. He also pointed out that the calculation of the heat transfer coefficient in evaporators is subjected to various physical laws that depend on whether boiling is nucleate or convective.

Houšová (1970) presented experimental data for falling film evaporation of water in a 3 metre long tube at the evaporation temperature range of 50 to 74°C. The data indicates that the change to nucleate boiling takes place above a wall superheat of 10°C.

Chen (1992) found that the overall heat transfer coefficient in a single tube falling film evaporator decreased with increasing of the temperature difference between the steam condensing and the liquid evaporating temperatures. There was a change in the rate of decrease of heat transfer coefficient with increases in the temperature differences between the steam condensing and the liquid evaporating temperature at about 8K, which was attributed to the changes of heat-transfer mechanisms in the thin liquid film from convective interface boiling to nuclear boiling.

Stephan (1992) stated that nucleate boiling is generally avoided in falling film evaporators because liquid is dragged along by the vapour bubbles resulting in dry spots forming on the wall, which can reduce the heat transfer rate and promote the fouling of the heating surface. However, Bouman *et al.* (1993) found that nucleate boiling starts at temperature difference, between the liquid and wall temperature, of about 0.5°C for milk and about 5°C for water. It also found that the transition from convective boiling to nucleate boiling takes place at much lower heat fluxes with skim milk than with water (van Stralen and Cole, 1979). This can partly be explained by the difference in surface tension, which for milk is lower (Walstra and Jenness, 1984), but may also be due to the presence of milk fat globules which may act as nuclei. Therefore, based on above discussions, Mackereth (1995) postulated that, with water, falling film evaporators are likely to operate solely under the convection boiling regime, while on milk, nucleate boiling may dominate.

3.4 Effect of the adjacent gas stream on the liquid film flow and heat transfer

In general, there are various correlations predicting that, as the velocity of the gas stream is increased, the mean film thickness for a given liquid flow rate decreases for downward concurrent flow of the two phases, due to the acceleration of the surface by the gas stream drag (Fulford, 1964).

The effect of the gas stream motion on the liquid film flow was first examined by Semenov (1944), he proposed an interrelationship among liquid throughput, film thickness and tangential force which can only be applicable for a film with a thickness not great than 150 microns and at moderate gas rates. A detailed analysis of the smooth film and gas streams inside vertical tubes was also carried out by Brauer (1956).

For wavy laminar flows, an equation published by Kapitsa (1948) predicts the mean film thicknesses based on the irrigation density and mean gas velocity, when the gas stream does not seriously affect the flow wavelength. Wavy film flow was shown to be more

stable than smooth film flow, and with a mean film thickness about 7% thinner than smooth film at the same flow rate.

For the turbulent film regime flow, Dukler (1960) provides numerical results relating the effects of a concurrent downward flowing gas steam on film thickness and liquid velocity. Film heat transfer under these circumstances is also determined.

Zhivaikin (1962) concludes that film thickness is slightly affected by concurrent downward flow for gas velocities up to 4 m/s, but that the film thickness decreases at higher gas velocities. He also presents a correlation to predict film thickness, for gas velocities between 4 m/s and the velocity at which spray formation commences.

Any pressure drop due to gas stream friction losses and the energy to create gas velocity will cause an increase in the evaporating temperature. Consequently, since falling film evaporators operate at low temperature difference, such pressure drop could significantly reduce the total available heat-transfer driving temperature difference (Schwartzberg, 1988).

Zhivaikin and Volgin (1964) showed experimental results which indicate that pressure drop per unit length is not always constant in the direction of gas flow. They explained that the reason is due to changes in the shape of the gas stream velocity profile and to changes in energy on accelerating the liquid film near the inlet. They found a particularly interesting feature in gas flows which is that the friction pressure drop in a wetted-wall tube is considerably larger than in the dry tube. This reason was not clear to them. But with gas flowing down the tube, there will be a drag force on the liquid film increasing its velocity. The energy required for this increase must be transmitted by an increased pressure drop in the gas.

Sinek and Young (1960) published an expression to calculate the friction pressure drop in falling film evaporators and they concluded that for most cases, the vapour rate per tube is not high enough for the friction pressure drop to deviate significantly from that

of the dry-tube value. However, the tube length employed in the commercial falling film evaporators has been increased considerably since 1960. At the same time the number of effects has also been increased, which results in the available heat-transfer driving temperature difference in each effect reduced. Hence the pressure drop in the falling film evaporators becomes significant.

Jebson (1988) and Jebson and Iyer (1991) found that the vapour momentum is an important and positive factor to influence the heat transfer coefficients in falling film evaporators used in the New Zealand dairy industry. The effect of vapour velocity over the liquid film was thought as that of an high wind blowing over a lake surface and causing waves. This effect probably increases heat transfer especially towards the bottom of the tube as the vapour velocity is increasing along the tube.

Carey (1992) argued that the vapour flow in the core of the tube would affect the heat transfer mechanism in the liquid film. The increasing vapour void fraction, as a result of vaporization will accelerate the liquid flow, which produce changes in the flow patterns. As vaporization continues, the thickness of the liquid film on the tube wall will decrease, reducing its thermal resistance and thereby enhancing the effectiveness of the heat convection mechanism.

3.5 Heat transfer enhancement by rotating the surface

Rotating heat transfer surface is a specific type of heat transfer intensification with mechanical aids, which has been classified as an "active" technique (Reay, 1991).

Within the field of intensified heat transfer, the so-called "passive" techniques (e.g. treated surface) are routinely used to improve evaporation and condensation heat transfer coefficients. However, the use of "active" methods, which appear to offer great potential rewards in terms of efficiency and compactness, are less well explored and, to a greater extent, less extensively applied. It has been pointed by Jachuck and Ramshaw (1994) that the use of high gravity field created by rotation is one of the most interesting and

potentially the most rewarding method among several active methods, such as stirring, scraping or vibration.

Rotation of the heat transfer surfaces offers the following advantages (Jachuck and Ramshaw, 1994; Yanniotis and Kolokotsa, 1996):

(1) Variable rotation speed offers a further degree of freedom on exchanger design and operation, and the equipment volume could be reduced due to the high heat transfer coefficient and high temperature difference that can be used;
(2) The increased "g" (acceleration due to rotating), coupled with a build-in surface structure roughness factor, enhances the liquid film process;
(3) There is a self-cleaning action whereby rotation can better handle liquids which contain solids as well as viscous products;
(4) Reduced fluid residence time in the heating zone will have a great influence in processing heat sensitive liquids.

The use of centrifugal force has been demonstrated to give significant degree of enhancement in both heat and mass transfer. A disadvantage of rotating equipment is the high cost of machining that is required. However, as automation in manufacturing is developed, this cost could decrease (Yanniotis and Kolokotsa, 1996).

Jachuck and Ramshaw (1994) have experimentally studied the convective heat transfer characteristics of water film on four discs, each with a different surface configuration, for various flow rates and rotational speed (250-890 rpm). Average heat transfer coefficients as high as 11 kW/m^2K were achieved by using a smooth disc. They observed by using a photographic technique that there were surface waves existing in the liquid film and claimed that the surface waves play an important role in the heat transfer performance of the thin film on rotating discs.

The increase in the average heat transfer coefficient for increasing rotational speeds may be due to better shear mixing, resulting from a thin film, which suggests that at higher

rotational speeds, the films get thinner and the surface waves become smaller and more concentrated. The surface waves will cease to exist when the rotation speed increases further.

Similar phenomena were observed by both Elsaadi (1992) and Lim (1980). Lim (1980) explained the existence of a maximum value for the mass transfer coefficient by suggesting that by increasing the flow rate, the film thickness increases, thereby creating waves which induce progressively more efficient mixing in the film. However, as the film thickness (resulting from increasing flow rate) increases beyond some optimum value, the waves are unable to produce the higher levels of mixing required to produce high mass transfer rates.

Convection heat transfer in axial flow through a horizontal heated tube, rotating about its axis, has been investigated experimentally by Kuo *et al.* (1960) with water and by Briggs (1959) with air.

Kuo *et al.* (1960) investigated experimentally the heat transfer with axial flow of water through a rotating horizontal annulus for the case that the liquid fills the entire annulus and for the case that the liquid fills only half the annulus. Their results indicated that there were at least three different flow regimes existing in the flow through a rotating tube. Under the conditions investigated, free convection effects were found to be of secondary importance compared to the phenomena produced by the rotation of the tube wall. Moreover, in the range of axial flow Reynolds numbers between 60 to 1,000, and rotational flow Reynolds numbers between 4,000 to 30,0000, rotational effects predominated also over those of the axial flow. They defined axial flow Reynolds numbers and rotational flow Reynolds numbers as $Re_a=Du/\nu$ and $Re_r=D^2\Omega/\nu$ respectively.

It is also worth noting that effective convection heat transfer coefficients for the half-filled annulus were found to be essentially equal to the values obtained with a full channel. The reason for this is that a thin layer of liquid adheres to the rotating surface

by virtue of the rotation and is carried upward through the air. The heated liquid film is then mixed with the cooler bulk of the main liquid stream. In this manner liquid is heated over the entire heating area and this quasi-periodic heat flow mechanism accounts for the large rates of heat transfer, as shown by Kuo *et al.* (1960). The phenomenon has been applied successfully in rotating heat exchangers (Mai, 195; Kern and Karakus, 1958).

With water in the tube, there may exist a free fluid surface, while a gas will always fill the entire cross-sectional area of the flow channel. The conclusion which can be drawn from Pattenden's work (1964) is that exceptionally large overall heat transfer coefficients can be achieved between two fluid streams separated by a rotating tube. Ferell *et al.* (1957) also claim that a significant reduction in axial pressure loss may be achieved in flow through a tube by increasing its rotational speed.

The details of the convection heat transfer in rotating system were given by Kreith (1968) in his comprehensive review.

More recently, Yonniotis and Kolokotsa (1996) reported an experimental work carried out on a heated smooth surface of a rotating disc. They investigated the effect of rotating speed and feed flow rate on heat transfer coefficients by using water and corn syrup as test liquids and boiling between 40 and 50°C. The heat transfer coefficient increased by 3-4 times when the rotating speed increases from 0 to 104.7 rad/s, but feed flow rate had no significant influence on the heat transfer coefficient.

3.6 Steam Condensation

The commonest medium for heating evaporators is steam. There are two mechanisms of condensation, which are well described by the terms dropwise and film type.

3.6.1 Film Condensation

If the liquid phase fully wets a cold surface in contact with a vapour near saturation conditions, the conversion of vapour to liquid will take the form of film condensation. The condensation takes place at the interface of the liquid-vapour film covering the solid surface. The vapour condensate travels down the surface as a continuous layer with an increase of the film thickness under the action of gravity. Because the latent heat of vaporization must be removed at the interface to sustain the process, the condensation rate is directly linked to the rate at which heat is transferred across the liquid film.

The theoretical analysis for laminar film condensation on a vertical surface was first proposed by Nusselt in 1916. In this analysis, a number of simplifying assumptions were made: (1) the liquid film is in laminar flow with smooth surface and its physical properties are constant; (2) the vapour is pure and stationary; (3) the shear stress acting at the vapour-liquid interface is negligible; (4) heat transfer across the liquid film only by conduction.

Nusselt's theory can be expressed in terms of a modified Nusselt number:

$$Nu' = 1.47\ Re^{\frac{1}{3}} \tag{3-3}$$

Where: Nu' is defined as:

$$Nu' = \frac{h_L}{k}\left(\frac{\mu^2}{\rho^2 g}\right)^{\frac{1}{3}} \tag{3-4}$$

h_L is surface heat transfer coefficient on the side of the liquid (W/m^2K);

k is thermal conductivity of the liquid (W/m.K);

ρ is the liquid density (kg/m^2);

g is the gravitational acceleration (m/s^2);

μ is dynamic viscosity (Pa.s).

Since then, a substantial number of modified versions of this analysis have been developed. A comprehensive review on the correlations for laminar and turbulent flow film condensation on a vertical surface is given by Chun and Kim (1990).

3.6.2 Dropwise condensation

Dropwise condensation is obtained only on a poorly wetted cooling surface (McCabe and Smith, 1965). A poorly wetted surface condition can result from contamination or coating of the surface with a substance that is poorly wetted by the liquid phase of the surrounding vapour.

In practice, this can be achieved for steam condensation by (1) injecting a non-wetting chemical into the vapour, which subsequently deposits on the surface; (2) introducing a substance such as a fatty acid (e.g. oleic) or wax onto the solid surface; (3) by permanently coating the surface with a low-surface-energy polymer or a noble metal (Holden *et al.*, 1987).

Each of these methods has its drawback and/or limitations. The effects of the first two methods are generally temporary, since the resulting surface films eventually are dissolved and washed off from condenser surface under common industrial operation conditions. The third method of promoting dropwise condensation is of particular interest because it holds the prospect of providing continuous dropwise condensation, but generally considerable cost will be added to the fabrication (Carey 1992).

Dropwise condensation is generally the preferred mode of condensation because the resulting heat transfer coefficient may be as much as an order of magnitude higher than that for film condensation under comparable circumstances. Billet (1989) stated that the heat transfer coefficients in dropwise condensation are higher than those encountered in purely film condensation by a factor of about 6-20.

During dropwise condensation, the condensate is usually observed to appear in the form of droplets, which grow on the surface and coalesce with adjacent droplets. When droplets become large enough, they are generally removed from the surface by the action of gravity or drag forces resulting from the motion of the surrounding gas. As the drops roll or fall from the surface, they merge with droplets in their path, effectively sweeping the surface clean of droplets. Droplets then begin to grow on the freshly exposed solid surface. This sweeping is renewal of the droplet growth process, which is responsible mainly for the high heat transfer coefficients associated with dropwise condensation.

Despite numerous studies of dropwise condensation over the years, its mechanism remains the subject of debate (Carey, 1992). Two different types of models have been proposed:

(1) The first model type is based on the premise that droplet formation is a heterogeneous nucleation process. Droplet embryos are postulated to form and grow at nucleation sites, while portions of the surface between the growing droplets remain dry. This type of model apparently was first proposed by Eucken in 1937.

(2) The second type of dropwise condensation model postulates that condensation occurs initially in a filmwise manner, forming an extremely thin film on the solid surface. As condensation continues, this film eventually reaches a critical thickness, estimated to be about 1 μm, at which point it ruptures and forms droplets. Condensation then continues on the surface between the droplets that form when the film ruptures. Condensate produced in these regions is drawn to adjacent drops by surface-tension effects. Droplets also grow by direct condensation on the droplet surfaces themselves. This second model was proposed by Jakob in 1936. Modified versions of this model have also been proposed by Kast (1963) and Silver (1964).

Both dropwise condensation models are supported by several experimental investigations. Using an optical technique to indicate changes in the thickness of very

thin liquid films, Umur and Griffith (1965) found that, at least for low temperature differences, the area between droplets was, in fact, dry. Their results indicate that no film greater than a monolayer existed between the droplets, and that no condensation took place in those areas. However, the results presented by Welch and Westwater (1961) and Sugawara and Katusuta (1966) indicate that condensation occurs entirely between droplets on a very thin liquid film.

As suggested by Collier (1981b), it may be that droplet nucleation dominates at low condensation rates, with the film disruption mechanism taking over at higher condensation rates.

A detailed discussion of theoretical aspects of dropwise condensation can also be found in a series of publications by Tanaka (1975, 1979, 1981).

Other methods of promoting dropwise condensation has been examined and reported, such as, surface vibration (Brodov *et al.*, 1977) surface rotation (Nocol and Gacesa, 1970; Sparrow and Gregg, 1959), electrostatic fields (O'Neill and Westwater, 1984).

3.6.3 Condensation in the presence of non-condensable gases

The most serious problem in steam or vapour condensation is the presence of non-condensable gases. Small amounts of non-condensing gases usually are dissolved or occluded in the liquid food being concentrated. Air also leaks into the vacuum system through joints and connections. It mixes with the steam or vapour flowing towards the condensing surface, and unless a means of steadily removing it is provided, it will accumulate at the condensing surface impeding the process of condensation, and impairing the heat transfer coefficient.

Air is heavier than steam and would be expected to collect at the bottom of the apparatus. However, diffusion and steam flows due to condensation ensure that the air

remains mixed with the steam and it was considered that there would be more air in dead corners where the flow is stagnate (Lyle, 1947).

As only the vapour is condensed, the concentration of the non-condensable gases at the condensing surface is higher. This, in turn, decreases the partial pressure of the vapour at the condensing surface and the corresponding saturation temperature at the condensing surface is lower than the bulk temperature. Therefore, the non-condensable gases reduce heat transfer coefficients in two different ways: (a) they form a layer on the condensing surface (air blanketing effect) and (b) non-condensable gases lower the condensation temperature at a given total pressure affecting the heat transfer efficiency.

Only traces of air could cause a steep decrease, as any concentration of air greater than 0.01% can have a drastic effect on the condensing heat transfer coefficient (Mincowycz and Sparrow; 1966, Sparrow *et al.*, 1967). Condensation rates are reduced by 10%, when flowing steam contains 2% air, whereas the reduction is 70% in stagnant zones (Collier, 1981a).

In order to maintain good heat transfer performance, non-condensable gases removal is usually accomplished by vacuum pumps or ejectors connected to the condensing vapour chamber. It is important to set the proper de-aeration rate, because the de-aeration rate determines the steam velocity at steam inlet and the average concentration of non-condensable gases at the condensing surface. Mackereth (1993) shown that at low de-aeration rates, the average concentration of non-condensable gases at the condensing surface increased. The heat transfer coefficient dropped slowly to approximately half the original value in a couple of hours in a single tube evaporator when the de-aeration line blocked. However, the removal of non-condensable gases reduces thermal efficiency. Schwartzberg (1988) pointed out that the mix of gas and vapour venting from a vacuum device often contain 97% to 98% vapour, which is wasted. Steam losses might be reduced if we were better able to control levels of non-condensable gases.

3.7 The development of evaporation technology in the dairy industry

The evaporation of milk has been known for many years, even as early as in the year 1200 A.D. when Marco Polo described the production of a pasta, which was effectively a sort of milk concentrate, in Mongolia (Westergard, 1983).

The most simple evaporator was an ordinary open pan heated with fire, hot water or steam. The simplest evaporator was used to produce storable milk with adding sugar by De Heine in 1810 (Wiegand, 1985).

In 1813, Howard invented a vacuum pan with a condenser to deal with the vapour produced (Taylor, 1982). This invention enabled the lowering of the evaporation temperature, improved the quality of products and was an important step on the way to industrial production of concentrated and durable liquid dairy products.

In 1850, Gail Borden was the first person to concentrate and sell milk on an industrial scale. He used a vacuum pan with a heating coil to enlarge the heating surface (Armerding, 1966). At this time sweetened condensed milk was produced in the United States.

In 1852, Robert Von Seelouitz was granted a patent for an evaporator, the so-called Robert evaporator, which had a vertical tube bundle arranged around a wide central circulation tube. A natural circulation, which improved the heat transfer, occurred in it. This kind of evaporator was improved and used in the dairy industry for quite a long time. Its use was animportant precondition for high capacities and continuous operation. In order to cope with highly concentrated solutions, the vertical tube bundle was separated from the separator, which made it possible to pump the concentrated milk to be cycled in the evaporator. This kind of evaporator is called a forced circulation evaporator.

In 1901, Kestner invented the so-called climbing-film evaporator, which was fitted with longer heating tube (about 7 m long and 50 mm diameter) and arranged with a chamber for the separation of the liquid from vapour alongside the calandria. This type of evaporator was developed on the basis of the Robert evaporator, but heat transfer coefficients were higher and was operated with less recycle than the Robert evaporator. In the climbing film evaporator, the amount of recycle is controlled, but not in the Robert evaporator.

With the development of production, high quality products were required. The problems in using a climbing film evaporator in dairy industry were shortly realised, because the hold up of the liquid in evaporator was high, that means the residence time of the milk in the evaporator was rather long. The high static pressure which prevents the liquid from boiling in the bottom parts of the tube, worsens the heat transfer in this area considerably. The evaporator cannot be used effectively with small temperature differences.

The disadvantages of the climbing film evaporator were recognized in the earlier 1930's. In 1935, the falling film concept was introduced by D. D. Peebles and P. D. V. Manning and the first patents were in this period (Hallström, 1988a).

However, because stainless steel was very expensive at that time, no suitable pumps were available and the problem of how to distribute the liquid evenly onto the heating tube was not resolved, a commercial falling film evaporator was not manufactured for use in industry until 1953 by Wiegand in Germany. Since then, falling film evaporator has been developed quickly. In many applications this type of evaporators have almost entirely displaced the other types of evaporators and this is true in the case of the dairy industry. Nowadays, all evaporators used in New Zealand dairy industry are falling film evaporators (FFE).

During the development of evaporating technology, two methods of reducing energy consumption were created and are still used today. One is multiple effect evaporation and another is vapour recompression.

In England in the year 1825, and in France in the year 1833, it was suggested to use the heat contained in the vapour produced in one evaporator for the heating of another evaporator and, if need be, to heat a third evaporator by means of the vapour produced in the second one, i.e. to operate according to the so-called multiple effect principle (Hallström, 1988b). But, before about 1910, most evaporation plants had only one effect. The first continuous multiple effect evaporator was used in the middle of 18th century in the sugar industry (Hahn, 1985). The multiple effect operation was introduced into dairy plants at the end of the nineteen thirties in Europe for producing evaporated cream (Wiegand, 1985). The theoretical specific steam consumption, in terms of the percentage of kg steam used per kg water evaporated, equal to the reciprocal value of the number of effects, it is therefore 100% with only one effect, 50% with two effects, 33.3% with three effects. The number of effects, however, is limited by the total temperature difference available. In the food industry it is often necessary to avoid boiling temperatures above 70 °C when dealing with sensitive products due to the formation of deposits on the heating surface and the effects on product quality. On the other hand it is very costly to operate with boiling temperature below 40 °C. Low temperatures not only result in a large increase in cooling water consumption, but also in a considerable increase of the evaporator size, because of the higher vacuum required, consequent larger vapour volumes and higher viscosity products with lower heat transfer. Nevertheless, the number of effects in an evaporator has been steadily increased and six and seven effects evaporators are now used.

In vapour recompression, the vapour can be compressed thermally by high-pressure steam-jet ejectors; or mechanically, by positive-displacement or centrifugal compressors as well as fans, to higher pressure and used as heating medium. It is obvious that a large saving in energy is obtained by compressing the vapour because the enthalpy difference between the vapour to be compressed and steam is about 24 kJ/kg, while

between water and steam about 2240 kJ/kg. Although steam jet compressors were equipped on milk evaporators in Europe after World War I, and mechanical vapour compressors were first found in the Swiss dairy industry during World war II (Wiegand, 1985), the oil crisis in 1973 greatly stimulated their use (Hallström, 1988b). In general, compressors can raise the saturation temperature of the vapour by 15-20°C, while fans can raise the saturation temperature by 4-6°C. Fans are now preferred, instead of compressors, because of their simplicity in design, ease of operation, and therefore lower cost (Mackereth, 1995).

After the two energy crises of 1973 and 1978, energy requirement became a serious problem, the number of effects increases greatly. In 1966, the first quadruple effect evaporation plant was produced, in 1974, the first five effect plant, in 1976, the first six effect plant and shortly after this, the first seven effect evaporator was installed (Hahn, 1985). In 1979, the mechanical vapour recompression was used once again in Germany in a triple effect plant for the evaporation of whey (Kessler, 1985).

The reasons for the widely use of falling film evaporator in the dairy industry are the peculiar characteristics of this evaporator, which can be described as follows:

(1) FFE can be operated at any low temperature difference. This means that FFE can be theoretically equipped with as many effects as one wanted;

(2) The lower temperature difference that can be used in FFE is also favourable to multiple effects operation and mechanical vapour recompression by fans;

(3) The very short residence time of the product in the evaporator is a result of the small amount of liquid hold up and the high flow velocity. Since the product is generally processed in single pass all liquid particles have an almost equal time of direct contact in the evaporator. Thus undesirable microbiological, physical and chemical changes in the milk resulting from excessive heat treatment are avoided;

(4) Due to the relatively high flow velocity and low temperature difference, the deposit on the tube wall is small, i.e. the operating time before cleaning can be largely extended;

(5) High final concentrations are possible in FFE since the high vapour velocity propels viscous products without plugging, and the low temperature difference used makes it possible to reach high concentration without scaling of the tubes;
(6) The capability of evaporation of FFE can be extended to satisfy any requirement due to single construction and the possibility of using longer tubes (15 m or more). Low operating costs, low steam consumption, and high quality can be achieved more easily in bigger evaporating plants (Wiegand, 1978);
(7) A relatively very small amount of cleaning agents is needed as the liquid volume in the evaporator is low.

It can therefore be seen that falling film evaporator fully satisfies the demands of the modern dairy industry of today, i.e. the possibility of large capacities, economical running, reliable and continuous operation, careful treatment of the products.

Evaporation is the only process used for the concentration of milk in New Zealand (Mackereth, 1995). The potential rival processes, which can also be used to remove water from milk, are reverse osmosis and freeze concentration. Reverse osmosis may become competitive with evaporation if maximum processing temperatures of 40-50°C are permitted, and only a low concentration product is required. It was reported that reverse osmosis can concentrate skim milk only up to 25% total solids, and the final concentration required must then be obtained by subsequent evaporation (Carić, 1994). With rapid decrease in capital cost and increase in membrane life, reverse osmosis is now been used as a first stage of whey concentration in whey powder manufacture (Bennet, 1996). Freeze concentration is only likely to be economic for low volume products that are hypersensitive to heat. Therefore, evaporation technology will remain an important process in the dairy industry, especially for the milk powder manufacturing process, for the foreseeable future (Mackereth, 1995).

It is well known that the efficiency of the evaporator is much higher than the drier. Therefore, concentrates with higher final total solids produced in the evaporator to the drier means that the total energy consumption in the whole process of milk powder

production will be reduced. In the present milk powder manufacturing process, the maximum allowable total solids of milk concentrates are mainly limited by the drier (Mackereth, 1995). If a breakthrough allows a higher viscosity feed to the drier, the falling film evaporator would soon limit the total solids of the concentrates. By then, an evaporator, which could produce a further higher total solids concentrate, will be needed. Thin film evaporators with rotating surfaces may will be chosen for this additional concentration (Bouman and Waalewijn, 1994a, b).

3.8 Thin film evaporators with rotating surfaces

It has already been recognized that the centrifugal force generated in a rotating system may be utilized to enhance the heat transfer performance. One of the applications of this phenomena is in the thin film evaporator with rotating heaters, which has been used for decades. From the aspect of modern process engineering, they are an interesting development and can be considered more as a welcome companion than as competitor to other types with short residence times, although the fields of application may overlap.

3.8.1 The development of this type of evaporator

For many years, it was believed that the concentration of heat sensitive materials should be carried out under very low temperature conditions to avoid damage. On this principle a number of evaporators were installed which were designed to boil liquid at temperature as low as 21°C (Gray, 1981). Unfortunately, this is very uneconomical and involves considerable practical difficulties with cooling water. Now, it has been shown that in many cases it is the time temperature integral which controls the extent of deterioration, and that it is possible to evaporate quite sensitive materials at relatively higher temperatures than had previously been thought, provided the length of time for which the product is maintained at this temperatures is sufficiently short. Therefore, much attention has been paid to reducing the heat contact times in evaporators to the very minimum (Leniger, 1986).

Experience gained in industrial practice has revealed that thin film evaporators with rotating wipers are by no means successful in all cases where heat unstable products have to be evaporated, because even residence times of about a minute are often still too long. Thus, if a residence time of a mere second were to be specified for a liquid with a viscosity as high as 20 Pa.s or more, no evaporators would be available. The mechanical and process engineering problems involved in problems of this nature have been approached from an entirely different angle, and a new principle has been devised to cope with them. Thus a design has been developed that permits evaporation under extremely mild conditions; for example, the residence time in the actual evaporation zone may be only a fraction of a second (Billet, 1989).

Rotating the surface on which evaporation takes place appears to be a logical way of developing this type of evaporator. The rotating conical heating surface was first developed in the US by Hickman, for sea-water distillation, beginning in 1935. The design was re-discovered and modified by Mautner in Yugoslavia and was presented as a commercial unit by Alfa-Laval in Sweden in 1959 (Hallström, 1969). In 1980's, a similar type of evaporator was built in Germany and Japan.

Depending on the orientation of the rotating cone, there are three different designs of this type evaporator available in the market. The most successful one is the Centritherm evaporator, which has a cone rotating about its vertical axis. There are three sizes: CT1B, CT6 and CT9. Their heating surfaces are $0.1m^2$, $2.4m^2$ and $7.1m^2$ respectively. For CT6 and CT9, there are multi-cones stacked upon each other. The largest capacity of Centritherm evaporator was reported as about 5,000 kg/h water evaporation (Mannheim and Passy, 1974).

The second one, called Liprotherm, has an inverted rotating cone. This design has a compact form as it includes the pre-heater and condenser in a same unit. A sight glass is also placed on the unit which can be used to observe the evaporating liquid film flow (Billet, 1989).

A recently developed model called Evapo has a horizontal rotating cone. There are six different available sizes for this evaporator. The heating surfaces are in the range of 0.1 to 5m^2, with water evaporation rates from 70 to 2,000 kg/h. The whole machine is automatically controlled and has a sight glass (Anon, 1990).

Figure 3.2 shows the different designs of this type of evaporator.

3.8.2 The features of the rotating surface evaporator

This type of evaporator offers the following features:

(1) It has an ultra short residence time, which is important for heat sensitive products such as enzymes, antibiotics, herbal medicines, protein solutions, fermented liquids, etc.. When evaporating or concentrating these heat-sensitive liquids, it is required that the process liquid receives a specific quantity of heat at a minimum temperature for an extremely short time period. The rotating surface evaporator satisfies all three of these important criteria. The liquid film produced by centrifugal force is a scant 0.1 mm thick, which is thinner than a mechanically spread film.

(2) It operates with high concentrated liquids. It was reported that the milk concentrate produced in the Evapor unit can be up to 85% dry matter (Anon, 1990). However it is unlikely for skim milk to be concentrated to such high level as gelling would occur when concentrate total solids is beyond 65% (Wood, 1982). So it would probably be used for sweetened milk concentrate (i.e. sugar may be added into the products).

(3) The centrifugal force generated by the rotating cone inhibits any tendency for the process liquid to foam, consequently improving efficiency. The application of centrifugal force to the liquid on the moving heat transfer surface, presses the liquid onto this surface and thereby eliminates foaming in a way not possible with other type

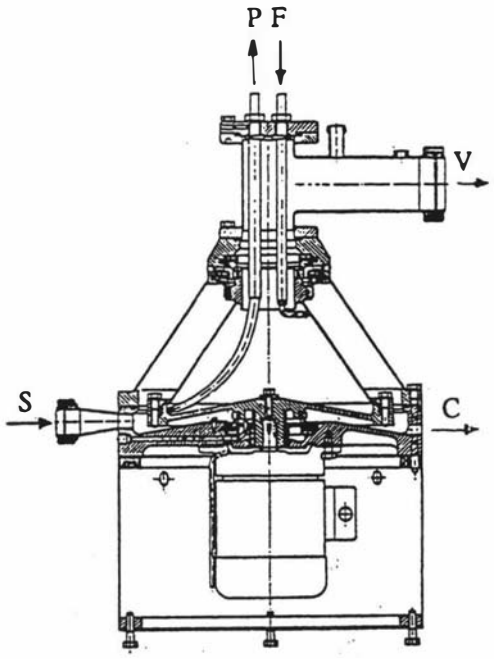

(1) Centritherm

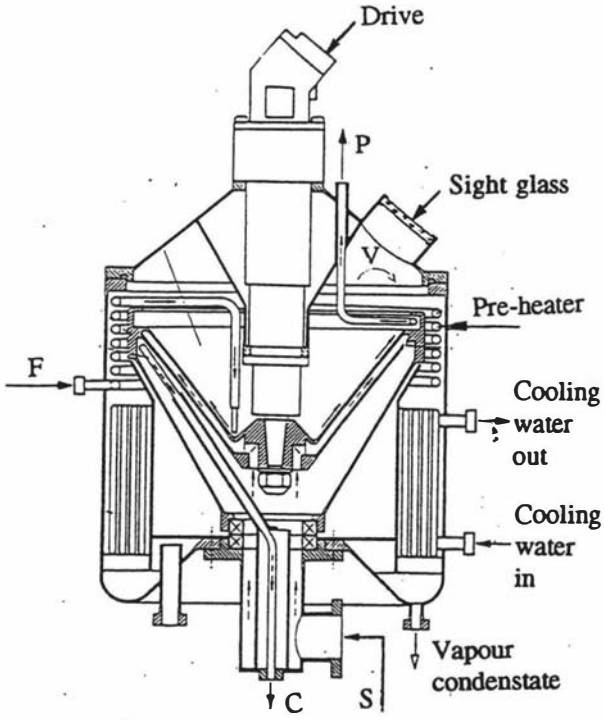

(2) Liprotherm

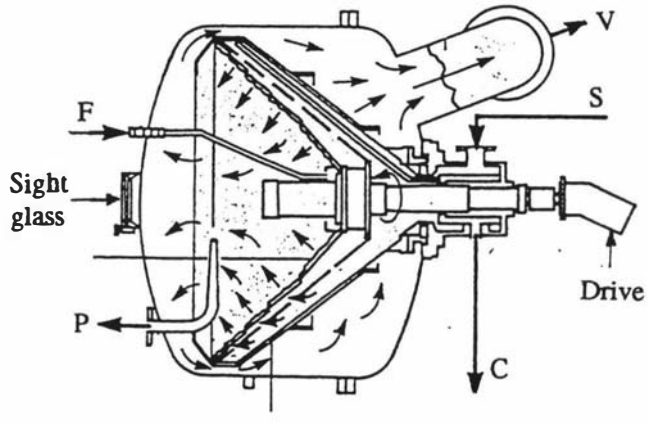

F - Feed
V - Vapour
S - Steam
P - Product (concentrate)
C - Condensate

(3) Evapo

Figure 3.2 The different designs of the film evaporators with rotating surfaces

of systems that use fixed heat transfer surfaces (e.g. downflow systems, mechanically-agitated systems, etc.).

(4) It has a high overall heat transfer coefficient. Rotation of the heating surface does not only improve the heat transfer on the liquid side by effectively distributing and quickly passing the liquid to be evaporated on the surface, but also benefits the steam condensation on the other side. As soon as the steam condenses on the outer surface of the cone, the condensate forms droplets, which are thrown off the rotating surface by centrifugal force. Therefore, no condensate film, which would offer resistance to heat transfer, is formed. The dropwise condensation is considered to be a major mechanism of condensation, which gives rise to very high heat transfer coefficients (Mannheim and Passy, 1974). Further, the fast moving liquid film also reduces the formation of deposit on the heating surface because the formation of deposit on the heating surface is controlled not only by the temperature but also by the movement of liquid on the heating surface (Wiegand, 1978).

(5) This type of evaporator is also highly suitable to concentrate high viscosity products. In conventional falling film evaporator the liquid film flow is assisted by vapour velocity, but at high liquid viscosities this is less effective (Jebson and Iyer, 1991). Hence, the final concentration of the products is limited. In the Centritherm evaporator, however, the transporting force can be greatly increased with mechanical assistance, which means considerably higher velocity and hence larger heat transfer coefficients and the possibility of obtaining a higher final concentration. The centrifugal force, generated in the rotating system at high rotational speeds, could be more than one hundred times greater than the force of gravity (Hallström, 1969). In addition, high viscosity liquids tend to form runnels which do not to wet the heating surfaces properly, but rotating the surface could overcome this problem.

(6) This type of evaporator meets the equipment for 'clean' production plants, since the amount of volatile decomposition products, which can enter the atmosphere or the effluent through the vacuum system, is reduced due to extremely short residence times.

In view of the increasing severity of legislation on the environment, this fact may be a convincing arguement in swaying decision on equipment selection in favour of these evaporators (Billet, 1989).

In this type of evaporator, energy must be supplied during start up to accelerate the rotating cone from unmoving to the angular velocity (Ω). Energy is also required in the rotor to give the liquid its final velocity and overcome the frictional losses. It was estimated that theelectric energy in this type of evaporator is between 1 and 10 % of thermal energy input (Yanniotis and Kolokotsa, 1996).

3.8.3 Industrial use of rotating surface evaporators

A literature search for the period 1969-1995 showed that there were 30 published papers dealing with the application of Centritherm evaporators. The Centritherm evaporator can be used in producing of a wide range of products, such as: fruit juices (Hallström, 1969), coffee and tea extracts, egg, yeast extracts (Pajunen *et al.*, 1974), milk products (Bouman and Waalewijn, 1994a,b), gelatin, meat extract (Traegardh, 1974), malt extract and brewery syrups, low-alcohol and alcohol-free beers (Oliver-Daumen, 1982, 1986), glucose products (Shinn, 1971), antibiotics, herbal medicines and enzymes (Anon, 1992).

Clarified apple juice containing 9-10 % dry matter was concentrated in a Centritherm evaporator. The feed flow (600 to 1,400 l/h), steam temperature (90 to 115°C) and evaporating temperature (45 to 60°C) were varied. It was concluded that the feed flow had a much greater effect on the degree of concentration than the other two variables (Nong, 1969).

Lewicki and Kowalczyk (1979) conducted experimental work using a Centritherm evaporator with apple juices (10, 20 and 30% dry matter, DM) and sweet whey (6 and 13% DM) by varying the temperature differences (20, 30, 40, 50K), evaporating temperatures (30 to 40°C), and the angular velocities of the rotating cone (72, 108 and 144 rad/s). The Reynolds numbers averaged for the feed and concentrate streams were

calculated to be in a range 21 to 213. They found that the overall heat transfer coefficients was independent of the type of food, its solids contents and the angular velocity and depended only on Reynolds number and temperature difference. It was also found that the residence time of material in the evaporator was 0.6 to 1.6 seconds and was longer for higher temperature difference at constant Reynolds number and inversely proportional to the Reynolds number at constant temperature differences.

CHAPTER 4
EXPERIMENTAL METHODS FOR DETERMINING HEAT TRANSFER COEFFICIENT

4.1 Objectives

The objectives of this experimental work were to assemble and operate a single-tube falling film evaporator with rotating surface and a cone evaporator with 10° top half angle and also to evaluate the effects of operating variables on the overall heat transfer coefficients in these two evaporators as well as the Centritherm evaporator.

4.2 Materials

4.2.1 Water

Tap water was used because it is a liquid with well known physical properties.

4.2.2 Sugar solution

Sucrose used was Chelsea white sugar produced by the New Zealand Sugar Company. The reasons for using sugar solution are that it is cheap, non-corrosive, not heat sensitive (in the temperature range of 50 to 70°C) and easily available. Its physical properties are also reasonably well known. The sucrose granules were dissolved in hot water to make up the desired sugar solutions.

4.2.3 Reconstituted skim milk

Low heat skim milk powder, manufactured by the Tui Milk Products Company, was used to make up the reconstituted skim milk solutions. The reason for using reconstituted skim milk instead of fresh milk is that the seasonal and compositional variation of milk is avoided.

4.2.4 Chemicals used for Cleaning-in-place (CIP)

1) Caustic alkaline solution (AC-180): caustic soda, made up to a strength of 1%;
2) Acid solution (AC-300): nitric acid and phosphoric acid, made up to a strength of 1%;
3) High strength sanitiser: Klenz Iodophor, made up to a strength of 1.5%.

All these chemicals were supplied by Economics Laboratory, Hamilton, New Zealand.

4.3 Equipment

The equipment used in the experimental work is listed below:
(1) A Centritherm evaporator (CT1B-2, ALFA-LAVAL, Lund, Sweden)
(2) A falling film evaporator with rotating surface, specially built at the Department of Food Technology;
(3) A cone evaporator with 10° top half angle, specially built at the Department of food Technology;
(4) A temperature recorder (32 channel recorder/datalogger, MOLYTEK, Japan);
(5) A refractometer (ATAGO, No.25870, Japan);
(6) A drying oven (Clayson, Catalogue 011 24, Laboratory apparatus Ltd, Upper Hurt, New Zealand);
(7) Other instruments used include an analytical balance, a measuring cylinder and a stop watch.
(8) Brookfild viscometer was used for measurement of skim milk viscosity.

4.3.1 Centritherm evaporator

The whole apparatus of Centritherm evaporator is shown in Figure 4.1. Figure 4.2 shows the schematic diagram of the Centritherm evaporator system.

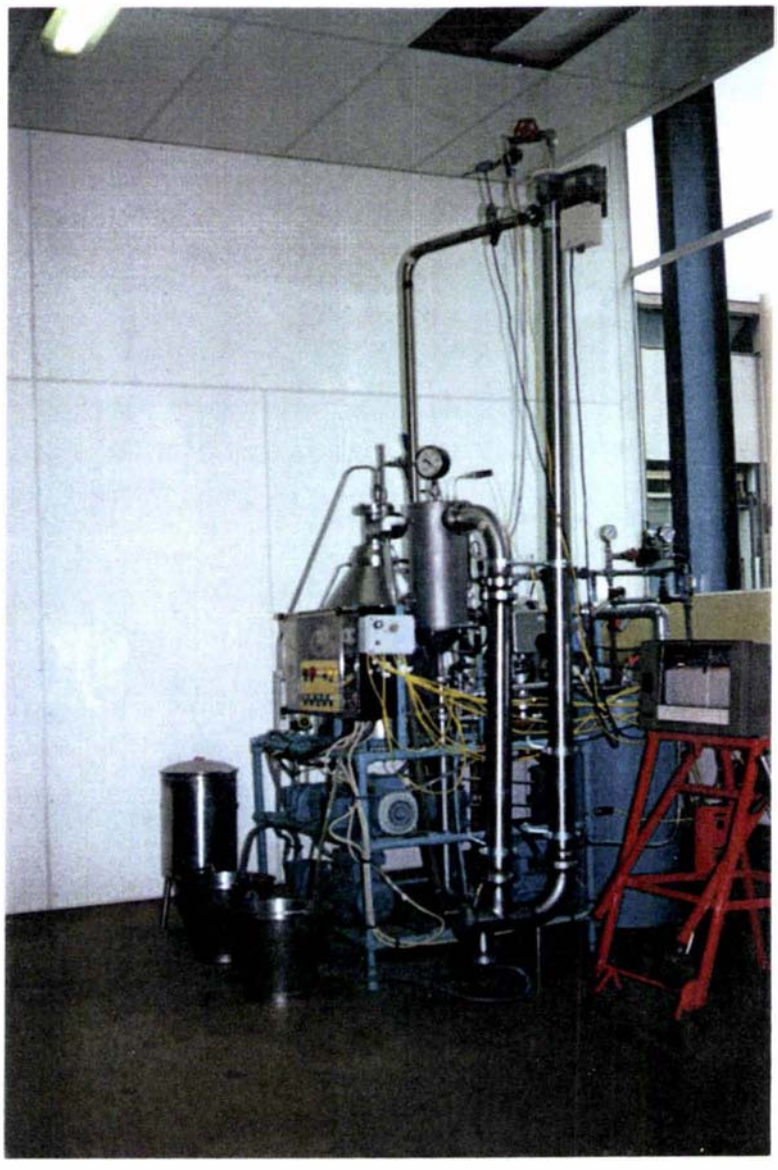

Figure 4.1 The whole apparatus of the Centritherm evaporator and the falling film evaporator with a rotating tube

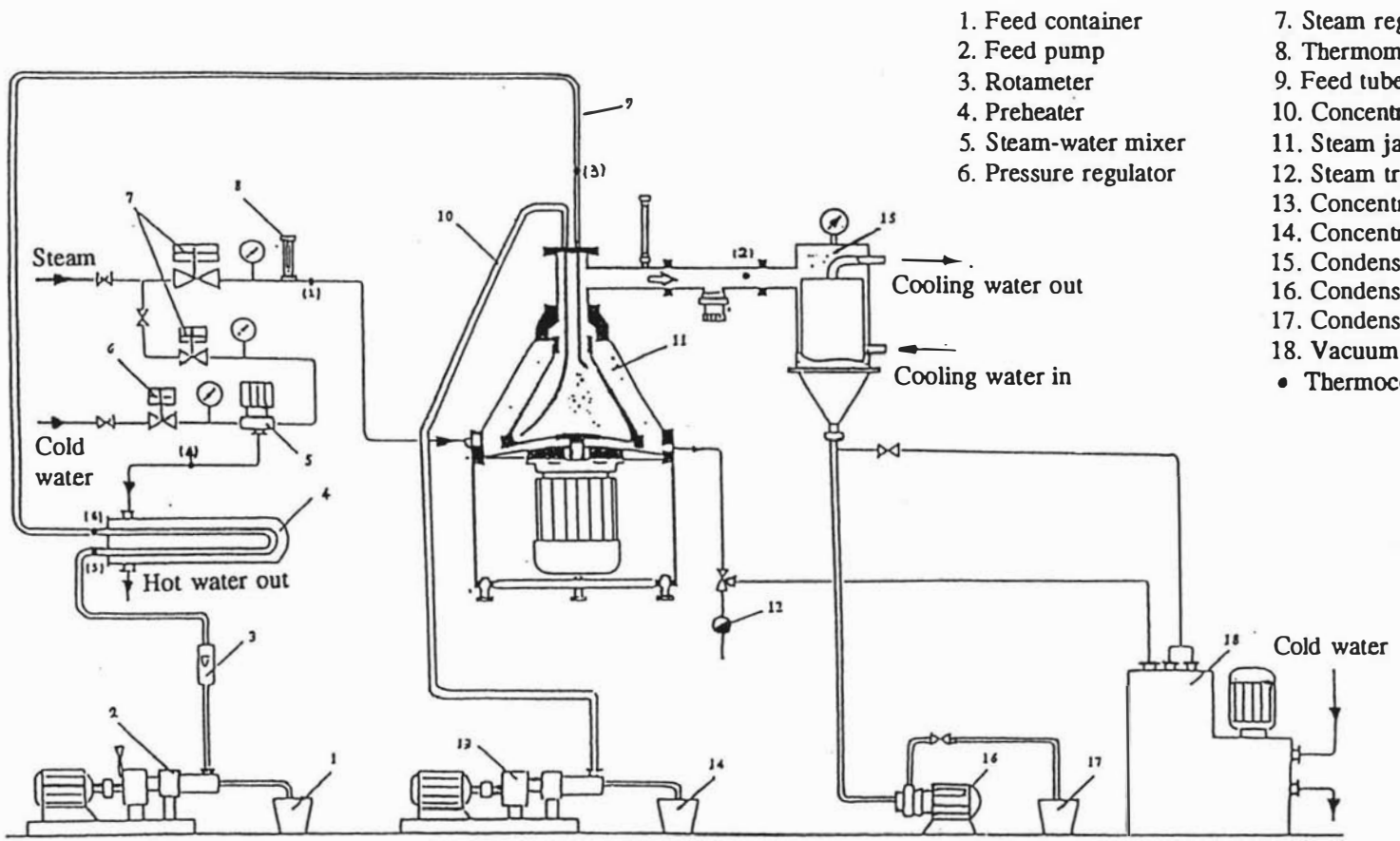

Figure 4.2 Schematic diagram of the Centritherm evaporator system

4.3.2 Single-tube falling film evaporator with rotating surface

A pilot scale single-tube falling film evaporator with rotating surface was linked to the Centritherm evaporator system. Thus, with the exception of the heating column, vapour chamber and temperature measurement system, all other parts of the apparatus were the same as those of Centritherm equipment, i.e. feed pump, concentrate pump, condensate pump, preheater, condenser, vacuum unit, and steam regulation system. Figure 4.3 shows the single-tube falling film evaporator with a rotating surface.

For this evaporator, the heating column contains a 32.00 mm O.D., 1.6 mm thick, 2 m length heating tube, which was coaxially placed inside a 73 mm I.D., 2 m length tube, forming a steam jacket between these two tubes. The total heating area (referring to outside surface) was 0.206 m^2. Because of the height of the pilot plant ceiling, the heating tube height of the falling film evaporator was limited to 2 m.

A 20 mm O.D., 0.75 m length tube (feed tube) was centrally inserted into the heating tube. The feed tube was fitted at the end with a distributor in which the gap between the tube and the plugger can be adjusted. The structure of the feed tube is shown in Figure 4.4.

A variable speed motor (LS80L-1, 0.75kW) was mounted on the top of evaporator. The heating tube was rotated through a driving chain.

Due to the rotation of the heating tube, the steam jacket required a bearing and a seal. After several trials, a stainless steel house which contained a seal was installed and a teflon strip of 0.7 mm thickness and 20 mm wide was used as a bearing.

A cyclone separator was mounted in the vapour chamber to separate liquid particles entrained in the vapour.

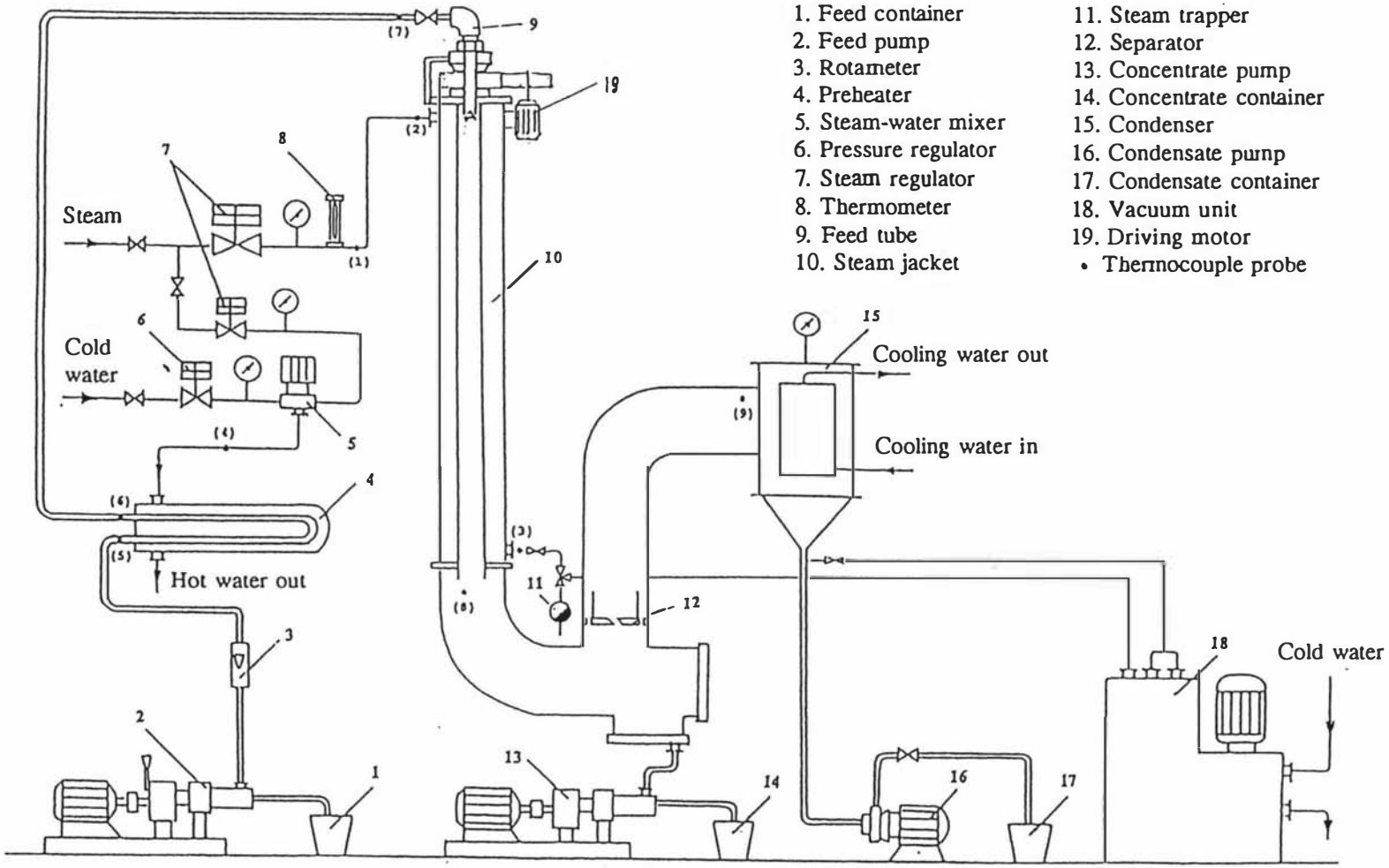

Figure 4.3 Schematic of the single-tube falling film evaporator with a rotating surface

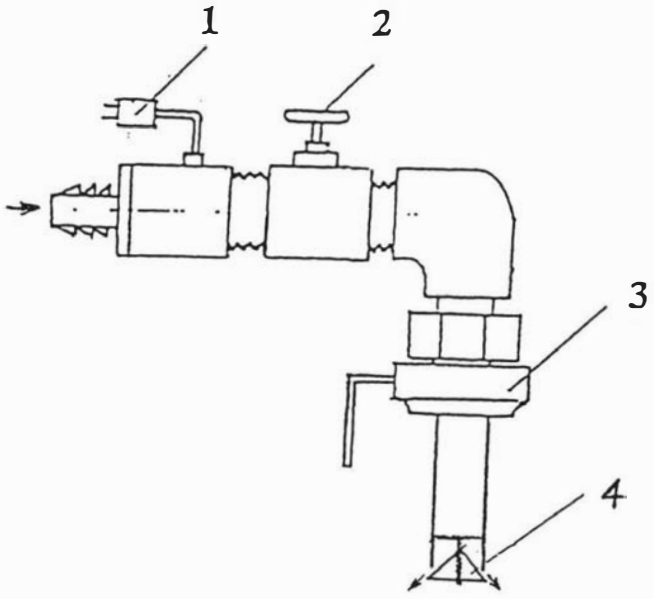

1. Thermocouple probe
2. Valve
3. Fixer
4. Adjustable distributor

Figure 4.4 Schematic diagram of the feed tube

4.3.3 Cone evaporator

The cone evaporator, made up of stainless steel, had a rotating cone with a 10° top half angle. The surface area for heat transfer in this evaporator was $0.1m^2$. The details of the dimensions of the cone evaporator are shown in Figure 4.5.

Similarly to the single tube falling film evaporator, the cone evaporator was also linked to the Centritherm evaporator system.

4.4 The evaporation process in thin film evaporators

The liquid to be evaporated was pumped by a variable speed feed pump (mono pump type 1) through a Spiraflo heat exchanger (Model TT 0.75/0.5-3), where the liquid was heated up by hot water to evaporating temperature, and then fed into the feed tube. After passing through the feed tube, the liquid flowed down the inside of the heating surface (cone or tube) as a thin evaporating film. The heat transfers from the inside of the heating surface to evaporate a portion of the liquid film. The unvaporized liquid and vapour flowed straight to the bottom of the vapour chamber where the unvaporized liquid (concentrate) was pumped out by a concentrate pump (mono pump type 1) and collected in a bucket. The vapour passed through a spiral plate condenser, where the vapour was condensed. The condensate was pumped out by a centrifugal pump (type GM) and was collected in a bucket for flow rate determination. Cold tap water flowing inside the spiral tubes of the condenser provided the heat sink for the condensation.

Steam was fed into the steam jacket. The heat flux, which was released by condensing steam outside of the heating cone or tube, was transferred to the liquid to be evaporated by conduction and convection. The steam condensate flowed down the outside of the heating cone or tube and was removed by means of an ejector into the vacuum unit located at the bottom of the steam jacket.

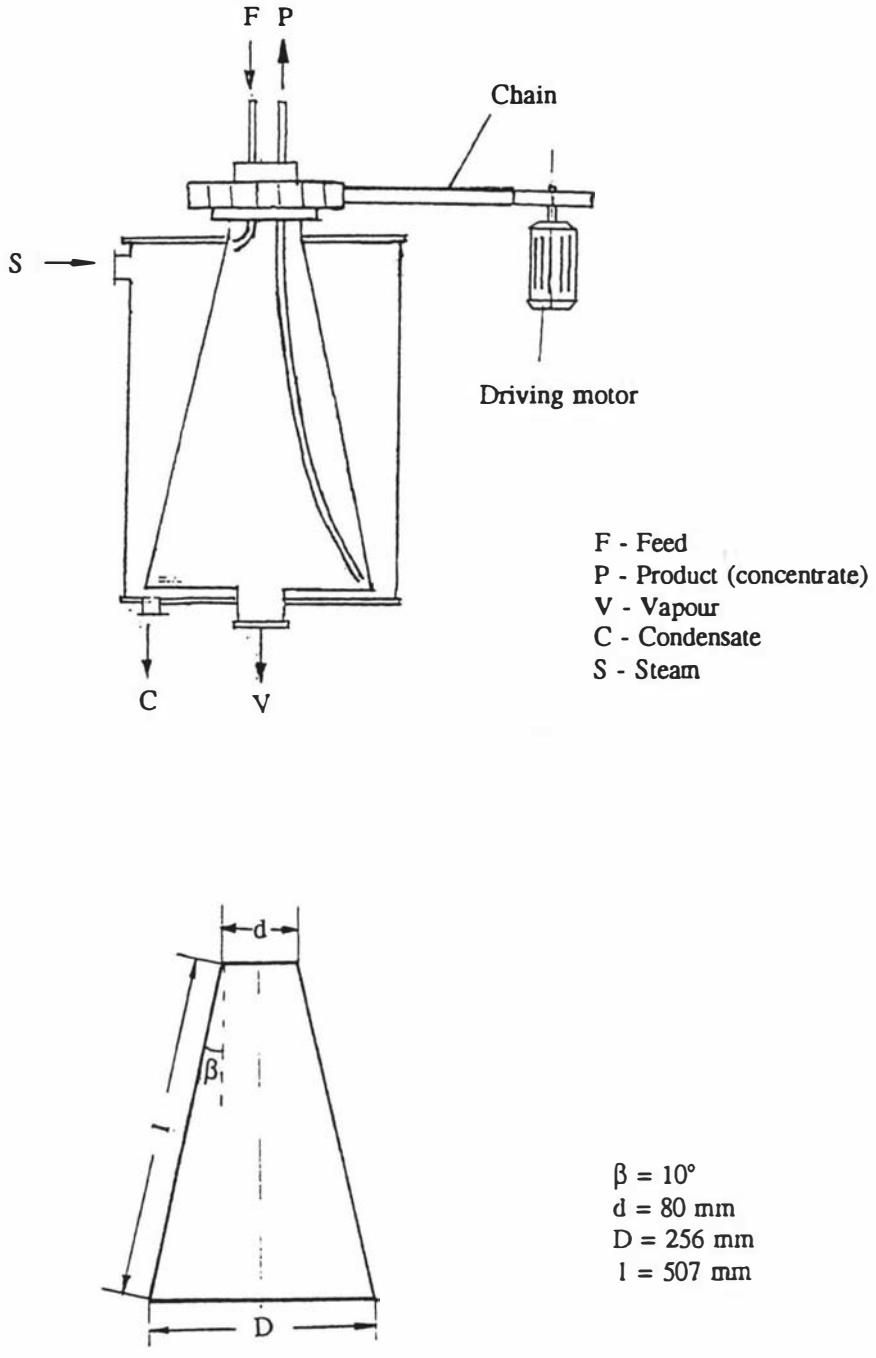

Figure 4.5 Schematic diagram of cone evaporator and the dimensions of the cone

The hot water used to heat up liquid in the Spiraflo heat exchanger was obtained by the use of a hot water mixer into which steam and cold tap water were fed. The pressures of steam and cold water were controlled by means of a steam regulator valve and a pressure regulator valve respectively.

Vacuum was provided by the Centritherm vacuum unit. This unit consists of a container for water, a circulation pump and three ejectors with built-in check valves. When the water was pumped by the circulation pump through the ejectors, a vacuum was created. One of the ejectors was used to remove steam condensate from the steam jacket. The other two were used to remove non-condensables from the evaporation side.

The vacuum was adjusted manually during operation, and released at the end of the operation, by means of a vent cock on the venting line.

The heating section and vapour stream tube lines were assembled with removable clamps and rubber gaskets. The liquid flow lines were made from transparent plastic hose. The system was carefully sealed and checked for air leakage during each run.

4.5 Instrumentation

4.5.1 Steam regulator

Steam pressure was controlled by means of a steam regulating valve (type SRV-5) with a temperature regulator. The adjustment of the steam regulating valve as well as the temperature regulator and more detailed information can be found in the ALFA-LAVAL Centritherm instruction book (1985).

4.5.2 Flowmeter

The inlet feed flow rate was measured by means of a stainless steel variable area rotameter with a capacity of 0.4-4.5 litres per minute of water at 20°C. The rotameter

was calibrated by discharge weight versus time measurements at the operating temperature.

4.5.3 Temperature measurement

Temperatures were measured by type J thermocouples (iron/constantan), which were connected to a recorder (32 channel recorder/datalogger, MOLYTEK). The thermocouple probes were monitored at nine different points, i.e. No. 1 measured the steam temperature after regulating; No. 2 measured the steam temperature entering the steam jacket; No. 3 measured the steam condensate temperature; No. 4 measured the hot water temperature. No. 5 and 6 measured the feed temperature at inlet and outlet preheater; No. 7 measured the feed temperature just before entering the feed tube; No. 8 measured the concentrate temperature; No. 9 measured the vapour temperature. All these measurement points are indicated in Figure 4.2. Before starting the experiments, all thermocouples were calibrated in a constant temperature bath at boiling and freezing points, and intermediate points against a standard mercury thermometer. The recorder plotted all measured temperature on a chart at 10 second intervals.

The thermocouples were calibrated in a water-ice mixture and in boiling water using an certified mercury-in glass thermometer.

4.5.4 Pressure measurement

A vacuum gauge was used to monitor vapour line. Two steam pressure gauges were used to monitor steam line pressure for the heating column and the water mixer respectively. A water pressure gauge was used to monitor water line pressure to the water mixer. The gauge positions are shown in Figure 4.2.

4.5.5 Rotating speed measurement

A digital tachometer (made in USA) was used to measure the rotating speed.

The details of using the tachometer can be found in its operation manual.

4.6 The variables and their ranges

The following variables were selected for this experimental work:

a) Overall temperature difference

b) Evaporating temperature

c) Rotating speed

d) Feed flow rate

e) Cone angle

After the apparatus was assembled, considerable time was taken to calibrate temperature measurements. Because temperature differences were used to calculate the heat transfer coefficient, the accurate measurement of temperature was a critical factor in the experimental setup.

After several runs to test the capacity of the evaporator system, ranges for the selected variables were chosen. These ranges are listed in Table 4.1.

Table 4.1. Ranges of experimental variables

Variable		Range
Flow rate	(m^3/s)	$6.67x10^{-6}$ - $6.67x10^{-5}$
Evaporating temperature	(°C)	40 - 70
Rotating speed	(rad/s)	0 - 210
Temperature difference	(K)	5 - 50
Feed liquid	(No.1)	Water
	(No.2)	Sugar solution (20 - 60%)
	(No.3)	Reconstituted skim milk (11%)

The ranges were suitable for all three evaporation systems utilised (Centritherm, rotating cone and rotating tube). To avoid excessive concentrate entrainment in the vapour in trials using skim milk, high temperature differences (greater than 30°C) were not used.

4.7 Operating procedure of thin film evaporator equipment

4.7.1 Starting

(1) Close all valves and set the feed tube at correct position;
(2) Turn on water to the condenser and the vacuum unit;
(3) Turn on the temperature recorder;
(4) Turn on the motor, which makes surface rotate;
(5) Start the vacuum pump;
(6) Check sealing of steam jacket and evaporating side (the pressure should be below -95 kPa);
(7) Start feed pump and check that the product enters the evaporator, adjust the feed flow rate to the desired value;
(8) Start concentrate pump and condensate pump, adjust the temperature of evaporating side through vacuum;
(9) Open drain valve and drain condensate from the steam supply line, close the drain valve;
(10) Open steam valve slowly, adjust steam pressure with the regulator until correct temperature is obtained;
(11) Open cold water valve to water mixer and then open the steam valve to it, adjust the hot water temperature to the desired value, which is the feed temperature just before entering the feed tube.

4.7.2 Cleaning

(1) Release vacuum in the evaporating side;
(2) Rinse the equipment with tap water;
(3) Recirculate 1% acid solution for 10 minutes;

(4) Rinse with tap water;

(5) Recirculate 1% alkali solution for 10 minutes;

(6) Rinse with tap water;

(7) If necessary, recirculate 1.5% sanitiser for 10 minutes.

4.7.3 Stopping

(1) Set the steam regulator to its minimum value;

(2) Close valves on the steam line and cold water line to the hot water mixer;

(3) Close steam supply valve;

(4) Release vacuum in the evaporating side;

(5) Stop vacuum pump and close supply vacuum valve;

(6) Stop feed and concentrate pumps;

(7) Stop condensate pump;

(8) Switched off motor;

(9) Close valve for cooling water to condenser and vacuum pump;

(10) Switch off the temperature recorder.

4.7.4 Operating cautions

(1) Never run the feed pump or the concentrate pump without liquid. If allowed to run dry for few seconds, the rubber stator in the pump will be destroyed;

(2) Maximum steam pressure before the steam regulating valve is 600 kPa, maximum steam pressure after the steam regulating valve is 200 kPa, corresponding to 120°C;

(3) The condenser should be supplied with enough cooling water to keep the outgoing water temperature 10°C below the evaporation temperature;

(4) Always keep an eye on temperature recorder during the experiment, because adjustment may be needed when desired temperature shifts due to fluctuation in steam and cold water pressures.

(5) Super heat was eliminated by cooling the outside of the steam line when super heat was present.

4.8 Experimental Procedure

In order to find the effect of individual variables on the heat transfer coefficients, only one parameter was varied during each run, while other parameters were kept constant.

A typical procedure was as follows:
(1) Start evaporator with water, and set steam temperature, evaporating temperature, feed flow rate, feed temperature and rotating speed at the desired values.
(2) After steady state was reached (about ten minutes), the feed was then switched to the solution to be used. The necessary adjustments were made to maintain the variables at desired values.
(3) The flow rate of vapour condensate was measured. Flow rates were calculated by using the values collected during a two minutes period at five minutes intervals during each test run. That means that the flow of condensate was diverted to an empty bucket and at the same time, time was recorded. After two minutes, the amount of condensate in the bucket was measured. For each run, three sets of measurements were usually made. If the error between the each measurement was greater than about 5%, further measurements were made.
(4) During the experiment, all temperatures were recorded on the temperature recorder. All data was recorded on a log sheet.
(5) After a test was completed, the feed was switched to water to flush out the remaining solution in the system, and then cleaning was done.

Initially, the feed temperature to evaporator was very difficult to control due to fluctuation of the pressure of cold water and steam in the water mixer (preheater). It became even more difficult to control when the feed temperature was very low before entering the preheater. Two pressure gauges and two pressure reducing valves were then installed on the cold water and steam lines respectively to monitor the feed temperature. The concentrate and the vapour condensate were fed back to feed tank after their weights were measured. This procedure kept the concentration of feed constant when running sugar solutions and reconstituted skim milk.

The feed temperature was kept ± 1°C around evaporating temperature during each run.

For falling film evaporator, the temperature difference between probes No.8 and No.9 was kept less than 0.5°C. When the temperature difference was greater than 0.5°C, which indicated that the concentrate might be accumulated at the bottom of the vapour chamber, adjustments were made.

A mass balance of the feed, concentrate and condensate was carried out at beginning of each run to check proper vapour condensation and accurate measurement.

4.9 Data processing

Based on the measured feed rate and vapour condensate flow rate, irrigation density as well as Reynolds number at the top and bottom of the heating tube were computed according to Equation 3-1.

The viscosity of sugar solution was computed according to the equation proposed by Campanella (1991).

The overall heat transfer coefficient (H_{exp}) was computed using vapour condensate flow rate and overall temperature difference (i.e. the temperature difference between probes No.3 and No.8 in the falling film evaporator and between No.2 and No.3 in the Centrithem evaporator) measurements. H_{exp} was calculated from the following formula:

$$H_{exp} = \frac{W_{exp}\, h_{fg}}{A\ \Delta T} \qquad (4\text{-}1)$$

Where: W_{exp} is vapour condensate flow rate (kg/s);

h_{fg} is the latent heat of vapour condensation, which is a function of the evaporating temperature (kJ/kg).

A Quattro Pro program, supplied by Honghton Mifflin Company (1993), was used for all data processing.

The raw experimental data and the results of calculations are given in Appendix I.

CHAPTER 5
DEVELOPMENT OF A THEORETICAL MODEL TO DETERMINE HEAT TRANSFER COEFFICIENTS ON ROTATING CONE SURFACES

5.1 Introduction

To gain a better understanding of the heat transfer through a liquid film on a rotating conical surface, it is necessary to develop a theoretical model for calculating the local liquid film thickness and liquid side heat transfer coefficient, as well as the overall heat transfer coefficient. In a rotating surface evaporator, the heating medium is usually steam, which is condensed on the outside surface of the rotating cone. The liquid to be concentrated is fed onto the inner surface. Steam condensation on the rotating surface has been studied intensively by Vasiliev and Khrolenok (1993). However, there are very few publications in the literature apart from Nikolaev *et al.* (1967) and Martynov (1984) dealing with the theoretical analysis of the liquid film flow on the inner surface of a rotating cone. Recently, Bouman and Waalewijn (1994a, b) presented a relationship of the liquid film thickness, the Reynolds number and the centrifugal acceleration on the rotating cone. The correlation was expressed as a Nusselt number function of the Reynolds number for concentrated whole milk.

5.2 Theory

5.2.1 Liquid film flow and energy analysis

A schematic of the system used in this study is shown in Figure 5.1.

As shown in the figure, a cone rotates about its vertical axis and the liquid is fed onto the inner surface. The co-ordinates used in the analysis are: x measures the distance

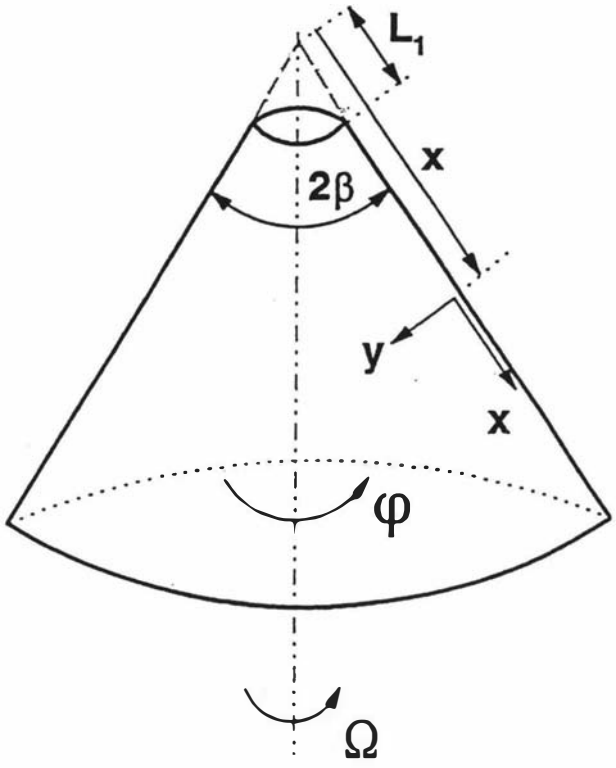

Figure 5.1 Schematic diagram of the system used in the theoretical analysis

along the cone surface from the apex; y measures the distance normal to the inner surface; and φ gives the angular position. The top angle of the cone is 2β. Under the action of gravity and centrifugal field, the liquid moves along the conical surface, in the x-direction, as a film.

The boundary-layer model for the conservation of mass, momentum and energy in the liquid film on the rotating cone can be written as (Schlichting, 1968):

Conservation of mass:

$$\frac{\partial U_x}{\partial x} + \frac{U_x}{x} + \frac{\partial U_y}{\partial y} = 0 \qquad (5\text{-}1)$$

x-momentum:

$$U_x \frac{\partial U_x}{\partial x} + U_y \frac{\partial U_x}{\partial y} - \frac{U_\varphi^2}{x} = \frac{\rho - \rho_v}{\rho} g \cos\beta + \nu \frac{\partial^2 U_x}{\partial y^2} \qquad (5\text{-}2)$$

φ-momentum:

$$U_x \frac{\partial U_\varphi}{\partial x} + \frac{U_x U_\varphi}{x} + U_y \frac{\partial U_\varphi}{\partial y} = \nu \frac{\partial^2 U_\varphi}{\partial y^2} \qquad (5\text{-}3)$$

Energy:

$$U_X \frac{\partial T}{\partial x} + U_y \frac{\partial T}{\partial y} = \alpha \frac{\partial^2 T}{\partial y^2} \qquad (5\text{-}4)$$

Similar equations were used by Chen *et al.* (1990) to solve the film flow of condensate in a rotating outer conical surface. These equations apply to axisymmetric conditions, which means that:

$$\frac{\partial U_x}{\partial \varphi} = 0, \qquad \frac{\partial U_\varphi}{\partial \varphi} = 0, \qquad \frac{\partial T}{\partial \varphi} = 0 \tag{5-5}$$

The y-momentum equation has not been included here since it only determines the pressure distribution along the film, and does not have influence on the heat-transfer calculation. To complete the statement of the problem, boundary conditions have to be imposed. They are:

$$at \quad y = 0, \qquad \left\{ \begin{array}{l} U_x = 0, \\ U_y = 0, \\ U_\varphi = r\Omega = (x \sin\beta)\,\Omega, \\ T = T_{ws} \end{array} \right\} \tag{5-6a}$$

$$at \quad y = \delta, \qquad \left\{ \begin{array}{l} \dfrac{\partial U_x}{\partial y} = 0, \quad \tau_{yx} = 0 \\ \dfrac{\partial U_\varphi}{\partial y} = 0, \quad \tau_{y\varphi} = 0 \\ T = T_{evp} \end{array} \right\} \tag{5-6b}$$

The boundary conditions at y = 0 assume that there is no liquid slip at the surface and the temperature of the liquid film is equal to the wall temperature. At the free surface of the liquid film y = δ, the boundary conditions assumption is that the effect of shear by the vapour inside the cone on the liquid film is negligible and the temperature of the film surface is equal to the evaporation temperature. Sparrow and Gregg (1959) demonstrated that for large Prandtl numbers these boundary conditions gave a good representation of the system. They also showed that for Prandtl numbers greater than one, a condition meet by most of the practical situations, energy transfer by convection is negligible.

Equations (5-2), (5-3) and (5-4) can be further simplified after deleting energy convection and assuming that:

$$\frac{U_\varphi^2}{x} >> U_x\frac{\partial U_x}{\partial x} + U_y\frac{\partial U_x}{\partial y} \tag{5-7}$$

Equation (5-7) can be obtained from the continuity equation (Eq (5-1)) and assuming that the secondary flow given by the velocity U_y is smaller than U^2_φ. To simplify equation (5-3), the boundary layer theory which considers that viscous effects are larger than fluid inertia inside the liquid film is assumed. Therefore, Equations (5-1) through (5-4) become:

$$\nu\frac{\partial^2 U_x}{\partial y^2} + \frac{\rho - \rho_v}{\rho} g\cos\beta + \frac{U_\varphi^2}{x} = 0 \tag{5-8}$$

$$\frac{\partial^2 U_\varphi}{\partial y^2} = 0 \tag{5-9}$$

$$\frac{\partial^2 T}{\partial y^2} = 0 \tag{5-10}$$

The boundary conditions become:

$$at \quad y = 0, \qquad \left\{ \begin{array}{l} U_x = 0, \\ U_\varphi = r_i\,\Omega = (x\sin\beta)\,\Omega, \\ T = T_{ws} \end{array} \right\} \tag{5-11a}$$

$$at \quad y = \delta, \qquad \left\{ \begin{array}{l} \dfrac{\partial U_x}{\partial y} = 0, \\ \dfrac{\partial U_\varphi}{\partial y} = 0, \\ T = T_{evp} \end{array} \right\} \tag{5-11b}$$

The solutions of Equations (5-9) and (5-10) associated with the boundary conditions (Eqs (5-11a,b)) are:

$$U_{\varphi} = r_i \Omega = (x \sin\beta)\ \Omega \tag{5-12}$$

$$T = T_{ws} - \frac{T_{ws} - T_{evp}}{\delta} y \tag{5-13}$$

Substitution of Equation (5-12) into Equation (5-8) yields the velocity distribution in the x direction, U_x:

$$U_x = \left(\frac{\rho - \rho_v}{\rho} \frac{g \cos\beta}{\nu} + \frac{x(\Omega \sin\beta)^2}{\nu} \right) \left(\delta y - \frac{y^2}{2} \right) \tag{5-14}$$

To obtain a dimensionless equation, dimensionless variables are introduced. Dimensionless distances, x^* and y^*, are as follows:

$$x^* = \frac{x}{L}, \qquad y^* = \frac{y}{L} \tag{5-15}$$

Whereas dimensionless velocity (U_x^*) and dimensionless film thickness (δ^*) are defined as follows:

$$U_x^* = \frac{U_x}{U_m}, \qquad \delta^* = \frac{\delta}{L} \tag{5-16}$$

The characteristic distance (L) and characteristic velocity (U_m) are defined as:

$$L = \left(\frac{\nu^2}{g\ \cos\beta}\right)^{\frac{1}{3}}, \qquad U_m = \frac{\nu}{L} \tag{5-17}$$

By substituting, Equation (5-14) becomes:

$$U_x^* = \left(\frac{\rho - \rho_v}{\rho} + R_o\, x^*\right)\left(\delta^* y^* - \frac{y^{*2}}{2}\right) \tag{5-18}$$

R_o represents the ratio between the centrifugal and the gravity forces, and it is defined as:

$$R_o = \frac{L(\Omega\ \sin\beta)^2}{g\cos\beta} \tag{5-19}$$

The liquid feed flow rate (Q_f) can be calculated as:

$$Q_f = \int_0^{\delta} 2\pi x \sin\beta\, U_x\, dy = 2\pi L^2 U_m \int_0^{\delta^*} U_x^*\, x^* \sin\beta\, dy^* \tag{5-20}$$

Substitution of Equation (5-18) into Equation (5-20) yields the dimensionless film thickness:

$$\delta^*(x^*) = \left\{\frac{3\ Q_f}{2\ \pi\ L^2\ U_m\ x^*\ \sin\beta\left(\frac{\rho - \rho_v}{\rho} + R_o\, x^*\right)}\right\}^{\frac{1}{3}} \tag{5-21}$$

By substituting Equations (5-15), (5-16), (5-17), (5-18) and (5-19) into equation (5-20) results in:

$$\delta(x) = \left\{ \frac{3\, Q_f\, \nu}{2\,\pi\, g\, x\, \sin\beta \cos\beta \left(\frac{\rho - \rho_v}{\rho} \right) + 2\,\pi\, x^2\, \Omega^2\, \sin^3\beta} \right\}^{\frac{1}{3}} \qquad (5\text{-}22)$$

5.2.2 Determination of the local heat transfer coefficient

The local heat flux to the liquid film can be calculated using the Fourier's Law:

$$q = - \left(k \frac{\partial T}{\partial y} \right)_{y=o} \qquad (5\text{-}23)$$

and the local liquid film heat transfer coefficient is defined as:

$$h_l = \frac{q}{T_{wl} - T_{evp}} \qquad (5\text{-}24)$$

Since the temperature profile across the liquid film is linear (Eq.5-13), the local heat transfer coefficient can be obtained from Equations (5-23) and (5-24) as:

$$h_l(x) = \frac{k}{\delta(x)} \qquad (5\text{-}25)$$

Substituting the film thickness given by equation (5-22) into equation (5-25) and integrating from the cone apex ($x=L_1$) to an arbitrary value of x, the local heat transfer coefficient can be calculated as:

$$h_l(x) = \frac{1}{x - L_1} \int_{L_1}^{x} \frac{k}{(3 Q_f \nu)^{\frac{1}{3}}} \left\{ 2\pi g x \sin\beta \cos\beta \left(\frac{\rho - \rho_v}{\rho} \right) + 2\pi x^2 \Omega^2 \sin^3\beta \right\}^{\frac{1}{3}} dx \quad (5\text{-}26)$$

5.2.3 Effect of liquid evaporation

During the evaporation process, the liquid film flow rate on the surface of the cone is reduced by the liquid vaporisation, which has to be taken into account. The evaporation rate from the inner surface of the cone can be written as follow:

$$W_{cal}(x) = \frac{1}{h_{fg}} \int_{L_1}^{x} h_l 2\pi x \sin\beta (T_{wl} - T_{evp}) dx \quad (5\text{-}27)$$

and the corrected local heat transfer coefficients ($h_l'(x)$) is calculated as:

$$h'_{cal}(x) = \frac{1}{x - L_1} \int_{L_1}^{x} \frac{k}{\left[3 (Q_f - W_{cal}) \nu \right]^{\frac{1}{3}}} \left\{ 2\pi g x \sin\beta \cos\beta \left(\frac{\rho - \rho_v}{\rho} \right) + 2\pi x^2 \Omega^2 \sin^3\beta \right\}^{\frac{1}{3}} dx \quad (5\text{-}28)$$

5.2.4 Overall heat transfer coefficient calculation

The overall heat transfer coefficients (H_{cal}) can be calculated considering the resistance to the heat flow of the steam condensate, the liquid film and the wall of the cone (thickness δ_w and thermal conductivity k_w):

$$H_{cal} = \frac{1}{\frac{1}{h_s} + \frac{2\delta_w}{k_w}\left(\frac{R_i + r_i}{2\delta_w} + 1\right)\ln\left(1 + \frac{2\delta_w}{R_i + r_i}\right) + \left(1 + \frac{2\delta_w}{R_i + r_i}\right)\frac{1}{h_l'}} \tag{5-29}$$

Where: h_s is the steam side heat transfer coefficient, which can be calculated using the Equation (5-30) proposed by Chen *et al.* (1991).

$$h_s = \frac{k}{L}\left(\frac{2}{3}\frac{Pr}{Ja}R_o\right)^{\frac{1}{4}} \tag{5-30}$$

Pr is the Prandtl number defined as:

$$Pr = \frac{C_p \mu}{k} \tag{5-31}$$

Ja is the Jacob number defined as:

$$Ja = \frac{C_p (T_s - T_{ws})}{h_{fg}'} \tag{5-32}$$

h'_{fg} is the effective latent heat defined as:

$$h_{fg}' = h_{fg}\left(1 + 0.68\frac{Cp\,(T_s - T_{ws})}{h_{fg}}\right) \tag{5-33}$$

Equation (5-30) is suitable for the rotating-dominated film condensation, which is applicable to thin film evaporators with rotating surfaces.

Calculations of surface areas on the rotating cone are given in Appendix II.

5.2.5 The relationship between rotational Nusselt number and Reynolds number

If $\rho >> \rho_v$, then $\rho-\rho_v/\rho \approx 1$, Equation (5-22) could be rewritten as:

$$\delta = \left(\frac{3 Q_f \nu}{2 \pi r g' + 2 \pi r a} \right)^{\frac{1}{3}} \tag{5-34}$$

Where: $r = x.\sin\beta$; $g' = g.\cos\beta$; $a = \Omega^2.r.\sin\beta$

If the Reynolds number is defined as $Re=4\Gamma/\mu$, where $\Gamma=Q_f\rho/2\pi r$, the equation can be rearranged as:

$$\delta = \left(\frac{3 \nu^2}{4 (g' + a)} \right)^{\frac{1}{3}} \left(\frac{4 \Gamma}{\mu} \right)^{\frac{1}{3}} \tag{5-35}$$

By substituting the Equation (5-25) into Equation (5-34), the following relationship can be derived:

$$\frac{k}{h_l} = \left(\frac{3\nu^2}{4(g' + a)} \right)^{\frac{1}{3}} Re^{\frac{1}{3}} \tag{5-36}$$

Therefore the relationship between a new defined rotational Nusselt number (Nu_{ro}) and the Reynolds number can be expressed as:

$$Nu_{ro} = \frac{h_l}{k} \left(\frac{\nu^2}{g' + a} \right)^{\frac{1}{3}} = 1.10 Re^{-\frac{1}{3}} \tag{5-37}$$

The above equation is a basic equation that can be used to predict local film heat transfer coefficients for rotating conical surface under laminar film flow and surface evaporation.

The liquid film Nusselt number (Nu) can be calculated using the dimensionless film thickness as follows:

$$Nu = \frac{h_l L}{k} = \frac{L}{\delta} = \frac{1}{\delta^*} \qquad (5\text{-}38)$$

5.3 Calculation procedure

To solve the equations given in the previous section, a numerical integration procedure was implemented in an applied mathematics software package (Mathcad 3.0, 1993). An iteration was started by assuming a initial value of wall temperature on the liquid side (T_{wl}) as the mean value of the steam condensing and the liquid evaporating temperatures, i.e. $T_{wl}=(T_s + T_{evp})/2$, and solving for the wall temperature on the steam side (T_{ws}), steam side heat transfer coefficient (h_s), liquid side heat transfer coefficient (h_l) as well as the overall heat transfer coefficient (H_{cal}) until convergence was finally obtained. A flow diagram for calculation is shown in Figure 5.2.

5.4 The determination of the physical properties of the liquids used

Three liquids were used in the experimental work: water, sugar solutions and skim milk. The physical properties of water are only a function of temperature and the physical properties of sugar solutions and reconstituted skim milk are mainly functions of the temperature and their concentrations. The correlations used for the theoretical calculation are given in the Appendix III.

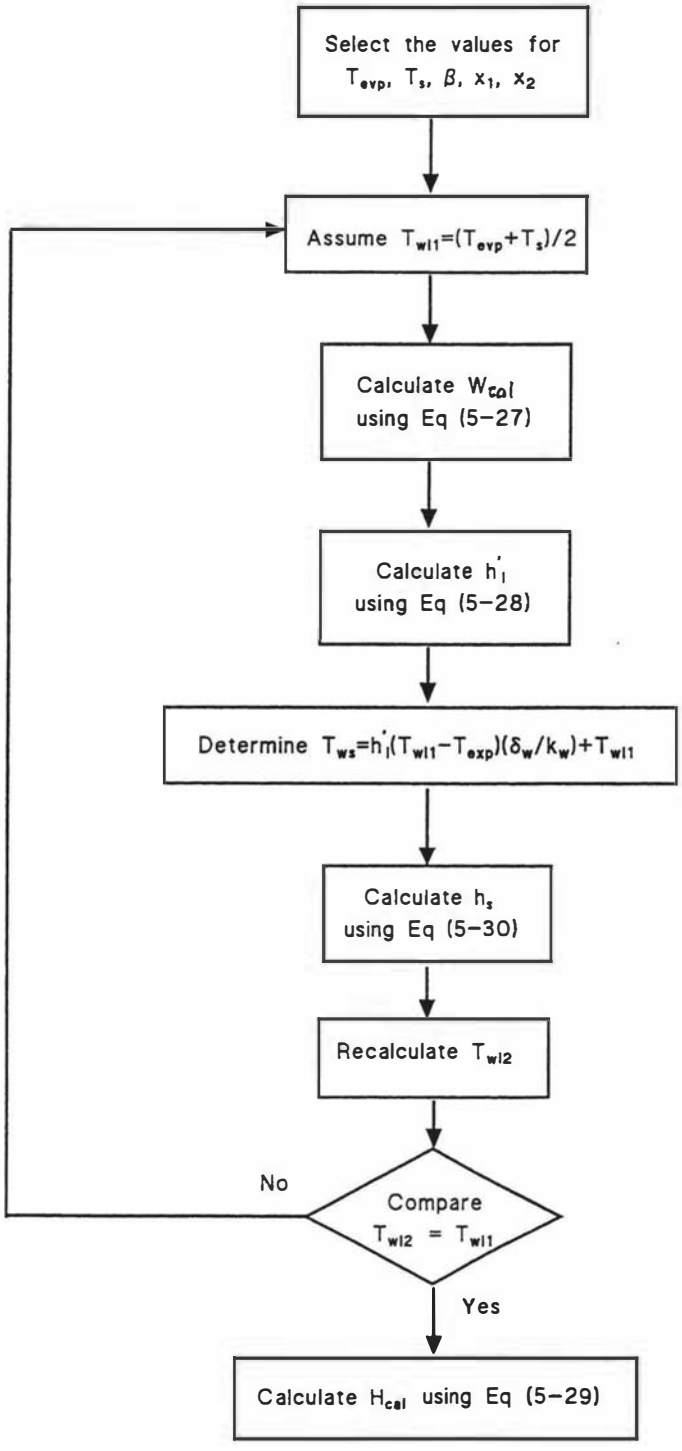

Figure 5.2 Flow diagram for the numerical calculation of the overall heat transfer coefficient

CHAPTER 6
HEAT TRANSFER IN FILM EVAPORATORS WITH ROTATING SURFACES - RESULTS AND DISCUSSION

6.1 Theoretical analysis results

The theoretical Equations (5-22) and (5-29), to predict the liquid film thickness and the heat transfer coefficient derived in the Chapter 5, show that the variables affecting the liquid film thickness and the overall heat transfer coefficient are: the feed flow rate, the cone rotating speed, the length of the cone, the cone angle, and the liquid viscosity.

To reveal the effect of these variables more clearly, the results obtained are presented graphically. The conditions used in the numerical calculations are those which are relevant to the Centritherm evaporator, i.e. rotating speed 157 rad/s, feed flow 5×10^{-5} m^3/s and evaporating temperature 70°C. Water was considered as the evaporating liquid for this part of the calculation. The results of the numerical calculations are given in the Appendix IV.

Figure 6.1 shows the local dimensionless film thickness for different cone angles. As the distance along the cone increases, the film thickness decreases due to the increase of the surface area, centrifugal acceleration and vaporisation. This figure also shows that the film thickness decreases with increasing cone angles. This is obviously a result of the increasing acceleration component in the direction along the cone surface.

Figure 6.2 shows the effect of feed flow rate on liquid film thickness. As the feed flow rate increases, the film thickness also increases. As depicted in the figure, this effect

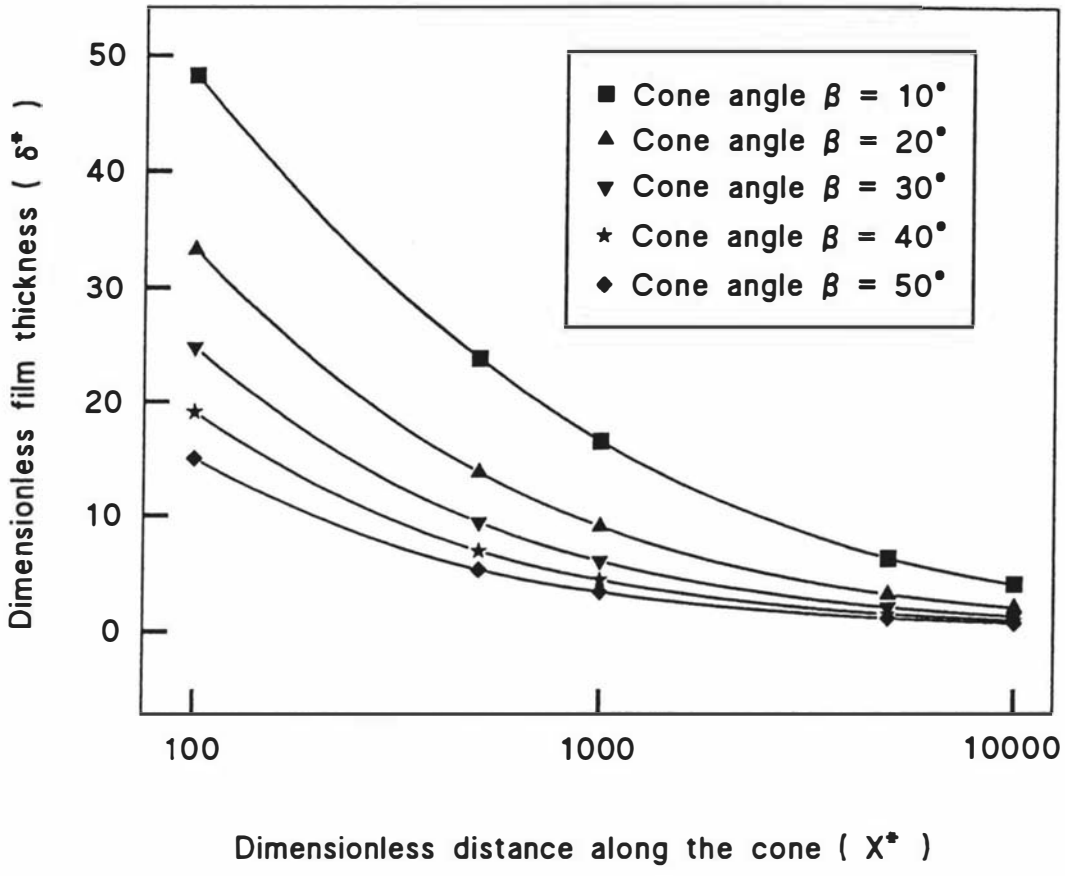

Figure 6.1 Dimensionless film thickness on a rotating cone at different cone angles. Rotating speed: 157 rad/s, feed flow: 5×10^{-5} m^3/s, water at 70°C.

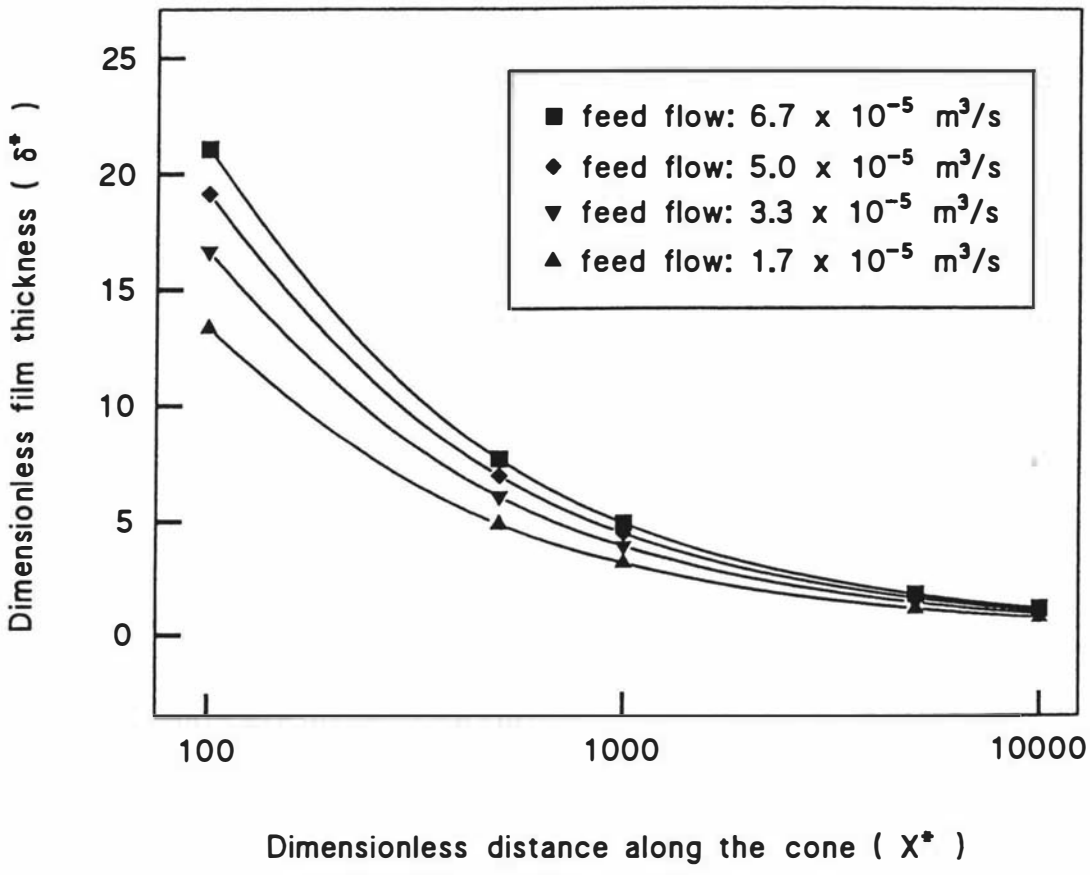

Figure 6.2 Dimensionless film thickness on a rotating cone at different feed flows. Rotating speed: 157 rad/s, cone angle: 40°, water at 70°C.

is more pronounced at the apex of the cone (lower values of x^*), whereas results appear to approximate to the same value towards the exit of the evaporator (large values of x^*).

Figure 6.3 shows the effect of rotation speed (defined by the rotation parameter R_o) on the dimensionless film thickness at a specific position (the middle of the conical surface). It clearly shows that the film thickness decreases with the increase of rotating speed. The figure also illustrates that this effect is reduced for higher cone angles.

The decreasing rate of dimensionless film thickness is bigger when rotation parameters are less than 0.01 than when rotation parameters are greater than 0.01. This implies that the effect of the gravity force becomes less important when the rotation parameter is bigger than 0.01.

Figure 6.4 shows the effect of rotating speed on the Nusselt number as a function of the cone angle. The Nusselt number increases as the rotating speed and cone angle increases.

The calculated local heat transfer coefficients as a function of the position for each of the heat resistances on the rotating cone (using conditions for the Centritherm evaporator) are shown in Figure 6.5. Conditions used in the calculation are rotating speed 157 rad/s, feed flow rate $5x10^{-5}$ m^3/s, evaporating temperature 70°C and temperature difference 10K. It can be seen that in the liquid side the heat transfer coefficient can vary from 12 to 23 kW/m^2K, which is due to the increase in the surface area and the evaporation of the liquid. While the steam side heat transfer coefficients are in the range 55-60 kW/m^2K. As a result the overall heat transfer coefficients increase slightly along the cone surface from the top to the bottom.

Figure 6.6 shows the calculated local surface temperature of the cone on both sides, the local liquid film thickness and the Reynolds number on the inner surface of the rotating cone with the same conditions as that used in the Figure 6.5. It can be seen that when steam temperature is 80°C and evaporating temperature is 70°C, the surface temperature

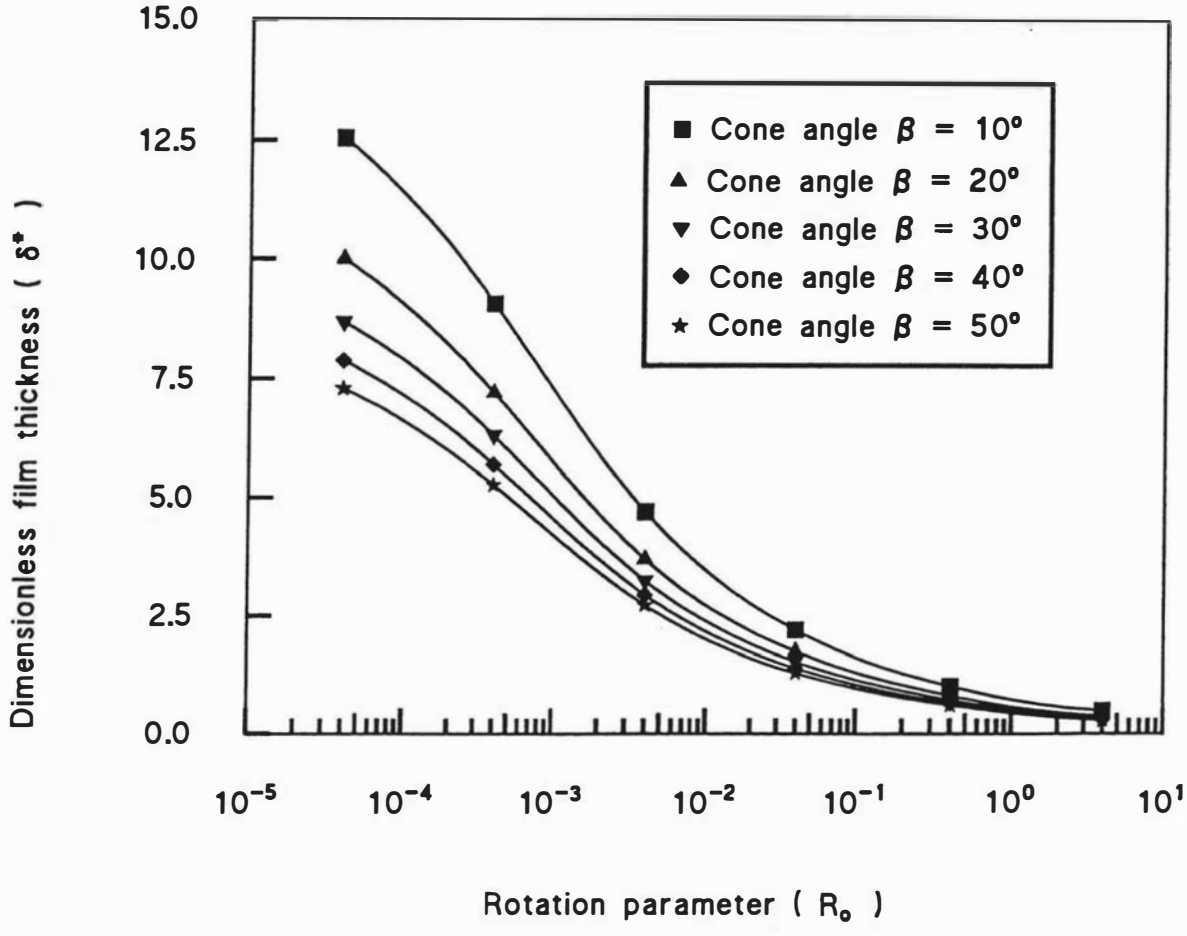

Figure 6.3 Dimensionless film thickness versus rotation parameter at different cone angles. Feed flow: 5×10^{-5} m^3/s, dimensionless distance (X^*): 5.57×10^3, water at 70°C.

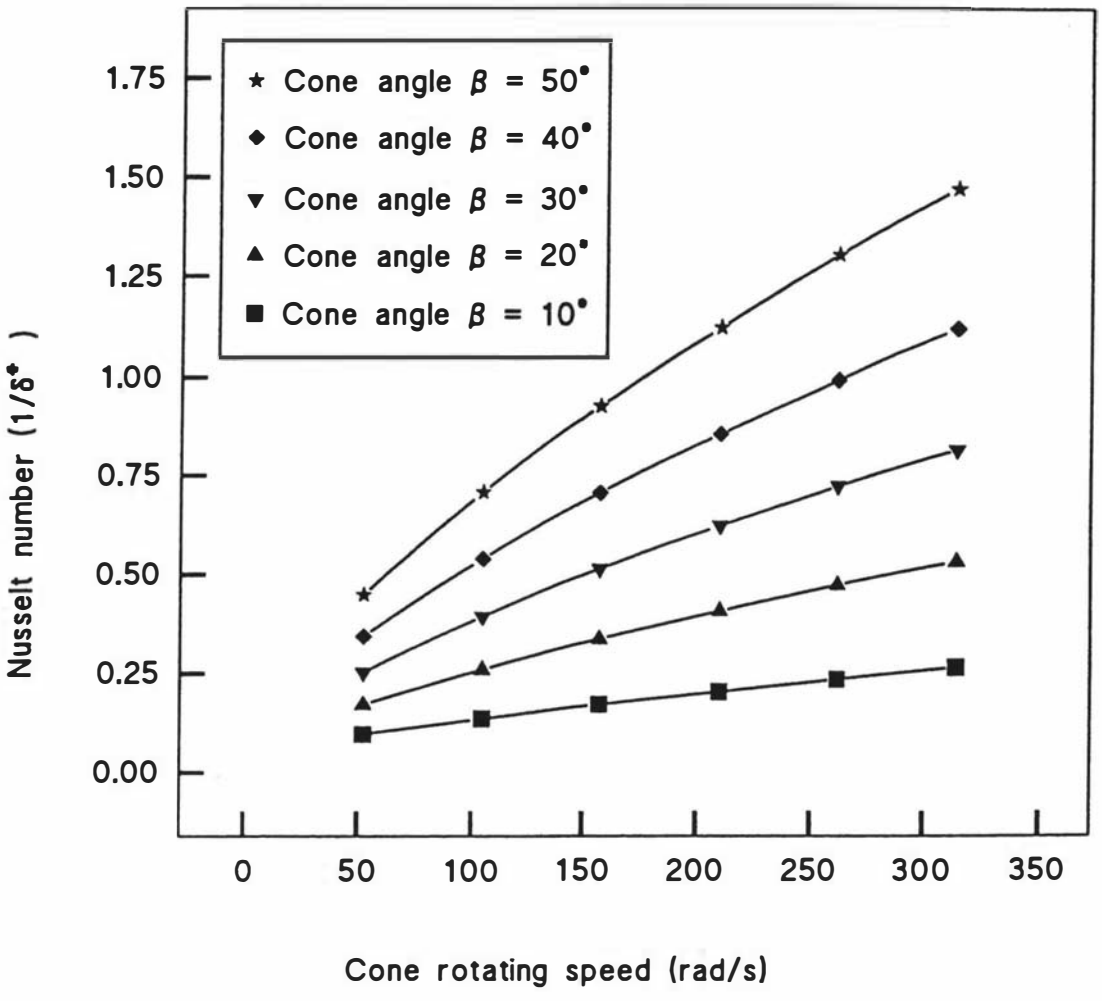

Figure 6.4 Effect of rotating speed on the Nusselt number at different cone angles. Feed flow: 5×10^{-5} m^3/s, water at 70°C, position given by $X^*=5.53 \times 10^3$ (X=0.155m).

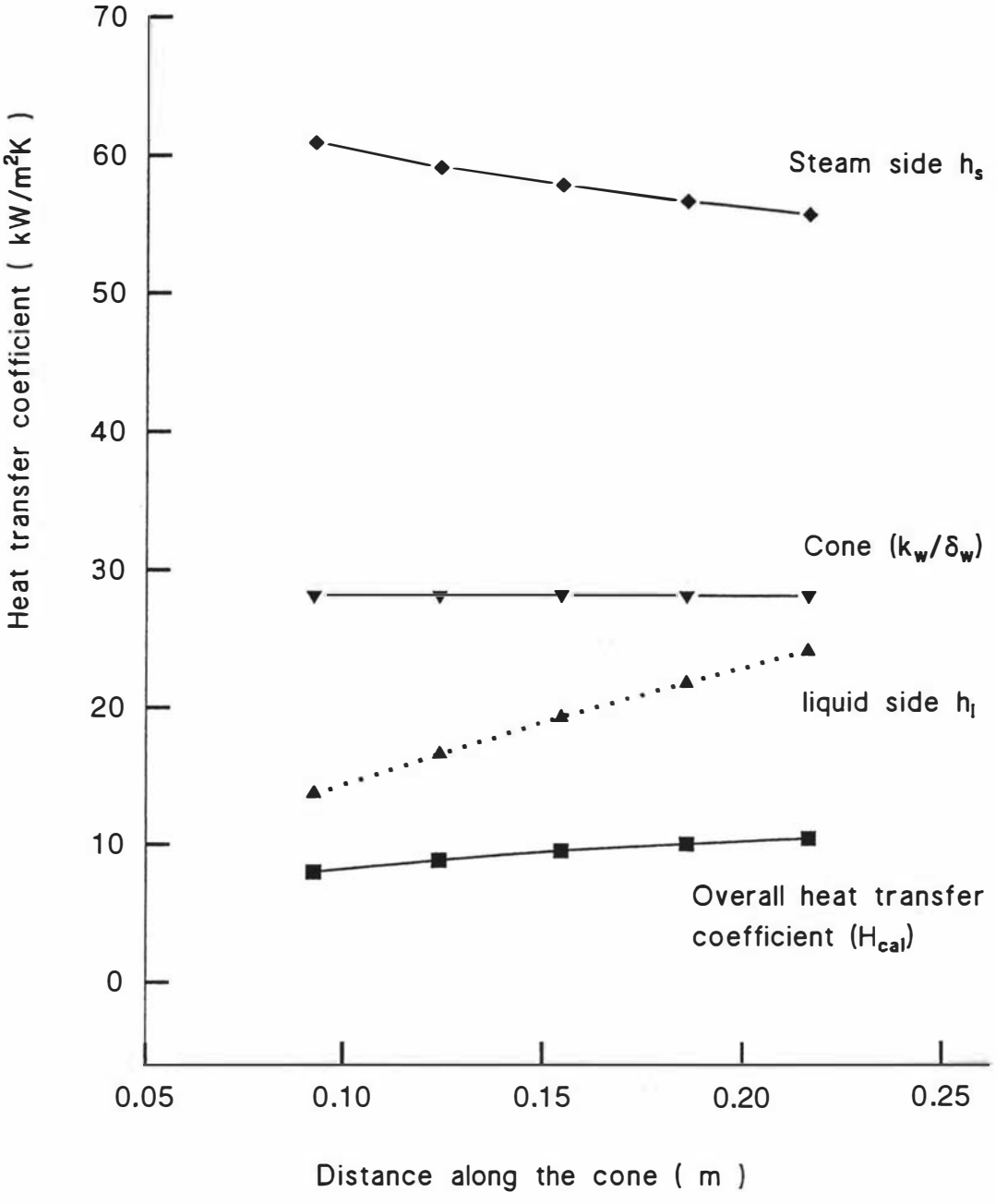

Figure 6.5 Calculated heat transfer coefficients on the rotating cone in the Centritherm evaporator. Rotating speed: 157 rad/s, feed flow: 5×10^{-5} m^3/s, evaporating temperature: 70°C, temperature difference: 10K, evaporating liquid: water.

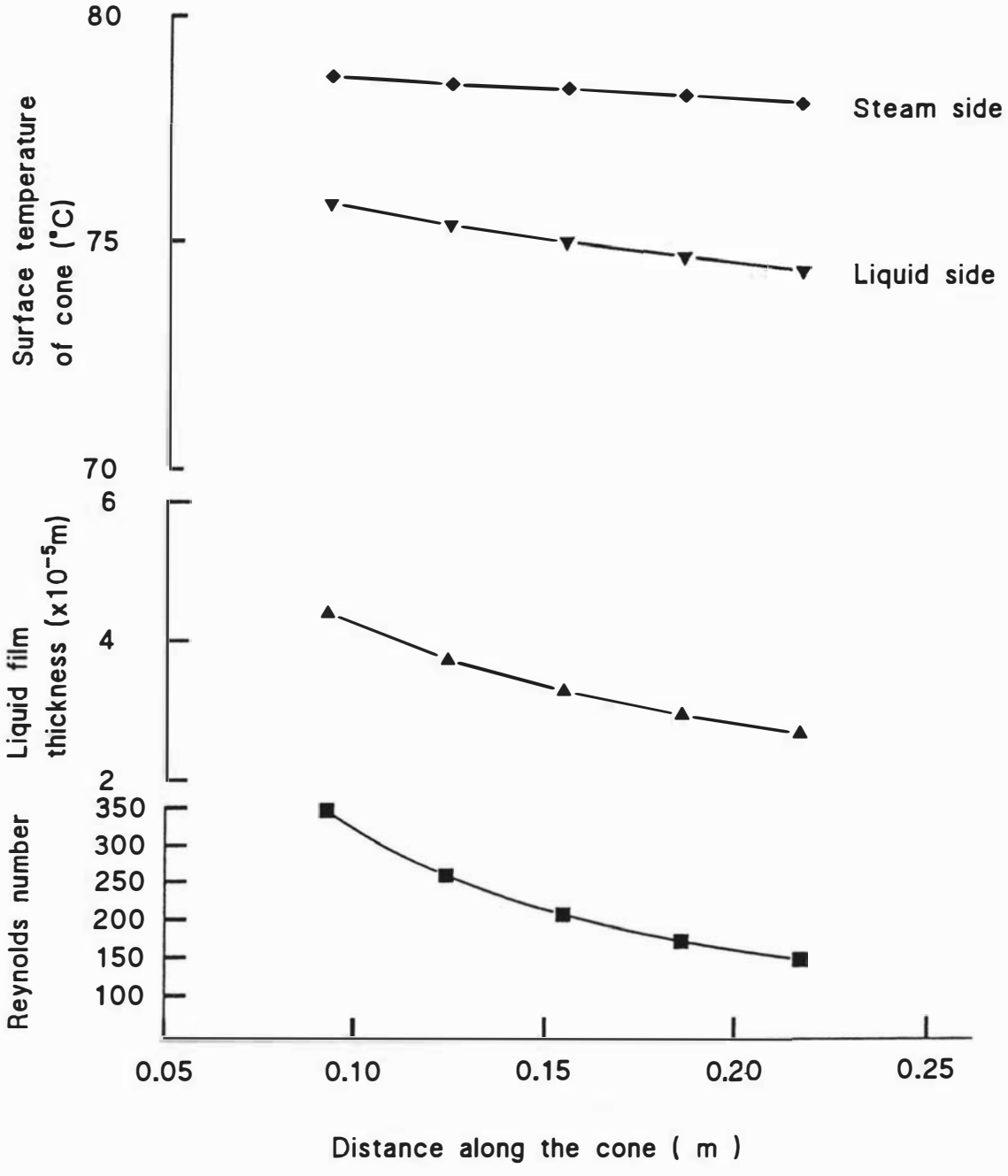

Figure 6.6 Calculated local surface temperatures, liquid film thickness and Reynolds number along the cone. Conditions used in the calculations were those of the Centritherm evaporator. Rotating speed: 186 rad/s, evaporating temperature: 70°C, temperature difference: 10K, feed flow: 5×10^{-5} m^3/s, evaporating liquid: water.

varies between 78.7 to 75.1°C on the steam side and between 75.8 to 74.4°C on the liquid side. The liquid film thickness is in the range of 0.025-0.044 mm. These results are in the same order of magnitude to the values (0.04-0.08 mm) reported by Hallström (1977) for water. Reynolds numbers for the inner surface liquid film are in the range of 150 to 350.

6.2 Experimental results and their comparison with those theoretically calculated with the model

Measured overall heat transfer coefficients were calculated as indicated in Chapter 4 (section 4.9). The uncertainty of the overall heat transfer coefficients calculated from these measured variables was determined to be 0.55 kW/m^2K. Therefore, the 95% confident interval of the measured heat transfer coefficients is around ±10% (an example of calculations is given in the Appendix V). By this reason, the error bar was not included in the figures.

Figure 6.7 shows typical recorded curves of steam temperature, evaporating temperature and feed temperature during an experimental run, which indicates the accuracy of the temperatures monitored.

An attempt was made to measure the surface temperature of the rotating surface by using a thermocouple, but it was not successful due to the heat generated by friction between the thermocouple and the rotating surface. Therefore, it was not practical in the setup used to measure the surface temperature of the rotating surface, and only overall heat transfer coefficients were calculated. The condensing side heat transfer coefficients were calculated using equation (5-28) and the values were in the order of 60 kW/m^2K under the conditions of this experiment (as shown in the Figure 6.5). These coefficients are considerable higher than the film coefficients on the evaporating side. Although the heat transfer resistance of the cone itself was calculated to be in the

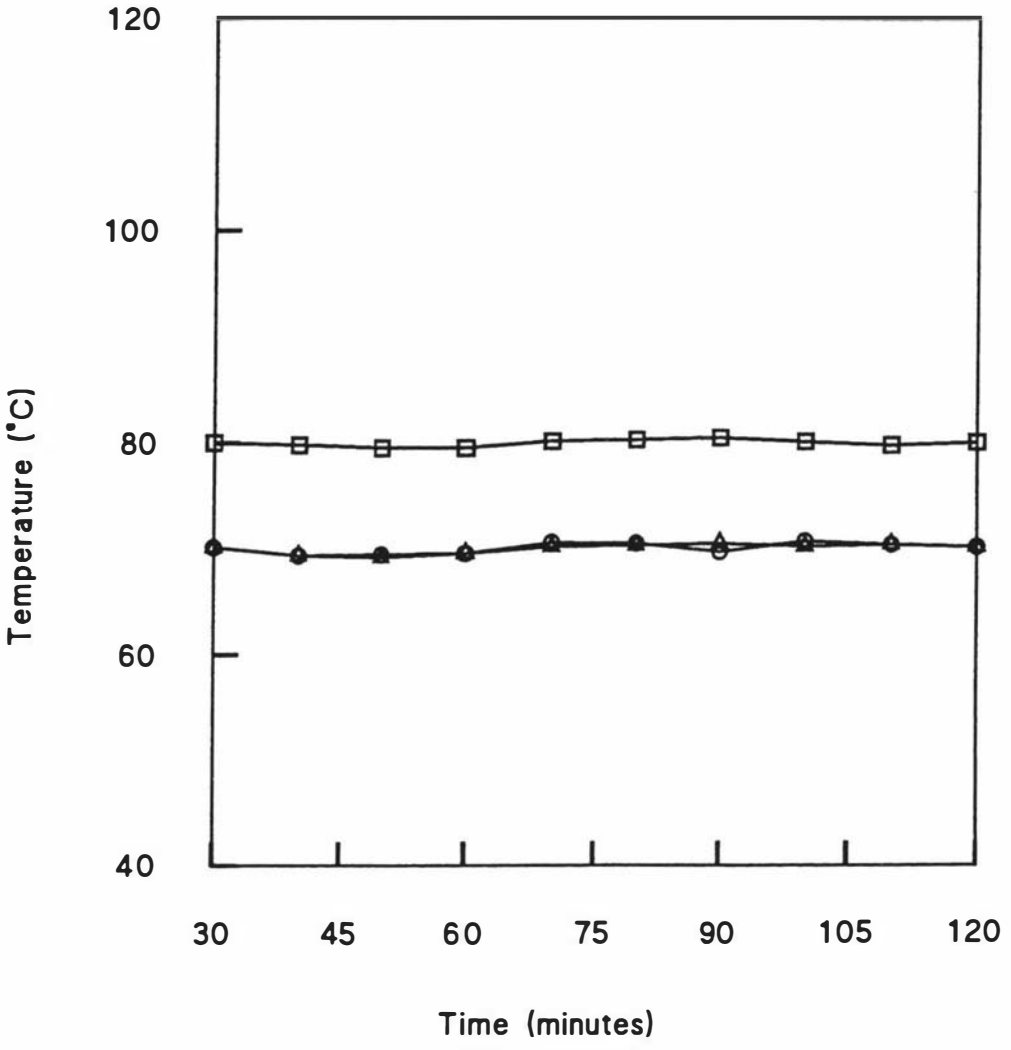

Figure 6.7 Recorded temperatures during an experimental run in the Centritherm evaporator.

□ Steam condensing temperature

△ Liquid evaporating temperature

○ Feed temperature

similar order of magnitude as the liquid film resistance, the evaporating liquid film is still the major controlling factor during the heat transfer process.

Experimental results obtained with the Centritherm, the cone evaporator and the single tube falling film evaporator with rotating surface are presented in the following sub-sections.

6.2.1 Centritherm evaporator

Experiments carried out using the Centritherm evaporator with water, a 20% sugar solution and skim milk are presented in this section.

A 4^2 factorial experiment with water was first conducted to get a basic understanding of the effects of selected variables, namely temperature difference between the steam condensing temperature and the liquid evaporating temperature, rotating speed, feed flow rate and liquid evaporating temperature. The following correlation was obtained using a multivariate analysis of the experimental data in the spreadsheet Quattro Pro:

$$H_{exp} = 0.289 + 0.055\Delta T + 0.18\,\Omega + 0.1\,T_{evp} + 0.055\,Q_f \qquad (6\text{-}1)$$

(R^2 = 86.4%, df=49)

where: ΔT is the temperature difference between the steam condensing temperature and the liquid evaporating temperature (K)

Ω is the rotating speed of the cone (rad/s)

T_{evp} is the evaporating temperature (°C)

Q_f is the feed flow rate (m^3/s)

(The t values for each variables are t_{Tevp}=15; $t_{\Delta T}$=7.75; t_{Ω}=5.15; t_{Qf}=0.025)

The results obtained show that the effects of temperature difference, evaporating temperature and rotating speed on the overall heat transfer coefficient were significant,

while the feed flow was less significant. The effect of each of these variables was investigated independently with the different liquids listed above.

6.2.1.1 Temperature difference

Figure 6.8 shows curves of measured overall heat transfer coefficient against the temperature difference between the steam condensing and the liquid evaporating temperatures for water, a 20% sugar solution and skim milk. Results obtained from the theoretical model were also plotted in the same graph. Solid lines indicate measured overall heat transfer coefficients, whereas dashed lines represent the theoretically calculated values, using Equation (5-29) under the same conditions of the experiment.

It can be observed that both measured and theoretical calculated values are close and the trend between measured curves is similar to that of the theoretical curves up to temperature differences of about 30K.

The dashed lines show that the calculated overall heat transfer coefficients increase slightly with the increase of the temperature difference. As the evaporation temperature was kept constant, an increase of temperature difference implies that the steam temperature and consequently the wall temperature of rotating cone is also increased. This affects the physical properties of the evaporating liquid and results in a slight increase of the overall heat transfer coefficient.

The solid lines show that the measured heat transfer coefficients increase with the increase of temperature difference until 30K and then decrease. This result suggests that an evaporation liquid-vapour interface may occur only at low temperature differences, and under that regime the heat transfer coefficient increases as the temperature difference increases. At constant feed flow, the increase in temperature difference causes more vapour to be produced, which in turn results in a reduction of the liquid film thickness and consequently an increase in coefficient of heat transfer.

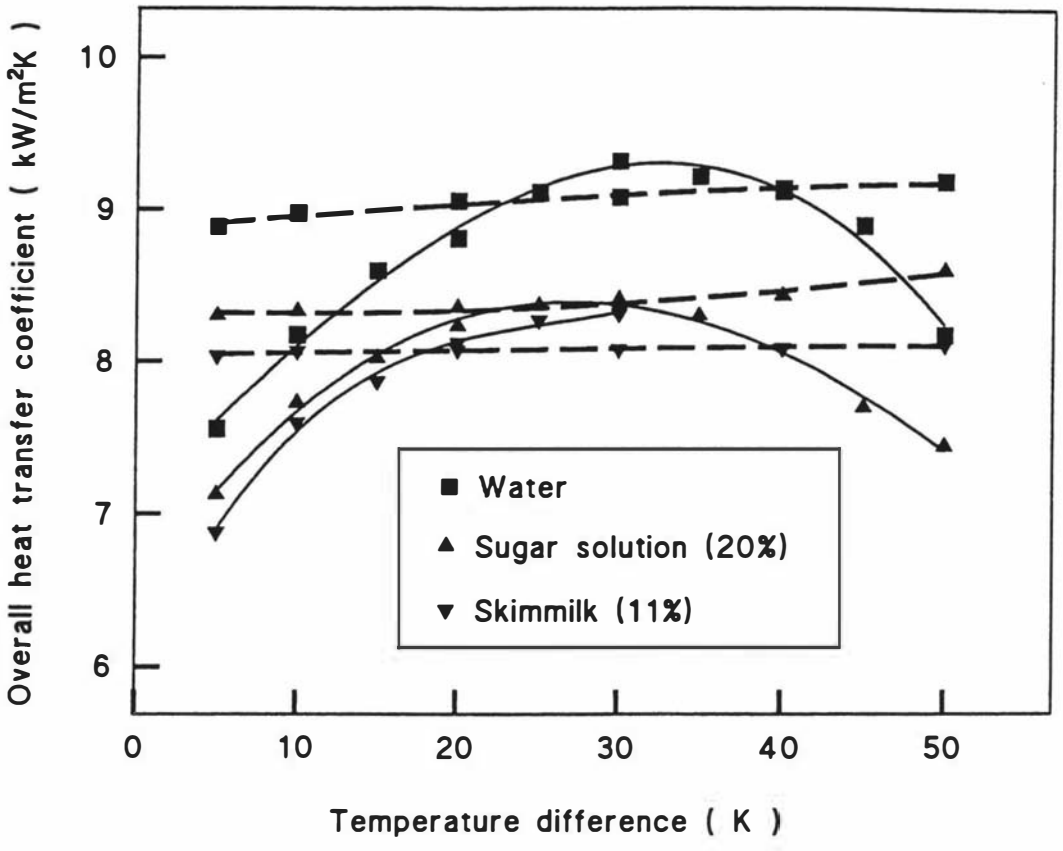

Figure 6.8 Effect of temperature difference on the overall heat transfer coefficient for water, 20% sugar solution and skimmilk in the Centritherm evaporator. Solid lines indicate experimental values while dashed lines indicate theoretical values. Evaporating temperature: 60°C, feed flow: 5×10^{-5} m^3/s, rotating speed: 186 rad/s.

Even though experimental and theoretical values appear to agree in some extent there is a degree of discrepancy between them. This discrepancy may be attributed to bubble formation in the evaporating liquid film. At low temperature differences, there may be incipient bubble formation and collapse. When bubble formation increases as a result of increasing temperature difference, bubbles tend to drag liquid with them and hence provide convection currents assisting the transfer of heat to the surface. However, the presence of bubbles could thicken the film and reduce heat transfer to the liquid-vapour interface. These two opposite effects result in that the heat transfer coefficients increases with the temperature difference between steam and liquid, but the rate of increase is reduced at higher temperature differences.

For water and sugar solution, it can be seen that the heat transfer coefficient decreases with further increase in temperature differences after 30K. This is probably because at high temperature differences, bubbles formation is very high and bubbles may start sticking to the surface and reducing the available surface. Hence the heat transfer decreases. Skim milk was not used when temperature differences were over 30K due to fouling of the surface.

6.2.1.2 Rotating speed

Figure 6.9 shows calculated (dashed lines) and experimental (solids lines) overall heat transfer coefficients as a function of the rotating speed in the Centritherm evaporator for water, a 20% sugar solution and skim milk. The increase of heat transfer coefficient with increases in the rotating speed is depicted in this figure. This indicates that the component of centrifuge force along the rotating surface plays a very important role in the heat transfer. As the rotating speed of the rotating surface increases, the centrifugal force is increased, then the speed of the liquid moving in the direction parallel to the surface will increase, and the film thickness will reduce, which results in a lower resistance to the heat transfer.

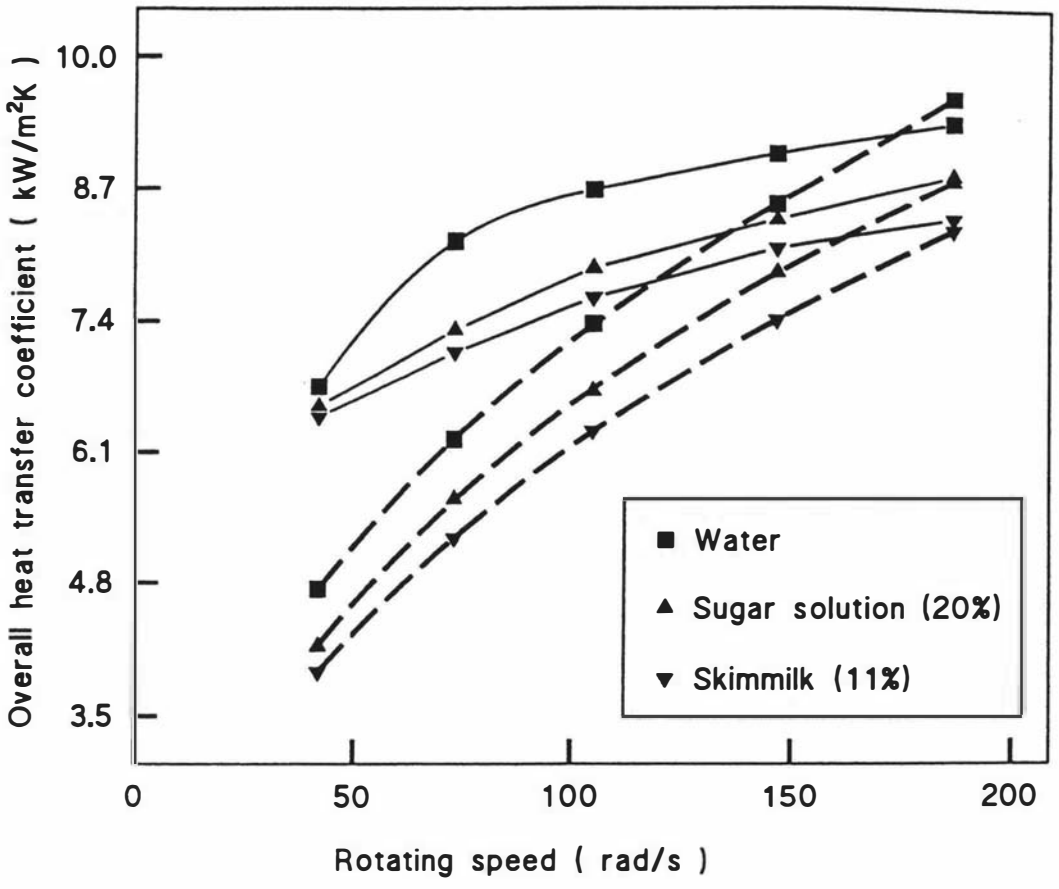

Figure 6.9 Effect of the cone rotating speed on the overall heat transfer coeficient for water, 20% sugar solution and skimmilk in the Centriterm evaporator. Solid lines are experimental values while dashed lines are theoretical values. Evaporating temperature: 70 °C, feed flow: 5×10^{-5} m^3/s, temperature difference: 10K.

Rotating the cone also beneficially influences heat transfer on the steam side. As steam is the heating medium, it condenses in the form of droplets (Mannheim and Passy, 1974) and is impelled from the surface. It can be deduced that the diameter of condensate droplets impelled from the rotating surface decrease as the speed of rotation rises. So the resistance to heat transfer lowers when the rotating speed is increased. It can be seen that both calculated and experimental overall heat transfer coefficients follow the same trend when the temperature difference is 10K. This means that for this temperature difference the heat transfer through the thin liquid film on the rotating surface is dominated mainly by the conduction and the main mechanism of evaporation is from the surface of the liquid film. If nucleate boiling contributed significantly to the mechanism of evaporation, there would be a change in the slope of curves in Figure 6.9, such as occurs in falling film evaporation (Chen and Jebson, 1992). Mälkki and Veldstra (1967) also stated that evaporation in the Centritherm evaporator takes place mainly from the liquid film surface.

Figure 6.9 shows there are some discrepancies between theoretical and experimental values at low rotating speeds. At low rotating speeds the film is comparatively thick. This encourages wavy laminar flow which increases the heat transfer. It was observed by Shinn (1971) that waves exist in the liquid film when it moves across the rotating conical surface. But when the speed increases the film thickness reduces the wave effect bringing the heat transfer coefficient closer to the theoretical value as observed in Figure 6.9.

6.2.1.3 Feed flow

Figure 6.10 shows the effect of feed flow rate on both experimental (solids line) and theoretical (dashed lines) overall heat transfer coefficients for water, 20% sugar solution and skim milk. Experimental results show a slightly increase in heat transfer coefficient with increasing feed flow rate. Two conflicting effects may be occurring in this experimental range. As the feed flow rate increases, the Reynolds number also

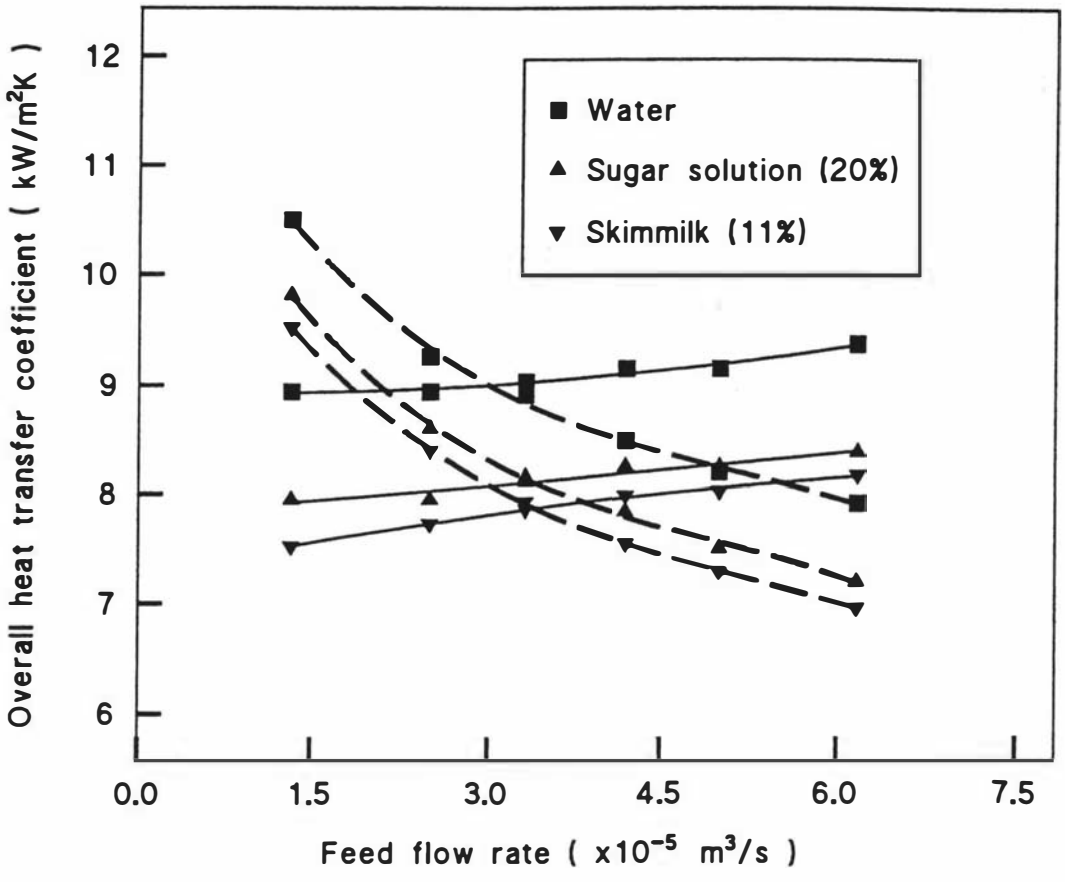

Figure 6.10 Effect of the feed flow rate on the overall heat transfer coefficient for water, 20% sugar solution and skimmilk in the Centritherm evaporator. Solid lines are experimental values while dashed lines are theoretical values. Evaporating temperature: 60°C, rotating speed: 146.6 rad/s, temperature difference: 10K.

increases, which would increase the wave motion and turbulence, hence, increasing the heat transfer coefficient. However, the increase of feed flow also increases the film thickness, decreasing the effect of liquid-vapour interface evaporation and lowering the heat transfer coefficient. The theoretical calculated values, which are based on the assumption of a laminar flow regime, illustrate the latter effect. Thus, the theoretical lines show a decrease in heat transfer with increasing flow rate. The combination of the above results shows that the heat transfer coefficient should increase slightly with increasing of feed flow. This result is in agreement with those obtained by Yanniotis and Kolokotsa (1996). They found that the feed flow rate had no significant influence on the heat transfer coefficient obtained from the heated surface of a rotating disc (feed flow in the range of 1.67×10^{-5} - 8.33×10^{-5} m^3/s, rotating speed in range of 21 - 63 rad/s).

Figure 6.11 shows the effect of the feed flow and the rotating speed on the heat transfer coefficient . The interaction between feed flow and rotating speed on the heat transfer coefficient was not significant under these conditions. By using the data of Figure 6.11, a regression equation was obtained:

$$\ln(9.77 - H_{exp}) = 1.252 - 0.002\Omega + 0.001\, Q_f - 1.24\, X\, 10^{-7}\, Q_f^2 \qquad (6\text{-}2)$$

$$(R^2 = 97.09\%, \text{ df}=9)$$

The results show that the feed flow has a slight effect of the feed flow on the heat transfer coefficient. It also appears that it is more important at low rotating speeds and high feed flow rates.

However, at some extreme conditions, it looks as there is an interaction between the rotating speed, feed flow and temperature difference. Figure 6.12 shows, for water, that the heat transfer coefficient increases with decreasing feed flow below 1.67×10^{-5} m^3/s at a temperature difference of 10K and a rotating speed of 186 rad/s. The heat transfer coefficient, however, decreases with decreasing the feed flow below 3.34×10^{-5} m^3/s for temperature difference of 30K and a rotating speed of 42 rad/s. The explanation may

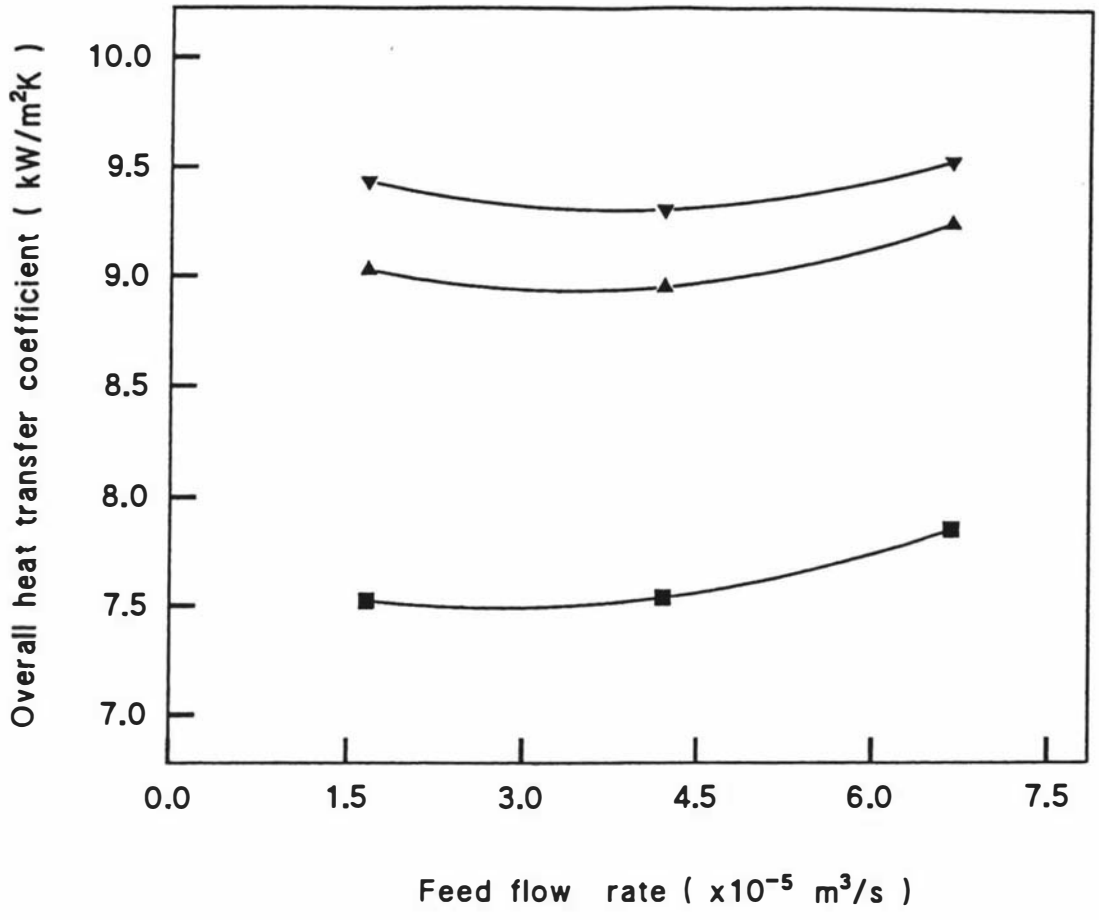

Figure 6.11 Effect of the feed flow rate and the rotational speed on the overall heat transfer coefficient for water in the Centritherm evaporator. Evaporating temperature: 70°C, temperature difference: 10K.

▼ Rotating speed 157 rad/s

▲ Rotating speed 105 rad/s

■ Rotating speed 52 rad/s

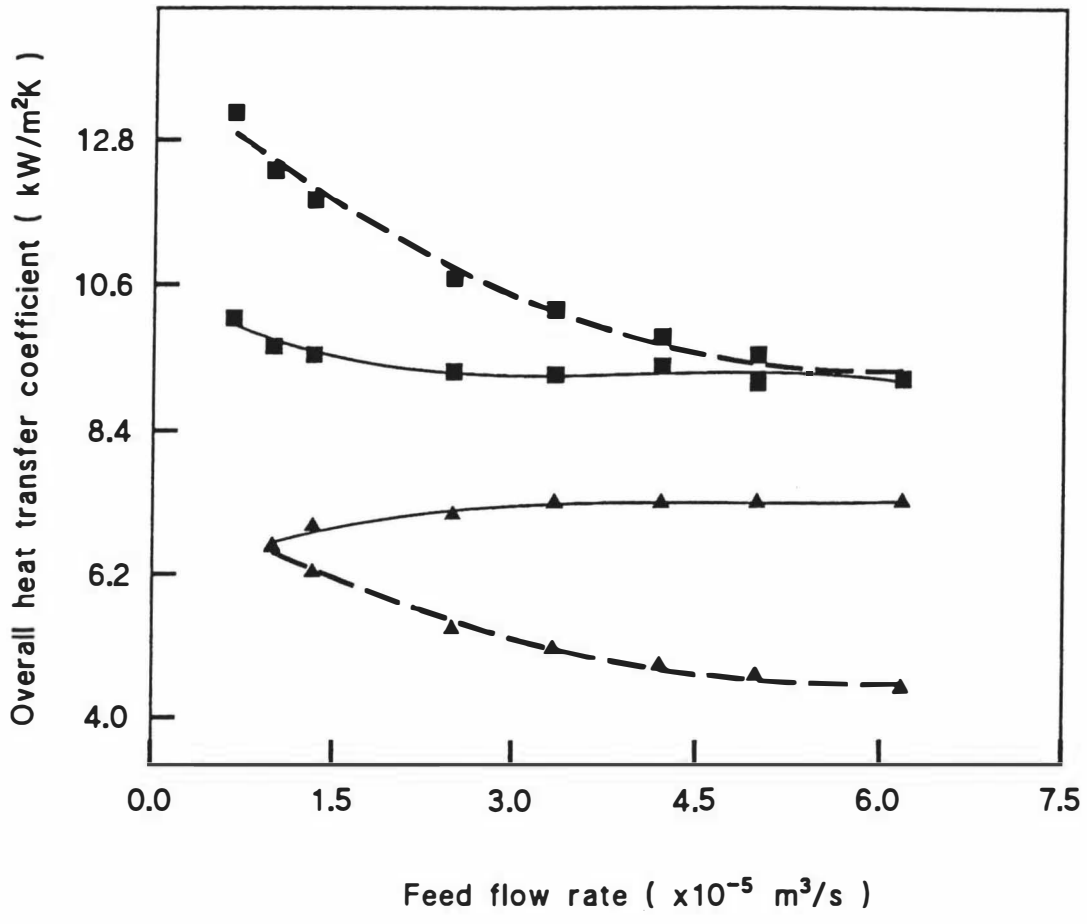

Figure 6.12 Effect of the feed flow rate on the overall heat transfer coefficient for water in the Centritherm evaporator. Solids lines are experimental values while dashed lines are theoretical values. Evaporating temperature: 70°C.

■ Temperature difference: 10K, Rotating speed: 186 rad/s

▲ Temperature difference: 30K, rotating speed: 42 rad/s

be that the reduction in feed flow at a low temperature difference and a high rotating speed causes a decrease in the film thickness, resulting in the increase of the heat transfer coefficient. This trend is also shown by the theoretical analysis. However, the reduction of feed flow at a high temperature difference and a low rotating speed may cause incomplete coverage of the liquid film on the rotating cone surface, which results in a decrease of the heat transfer coefficient. For the high temperature difference, the theoretical model does not predict the trend of the curve shown in Figure 6.12. The main reason could be attributed to a phenomena of natural convection which increases the heat transfer coefficient. Bubble formation at high temperature differences and low feed flow rates may also disturb the film coverage. At high temperature differences there would be much more bubble formation, to the extent that the measured heat transfer coefficients are actually higher than the theoretical ones.

6.2.1.4 Evaporating temperature

The effect of the evaporating temperature on the overall heat transfer coefficient for water, 20% sugar solution and skim milk is shown in Figure 6.13. It can be seen that both theoretical and experimental overall heat transfer coefficients increase as the evaporating temperature increases. At these experimental conditions, both experimental and theoretical values are within 12% agreement. However, the experimental values are lower than the theoretical values.

The effect of evaporating temperature is attributed to the changes in the liquids' physical properties (liquid viscosity and thermal conductivity) with temperature. The values of viscosity, thermal conductivity and Prandtl number at different temperatures for liquids studied in this research are given in Tables 6.1 - 6.3. It can be seen that as the evaporating temperature increases, the liquid viscosity decreases and the thermal conductivity slightly increases. The changes in these properties result in a thinner film with increased heat transfer conduction an therefore a higher heat transfer coefficient.

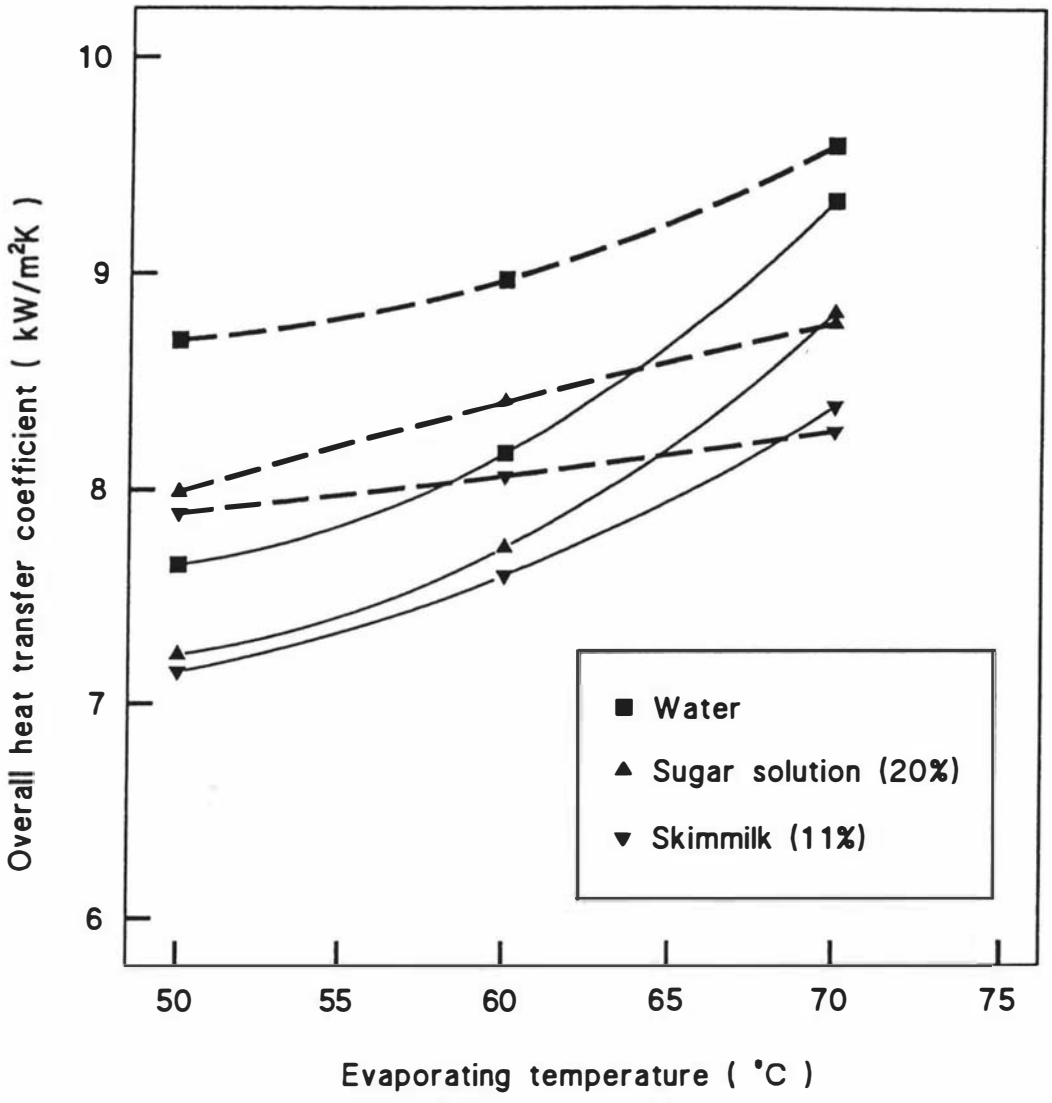

Figure 6.13 Effect of the evaporating temperature on the overall heat transfer coefficient in the Centritherm evaporator. Solid lines are experimental values while dashed lines are theoretical values. Rotating speed: 186 rad/s, feed flow: 5×10^{-5} m^3/s, temperature difference: 10K.

Table 6.1 Physical properties of water as a function of temperature (from Rogers and Mayhew, 1984)

Water	50°C	60°C	70°C
Viscosity (Pa.s)	$5.4x10^{-4}$	$4.6x10^{-4}$	$4.0x10^{-4}$
Thermal conductivity (W/m.K)	0.643	0.653	0.662
Prandtl number	3.9	3.0	2.5

Table 6.2 Physical properties of a 20% sugar solution as a function of temperature (from Campanella, 1991)

20% sugar solution	50°C	60°C	70°C
Viscosity (Pa.s)	$9.4x10^{-4}$	$7.8x10^{-4}$	$6.7x10^{-4}$
Thermal conductivity (W/m.K)	0.642	0.651	0.660
Prandtl number	6.1	5.0	4.2

Table 6.3 Physical properties of skim milk as a function of temperature (from Wood, 1982)

Skim milk (11%)	50°C	60°C	70°C
Viscosity (Pa.s)	$8.56x10^{-4}$	$7.8x10^{-4}$	$7.5x10^{-4}$
Thermal conductivity (W/m.K)	0.616	0.625	0.632
Prandtl number	5.8	5.2	5.0

6.2.1.5 Experiments of sugar solutions at different concentrations

Typical curves of overall heat transfer coefficient versus temperature difference for different concentrations of sugar solution are shown in Figure 6.14. Both experimental and theoretical values are reasonab ly close except for the highest concentration (60%TS) at low temperature differences (below 15K).

The evaporation mechanism in this experiment is likely to be a combination of film surface evaporation and bubble formation on the surface of the rotating cone. When the temperature difference increases, the heat transfer by conduction will increase, because thermal conductivity of the film increases slightly. At the same time, more bubbles are formed and present in the liquid film, which increases the film thickness, decreasing the rate of heat transfer to the liquid-vapour interface. In addition, the motion of bubbles through the liquid film encourage the turbulence and has a positive effect on heat transfer coefficient as mentioned on section 3.2.1.1. As a consequence of these effects, the overall heat transfer coefficient slightly increases with an increase of temperature difference.

The experimental values show that when the concentration rises to 60%, the heat transfer coefficient reduces significantly with decreasing temperature differences. The reason for this decreasing is not clear. In general, as the concentration of the solutions increases, the overall heat transfer coefficient reduce gradually. The heat transfer coefficients, however, are still around 5 kW/m^2K at concentrations of 60% when the temperature difference is greater than 15K.

Figure 6.15 shows the effect of concentration on the overall heat transfer coefficient when the evaporating temperature is 70°C, feed flow $5x10^{-5}$ m^3/s, temperature difference 10K and rotating speed 186 rad/s. It is clearly illustrated in this figure that when the concentration increases, the associated increase in film viscosity and thickness decreases the heat transfer coefficients. Both calculated and experiment overall heat transfer coefficients follow the same trend and are in reasonable agreement, which again

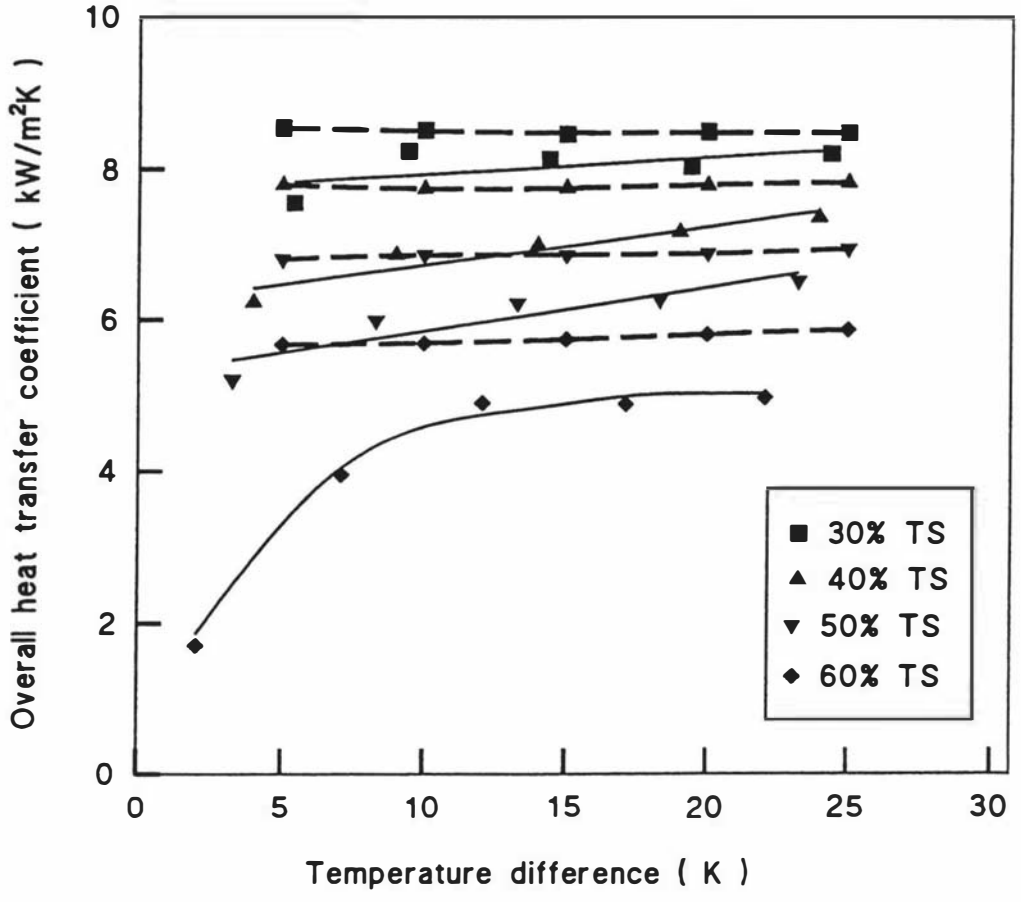

Figure 6.14 Effect of the temperature difference on the overall heat transfer coefficient for sugar solutions in the Centritherm evaporator. Solids lines are experimental values while dashed lines are theoretical values. Rotating speed: 186 rad/s, feed flow: 4.2×10^{-5} m^3/s, evaporating temperature: 70°C.

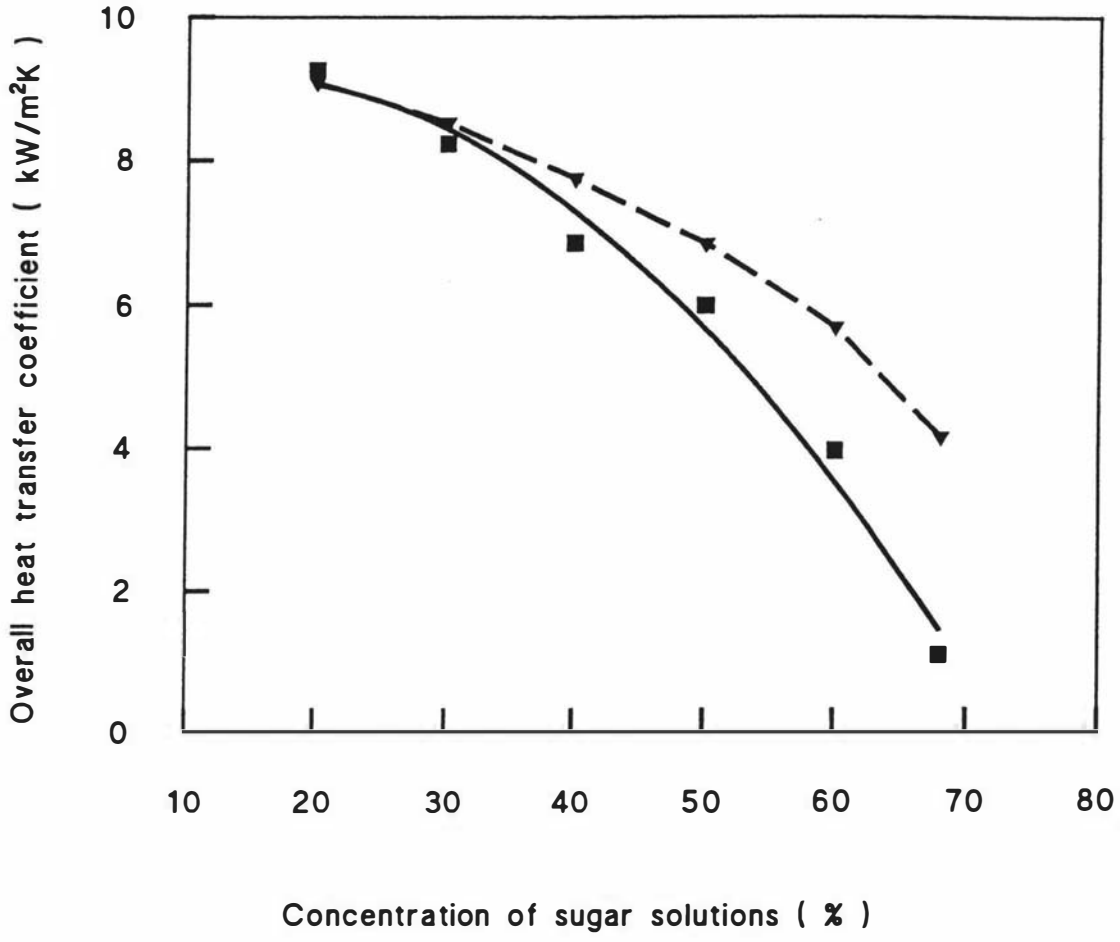

Figure 6.15 Effect of sugar concentration on the overall heat transfer coeficient in the Centritherm evaporator. Evaporating temperature: 70°C, temperature difference: 10K, feed flow: 4.2×10^{-5} m^3/s, rotating speed: 186 rad/s.

■ Experimental results (solid line)

▼ Theoretical results (dashed line)

indicates that the heat transfer through the thin liquid film on the rotating surface at low temperature differences occurs mainly by conduction and the main mechanism of evaporation is from the surface of the liquid film.

6.2.2 Cone evaporator

The cone evaporator was specially built to study the effect of the cone angle (formed by the rotating surface around the vertical axis) on the overall heat transfer coefficient. Only water was used in the experiments.

6.2.2.1 Temperature difference

Figure 6.16 shows the measured and calculated overall heat transfer coefficients versus the temperature difference in the cone evaporator. It is found that the temperature difference, in the range studied, does not affect these overall heat transfer coefficients. The experimental results follow a similar trend to the theoretical ones, but the heat transfer coefficients, however, are not in as a close agreement as those for the Centritherm evaporator.

6.2.2.2 Rotating speed

Figure 6.17 shows the effect of the rotating speed on the overall heat transfer coefficient as a function of the evaporation temperature. Both the theoretical and experimental curves follow the same trend. This again indicates that the component of centrifugal force along the rotating surface plays an important role in the heat transfer. The film thickness will reduce as the speed of the liquid moving over the surface increases (due to the increases of rotating speed), which results in a lower resistance to the heat transfer.

At low rotating speeds the concentrate extraction pump was not able to handle higher flow rate. Hence it was not possible to make measurements in this region.

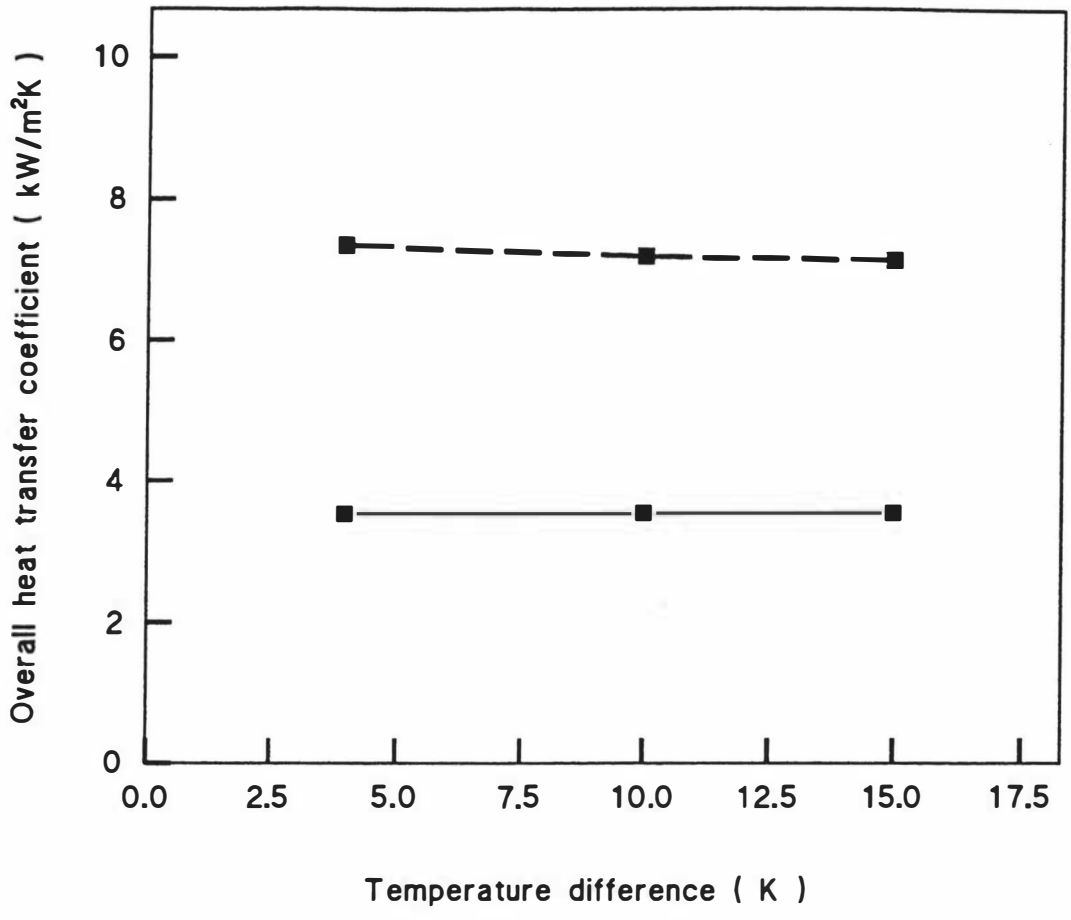

Figure 6.16 Effect of the temperature difference on the overall heat transfer coefficient for water in a cone evaporator. The solid line is connecting experimental values and the dashed line is connecting theoretical values. Rotating speed: 230 rad/s, feed flow: 4.2×10^{-5} m^3/s, evaporating temperature: 70°C.

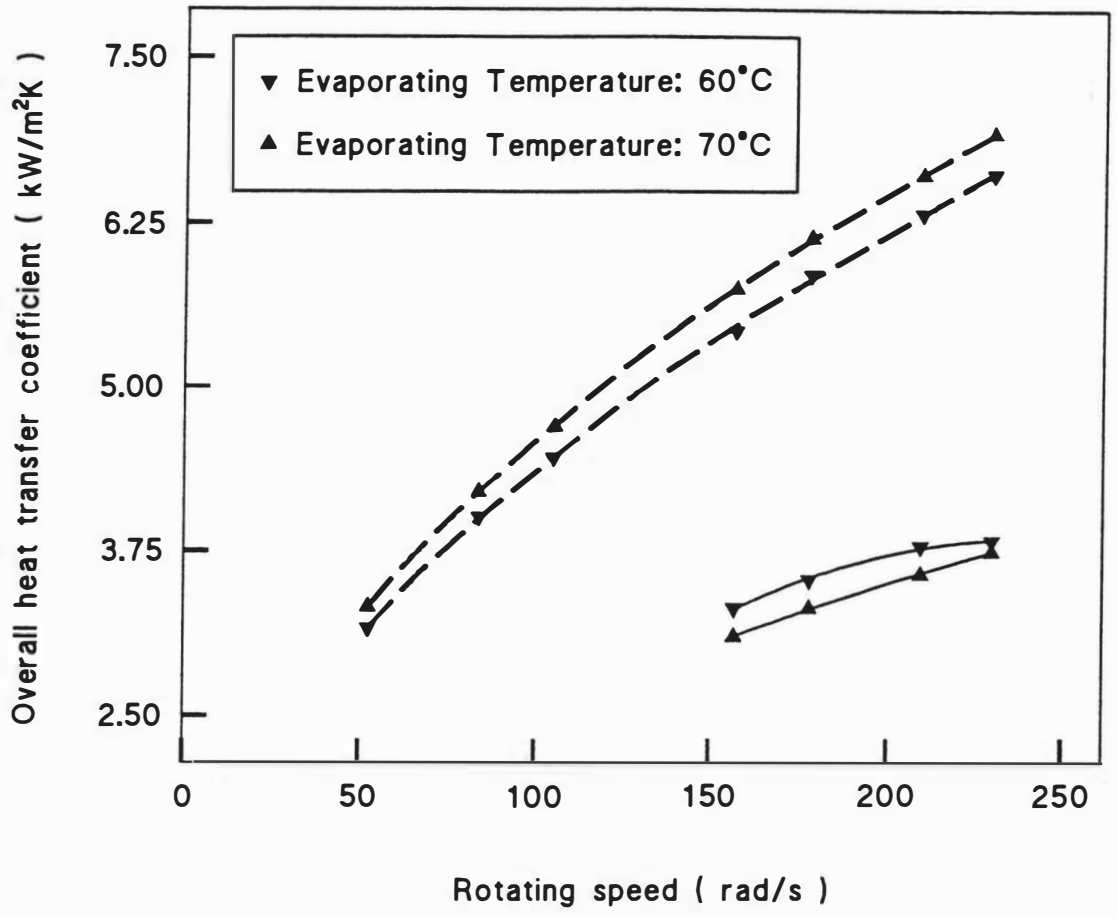

Figure 6.17 Effect of rotating speed on the overall heat transfer coefficient at different evaporating temperature in a cone evaporator for water. Solid lines are experimental values while dashed lines are theoretical values. Temperature difference: 10K, feed flow: 4.2×10^{-5} m^3/s.

6.2.2.3 Feed flow

Figure 6.18 shows that the feed flow has only a slight effect on the heat transfer coefficient in these conditions, the results are similar to those for the Centritherm evaporator. As the feed flow rate increases, the Reynolds number also increases, which would increase the wave motion and turbulence, hence, increasing the heat transfer coefficient. However, the increase of feed flow also increases the film thickness, decreasing the effect of liquid-vapour interface evaporation and lowering the heat transfer coefficient. The later effect is illustrated in the theoretical line. The net effect of these two conflicting effects means that the heat transfer coefficient increases only slightly with increasing feed flow rate.

6.2.2.4 Evaporating temperature

Figure 6.19 shows the effect of evaporating temperature on the overall heat transfer coefficient. It can be seen that both the theoretical and experimental heat transfer coefficients follow the same trend. The experimental heat transfer coefficients, however, are lower than the theoretical ones.

The results above reported show that measured overall heat transfer coefficients are considerably lower than the theoretically calculated values in the cone evaporator. No explanation for the difference could be found, but it is thought that a poor feed distribution may be one of the cause for the discrepancies. It is important to note, however, that in general, the overall heat transfer coefficient experimentally measured in the cone evaporator were lower than those measured in the Centritherm evaporator, which indicates that the cone angle has an important role in determining the overall heat transfer coefficients in this type of evaporator.

6.2.3 Falling film evaporator with a rotating tube

The initial idea of rotating the tube in a falling film evaporator arose from the observation that the heat transfer coefficient in the Centritherm evaporator is much

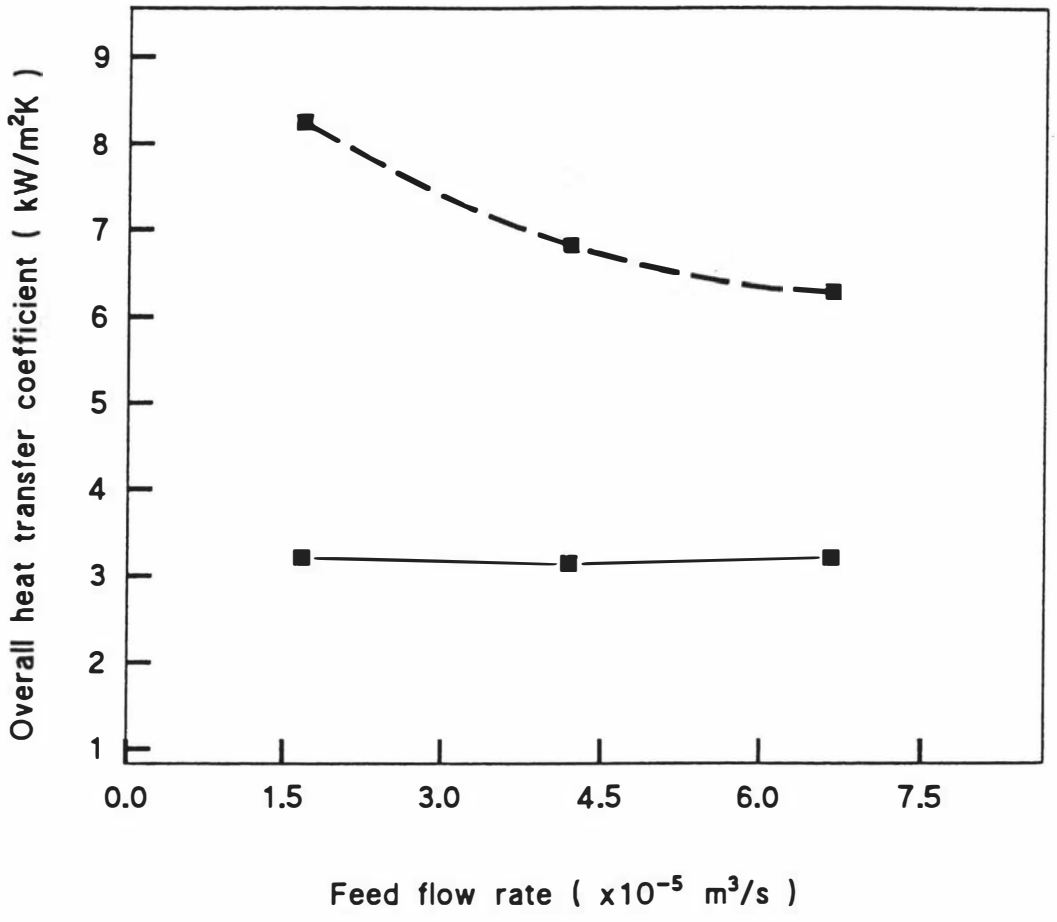

Figure 6.18 Effect of the feed flow rate on the overall heat transfer coefficient for water in a cone evaporator. Temperature difference: 10K, rotating speed: 230 rad/s, evaporating temperature: 60°C. The solid line is connecting experimental values while the dashed line is connecting theoretical values.

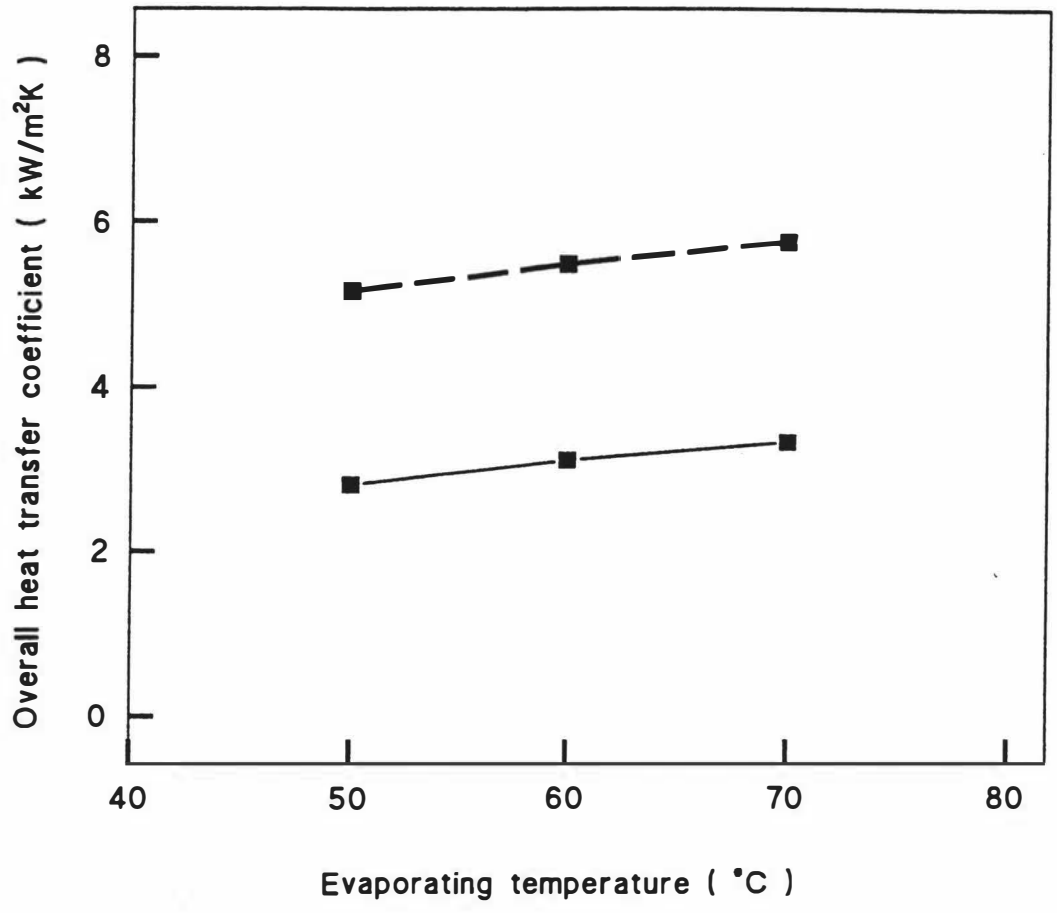

Figure 6.19 Effect of the evaporating temperature on the overall heat transfer coefficient for water in a cone evaporator. The solid line is connecting experimental values and the dashed line is connecting theoretical values. Temperature difference: 10K, feed flow: 4.2×10^{-5} m^3/s, rotating speed: 157 rad/s.

higher than that in falling film evaporators. It was thought that if the energy of the vapours could be used to rotate the tubes, the heat transfer coefficient in a falling film evaporator could be increased to match that of the Centritherm evaporator without expending extra energy. The vapour velocity down the tubes in a falling film evaporator is very high, as much as one third the velocity of sound (Jebson and Iyer, 1991). The kinetic energy of vapours leaving the bottom of the tubes is mostly dissipated, although some is used to pass the vapours through the vapour-liquid separator. The tubes could be rotated by mounting a simple bearing at their tops and bottoms, extending the tubes sightly at the bottom, and cutting and twisting the extended portion so that a simple turbine is formed. By this means it would be hoped that high speed rotation could be achieved simply, effectively and cheaply.

In order to test the effectiveness of rotating the tube on the overall heat transfer coefficient, a motor driven rotating tube falling film evaporator was constructed and tested. The effect of feed flow, tube rotating speed, temperature difference between condensing and evaporating temperatures, evaporating temperature and feed temperature on the overall heat transfer coefficient was investigated.

6.2.3.1 Reynolds number

Figure 6.20 shows the change in the overall heat transfer coefficient in the rotating tube falling film evaporator with the average liquid film Reynolds number. The Reynolds number was varied by changing the feed flow. In the figure two regimes can be identified and these flow regimes are probably related to changes in the liquid flow pattern, as the Reynolds number is varied. The initial steep rise in heat transfer coefficients is probably related to a change from laminar to wavy laminar and starts at a Reynolds number of 30 (Hallström, 1985). Then the heat transfer coefficients increase slightly with the increase of the Reynolds number. The second regime (flow rate beyond 0.03 kg/s, corresponding to Reynolds number of 3500) shows the heat transfer coefficients increase again with increasing of the Reynolds numbers, which is likely to correspond to a turbulent regime. These changes of the heat transfer coefficient with

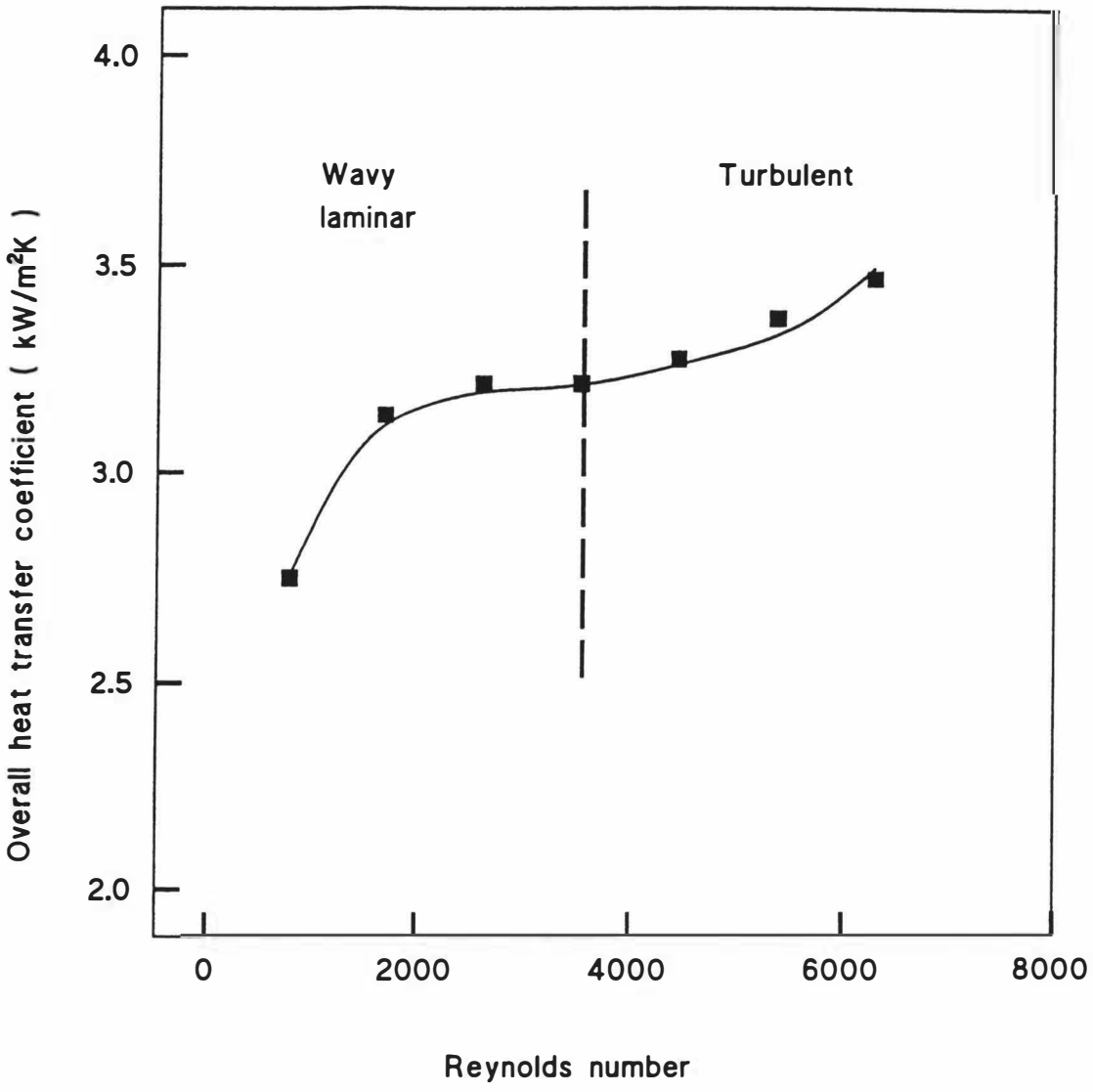

Figure 6.20 Effect of the Reynolds number on the overall heat transfer coefficient of a rotating tube falling film evaporator. Evaporating temperature: 70°C, temperature difference: 10K, rotating speed: 72.3 rad/s, tube length: 2 m, evaporating liquid: water.

the Reynolds number in rotating tube falling film evaporator are similar to the results obtained in falling film evaporator (Schwartzberg, 1988). But the Reynolds number where the changes in flow regime are apparently taking place in the rotating tube evaporator are higher than those observed in a stationary tube (Chen, 1992). The rotation of the tube probably favours the changes towards more turbulent regimes at higher Reynolds numbers. This has been called the re-laminar phenomena (Cannon and Kays, 1969).

6.2.3.2 Rotating speed

As the rotating speed and feed flow rate were both likely to interact and influence the flow regime, these factors were studied together using a factorial design with five levels for the rotating speed and three levels for the feed flow rate.

Figure 6.21 shows the effect of the Reynolds number on the overall heat transfer coefficient as a function of the rotating speed, which is varied by changing the feed flow rate. Experimental data shown in Figure 6.21 was statistically analyzed and yielded the regression equation:

$$H_{exp} = 2.62 + 0.925\Omega - 0.836\Omega^2 + 0.177\Omega^3 + 0.000104\,Re - 0.000412\Omega\,Re + 0.000536\Omega^2\,Re - 0.000134\Omega^3\,Re \quad (6\text{-}3)$$

$$(R^2 = 87.3\%,\ df=37)$$

It can be seen in Figure 6.21 that the heat transfer coefficient increases then declines as the rotating speed increases, and the peak heat transfer coefficient increases with the Reynolds number. When the tube starts to rotate, the liquid film on the inner surface of the tube changes the configuration due to tube vibration, which results in better heat transfer through the liquid film. At low Reynolds numbers, the rise of heat transfer coefficient occurs at a rotating speed of 10 rad/s, then the heat transfer coefficient decreases as the rotating speed increases. For high Reynolds numbers, the peak heat transfer coefficient occurs at 80 rad/s, which may be explained as the film thickness is thicker at high Reynolds numbers (high feed flow rates), and the change of the

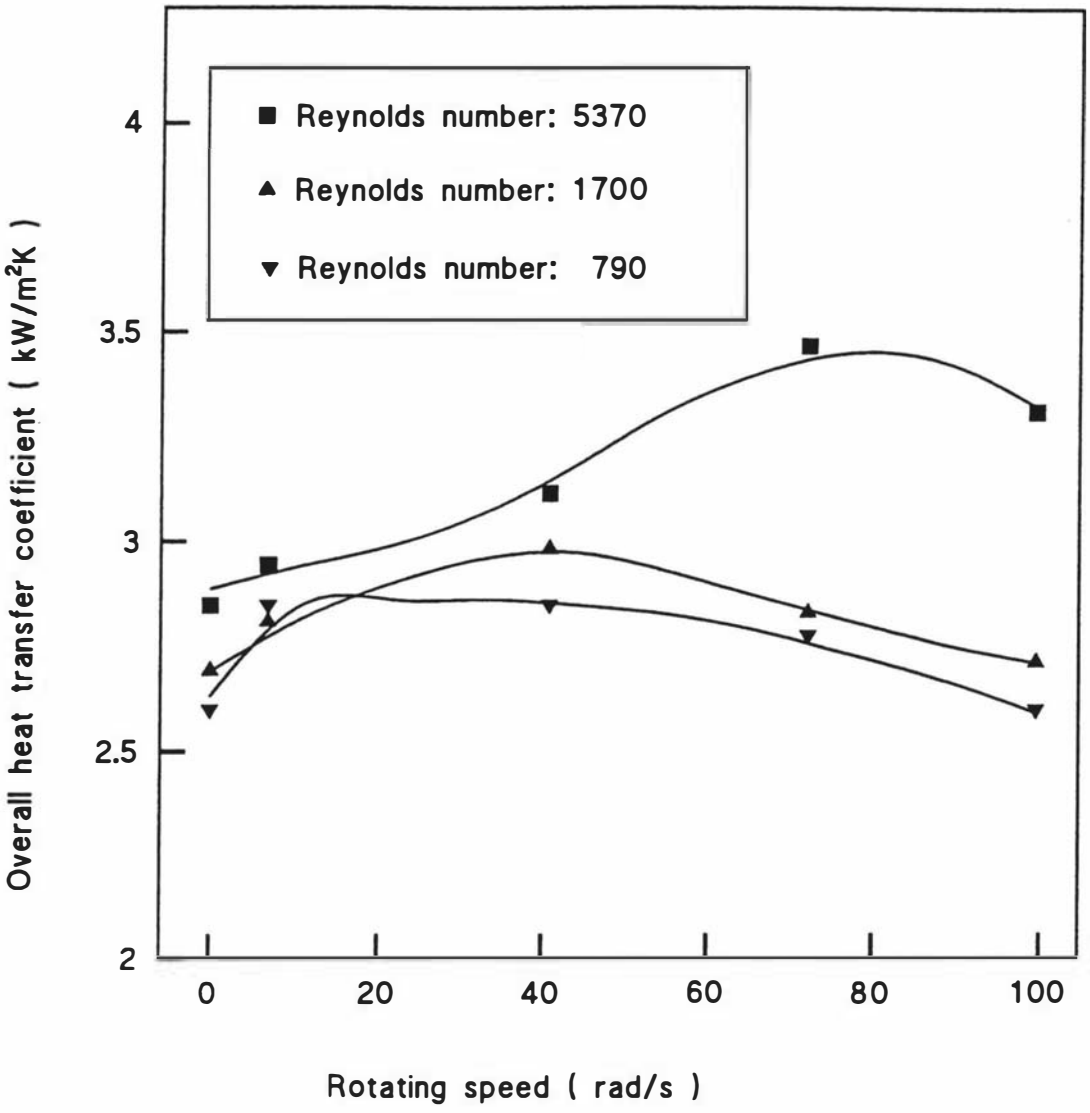

Figure 6.21 Effect of the tube rotating speed on the overall heat transfer coefficient in a rotating tube falling film evaporator at different Reynolds numbers. Evaporating temperature: 70°C, tube length: 2 m, temperature difference: 10K. evaporating liquid: water.

configuration will last longer, so the heat transfer coefficient reaches the peak at a high rotating speed. However, when the rotating speed is towards the higher limit, a severe vibration was observed in the experiments. This may result in the detachment of the liquid film from the rotating surface, consequently reducing the heat transfer coefficients at high rotating speed. Even if the vibration problem was overcome, the maximum increase in heat transfer coefficient is likely to be only of the order of 30%. Under these conditions the use of a rotating tube falling film evaporator is unlikely to be economic.

6.2.3.3 Evaporating temperature

Figure 6.22 shows the effect of increasing evaporation temperature on the heat transfer coefficient. As comparison the results of Chen and Jebson (1992) for a fixed tube evaporator are indicated in the same figure. The increase is probably due to the changes in the liquid properties with the temperature. Viscosity will decrease, and thermal conductivity, and thermal capacity increase, the later only very slightly. The figure also illustrates clearly that higher heat transfer coefficients are obtained with a rotating tube. The increase of both heat transfer coefficients for rotating and fixed tube with evaporating temperature appears to follow a linear relationship being the slope for the rotating tube higher than that for the fixed tube. The rotating tube at higher evaporation temperature seems to encourage the film being thinner than the film on stationary tube at same evaporation temperature.

6.2.3.4 Feed temperature

The effect of the feed temperature for both fixed and rotating tube evaporators is illustrated in Figure 6.23. This figure shows that the heat transfer coefficient increase slightly with increase in feed temperature into the evaporator. A similar effect was also observed in a falling film evaporator (Chen, 1992) and the results are also plotted in Figure 6.23.

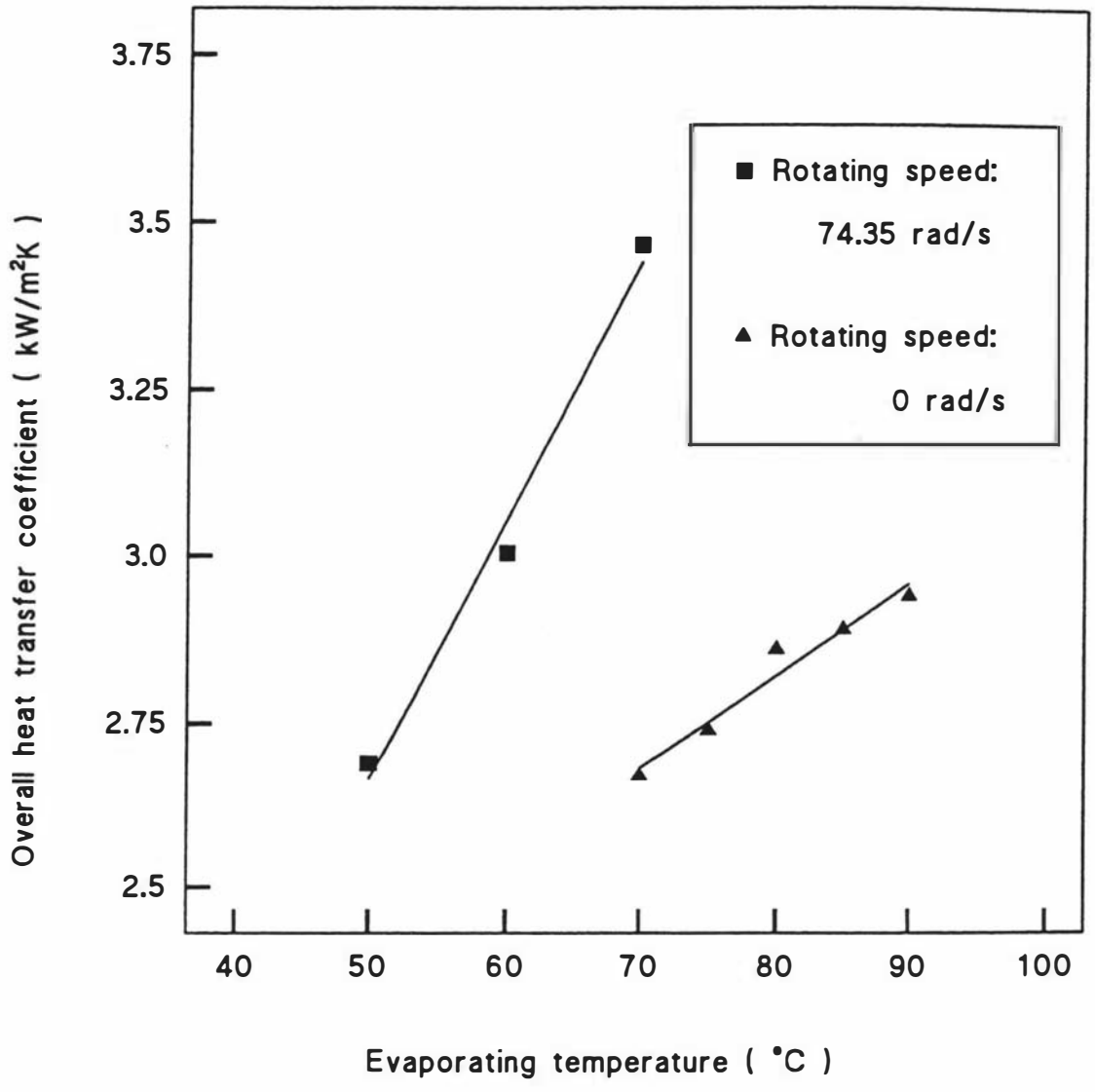

Figure 6.22 Effect of the evaporating temperature on the overall heat transfer coefficient in a rotating tube falling film evaporator. Temperature difference: 10K, feed flow: 5×10^{-3} m^3/s, tube length: 2 m. evaporating liquid: water.

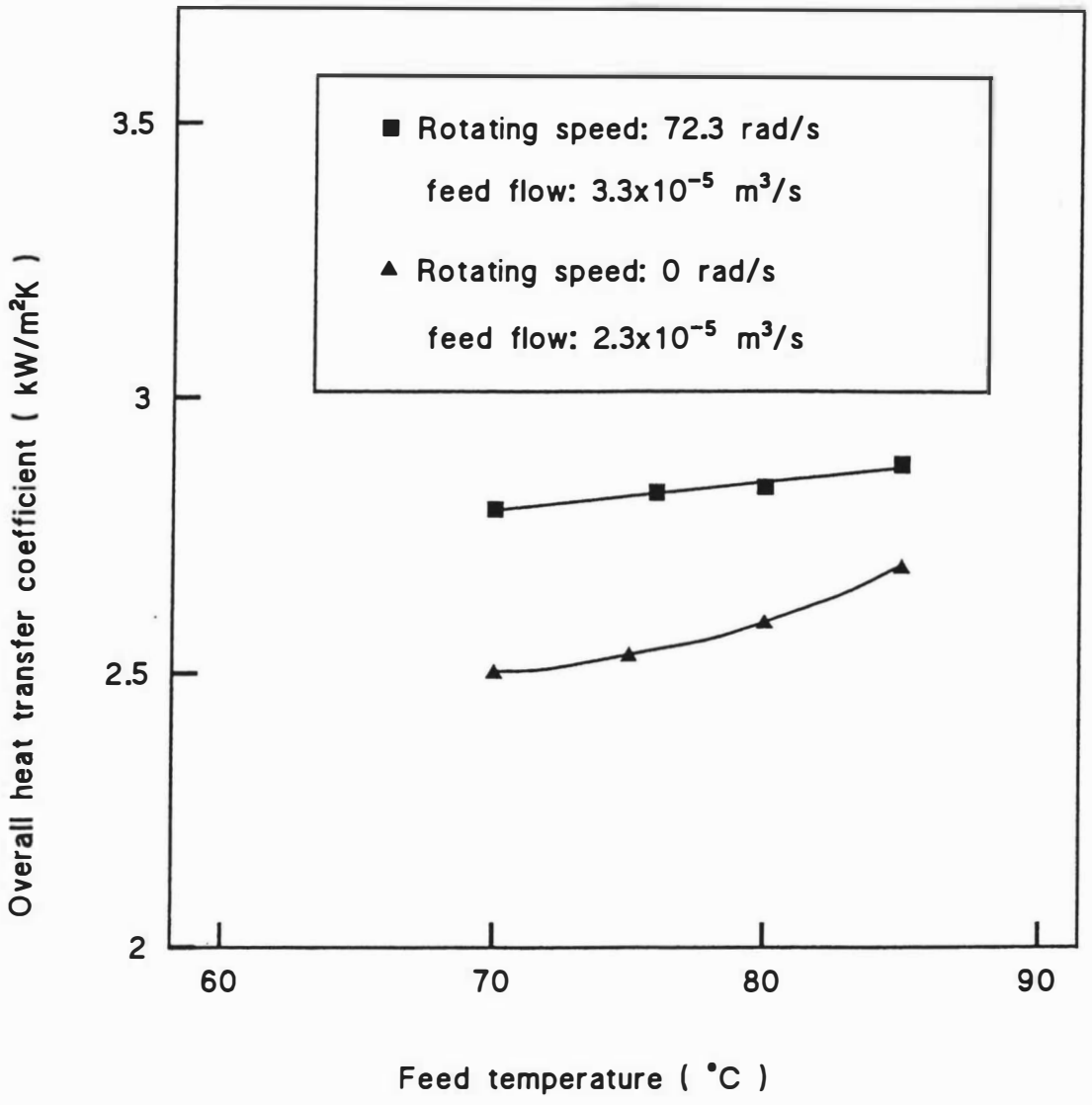

Figure 6.23 Effect of the feed temperature on the overall heat transfer coefficient in a rotating tube falling film evaporator. Temperature difference: 10K, evaporating temperature: 70°C, tube length: 2 m. evaporating liquid: water.

With the short tube length used in these experiments, the entrance effect will have a significant effect on the heat transfer coefficient for the tube as a whole. As the feed temperature increases, while the evaporating temperature keeps constant, there is more flashing and higher vapour velocities at the top of the tube. The normal flow regime is then achieved more quickly. This consequently will cause an increase in the overall heat transfer coefficient. However, when the tube is rotating the centrifugal forces may also encourage the flow to reach the normal regime fast, and the effect of the vapour velocity at the top of the tube will become relatively smaller. Hence the effect of increasing the feed temperature on a rotating tube evaporator will be smaller.

6.2.3.5 Temperature difference

An experimental design with five levels of rotating speeds and three levels of temperature differences was used to determine the effect of rotating speed on the overall heat transfer coefficient as a function of the temperature difference.

Figure 6.2 shows the results of the experimental design. The data shown in Figure 6.24 was statistically analyzed giving the following regression equation:

$$H_{exp} = 4.19 - 0.134\,\Delta T + 0.499\,\Omega - 0.0493\,\Omega^3 \qquad (6\text{-}4)$$

$$(R^2 = 94.4\%,\ df = 41)$$

It is noted that in this case there is no interaction between the temperature difference and the rotating speed, and hence the maximum occurs at a constant speed of 75 rad/s.

Chen and Jebson (1992) showed that for a falling film evaporator there is a rapid linear fall in the heat transfer coefficient with increase in temperature differences up to 8K, after which the heat transfer coefficient decreases more slowly. The change in the slope of the line is thought to be associated with the onset of nucleate boiling. Figure 6.24 shows that for a small temperature difference there is a rapid increase in the heat

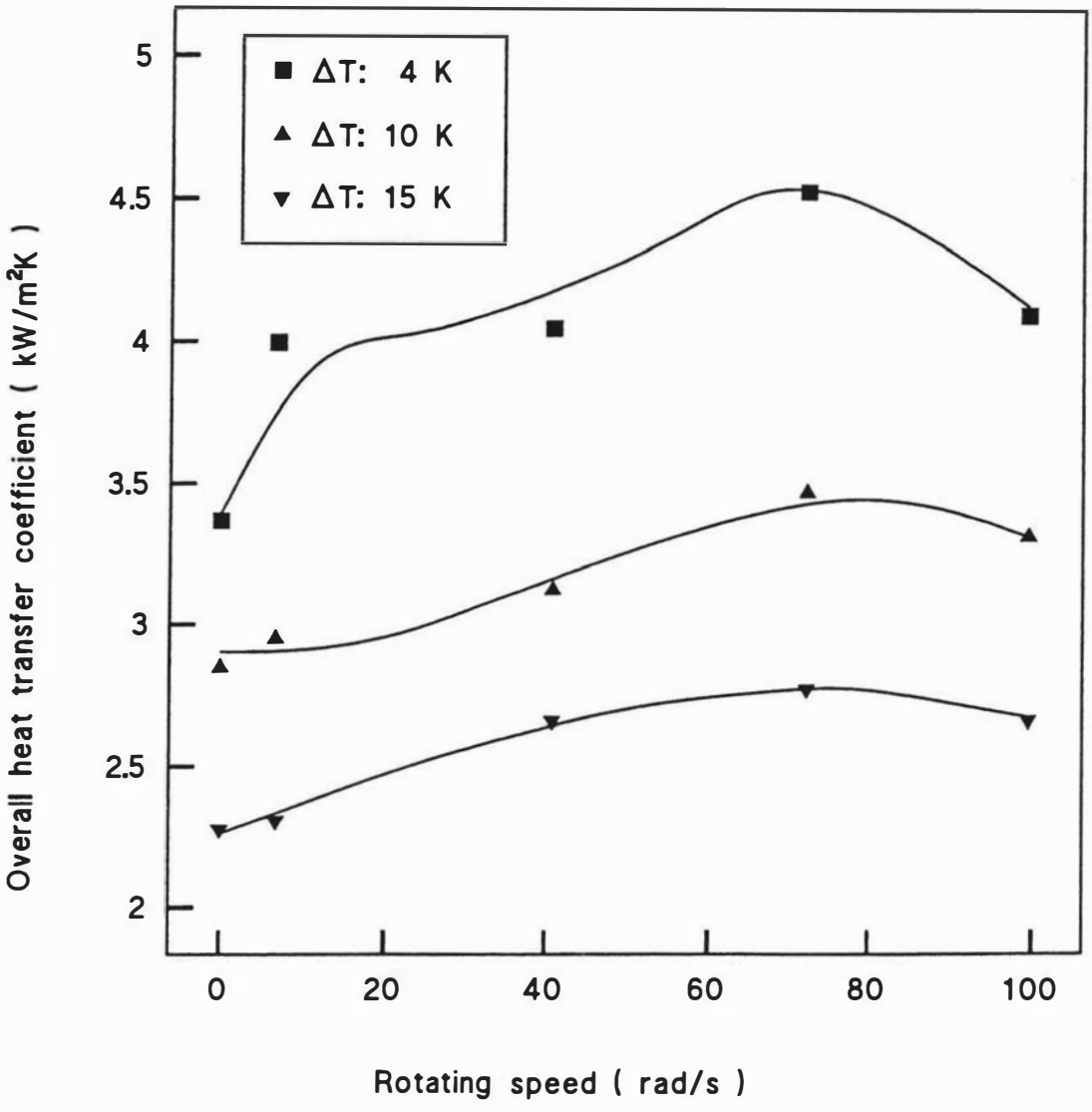

Figure 6.24 Effect of the tube rotating speed on the overall heat transfer coefficient in a rotating tube falling film evaporator at different temperature differences. Feed flow rate: 5×10^{-5} m^3/s, tube length: 2 m, evaporating temperature: 60°C. evaporating liquid: water.

transfer coefficient with the commencement of rotation, but after that the increase is slower. In this case it may be attributed that even a low rotating speed there is a rapid decrease in film thickness and hence a higher heat transfer coefficient, but higher speeds are not correspondingly effective in decreasing film thickness. It is noted that at the higher temperature differences there is no rapid increase in heat transfer coefficient at low speeds. If the main mechanism at these speeds is ebullition, then the effect of increasing speed may be to remove bubbles more quickly, and this would explain the steady increase with increase of rotating speed. The decline of the heat transfer coefficient at high speeds is again thought to be the result of vibration disturbing the film.

6.3. Conclusions

A theoretical model that describe the flow of a film on a rotating surface has been developed. Although the model was simple, it revealed basic relationships among variables for the evaporating heat transfer of the liquid film on the surface of a rotating cone.

The theoretical equations obtained from the proposed model show that the liquid film thickness and the heat transfer coefficients are affected by the feed flow rate, rotating speed of the cone, length of the cone, angle of the cone, and liquid viscosity.

The local film thickness decreases with decrease in feed flow rate, increase of cone length and rotating speed. Increase of cone angle results in thinner liquid films and higher heat transfer coefficients.

The theoretical calculated overall heat transfer coefficients show similar trend to experimental results obtained using the Centritherm and a constructed cone evaporators.

The discrepancies between experimental and theoretical results could be attributed to the following reasons:

1) It was assumed in the theoretical model that the liquid film moves across the conical surface as a smooth film without waves. However, it was observed by Shinn (1971) that waves exist in the liquid film when it moves across the rotating conical surface. Waves are likely to increase turbulence and hence heat transfer.

2) It was also assumed in the theoretical model that evaporation takes place only at the surface of liquid film, which is true only at lower temperature differences. At high temperature differences, bubbles are likely to be formed on the heating surface, which will affect the heat transfer.

3) Centrifugal forces acting on the liquid film increase the pressure in the film as the rotating speed rises. This causes that the saturation temperature of the liquid on the conical surface increases slightly and therefore reduces the temperature difference between the conical surface and the liquid film.

4) Differences between calculated and experimental heat transfer coefficients could also be caused by the presence of non-condensable gases in the steam jacket, which depend on the efficiency of non-condensable gases removal by the steam-trap system. The concentrations of non-condensable gases were not measured but it has been reported that it could seriously affect the steam side heat transfer coefficients (Mincowycz and Sparrow, 1966; Machereth, 1993).

The results obtained in falling film evaporator with rotating tube showed that rotating the tubes of a falling film evaporator will increase the overall heat transfer coefficient but the increase obtained is very dependent on feed flow rate, and is not sufficient to justify the use of this evaporator in the industry. Rotation also appears to delay the onset of bubble formation in evaporation, and reduce the effect of vapour velocity at the top of the tubes.

PART III

FOULING IN EVAPORATORS WITH ROTATING SURFACES

CHAPTER 7
LITERATURE REVIEWS OF FOULING IN MILK PROCESSING

In virtually all types of heat transfer plants, fouling of heat transfer surfaces is the main cause of progressive decline in efficiency and performance of the equipment with time. To overcome fouling, frequent cleaning of equipment is required. Fouling is of considerable importance in the dairy industry (Tissier and Lalade, 1986). The fouling of a heating surface during the processing of milk, especially at high temperatures, is an important practical problem, with implications for operating costs and product quality. The understanding of the fouling process will assist in the determination of methods to prevent or delay the undesirable deposit formation on the heat transfer surfaces, and will be more practically important in the design of an efficient cleaning system.

After looking at the general aspects of the fouling problem, this review mainly focuses on fouling in milk processing.

7.1 The costs of fouling

Surveys of fouling in the British industry (Pritchard, 1979) estimated that fouling costs were about £300-500 million per annum, which was between 0.2 to 0.33% of the Gross National Product (GNP) of the United Kingdom in 1978. The fouling costs include more than £50 million per annum for the food industry (Fryer and Gotham, 1988). A survey in the United States showed that the annual cost of fouling of heat exchangers run between US $8 to 10 billion per annum (Garrett-Price, 1985). This represents 0.228 to 0.35% of the American GNP for the year 1984. A survey of fouling in New Zealand industry estimated that fouling costs were between 0.1% to 0.15% of GNP in 1988 (Steinhagen *et al.*, 1990).

These figures show that the costs of fouling in the industry are quite significant. Therefore, the study of fouling is an important aspect in heat transfer equipment and process design. However, this is still the major unresolved problem (Whalley, 1992).

Although the precise costs of fouling are difficult to quantify, it is important to examine the areas in which fouling affects production (Fryer *et al.*, 1995). The total costs attributable to fouling in heat transfer equipment are made up of the following components (Pritchard, 1988; Bott, 1989, 1995 and Steinhagen *et al.*, 1990):

(1) Capital costs

Extra heat transfer area is included in the design of plant to take account of the reduction in heat transfer efficiency due to fouling. In practice, the heat exchangers are between 10%-50% overdesigned, with the average around 30% (Garrett-Price, 1985). In some instances of severe or perhaps unknown fouling potential, the allowance of heat transfer area for fouling might be as high as 100% (Bott, 1988), or even 500% (Sandu and Lund, 1982). In addition, extra pump capacity is also installed.

(2) Energy costs

Fouling results in increased energy costs via the extra heat and pumping duties required.

(3) Maintenance costs

This includes the costs for installing complex cleaning processes systems and costs for chemicals.

(4) Loss of production

The necessity of frequent cleaning of the plant, and operation during production at a reduced efficiency due to fouling, results in a loss of production.

(5) Impairing product's quality

Fouling in the food processing industry can give rise to problems of texture, taste and sometimes aroma of food products (Bott, 1988) and has to be regarded as a potential

source of biological contamination (Pritchard, 1988). The quality of the processed milk may be impaired by the presence of detached pieces of deposit, which break away from the vessel walls under the action of high shear forces in the final products (Swartzel, 1983, Marrs and Lewis, 1986, Grandison, 1988a).

7.2 The types of fouling

Fouling is normally classified into following six major categories according to the underlying process (Hallström, 1988a, Bott, 1995):

(1) Precipitation fouling

This involves precipitation of dissolved substances and/or formation of crystals on the surface. If the dissolved substances have inverse solubility the precipitation takes place on heating surfaces at a higher temperature than the liquid. This type of precipitation is also called scaling.

(2) Reaction fouling

This type of fouling is the result of one or more chemical reactions between reactants contained in the flowing fluid at, or near, the surface due to the change in temperature.

(3) Particulate fouling

This is the name given to the accumulation of suspended solid particles from the fluid stream onto the surface. In a few cases the deposition occurs as a result of gravity, in which the process is referred as sedimentation fouling.

(4) Biological fouling

This type of fouling is due to the attachment and growth of micro-organisms originating from the process stream on the surface.

(5) Corrosion fouling

Chemical reactions in the material of the heating surface itself.

(6) Freezing fouling

Solidification of the fluid or a fluid component due to a temperature lower than the melting point at the surface.

In most cases, more than one type of fouling occurs in the system. However, it is useful to study the mechanisms separately in order to have some appreciation of the factors that are likely to influence the fouling problem, although in combined fouling systems there may be modification of the effects of certain variables (Bott, 1989).

Milk fouling on the heating surface may fall into the first, second and fourth categories.

7.3 The research history of fouling in dairy industry

Fouling problems associated with food processing have been studied in processing sugar-beet liquor and sugars, fruit and vegetable juices, brewing fluids, soya and egg proteins (Marrs and Lewis, 1986; Fryer and Gotham, 1988). In the dairy industry, its importance has also long been recognised. The research work started in the early thirties (Parker and Johnson, 1930). As the processing plant required cleaning before the deposit layer became severe due to hygienic reasons, the initial research of milk fouling concentrated on plant cleaning as a practical solution (Johnson and Roland, 1940a,b; Bell and Sanders, 1944). Only in the last two decades, the fouling of process plant had been accepted as a part of a larger problem and studied more widely and in greater detail (Burton, 1988). This is because that the volume of milk processed in a dairy plant has steadily increased, as well as the reductions in energy consumption, amounts of cleaning material used and time spent in cleaning have become considerably more important (Hege and Kessler, 1986a). The research work carried out at the National Institute for Research in Dairying (NIRD), Shinfield (UK), started in the mid sixties, provides a starting point for many other fouling studies in the milk industry (Fryer *et al.*, 1995). Now the literature on milk fouling is extensive and significant progress has been made in understanding the composition and structure of fouling deposits as well as the fouling mechanisms. The results of these works can be found

in several conference proceedings (Melo *et al.*, 1988; Kessler and Lund, 1989; Belmar-Beiny and Fryer, 1994), reviews (Burton, 1968, 1988; Bott, 1989; Fryer *et al.*, 1995, Jeurnink *et al.*, 1996) and a book (Bott, 1995).

The composition of the deposits is now known, and the chemical changes that occur when milk is heated are fairly well understood. However, the interaction between the chemistry and the engineering factors in processing plant are not, and the progress made towards the reduction of fouling in commercial processing plant has been largely empirical (Fryer *et al.*, 1995).

The difficulty of interpreting the interrelationships of the chemical reactions, which give rise to fouling, with the fluid mechanics of the heat transfer equipment is due to a number of reasons (Belmar-Beiny *et al.*, 1993):

(i) The milk fouling deposit is complex. Deposit is mainly formed by a mixture of proteins and inorganic salts.

(ii) Fouling from milk shows strong seasonal variations, as a result of differences in its composition. This makes it difficult to interpret results in terms of basic kinetics unless a well-defined fluid, which does not show such a variation, is used.

(iii) Fouling is generally considered to be the result of several temperature-dependent effects; chemical reactions which result in the denaturation of whey proteins and the formation of insoluble protein aggregates, and solubility limits which result in the precipitation of salts.

(iv) The milk fouling is also a function of many other factors, such as the fluid velocity, surface conditions, air content, etc.. Fluid travelling through the heat transfer equipment may experience a range of shear rates and temperatures, both of which affect the rate of fouling.

7.4 Composition and structure of milk fouling deposit

The extent of fouling on the heat transfer surface and the composition of the deposit formed from the milk are largely dependent on the temperature of milk. Two distinct types of deposits were described by Burton (1968):

(i) The first, called Type A, is a voluminous material, which starts to form at temperatures above 70°C, is maximum in the range 95 to 110°C, and then decreases at higher temperatures (Burton, 1968; Lalande *et al.*, 1984). The deposit has a high protein content (50 to 70%) and a lower mineral content (30 to 40%) (Lyster, 1965, Lalande *et al.*, 1984; Tissier *et al.*, 1984). At the lower end of the temperature range at which this deposit is formed, most of the protein is β-lactoglobulin, but at the higher end of the range it is predominantly casein (Tissier *et al.*, 1984; Lalande *et al.*, 1985). This deposit is predominantly soft, white and spongy: however, if overcooked it can become brown and very much harder (Lyster, 1965; Burton, 1968).

(ii) The second type of deposit, called Type B, forms at higher temperatures than Type A, above 120°C. It is hard and granular, and has a high mineral content (70 to 80%) and a small amount of protein (10 to 20%), largely casein (Lyster, 1965; Burton, 1968; Lalande *et al.*, 1984).

Table 7.1 gave a detailed chemical analysis of fouling deposits at pasteurization and UHT temperatures (Tissier *et al.*, 1984). The deposit formed in a pasteurizer is of the Type A while in a UHT sterilizer is close to Type B deposits. The protein composition of these deposits is shown in the Table 7.2.

As shown in the tables, the composition of milk fouling deposits is highly temperature dependent. Type A deposit (72°C) contains mainly whey proteins and Immunoglobulins while the sterilizer Type B deposit contains only casein. There are large differences between deposit protein compositions and those of raw milk. Therefore fouling results from preferential deposition of certain milk components.

Table 7.1 The composition of milk deposits in a pasteurizer and a sterilizer (From Tissier *et al.*, 1984).

Composition in the deposit (%)	Pasteurizer (72°C)	Sterilizer (138°C)
Protein	50	12
Mineral	15	75
Fat	25	3
Minor components	10	10
Total	100	100

Table 7.2 The protein composition of milk deposits in a pasteurizer and a sterilizer (From Tissier *et al.*, 1984).

Protein composition (%)	Pasteurizer (72°C)	Sterilizer (138°C)
β-lactoglobulin	50	-
α-Casein	18	27
β-Casein	-	50
Immunoglobulins	23	-
Minor components	9	23
Total	100	100

Although fat is present in the deposits, it does not play a significant role in the process of fouling (Maas *et al.*, 1985, Burton, 1988). It is thought that fat occurs in the deposit

when it is trapped by other constituents (Burton, 1988). In directly heated UHT systems Burton (1968) found that after steam-injection heating, a different deposit on the unheated surface of the holding section of the plant was formed. This deposit had an unusually high fat content (30 to 35%), with a mineral composition similar than deposits produced in indirect systems. Lalande *et al.* (1984) found a similar type of deposit after homogenization of milk at 138°C in an indirect heat exchanger. Burton (1988) proposed that this deposit is due to destabilization of the fat globules by mechanical action at high temperature.

Lactose is hardly found in milk deposits because it is water soluble. So even if it was incorporated in a deposit, it would dissolve again in the milk stream (Jeurnink *et al.*, 1996).

The fouling material not only varies in composition according to the temperature at the point where it forms, but it also varies throughout the thickness of the fouling material (Burton, 1988). A number of detailed examinations about the structure of fouling deposits have been reported (Hege and Kessler 1986b; Daufin *et al.*, 1987; Britten *et al.*, 1988; Foster *et al.*, 1989). Tissier and Lalande (1986) reported that, for a process time greater than about 1 hour, Type A deposits consist of two layers: a protein-rich outer layer and a sublayer, near to the heat exchange surface, that is rich in calcium and phosphorus. They ascribed the formation of the sublayer to the diffusion and subsequent crystallization of insoluble calcium phosphate. Due to the distinct two layers structure, there is an argument about the nature of the initial layer of deposits formed on the heating surfaces. More discussions regarding initial deposition are given in the section 7.9.

Type B deposit is hard, granular and brittle in structure (Lyster, 1965; Lalande *et al.*, 1984). Foster and Green (1990) studied the structure using scanning electron microscopy (SEM), and reported that Type B deposits become rougher as the surface temperature increases. The depth profile of Type B deposits was also studied; no distinct structural layers were found, but, like Type A deposits, protein was concentrated

near the outside of the deposit with calcium, phosphorus and magnesium near the heat exchange surface. In addition, calcium phosphates tended to be located nearer to the surface than magnesium phosphates.

Lyster (1965) noted that calcium and phosphate typically accounted for 90% of the mineral content of milk fouling deposit, but only represent 30% of mineral content in raw milk. The calcium/phosphate ratio for Type A deposit was found to be about 1.5. This, which has been also verified by others researchers (Ito and Nakanishi, 1967; Skudder *et al.*, 1981; Lalande *et al.*, 1984; Tissier and Lalande, 1986), indicates the presence of calcium triphosphate.

7.5 Factors affecting milk fouling on the heating surface

Dairy fluid fouling is a function of many variables, including chemical and physical properties. The seasonal changes in milk composition are also reflected in fouling. The factors which affect the milk fouling on the heating surface can be classified as: milk properties; and, plant construction and operation.

7.5.1 Milk properties

7.5.1.1 Compositional variations with season

Milk is a complex biological fluid subject to compositional variations (Walstra and Jenness, 1984), which are reflected in fouling. Burton (1968) found that different milk supplies vary widely in their ability to deposit fouling material during heat treatment. The amount of deposit formation during milk processing can vary from one milk supply to another, from day to day with a single milk source, and from season to season for milk from a single herd supply, although the underlying chemical factors are not very clear (Burton, 1966, 1967, 1968, 1972, 1988 and Grandison, 1988a,b,c). Grandison (1988c), however, was unable to correlate herd diet and fouling deposit.

7.5.1.2 pH values of milk

The effect of milk pH on deposit formation has been widely studied (Hege and Kessler, 1986a; Skudder *et al.*, 1986; Visser *et al.*, 1986; Chaplin and Lyster, 1988). Milk pH typically varies between 6.6 to 6.8. Skudder *et al.* (1986) showed that the amount of fouling increased markedly at an acidic pH, but remained unaffected at alkaline values. These results were consistent with the reports of others (Yoon and Lund, 1989). Hege and Kessler (1986a) concluded that the denaturation of protein is accelerated by lower pH values, because a decrease in pH causes a reduction in the negative charges of the protein molecules. This in turn reduces the electrostatic (repulsive) force between the molecules, thus, promoting aggregation.

7.5.1.3 The amino nitrogen level of the milk

A strong positive correlation between depositional rate in a heat exchanger and the amino nitrogen level of the milk has been shown by Lalande and Corrieu (1981). This may depend on the association of the amino group concentration with urea content (Burton, 1988). It is known that added urea increases milk heat stability (Robertson and Dixon, 1969; Muir and Sweetsur, 1976) and decreases deposit formation.

7.5.1.4 Calcium phosphate

Burton (1968) hypothesized firstly that mineral deposition occurred because of the lower solubility of calcium phosphate at higher temperatures. This view was supported by Visser *et al.* (1986). A precipitation fouling was suggested for calcium phosphate deposition on the heating surface by Barton *et al.* (1985). The rate of precipitation of phosphate is a function of the temperature and the resulting degree of supersaturation (Sandu, 1989). Jeurnink and de Kruif (1995) found that either increasing or decreasing the calcium concentration in respect to standard calcium concentration in milk led to more fouling, due to the effect of calcium on the stability of casein micelles. Daufin *et al.* (1987) showed that dairy fluids not containing calcium did not produce any

fouling and when no precipitable calcium was presented, deposit growth was in fact stopped. These results might be an explanation for the effect of the seasonal variation of milk composition on fouling and the inhibiting precipitation of calcium phosphate could be a method to prevent or minimize fouling.

7.5.1.5 Air content in milk

The presence of air in milk has the effect of increasing fouling rates (Gynning *et al.*, 1958; Burton, 1968; Marrs and Lewis, 1986; Fryer, 1986). It is thought that air bubbles are formed at heated surfaces, which promotes protein coagulation and denaturation. Marrs and Lewis (1986) concluded that the dramatic reduction in fouling rates, which resulted from an increase in the back pressure applied to the product side of the heat exchanger, was almost certainly due to the suppression of air bubble formation at the heated surface. The air content of bovine milk may be increased by entrapment during milking (Butler, 1988). Deaeration of the milk prior to heating reduces the degree of fouling by anything up to 50% (Gynning *et al.*, 1958).

The enhancement of fouling through air bubble formation on the heated surface was regarded as a distinctive mechanisms of milk fouling (Jeurnink *et al.*, 1996). Visual observations showed that air bubbles were nuclei for the formation of deposit (Jeurnink, 1995a). The fouling process induced by the air bubbles can be described as follows: when the bubbles are formed, the surface becomes dry (Visser, 1988) and as a consequence, there is an increase in the temperature difference between the hot stainless steel surface and the bulk of the liquid, resulting in evaporation of water at the vapour-liquid interface. Due to this evaporation milk is transported from the bulk to the surface where the air/vapour bubbles are attached. Here milk protein accumulates and because of the local increase in concentration and the high temperature the protein may coagulate and deposit on the surface. Eventually the air/vapour bubble bursts and part of the membrane is carried away with the liquid. The schematic representation of this process is shown in the Figure 7.1. The contribution of air/vapour bubbles to the deposit is determined by the amount of air present in the milk, the temperature difference between

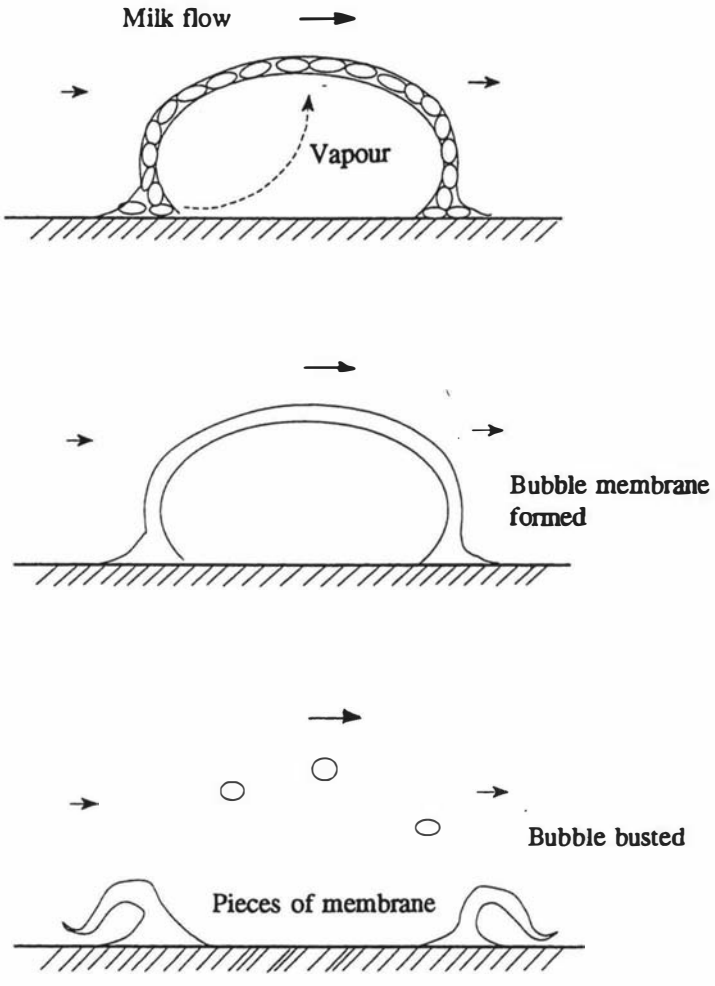

Figure 7.1 The schematic presentation of the milk fouling process induced by an air bubble at a hot stainless steel surface (From Jeurnink, *et al.*, 1996)

the surface and the bulk, the operational pressure in the heat exchanger and the wall shear stress (Jeurnink, 1995a). It is also thought the similar phenomena may occur in film evaporators for dairy products as a result of nucleate boiling (Jeurnink *et al.*, 1996).

7.5.1.6 Concentration of milk

The depositional rate increased with the rising of the milk concentrations. Fryer *et al.* (1992) found that the total amount of deposit from whey protein concentrate increased linearly with protein concentration. It was deduced that the increased concentration resulted in higher viscosity and low turbulence, an increased probability of non-uniform heating, low heat transfer rates which caused an increased product depositional rate (Jelen, 1981).

7.5.2 Plant construction and operation

7.5.2.1 Storage time

Storage of milk at room or refrigerated temperature for 12-24 hours prior to processing, without change in pH, significantly reduced deposit formation (Burton, 1966, 1968; Ashton, 1966), although longer-term aging led to a rise in deposit formation (Burton, 1968; Jeurnink, 1991). The reason for the initial drop of deposit may result from the lipolysis of the milk fat by natural lipases in the milk. One of the fatty acids (capric acid) liberated during lipolysis was found to have a specific effect, at very low concentrations (about 1 mg/litre), of reducing the amount of deposit on the heated surface (Al-Roubale and Burton, 1979). The late rise of deposit after longer storage may be due to the action of proteolytic enzymes, secreted by pschrotrophic bacteria (species growing at temperatures of 5 to 10°C) in the milk. κ-casein is hydrolysed by proteolytic enzymes during storage, resulting in a decreased heat stability of casein micelles, which will coagulate on heating and cause an additional protein deposition (Jeurnink, 1991). If milk cannot be effectively refrigerated, bacteriological spoilage may occur in milk. Therefore, a compromise will be required between beneficial effects of aging and the adverse effects of bacterial growth and a drop in pH.

7.5.2.2 Preheating

Preheating milk was found to reduce fouling in later processes (Bell and Sanders, 1944). Foster *et al.* (1989) found that preheating of whole milk at 70 to 95°C for 5 minutes caused a 10 to 20 % decrease in the amount of deposit produced at the heating temperature of 100°C, compared with raw milk. It is now known that the denaturation of whey proteins, especially ß-lactoglobulin, during preheating and preholding stage, reduces the formation of proteinaceous deposits in later processes. It was also thought that the supersaturation and crystallization of calcium and phosphorus from solution at high temperature was responsible for the effect of preheating (Burton, 1968). Proper selection of preheating conditions (temperatures and preholding time) could be used as a method to reduce fouling in the following heat treatment steps. It was also suggested that in order to minimize the deposition in the holding section, the holding vessels should be high-volume one, which give a high volume/surface ratio, i.e. reducing the surface area (Burton, 1988; Jeurnink, 1995b), or a continuous stirred tank reactor rather than a plug flow reactor or a holding tube (de Jong *et al.*, 1992).

7.5.2.3 Absolute liquid velocity

In general, the higher the liquid flow velocity, the less the amount of fouling. This is probably because at lower velocities the thickness of the laminar sublayer adjacent to the heat surface is greater, so that the volume of material subject to high temperature, and the volume which remains for relatively long periods near to the surface, are greater (Burton, 1988). It was demonstrated by Gordon *et al.* (1968), Fryer (1986) and Gotham (1990) that both the amount and extent of fouling decreased with increasing flow rate in a tubular heat exchanger, in which it is clearly possible to relate flow rate to the shear stress in the equipment. It was found that deposition was prevented if the wall shear stress exceeded 15 Pa when heating simulated milk ultra filtrate in a rotating disk device (Jeurnink *et al.*, 1996). It is much more difficult to relate fouling to flow rate in plate heat exchangers because of the complex flow geometries involved (Fryer *et al.*, 1995). It was pointed out by Bott (1989) that the benefits of reducing fouling at high liquid

flow velocity must be balanced against the additional pressure drop and associated pumping costs.

7.5.2.4 Surface conditions

As the milk fouling occurs on the solids and liquid interface, the roughness of the surface could be important in the fouling. Rough surfaces, in general, appear to favour deposit growth (Bott, 1989). It is conceivable that modification of the surface could prevent or limit fouling. Much theoretical attention, e.g. coating the surface, high polish of the surface, and electrochemical modification, has been given to this possibility (Baier, 1981), but so far with little practical effect (Burton, 1988). It was also found that after the first deposit layer is established, the surface roughness will no longer affect the growth of deposition (Dupeyrat *et al.*, 1987; Britten *et al.*, 1988; Yoon and Lund 1989). This is not surprising, as once a surface has become covered with fouled material it is the deposit-deposit interaction, rather than the deposit-metal surface interaction, which is the most significant factor. Britten *et al.* (1988) found that different coatings on the heating surface did not affect the amount of deposit formed, but did affect the strength of adhesion; the interfacial energy parameters of the surface appeared to be the main factors affecting the adhesive strength. They concluded that the polar binding potential of the coated surfaces was the main factor influencing the strength of adhesion. It thus appears that the first material to adsorb is responsible for the strength of the deposit-surface bond; this may affect the cleaning rate (Fryer *et al.*, 1995).

The precleaning conditions should be given major attention before operations are started, because the predeposited dirt on the surface will act as kernels for secondary deposition (Visser, 1988).

7.5.2.5 Temperature

Temperature directly determines the severity and type of fouling on the surface. As the temperature rises both on the heat transfer surface and in the liquid stream, the whey proteins start to denature, aggregate and deposit and the calcium phosphate may start to precipitate. If temperature increases further, the colloidal stability of casein micelles in milk decreases, then the coagulation of casein micelles may be become a major controlling factor in the deposition process. Table 7.1 demonstrates that at 75°C, heat-denatured ß-lactoglobulin accounted for the majority of the protein in the deposit, whereas at 138°C, ß- and α- caseins were present in greater quantity. This is presumably because the ß-lactoglobulin is denatured at temperature of 75°C, while the casein micelles become destabilised at higher temperatures.

7.5.2.6 Processing time

In practice, the amount of fouling deposit always increases with time. Fouling in the dairy industry is more severe than that in other industries. For example, in the petrochemical industry, it is common to clean only once a year or less (Crittenden *et al.*, 1992). In comparison to the dairy industry, it is necessary to clean the processing plant daily or even more often.

The fouling process is a transient process. If fouling resistance (R_f) is plotted against processing time, different fouling curves may be produced depending on the conditions.

Figure 7.2 summaries the ideal curves that are possible in fouling process (Sandu and Lund, 1982; Bott, 1988, 1995):

Curves A and A' represent linear fouling processes, in which the masses of deposit gradually increase with time but the rates of deposition are constant. Curves B and B' denote the asymptotic fouling processes, in which the rates of fouling for whatever reasons, gradually fall with time and eventually reach steady state when there is no net

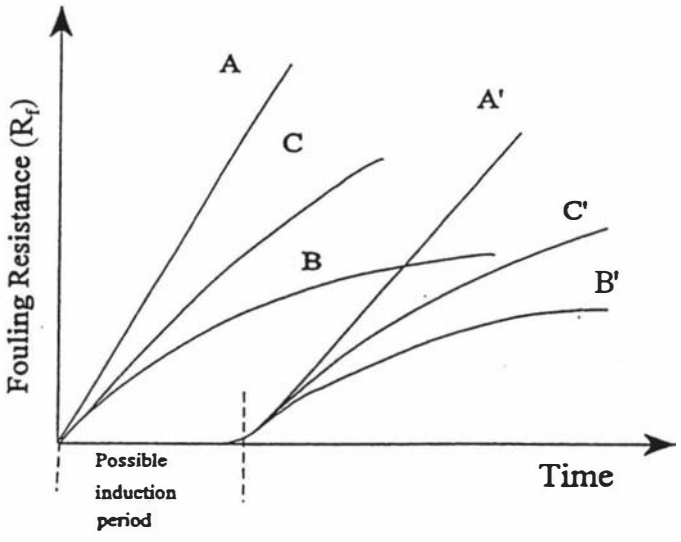

Figure 7.2 Idealised fouling curves

increase of deposit on the surface. Curves C and C' represent falling rate fouling processes.

For Curves A', B' and C', the fouling processes are further complicated by the fact that a period time has to elapse before significant fouling begins. This period is referred to as the induction period and usually attributed to the time required to "condition" the surface (Bott, 1988). This phenomenon is often observed in food fouling and has resulted in two-stage model for the food fouling process being proposed (Fryer, 1989).

In tubular geometries an induction period, which is characterised by unchanged conditions of heat transfer and pressure drop, is seen (Delsing and Hiddink, 1983), whereas in plate heat exchangers the induction period is less obvious due to its complex geometry (Fryer and Gotham, 1988). In a recent experimental work using a plate heat exchanger and at heating temperature below 95°C, Delplace *et al.* (1994) did find that fouling by whey protein solutions is a two-stage phenomenon.

7.6 Possible mechanisms for milk fouling on the heating surface

A large number of studies were focused on the fouling mechanisms using a variety of different dairy fluids, processing conditions and analytical techniques.

In general, fouling is a process that can be also described in terms of colloid chemistry. Since in almost any conceivable case, the nature of solid surface will be different from those of the contaminating materials, initial fouling can be described by a process of heterocoagulation. Once the first layer has been deposited, a second layer can be formed, either by homocoagulation when identical particles deposit onto the already deposited ones, or by a second heterocoagulation process, when "other" particles are attracted by and bound to the initially deposited material (Visser, 1988).

General considerations for a possible mechanism of milk fouling process were proposed as follows (Burton, 1988):

(1) Converting--one or more of the constituents in the product is converted into a form capable of being deposited on the surface;
(2) Transporting--transfer of the depositable material (foulant or foulant precursor) to a surface;
(3) Absorption--fouling material attached to the surface to form an initial layer;
(4) Build-up--deposition of further fouling material on the initial layer;
(5) Balance--between deposition and removal through the shear forces caused by the flow of the products across the deposit-liquid interface.

More recently Visser *et al.* (1995), from their experimental results, proposed a similar but more specific milk fouling process which was distinguished by four independent steps.
(1) The formation of particles in the bulk solution generated by heat;
(2) The deposition of these particles onto the heating surface through diffusion;
(3) The adherence of particles;
(4) The conversion of the adhering particles into a two dimension gel when the surface concentration is sufficiently high.

There is general agreement that at least two separate reactions occurring during heating of milk play an important part in fouling: denaturation and aggregation of whey protein, especially ß-lactoglobulin, and the precipitation of calcium phosphate from solution (Burton, 1988). A schematic presentation of fouling mechanisms during heating whey and milk (below 100°C) was proposed by Jeurnink *et al.* (1996) and shown in Figure 7.3.

The whole process can be described as follows: At room temperature a monolayer of protein is immediately absorbed. Further deposition of protein on top of this monolayer occurs if whey protein undergoes heat denaturation. The active ß-lactoglobulin molecules and aggregates are formed in the bulk and transported to the surface. Their deposition is through reactions with already deposited molecules and this process is enhanced in the presence of calcium. Calcium phosphate may precipitate directly on the

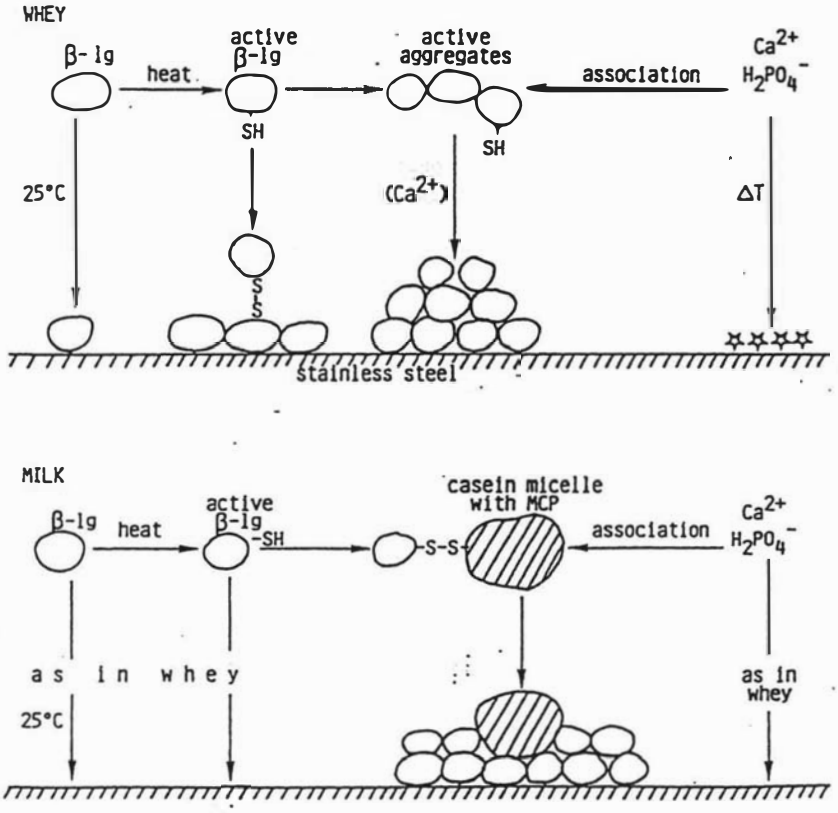

Figure 7.3 Schematic presentation of the fouling mechanisms during heating of whey and milk. (From Jeurnink *et al.*, 1996)

stainless steel wall, promoted by a large temperature difference between the heating surface and the bulk, or it may associate with ß-lactoglobulin aggregates. In milk, where casein micelles are present, calcium phosphate may also associate with the micellar calcium phosphate and the active ß-lactoglobulin molecules may associate with the κ-casein at the surface of the casein micelle and may so entrap the micelles in the deposit.

In milk fouling, other reactions, such as reactions of lactose with the formation of organic acids and the removal of carbon dioxide which result from changes in pH of the solution, may also be involved and their effect in causing the fouling appears to be interrelated with the deposition mechanisms discussed above (Fryer *et al.*, 1995).

7.7 The initial deposited layer of milk fouling

In order to understand the fouling process, many studies were focused on the initial events occurring in milk fouling. It is thought that if the processes which govern the initial period of deposition were understood, it might be possible to extend induction period and thus improve the industrial heat transfer perfomance. Therefore the sequence and the rate of events which make up the initial stage are very important (Fryer *et al.*, 1995).

Although it is well known that the fully-developed deposit consists of a thin mineral-rich layer adjacent to the metal surface, there is still an argument about the nature of the initial layer adsorbed on the metal surface. The described fouling mechanisms proposed by Jeurnink *et al.* (1996) was based on results that as soon as a stainless surface comes into contact with a whey protein solution, even at room temperature, immediately a monolayer of protein adsorbs. However, Burton (1988) described that the first species formed at the heating surface are mineral crystal nuclei. This deposit is formed due to the supersaturation of the mineral salts produced by the higher temperature in the thin liquid layer adjacent to the surface. The results of Daufin *et al.* (1987) and Green *et al.*

(1988) suggest that mineral deposition is crucial in the initial stage of fouling and the minerals are the most likely species to adsorb first.

Many other workers' results support the theory that proteins adsorb first at the surface. Baier (1981) used internal reflectance spectroscopy to study a system at 50°C and found that proteins were the first species to adsorb in milk fouling. Delsing and Hiddink (1983) (bulk temperature of 76°C), followed by Daufin *et al.* (1987) (bulk temperatures from 25 to 88°C), found, using X-ray photoelectron spectroscopy (XPS) and different test fluids, that proteins were the main, though not the only, species to adsorb first. Tissier and Lalande (1986) did not find any minerals in a deposit of 0.0169 μm thickness formed after 1 min. However, when using X ray microanalysis they found high concentrations of calcium and phosphorus at the interface.

Belmar-Beiny and Fryer (1993) used X-ray photoelectron spectroscopy to study the deposits formed by whey protein concentrate after 4 and 150 seconds and found that the composition of deposit film after 4 seconds was close to the theoretical composition of pure ß-lactoglobulin. Only after 150 seconds of contact time were sulfur and calcium detected; no phosphorus was found. These results indicate that proteins are most likely to be the first species to adhere to the stainless steel surface. Proteins are very surface active, and a clean metal surface has a large free surface energy gradient so it would be expected that a layer would form very rapidly. The role of calcium and phosphate ions in milk and whey fouling is quite complex. In the bulk, calcium ions promote aggregation of ß-lactoglobulin not only by binding to the ß-lactoglobulin molecule but also by decreasing the denaturation temperature (Xiong, 1992); on the surface, calcium will form bridges between adsorbed protein and the protein aggregates formed in the bulk and then adhering to the surface (Fryer *et al.*, 1995).

7.8 The rate-controlling processes in milk fouling

From the proposed milk fouling mechanisms, it can be considered that the fouling rate is controlled by two processes, i.e. the mass transfer of active molecules and aggregates

to the surface, and the chemical reactions, which involves a surface reaction and a bulk reaction. The slowest of these processes will be the rate-controlling process. Based on these hypothesis, three cases can be considered (Fryer *et al.*, 1995):

(i) If fouling is mass transfer controlled, the transfer of reacted protein to the wall is the slowest step, and the rate of deposit formation will not be a strong function of temperature.

(ii) If fouling is controlled only by surface processes, deposition will occur wherever the wall temperature is hot enough for protein denaturation and aggregation to occur, regardless of the bulk temperature, the fouling should depend only on the wall temperature.

(iii) If the controlling reaction for fouling takes place in the bulk, then two conditions can be envisaged:

(a) If the wall temperature is such that protein denaturation and aggregation will occur, but the bulk temperature is such that native protein is thermally stable, fouling will result from deposition of protein which has denatured and aggregated in the thermal boundary layer adjacent to the wall.

(b) If both the boundary layer and the turbulent core are hot enough for protein denaturation and aggregation, protein denatured and aggregated in both regions will contribute to deposit formation.

Gotham *et al.* (1989) identified two regimes of protein deposition during the fouling period in a tubular heat exchanger with a 35% whey protein solution; fouling from the thermal boundary layer (controlled by surface reaction at the wall temperature) and fouling from the bulk of the fluid (controlled by bulk reaction, mass transfer and adhesion of active protein aggregates). In the former regime, the rate and extent of fouling depends on the wall temperature regardless of bulk fluid temperature, while in the later regime, fouling occurs when the bulk milk becomes hot enough to produce denatured and aggregated proteins.

Gotham (1990) demonstrated that when whey protein concentrate passes through a tubular heat exchanger with the same temperature difference, an increase in fouling

occurred when the bulk temperature exceeds 75°C, which suggested that the bulk reaction of whey proteins and mass transfer is the controlling process. Bradley and Fryer (1992) also showed that, when the bulk fluid is hot enough to produce denatured and aggregated proteins, fouling deposits will increase when mass transfer to the surface is increased due to a higher denatured protein concentration gradient.

Belmar-Beiny *et al.* (1993) outlined two simple models, based on wall and bulk reactions, that demonstrate that wall reactions alone cannot be responsible for fouling. It is not proposed that bulk processes are the only ones involved, or that they will be important in all situations; the final stage in fouling must be the incorporation of deposit into the surface, which must involve a surface reaction.

The above results suggest that fouling due to milk fluids is not purely controlled by surface reactions but that bulk reaction of milk fluid and mass transfer may be involved, depending on the configuration of the system and its operating variables, such as temperature and flow rate.

7.9 Whey proteins and their denaturation

From a colloid chemistry point of view, the colloidal components in milk, casein micelles and fat globules, are sufficiently stabilised by double-layer forces and hydration layers so that fouling problems at temperature below 100°C are mainly related to its soluble components, i.e. whey proteins, soluble casein and calcium phosphate (Visser, 1988). Therefore it is necessary to know the details of the chemistry of whey proteins as well as their denaturation processes.

Whey proteins comprise about 20% of the protein in bovine milk. They are mainly composed of the 4 compact globular proteins: ß-lactoglobulin (ß-lg), α-lactalbumin (α-la), bovine serum albumin (BSA) and several classes of immunoglobulin (Ig). Comprehensive reviews concerning the whey protein system of bovine milk are available (Eigel *et al.*, 1984; Mulvihill and Donovan, 1987; Fox, 1989).

7.9.1 ß-lactoglobulin (ß-lg)

ß-lg represents about 50% of the total whey proteins in bovine milk or 12% of the total milk proteins. A molecule of ß-lg consists of 162 amino acid residues, has a monomeric molecular weight of about 18,300 Da (Eigel *et al.*, 1984) and exhibits well developed secondary, tertiary and quaternary structures. The secondary structure of bovine ß-lg consists of about 45% ß-sheet, 10% α-helical and 45% unordered structures (Timasheff *et al.*, 1966, 1967, Creamer, *et al.*, 1983). Depending on the pH, ß-lactoglobulin molecules may exist as a monomer, dimers or octamer. Below pH 3.5, the dimers dissociate to monomers due to strong electrostatic repulsion forces. In the pH range from 3.5 to 5.2, the dimers combine to form octamers. Between pH 5.5 and 7.5, the molecules exist as stable dimers. Above pH 7.0, the molecule undergoes reversible conformational changes, and above pH 8.0, the protein is unstable and forms aggregates of denatured protein (Lyster, 1970). It was also found that the monomer-octamer association is not only affected by pH, but also by factors such as protein concentration, temperature and ionic strength (Langton and Hermansson, 1992). The quaternary structure is maintained largely by electrostatic forces (Jelen and Rattray, 1995).

7.9.2 α-lactalbumin (α-la)

α-la is a small protein molecule with a molecular weight of 14,200 Da. It comprises about 20% of the whey proteins, and is generally reported as being the second most important protein. The molecule consists of 123 known amino acid residues (Fox, 1989; Walstra and Jenness, 1984). It is a very compact molecule and nearly spherical in shape. Its secondary structure consists of 26% α-helix, 14% ß-sheet and 60% unordered structure at physiological pH (Robbins and Holmes, 1970). α-la normally exists as a monomer.

7.9.3 Bovine serum albumin (BSA)

BSA is a major component of blood serum, but is also found in whey. It is synthesized in the liver, and goes into the milk via the secretary cells. It represents about 10% of the whey proteins, contains 17 disulphide bonds and one free thiol group per molecule (Reed *et al.*, 1980). This holds the molecule in a multiloop structure. BSA consists of 582 amino acid residues and has a molecular weight of about 66,000 Da (Peters, 1985). The secondary structure of BSA consists of about 10% ß-sheet, 55% a-helical and 25% unordered structures (Reed *et al.*, 1975).

7.9.4 Immunoglobulins (Igs)

Igs represent 10% of the whey proteins. Igs are polymers of two identical light chains and two identical heavy chains joint together by disulphide bridges. They are far the heaviest proteins in whey with the molecular weight of 1.5×10^5 - 9×10^5 Da (Jelen and Rattray, 1995). The Igs are among the most heat-sensitive of the whey proteins (Fox, 1989).

7.9.5 Whey protein structure

Whey proteins in their native state are globular proteins having secondary and tertiary structures. The three dimensional globular structure of the individual whey proteins are stabilised by intramolecular disulphide bonds, hydrogen bonds, hydrophobic interactions and ionic bonds.

The majority of the non-polar hydrophobic amino acid side chain residues are on the interior, and the polar hydrophillic residues are on the exterior part of the molecule. The intramolecular bindings and a loosely held water layer around the molecules make interactions with other molecules difficult (Clark *et al.*, 1981).

7.9.6 Whey protein denaturation and aggregation

Protein denaturation is a process in which the native protein structure changes without alterations in the original amino acid sequence. Thermal denaturation is due to a sudden entropically induced disruption of the native state (Clark *et al.*, 1981). When heated above about 70°C, the structure of ß-lactoglobulin is irreversibly altered by two separate processes of denaturation and aggregation. These processes are consecutive; the native conformation of the protein first is partially unfolds into disordered and non uniform molecules. This is an intramolecular process which exposes the hydrophobic molecular core, together with reactive disulfide and sulfhydryl (-SH) bonds, to an aqueous environment. This unstable configuration is then stabilized by polymerization with other denatured molecules in intermolecular aggregation that may lead to bind the protein molecules to dimers, quatromers, and oligomers and further on to gels (Clark *et al.*, 1981, Hege and Kessler, 1986a). Although denaturation is reversible at low temperatures, as molecules can return to their folded state on cooling, aggregation of whey proteins is totally irreversible; the resulting aggregates are insoluble in water (Fryer *et al.*, 1995). The rate of reaction increases significantly between 71 and 75°C (Donovan and Mulvihill, 1987). One difficulty in interpreting the literature in this area is that the two processes are very difficult to separate, and the whole process is often described as denaturation (Fryer *et al.*, 1995).

7.10 The relationship of whey protein denaturation and milk fouling

Although the exact mechanisms of milk fouling are still not very clear, the correlation between protein denaturation and fouling of heat exchangers has been confirmed by many investigators (de Jong *et al.*, 1992, 1993; Belmar-Beiny *et al.*, 1993). Results obtained by Tissier *et al.* (1984) showed that ß-lg has an important role in the fouling process of heat exchangers. It appears that denaturation of ß-lg and the formation of deposits evolve in parallel along the heat exchanger. Even for whipping cream the correlation between the denaturation of whey proteins and the fouling rate has been demonstrated (Hiddink *et al.*, 1986). Hegg *et al.* (1985), working with solutions of

whey proteins, showed that deposit formation and denaturation was greatest at the isoelectric point of the proteins. They therefore suggested that there was a close connection between protein denaturation and deposit formation.

The measurements of Hegg and Larsson (1981) have shown that in milk, ß-lg is most prone to deposit on metal surface, whereas α-la has a lesser tendency to attach to surfaces.

Hege and Kessler (1986a) pointed out that both the effect of temperature and the activation energy for the process of deposit formation are similar to that on whey protein denaturation. Kessler *et al.* (1986) found that the activation energy for demineralized whey fouling was 315 kJ/mol, whereas the activation energy for protein denaturation was 300 kJ/mol. However, Fryer (1986) and Lalande and Corrieu (1981) found lower values for milk fouling: 87 kJ/mol and 90 kJ/mol respectively. It is likely that different controlling reactions have different rate-limiting steps and therefore different activation energies.

Gotham *et al.* (1992) suggested that aggregation rather than denaturation of whey proteins is the controlling step in deposit formation. Jeurnink (1995b) concluded from his experimental results that the denaturation of the whey proteins, specially the formation of the active ß-lg molecules and aggregates, in the vicinity of the surface is a prerequisite to obtain deposition.

7.11 Conclusions

This review shows that the fouling in milk processing has been studied considerably, but most of the research work was concentrated on tubular or plate heat exchangers and UHT plants. There is lack of knowledge of fouling in other processing units. For example, fouling in evaporators has received little attention. It was known that fouling in multistage evaporators were severe at both first effect and last effect, which were due to the high temperature in the first effect and the high concentration in the last effect.

Little information regarding fouling in the evaporators is available in the published literature (Kessler, 1989; Jeurnink and Brinkman, 1994). The objective of this research work is to study the fouling in an evaporator with a rotating surface.

CHAPTER 8
FOULING IN EVAPORATORS - MATERIALS AND METHODS

8.1 Introduction

The study of fouling in the evaporation process is limited. No publication of fouling in the Centritherm evaporator is available in the literature at present. The objectives of this part of the work were to investigate the fouling phenomena occurring in a Centritherm evaporator and to evaluate the effect of operation variables on the onset and rate of fouling.

8.2 Materials

8.2.1 Equipment

(1) A Centritherm Evaporator (CT1B-2, ALFA-LAVAL) and a rotating falling film evaporator were used;
(2) A temperature recorder (Monitech);
(4) A refractometer (ATAGO, No.25870, Japan);
(5) A PAGE system (Mini protein II equipment, Bio-Rad Laboratories, Richmond, USA);
(6) A pH meter (PHM 61 Laboratory pH meter, Copenhagen, Denmark)
(7) A drying oven (Clayson, Catalogue 011 24, Laboratory apparatus Ltd, Upper Hutt, New Zealand);
(8) Other instruments used include an analytical balance, a stop watch and a measuring cylinder.

8.2.2 Model solutions

To avoid compositional and seasonal variations in feed material, two model feeds were first used in the preliminary trials.

(1) Low heat skim milk powder from Tui Milk Products Company was used to make reconstituted skim milk solutions at 10, 20 and 25% TS.
(2) Powdered whey protein concentrate (ALACEN 134) from the New Zealand Dairy Board was used to make up a reconstituted whey solution at 26% TS.

The solutions were made by sprinkling weighed powder onto a weighed quantity of water (to avoid the formation of agglomerates) in a locally designed milk powder mixer, which was available in the pilot plant at the Food Technology Department, Massey University. Mixing was continued for 5 minutes after all the powder was added, to make sure that any agglomerates or any powder sticking to the walls of the container were dissolved. The solutions were then stored in a chill room before use.

As no detectable fouling was found in the preliminary trials, a sweet cheddar cheese whey solution (total solids = 6.5 - 7.5%, pH = 4.4 - 4.8) from a local cheese factory (Tui Milk Products Company) was chosen for the remainder of the experimental work. All the experimental work was carried out within a two months period in the spring. Thus the compositional, seasonal and daily variations of whey solutions could be regarded as negligible. Manufacture of the cheddar cheese was normally done in the early morning (4-5 am), therefore the whey solution was collected in plastic milk cans and stored in a chill room (4°C). The whey then was transferred to the pilot plant at the Food Technology Department and stored in a chill room until the experiment was carried out.

8.2.3 Chemicals used for cleaning

The caustic alkaline solution, the acid solution and the sanitiser solution used in this part of experimental work were the same as described in section 4.2.4.

8.3 Methods

8.3.1 The Centritherm evaporator and the falling film evaporator

The experimental work was mainly carried out on the Centritherm evaporator system. which was described in section 4.3.1. Some experimental work was also conducted on a falling film evaporator, which was described in section 4.3.2. A comparison of the results obtained with these two evaporators were made. The falling film evaporator was operated without rotation.

8.3.2 The recycle system

One problem with fouling experiments is that good quality milk is relatively stable in the evaporator and the decline in heat transfer coefficient will be detected only after a quite long time (several hours), which means that experimental work on milk fouling is time-consuming and expensive. Alternative approaches to understanding milk fouling have focused on breaking milk down and examining whey protein concentration, or permeates. These solutions foul at a much faster rate than milk, and provide an insight into the fouling process although they may have different fouling characteristics to milk (Kastanas *et al.*, 1995).

To obtain a proper picture of the fouling process in an evaporator, the processing time has to be 4 to 6 hours or even longer. This necessitates the use of large amounts of feed material, which incurs in high costs and practical difficulties to carry out the experiment in a pilot plant. Therefore, to minimize raw material utilisation, a recycled whey solution was employed in this experiment. About 40 litres of whey were recycled in each trial.

To recycle the whey solution in the system and maintain a constant concentration of the feed, the concentrated solution and the vapour condensate were measured and fed back to the feed container.

When using whey with this recycling system, it was found that the fouling resistance would reach a constant value after running for 4 hours. Therefore, the rest of runs were stopped after this time.

8.3.3 The examination of denatured whey proteins

Polyacrylamide Gel Electrophoresis (PAGE) was used to determine the extent of whey protein denaturation during processing in the Centritherm. The gel preparation and the procedures of using PAGE are given in the Appendix VI.

8.4 Instrumentation

This part was the same as that described in section 4.5.

8.5 Experimental

8.5.1 Experimental variables

The levels of experimental variables used are shown in Table 8.1.

Table 8.1 Ranges of experimental variables

Evaporating Temperature (ET)	60, 70°C
Temperature difference (ΔT)	10, 20K
Rotating speed (RS)	105, 186 rad/s
Feed flow (FF)	1.67×10^{-5}, 4.2×10^{-5} m^3/s

8.5.2 Experimental design

A 4^2 factorial experimental plan was employed using the Plackett-Burman experimental design program (supplied by the Food Technology Research Centre, Massey University) to find out interactions between variables.

Table 8.2 The arranged trials with selected variables.

Trial	ET	ΔT	RS	FF
1	-	-	-	-
2	-	-	+	+
3	-	+	-	-
4	-	+	+	+
5	+	-	-	+
6	+	-	+	-
7	+	+	-	-
8	+	+	+	+

Note: '+' represents a high value, '-' represent a low value

Two trials of the middle point and duplicate of each trial were made.

To assess the effect of individual variables, other trials were also carried out.

8.5.3 Experimental Procedure

The use of the Centritherm evaporator and experimental procedures were the same as those described in sections 4.7 and 4.8. One modification was made to the experimental procedure for the measurement of vapour condensate flow. As the fouling process is a transient process, the measurement of vapour condensate flow rate was done as quick as possible. Therefore flow was measured for a two minute period (triplicate) at every hour during each test run.

8.5.4 Evaporator Cleaning

A special attention was given to the cleaning procedure described in section 4.7.2.

An extended long time cleaning procedures was employed in order to achieve maximum removal of organic or inorganic deposits so that no deposit nucleation sites remain, which might accelerate subsequent deposition.

After the completion of the trial, the flow was switched to water and the flow rate was increased to the maximum possible, until the water coming out from the evaporator becomes clean, which took about two minutes. The flow were then switched from water to detergent. Two kinds of detergents were used: an alkaline-based solution (AC-180) and an acid-based solution (AC-300). The action of alkaline detergent lasted for 30 minutes, at a concentration of 1% (w/w), to remove the deposited proteins, then acid detergent, at concentration of 1% (w/w), was circulated for 30 minutes to remove the deposited minerals. Between the detergent stages, and at the end of cleaning, rinsing with water stages, each lasting 10 minutes, were used.

The cleanliness of the surface was checked once by disassembling the apparatus. It was observed that the deposits had been removed completely after the cleaning using the above procedures. Before each test, the heat transfer coefficient with water was

measured to check that the heat transfer coefficient had not changed, to ensure that the surface was clean.

8.6 Theory and data processing

The equation for the overall heat transfer coefficient in an evaporator with a clean surface can be written as:

$$\frac{1}{H_o} = \frac{1}{h_s}\frac{A_m}{A_s} + \frac{1}{h_l}\frac{A_m}{A_l} + \frac{\delta_w}{k_w} \qquad (8\text{-}1)$$

If the effect of fouling is taken into account, a fouling resistance (R_f) can be included in the equation as:

$$\frac{1}{H(t)} = \frac{1}{H_o} + R_f(t) = \frac{1}{H_o} + \frac{\delta_d(t)}{k_d} \qquad (8\text{-}2)$$

or

$$\frac{1}{H(t)} = \frac{1}{h_s}\frac{A_m}{A_s} + \frac{1}{h_l}\frac{A_m}{A_l} + \frac{\delta_w}{k_w} + \frac{\delta_d(t)}{k_d} \qquad (8\text{-}3)$$

where

$$R_f(t) = \frac{\delta_d(t)}{k_d} \qquad (8\text{-}4)$$

$\delta_d(t)$ is the thickness of the fouling layer at time t.

k_d is the thermal conductivity of the fouling layer.

The fouling resistance can be calculated from the overall heat transfer coefficients using the following equation:

$$R_f(t) = \frac{1}{H(t)} - \frac{1}{H_0} \qquad (8\text{-}5)$$

The overall heat transfer coefficients (H_o and H(t)) are computed by using the measured flow rate of vapour condensate (W_{exp}), the temperature difference between the steam condensing and the liquid evaporating temperatures (ΔT), and the latent heat (h_{fg}), which is a function of the evaporating temperature. The calculation formula is the same as the Equation 4-1 given in the Chapter 4. Thus, the fouling behaviour in the evaporator can then be estimated by measuring the change in the overall heat transfer coefficients with time.

Changes in the flow rate of vapour condensate which result from fouling were monitored in order to determine the changes of overall heat transfer coefficient and the fouling resistance changes with the time.

All collected data were loaded into the Quattro program. The calculated results are given in the Appendix VII.

CHAPTER 9
FOULING IN EVAPORATORS - RESULTS AND DISCUSSION

The experimental work presented in this chapter deals with the fouling in a Centritherm evaporator under different operating conditions using whey solutions as the fouling material. The effects of variables, such as evaporating temperature, difference between the liquid evaporating and the steam condensing temperatures, and rotating speed of the heating surface on fouling are discussed. The interaction of the experimental variables on the evaporator surface fouling are also discussed. Possible mechanisms of whey fouling on the rotating surface are then proposed.

9.1 Preliminary experimental results

Initially, several exploratory experiments were carried out, using reconstituted skim milk solutions with concentrations of 10%, 20% and 25% total solids, and a reconstituted whey powder solution with a concentration of 25% total solids, at evaporating temperatures of 50, 60 and 70°C, a temperature difference of 20K, a rotating speed of 186 rad/s, and a feed flow rate of 4.2×10^{-5} m^3/s.

A summary of the experimental results are presented in Table 9.1. As can be seen in this table, there was no fouling detectable for these solutions after running for more than 6 hours. These results were not expected. One possible reason for this results is that materials which are responsible for forming the deposits on the surface have been removed (inactivated) or reduced during the manufacture of powders. Analysis of fouled deposits in evaporators has shown the deposits were mainly whey proteins and minerals (Jeurnink and Brinkman, 1994). The depositable materials, therefore, could include some minor constituents in their native form (Burton, 1988), minerals and denatured whey protein. It has been found that aggregated whey proteins are less active in the fouling process (Jeurnink, 1995a). Jeurnink (1995b), similarly, found that reconstituted milk gave much less fouling than fresh milk in tubular heat exchangers.

It was suspected that the process of reconstitution presumably caused other changes affecting the fouling behaviour.

Table 9.1 Summary of preliminary experimental results after 6 hours evaporation running

Trials	Solutions	ET (°C)	ST (°C)	RS (rad/s)	FF (m^3/s) x 10^{-5}	Time (hrs)	Final R_f (m^2K/kW)
1	10% TS Skim milk	50	70	186	4.2	6	0
2	20% TS Skim milk	60	80	186	4.2	8	0
3	25% TS Skim milk	70	90	186	4.2	7	0
4	25% TS WPC	60	80	186	4.2	7	0

Another possible reason is that the liquid evaporating temperature and the temperature of the heating surface in evaporators is much lower, when compared with that in sterilizers and UHT plants. Thus, there is no fouling to be detected on the surface of the Centritherm evaporator by using these solutions.

Hence, reconstituted skim milk and whey solutions, which are frequently reported in the literature for fouling studies in sterilizers and UHT plants, were not used, instead, fresh sweet cheese whey was used for the remainder of this study.

9.2 Effect of evaporation temperature and temperature difference on fouling

Figures 9.1 and 9.2 show the fouling resistance as a function of time at different temperature differences, feed flow rate and evaporating temperature. The figures clearly illustrate that fouling resistance increases with time for cheese whey at both evaporation temperatures 60°C and 70°C (Figure 9.1 and 9.2 respectively).

All the fouling curves depicted in Figure 9.1 (evaporating temperature 60°C) show an induction period less than one hour. However there is no induction period for an evaporating temperature of 70°C and a temperature difference of 20K. An induction period of about half an hour was observed for an evaporating temperature of 70°C and a temperature difference of 10K. It appears that this period was needed to achieve sufficient denaturation of whey protein to induce fouling.

It was demonstrated by other investigators (Jeurnink, 1995a, b; de Jong *et al.*; 1992, Hege and Kessler, 1986a) that the denaturation of the whey protein is strongly associated with the milk fouling and that the rate of whey protein denaturation increased as the temperature rose.

As illustrated in the figures there is a strong influence of the temperature difference on the evaporator fouling, whereas the influence of the feed flow is much weaker. If Figures 9.1 and 9.2 are combined for a given feed flow and temperature difference, it can be clearly seen that evaporation temperature increases fouling rate (Figure 9.3).

In general, the higher the evaporation temperature and temperature difference, the greater the fouling on the surface. This can be attributed to the fact that depositable materials adsorb on the surface more quickly at a high temperature than at a lower temperature (Hegg *et al.*, 1985; Roscoe and Fuller, 1994).

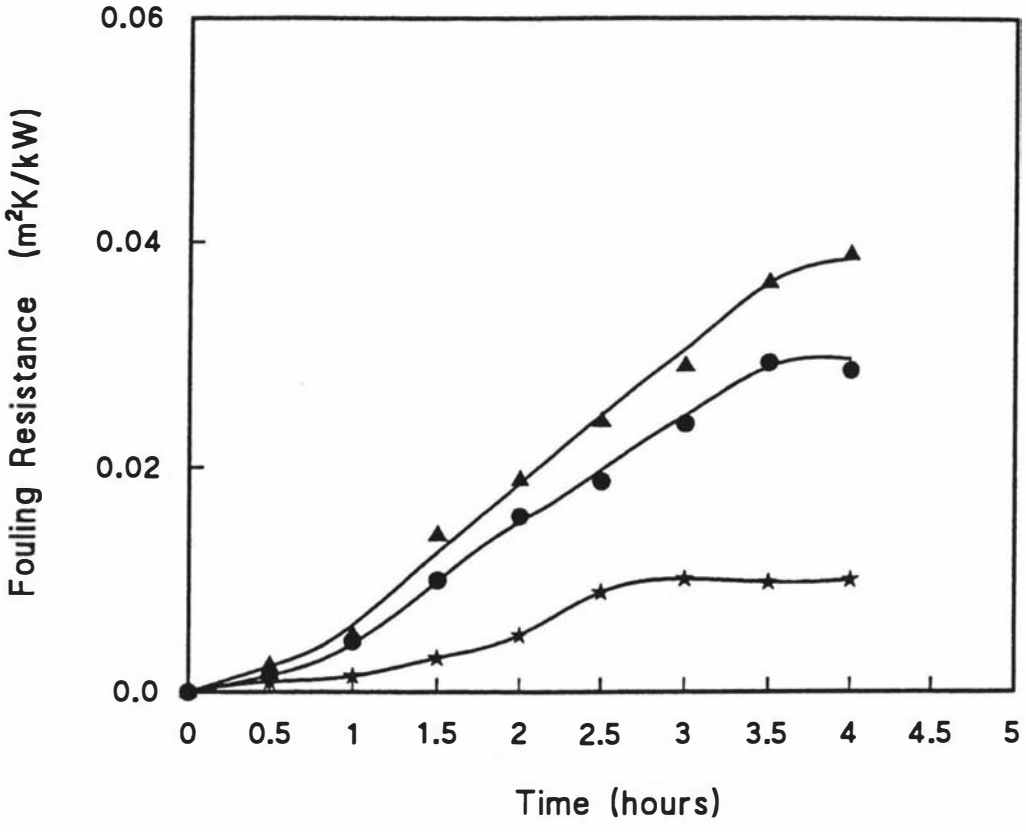

Figure 9.1 Fouling resistance as a function of time for recycled sweet cheese whey in the Centritherm evaporator at an evaporating temperature of 60°C and a rotating speed of 105 rad/s.

▲ Temperature difference: 20°C, feed flow: 1.67×10^{-5} m^3/s

● Temperature difference: 20°C, feed flow: 4.2×10^{-5} m^3/s

★ Temperature difference: 10°C, feed flow: 1.67×10^{-5} m^3/s

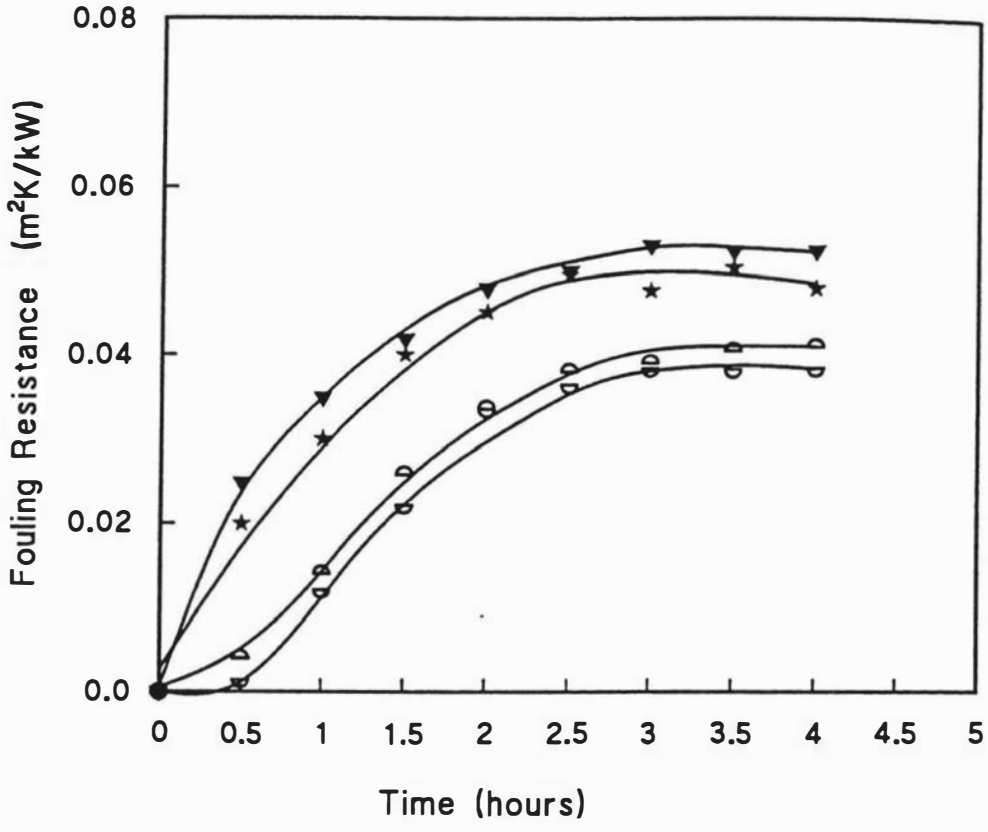

Figure 9.2 Fouling resistance as a function of time for recycled sweet cheese whey in the Centritherm evaporator at an evaporating temperature of 70°C and a rotating speed of 105 rad/s.

▼ Temperature difference: 20°C, feed flow: 1.67×10^{-5} m^3/s

★ Temperature difference: 20°C, feed flow: 4.2×10^{-5} m^3/s

⌓ Temperature difference: 10°C, feed flow: 1.67×10^{-5} m^3/s

⌓ Temperature difference: 10°C, feed flow: 4.2×10^{-5} m^3/s

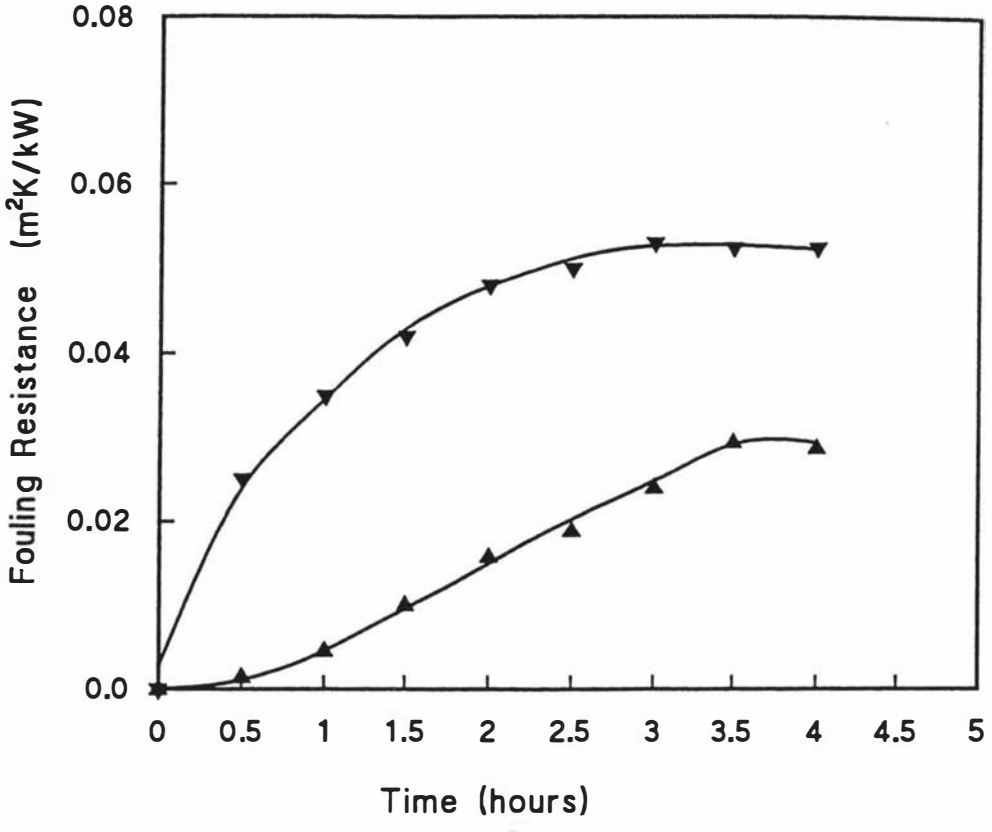

Figure 9.3 Fouling resistance as a function of time at different evaporating temperatures for recycled sweet cheese whey in the Centritherm evaporator. Rotating speed: 105 rad/s, feed flow: 1.67×10^{-5} m^3/s, temperature difference: 20°C.

▼ Evaporating Temperature: 70°C

▼ Evaporating Temperature: 60°C

The change in the state of protein in cheese whey solutions after running (recycled) in the evaporator at 60°C and 70°C for 6 hours was determined using PAGE. It was found that there were no detectable denatured proteins at 60°C, and only loss of BSA was found at 70°C.

Table 9.2 Percentage loss of native whey protein during evaporation at a temperature of 70°C and a temperature difference of 20K

Time (hour)	1	2	3	4	5	6
α-la	0	0	0	0	0	0
β-lg	0	0	0	0	0	0
BSA	44%	50%	61%	72%	72%	72%

Results for the more severe conditions are presented in Table 9.2. The gel photograph of PAGE is given in the Appendix VIII.

By using equations derived in Chapter 5, the inner surface temperature of the rotating cone was calculated to be about 77°C, when the evaporation temperature was 70°C, the temperature difference 20K, the rotating speed of cone 186 rad/s, and the feed flow 4.6 x 10^{-5} kg/s. This reveals that although the steam temperature was 90°C, the temperature at which the whey solutions were subjected was not very high. At this temperature only BSA would be expected to denature. This explains why only the BSA was 72% denatured but other whey proteins were undenatured after running the evaporator at 70°C for 6 hours.

Although the content of BSA in the whey is small, a thin layer of denatured BSA could be easily attached on the surface and be associated with other depositable materials existing in the whey. Most of the research work regarding fouling in milk processing was found that other proteins mainly contribute to deposits. One example is given in section 7.4. When a pasteurizer was operating at 72°C, only β-lg, Igs, and α-Casein were included in milk deposits. Given that the temperature difference used in pasteurization is usually higher than that for evaporation, the temperature of the steel surface is appreciably higher in pasteurization. Hence in this process denaturation of β-lg, Igs, and α-Casein, may occur as is shown in Table 7.1 (p129), but is much less likely in evaporation. BSA has not been

literature as a precursor of fouling. The results obtained in this work show that BSA plays an important role in the initial stage of fouling, especially for fouling in the evaporation process.

9.3 Visual observation of the whey deposits on the surface.

After a run was completed, the Centritherm evaporator was disassembled and the fouled cone was carefully taken of the machine and visually observed. A photograph of the evaporator cone is presented in Figure 9.4. Visual inspection showed that the deposited film was thin and soft, which appears to be of the type A milk deposit described by other investigators (Burton, 1968, Lalande *et al.*, 1984, Tissier *et al.*, 1984). It was planned to weigh the mass of deposited materials and make a chemical analysis of the deposit, but it was very difficult to remove a deposit sample from the cone surface. It was also not practical to insert a test section, which could remove a sample after the experiment in order to examine the fouled surface. Therefore only a visual observation was done.

If the k_d is taken as 0.3 W/m.K (Wood, 1982), from a theoretical calculation, the fouled deposit thickness on the cone surface, assuming a fouling resistance of 0.04 (m^2K/kW), could be determined as 12 μm. Obviously, the low conductivity of the fouling layer makes such a thin deposit layer to have a significant reduction in the overall heat transfer coefficient.

9.4 Effect of the rotating speed on fouling

The effect of rotating speed on the fouling resistance at two different feed flows and temperature differences can be observed in Figure 9.5. It appears that the increase of rotating speed reduces fouling at low temperature differences. This effect, however, is not significant at higher temperature differences. This result suggests that temperature is more important than the liquid flow velocity. It may be explained that at higher temperature difference, the wall temperature (temperature differences were altered

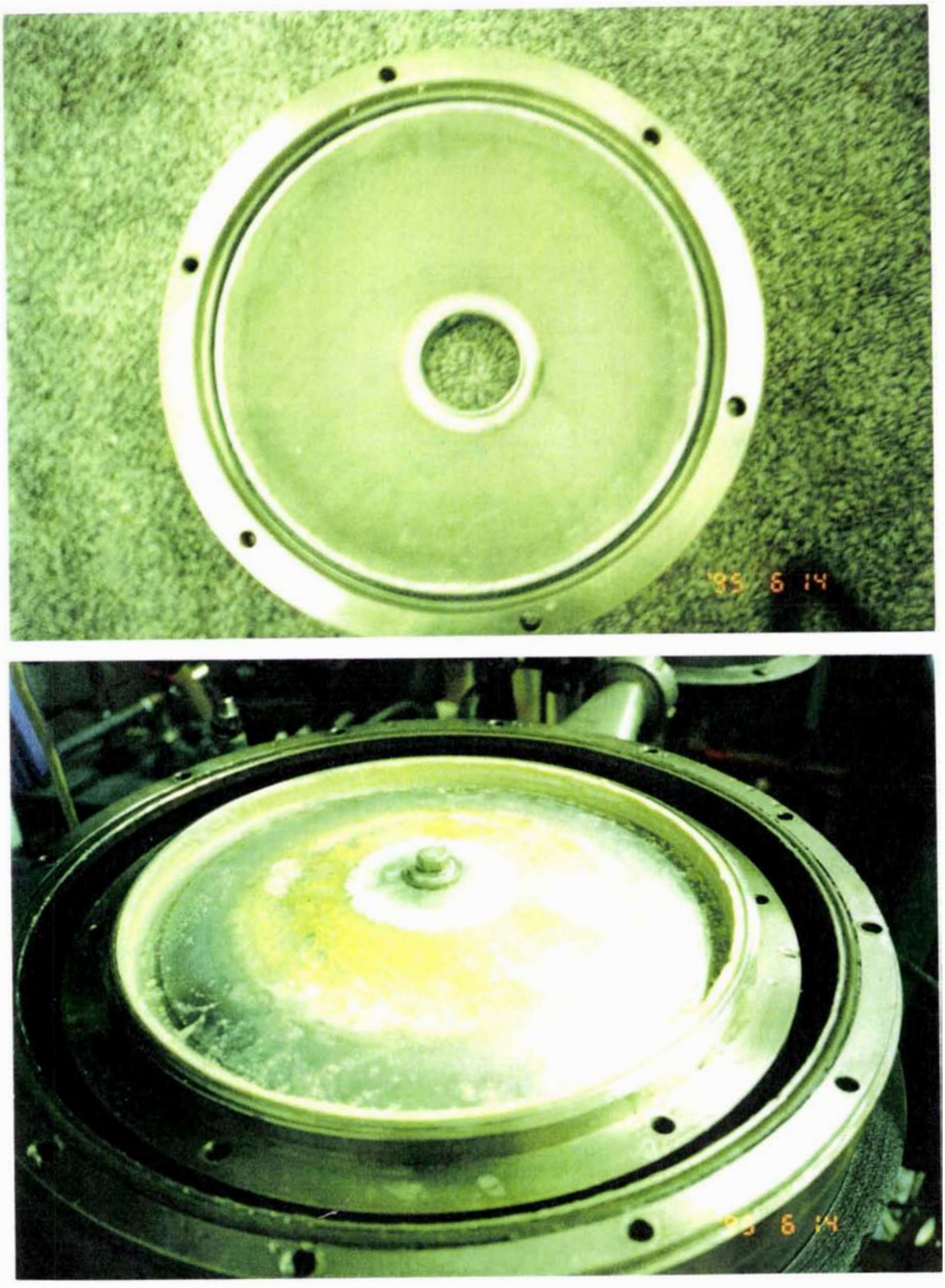

Figure 9.4 The fouled rotating surface of the Centritherm evaporator

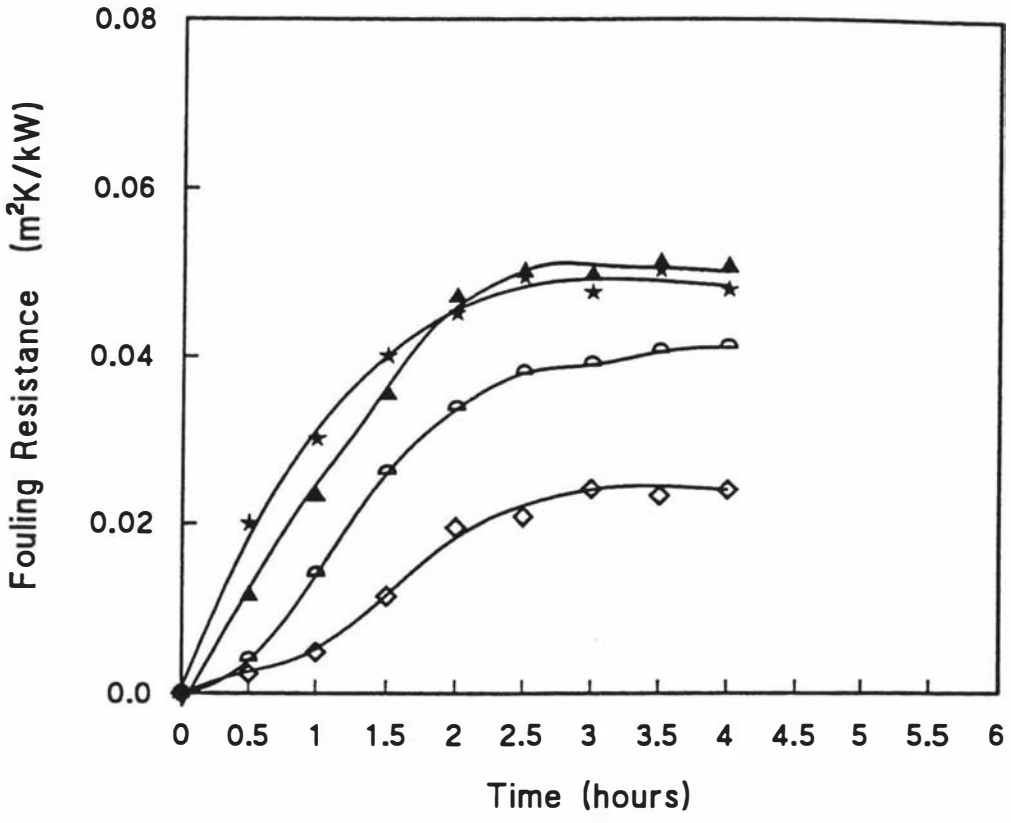

Figure 9.5 Fouling resistance as a function of time for recycled sweet cheese whey in the Centritherm evaporator at an evaporating temperature of 70°C and different rotating speed.

★ ΔT: 20°C, FF: 4.2×10^{-5} m^3/s, RS: 105 rad/s

▲ ΔT: 20°C, FF: 4.2×10^{-5} m^3/s, RS: 186 rad/s

○ ΔT: 10°C, FF: 1.67×10^{-5} m^3/s, RS: 105 rad/s

◇ ΔT: 10°C, FF: 1.67×10^{-5} m^3/s, RS: 186 rad/s

by changing the steam temperature) is higher and activated molecules are formed at the liquid film close to the wall and attached to the deposited layer, whereas, at lower temperature difference, the activated molecules are formed in the bulk solution and then transferred by mass transfer to the surface, which is affected by the liquid film velocity. It can also be seen that the final measured fouling resistances after 4 hour operation depended of the temperature differences.

Figure 9.6 shows a comparison between fouling in the falling film evaporator and the Centritherm evaporator. It can be seen that the fouling rate is higher in the falling film evaporator than that in the Centritherm evaporator. This shows that the high velocity of liquid film delays the formation of the deposit on the heat transfer surface. In theory, the higher the rotating speed, the higher the centrifugal force applied on the liquid film. Under the action of a higher centrifugal field, the velocity gradient in the liquid film becomes large and the thickness of the laminar sublayer is reduced. Therefore, the deposition rate is delayed and the increasing rate of thermal resistance with time will be lower. Taborek *et al.* (1972) also found that increased flow velocity results not only in higher heat transfer coefficients, but in a decreased tendency towards fouling.

One point which should be taken into account is that the same amount of whey solutions were used in each trial for the falling film evaporator and the Centritherm evaporator, but the heat transfer area in the falling film evaporator was more than the double that in the Centritherm (0.2 m^2 in the falling film evaporator and 0.09 m^2 in the Centritherm). Therefore, the final fouling resistance corrected by area in the falling film evaporator (about 0.16 m^2K/kW) will be much higher than that in the Centritherm evaporator (about 0.047 m^2K/kW).

9.5 The interaction of variables on the fouling resistance

The fouling process is a transient process. To find out the interaction between variables, the values of fouling resistance after 4 hours operation, obtained in the 4^2 factorial experiment, were loaded into a regression analysis program (Quattro).

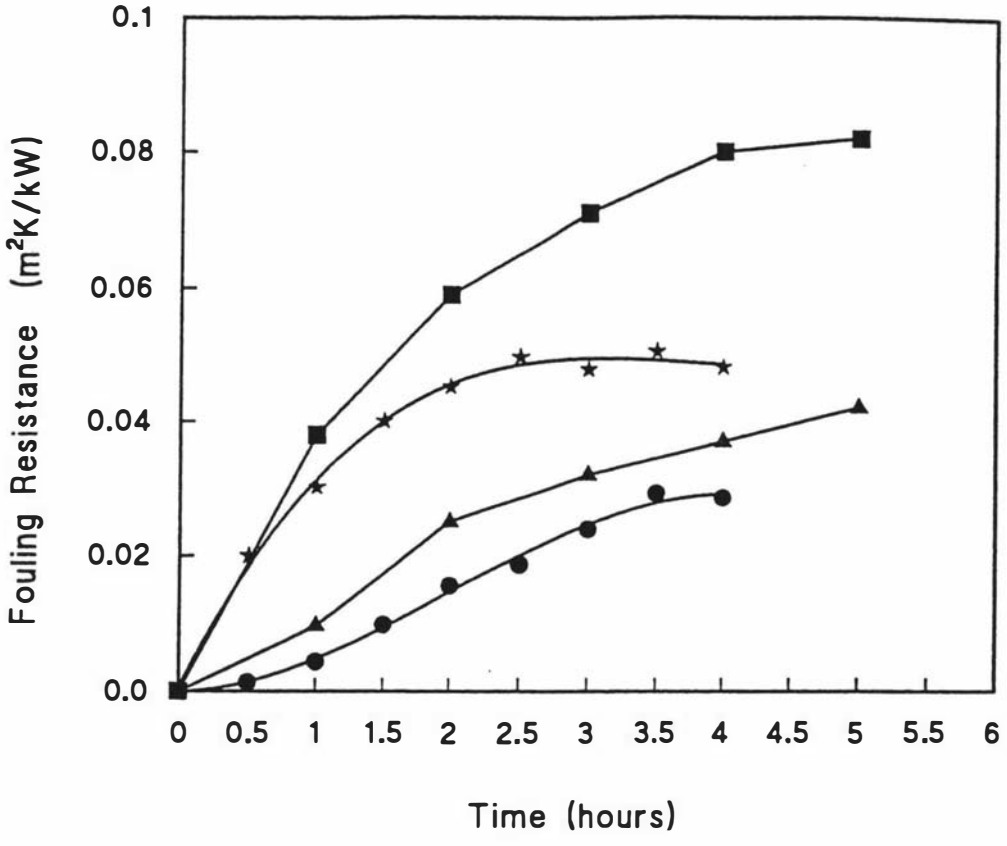

Figure 9.6 Comparison of fouling resistances in the falling film evaporator and the Centritherm evaporator for sweet cheese whey at a temperature difference of 20°C.

■ ET: 70°C, FF: 4.2×10^{-5} m^3/s (Falling film evaporator)

★ ET: 70°C, FF: 4.2×10^{-5} m^3/s, RS: 186 rad/s (Centritherm)

▲ ET: 60°C, FF: 1.67×10^{-5} m^3/s (Falling film evaporator)

● ET: 60°C, FF: 1.67×10^{-5} m^3/s, RS: 105 rad/s (Centritherm)

The following equation was obtained:

$$R_f = 3.4\times10^{-3}T_{evp} - 3.1\times10^{-5}\Omega + 5.2\times10^{-2}Q_f - 7.5\times10^{-4}T_{evp}Q_f + 1.4\times10^{-6}\Delta T\Omega \quad (9\text{-}1)$$

(R^2 = 95.0%, df = 10)

It was found that the interaction between evaporating temperature and feed flow rate causes a decrease in the fouling resistance. A possible explanation may be that the higher evaporating temperature causes a reduction on the viscosity of the evaporating solution, which in turn encourages turbulence and decreases the fouling rate (Taborek *et al.*, 1972).

It was also found that the interaction between the temperature difference and rotating speed causes the fouling resistance to increase. This would be showing that the effect of the temperature difference on the fouling rate is larger than that of the rotating speed.

9.6 The building up of the deposits

During the experimental trials, an interesting phenomena was found. For the same operation conditions fouling rate increased when a new whey solution was introduced in the evaporator. It can be seen from Figure 9.7 that the fouling resistances increase with time after new whey solutions were introduced into the system. The whole process for the first whey solution was run for the first four hours and then second and third whey solutions were introduced and run for another three hours respectively. These results would indicate that depositable materials in the whey would be used up or inactivated after running for some period and the deposit rate largely depends on the concentration of the depositable materials (activated molecules). This result agrees with the fouling model proposed by Jeurnink (1995b). He found that the fouling rate is strongly related to concentration of activated molecules (e.g. unfolded whey protein) in the solutions. Therefore, the results of this research seem to indicate that the

denaturation of whey proteins in the vicinity of the surface is a prerequisite to obtain fouling.

Figure 9.7 clearly illustrates that there is an induction period after a new whey solution is introduced. However, the induction period decreases, i.e. it is about one hour for the first solution and about half an hour for the next introduced solutions. This may be due to the fact that it takes less time for depositable materials to be adsorbed on the fouled or unclean surface than on the clean surface (Burton, 1988). So the first induction period is longer than the following induction periods.

These results suggest that the formation of the activated molecules is a critical factor to influence the fouling process. At the higher temperature, the activated molecules formed fast and the rate of deposition was therefore quicker, while at lower temperatures, the activated molecules formed at relatively slow rate.

9.7 The possible fouling mechanism of whey solutions on the rotating surface

The above results suggest that the fouling mechanism is due to the formation of activated molecules and it is a critical factor to influence the fouling process. The formation of activated molecules, largely due to the denatured whey proteins (in this experimental work, BSA was found as a major activated molecule), is a combination of time and temperature. At high temperatures, the activated molecules form fast and the rate of deposition is, therefore, quicker, while at low temperatures, the activated molecules form relatively slowly and the rate of deposition is also low. The increase of liquid velocity over the surface delays the formation of the deposits at low temperatures, which results in a low concentration of activated molecules.

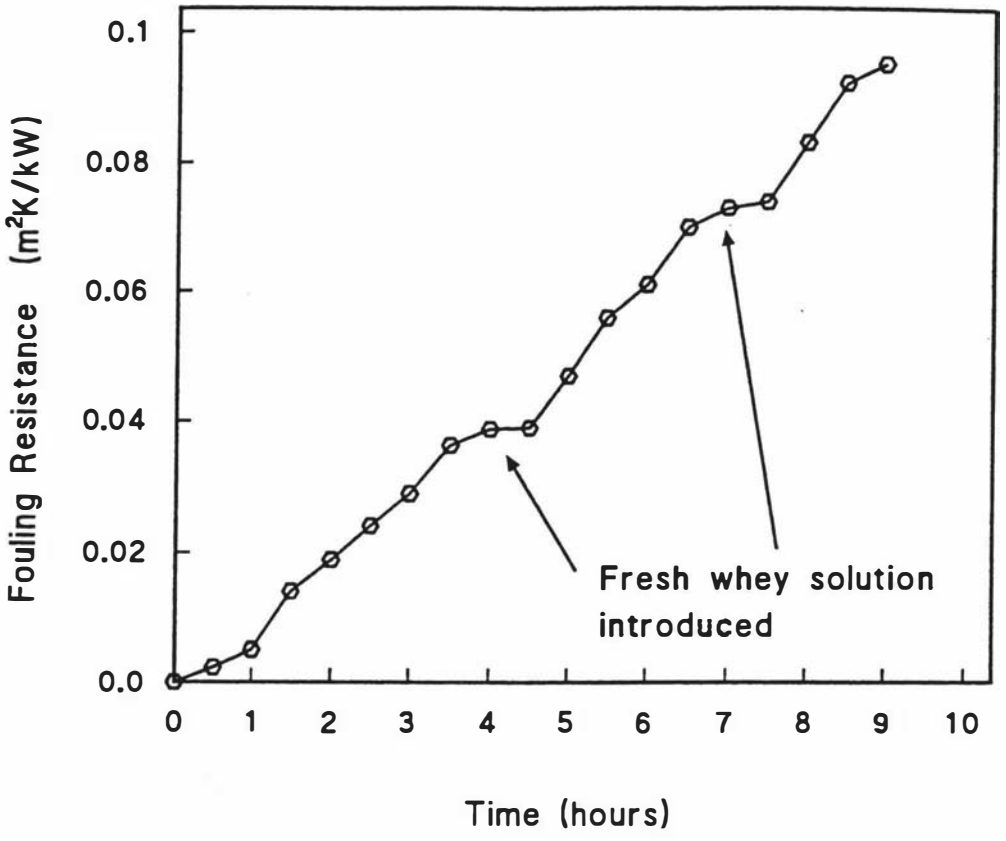

Figure 9.7 Fouling resistance as a function of time for recycled sweet cheeese whey, when a new whey solution is introduced. Rotating speed: 105 rad/s, evaporating temperature: 60°C, temperature difference: 20°C, feed flow: 4.2×10^{-5} m^3/s.

9.8 The evaporation mechanism on a fouled heat transfer surface

In order to study the effect of deposited layer on the overall heat transfer coefficient, a fouled heat transfer surface (whey solution was run more than 5 hours until a constant fouling resistance was achieved) was then used to find out how the overall heat transfer coefficient changed with the temperature difference. The results are depicted in Figure 9.8.

Figure 9.8 shows that the temperature difference affects the overall heat transfer coefficient after a deposit layer was established on the surface. The same trend was found for both the fouled and the clear surfaces. It can be then assumed that a similar mechanism of evaporation exists on fouled and clean surfaces.

9.9 Conclusions

The results obtained can be summarised as follows:

(1) Fouling is strongly linked with evaporation temperature and temperature difference because of the denaturation of whey proteins, which are temperature dependent.

(2) BSA was found to be an important depositable material involved in the fouling process with whey solution.

(3) The presence of denatured whey proteins in the vicinity of the surface is a prerequisite to obtain deposition. Aggregated whey proteins have less ability of depositing onto the surface.

(4) A small amount of denatured whey protein could reduce the heat transfer coefficients significantly.

(4) Fouling is also a function of liquid velocity. The effect is more significant at lower evaporation temperature. Increasing the rotating velocity will delay the formation of an initial layer and reduce the rate of fouling.

(5) Fouled and clean surfaces have the similar evaporation mechanism.

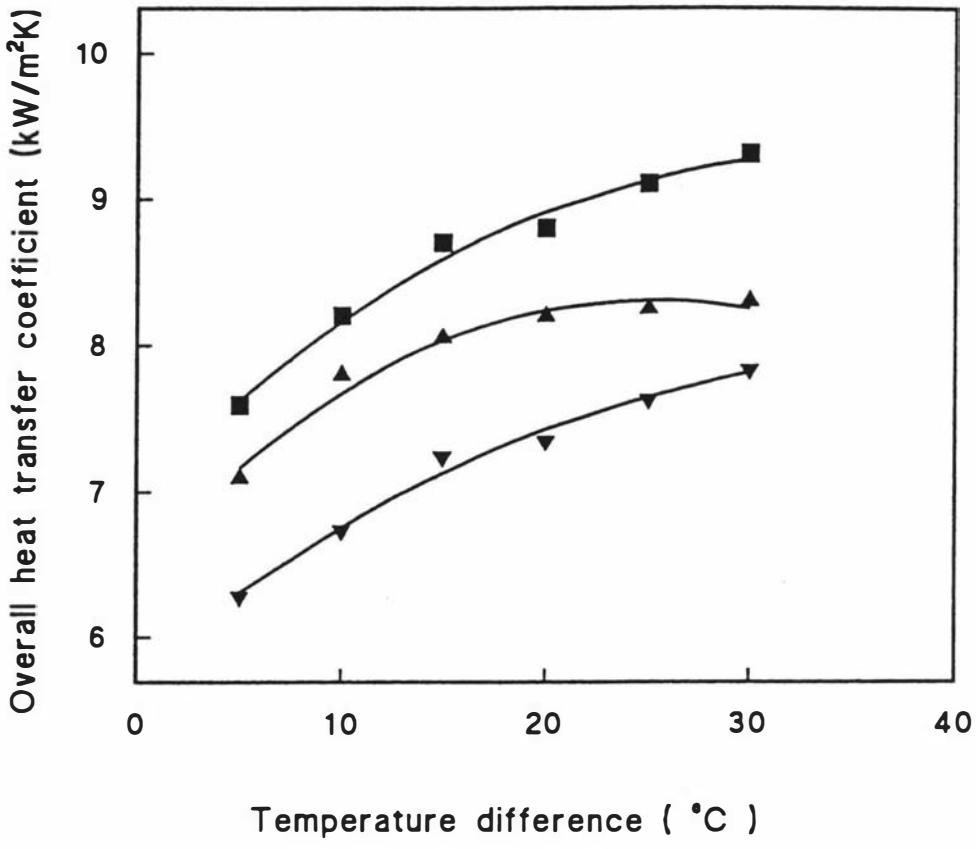

Figure 9.8 Overall heat transfer coefficient as a function of temperature difference for different liquids and clean and fouled rotating surfaces in the Centritherm evaporator. Rotating speed: 186 rad/s

■ Water on clean surface, ET: 60°C, FF: $5x10^{-5}$ m^3/s

▲ Sugar solution (20%) on the clean surface, ET: 60°C, FF: $5x10^{-5}$ m^3/s

▼ Whey solution on fouled surface, ET: 65°C, FF: $4.2x10^{-5}$ m^3/s

CHAPTER 10
OVERALL DISCUSSION AND RECOMMENDATIONS

10.1 Overall discussion

10.1.1 Background of the Ph.D. programme

The starting point of this research work was to evaluate the feasibility of a new on-farm evaporation system, in which a small scale evaporator could be used to pre-concentrate milk on farms.

The proposed on-farm evaporator consisted of a rotating heating surface to improve heat transfer and at the same time compresses the vapour. Thus, an understanding of the factors controlling heat transfer coefficients on the rotating surface was an important step for the design of the on-farm evaporator and constitute one major part of this Ph.D. thesis.

The initial idea was to develop a highly efficient falling film evaporator with rotating surfaces. This was based on the fact that the Centritherm evaporator (rotating surface evaporator) could provide very high heat transfer coefficients (of the order 10 kW/m^2K). If this could be achieved in the falling film evaporator with rotating tubes, the efficiency of the evaporator could be improved significantly. After a series of trials on a falling film evaporator with a rotating surface, it was realized that the cone angle was a crucial factor in the Centritherm evaporator design to produce the high heat transfer coefficient.

Then a cone evaporator (with a 10° of half top angle) was built to study the effect of the cone angle on the heat transfer coefficient in a rotating surface evaporator. At same time, another idea was generated to develop an evaporator in which the evaporator body is connected with a vapour compressor. This evaporator was expected to be operated

in an efficient way by taking the advantages of the high heat transfer coefficient of a rotating surface evaporator and the nearly isothermal compression of the vapours. A lot of efforts were made to develop the prototype for this evaporator and a lot of time was spent to test it. Unfortunately, this idea was not successful as no compressed vapour was able to be generated.

Then the main attention was focused on the factors affecting heat transfer coefficient in the rotating surface evaporator and a theoretical model was developed. After that, the aspect of fouling in this type of evaporator was also investigated.

From this work, a possible design of a suitable evaporator to be used in on-farm evaporation system has been developed.

10.1.2 Liquid film flow and heat transfer on the rotating surface

The developed analytical model gave a clear picture of what occurs in a thin film evaporator with rotating surface in terms of film thickness and heat transfer coefficient.

It is shown that the liquid film thickness and the heat transfer coefficients are affected by the feed flow rate, rotating speed of the cone, length of the cone, angle of the cone, and liquid viscosity. The local film thickness decreases with decrease in feed flow rate and liquid viscosity, increase of cone length and rotating speed. Increase of cone angle results in thinner liquid films and higher heat transfer coefficients.

10.1.3 Heat transfer in the Centritherm and the cone evaporators

The theoretical calculated overall heat transfer coefficients show a similar trend than the experimental results obtained in the Centritherm and the cone evaporators.

In general, the overall heat transfer coefficient increase with the increase of the rotating speed. Good agreement between theoretical and experimental values of overall heat transfer coefficients as a function of rotating speed was obtained with the Centritherm evaporator, when evaporating temperature was 70°C and difference between the steam condensing and the liquid evaporating temperatures was 10K.

The measured overall heat transfer coefficient in the Centritherm evaporator increases with the increase of temperature difference until 30K and then decreases. This result can be explained by the fact that the liquid-vapour interface evaporation may occur only at low temperature differences. Bubble formation on the heating surface may occur when high temperature differences are used. The bubble formation could create turbulence in the liquid film, which improves heat transfer, but it could also thicken the film, which reduces heat transfer to the liquid-vapour interface. When the temperature difference becomes too high, bubbles may start sticking to the surface and reducing the available surface, which causes the decrease of overall heat transfer coefficient.

The overall heat transfer coefficient increases with increase in evaporating temperature due to the change in the liquid physical properties, namely the viscosity and thermal conductivity.

The overall heat transfer coefficient was expected to decrease with increase of the concentration of sugar solutions, mainly due to the increase of liquid viscosity. However, it was found that heat transfer coefficients were of the order of 5 kWm^2/K for 60% sugar solutions at temperature differences greater than 15K in the Centritherm evaporator.

The overall heat transfer coefficients experimentally obtained with the cone evaporator were lower than those measured in the Centritherm evaporator. This shows that the cone angle plays an important role in the overall heat transfer coefficient of rotating thin film evaporators. There was a large difference between theoretical and experimental

values in the cone evaporator which may be due to a poor distribution of the liquid film.

The discrepancies between experimental and theoretical results could be attributed to the following reasons:

1) It was assumed in the theoretical model that the liquid film moves across the conical surface as a smooth film without waves. However, it was observed by Shinn (1971) that waves exist in the liquid film when it moves across the rotating conical surface. This may be due to the vibration of surface when it rotates. Waves are likely to increase turbulence and hence the heat transfer.

2) It was also assumed in the theoretical model that the evaporation takes place only at the surface of liquid film, which is true only at the lower temperature difference. At higher temperature differences, bubbles are likely to be formed on the heating surface, and affect the heat transfer.

3) Centrifugal forces acting on the liquid film increase the pressure in the film as the rotating speed rises. This causes that the saturation temperature of the liquid on the conical surface increases slightly and therefore reduces the temperature difference between the heating surface and the liquid film.

4) Differences between calculated and experimental heat transfer coefficients could also be caused by the presence of non-condensable gases in the steam jacket, which depend on the efficiency of non-condensable gases removal by the steam-trap system. The concentrations of non-condensable gases were not measured but it has been reported that it could seriously affect the steam side heat transfer coefficients (Mincowycz and Sparrow, 1966; Machareth, 1993).

10.1.4 Heat transfer in falling film evaporator with rotating tube

From the results obtained with the falling film evaporator, it can be concluded that rotating the tubes of a falling film evaporator will increase the overall heat transfer coefficient but the increase obtained is very dependent on feed flow rate, and is not sufficient to justify the use of this evaporator in the industry. Rotation also appears to delay the onset of bubble formation in evaporation, and reduce the effect of vapour velocity at the top of the tubes.

10.1.5 Fouling with whey solution in the Centritherm evaporator

This work only provides preliminary data on the fouling of the rotating surface during the evaporation process of fresh whey. It was found that reconstituted skim milk and whey solutions did not cause any fouling problem after running for more than 6 hours in the Centritherm evaporator. This indicates that the aggregated whey proteins, which were formed in the manufacture of skim milk powder and whey powder, were less active to produce fouling.

The results obtained confirmed that temperature strongly influences the fouling behaviour. In general, the higher the evaporating temperature and the temperature difference, the faster is the deposition rate and the greater the fouling on the surface. Bovine Serum Albumins (BSA) denatured 72% after running the evaporator at a evaporating temperature of 70°C and a temperature difference of 20K for 6 hours. Though the content of BSA in whey is small, the denatured BSA could be easily attached to the surface. By associated with other depositable materials existing in the whey solution, the thin layer of deposit could reduce the heat transfer coefficients significantly. This was attributed to the lower thermal conductivity of deposit layer.

An induction period was observed when the evaporating temperature was 60°C. It was also found that the induction period decreased when new whey solutions were

introduced into the evaporator. It proved the fact that depositable materials are much easier to be adsorbed on fouled or unclean surfaces than on clean surfaces. The results of increasing fouling rate after new whey solutions were introduced suggested that the concentration of activated molecules in the solutions strongly affected the fouling process.

Increasing the rotating velocity would delay the formation of an initial layer and reduce the rate of fouling. The effect of liquid velocity was more significant at high temperature than at low temperature.

A possible mechanism for whey fouling on a rotating surface was first the formation of activated molecules, namely denaturation of proteins (mainly BSA), which is the prerequisite for the deposition. The concentration of the activated molecules, which were affected by the evaporating temperature and the temperature difference, determined the rate of deposition on the surface. When activated whey proteins are aggregated, they have less ability of depositing onto the surface.

10.2 Recommendation for the future work

(1) A more complicated model using numerical methods could be developed to describe the evaporation process in rotating surface evaporators. Two particular aspects, which are the formation of the waves in the liquid film and the wall superheat required for onset of nucleate boiling in liquid film flow, should be given consideration.

(2) More experimental work could be conducted to gain a further understanding of the operation variables, e.g. the effect of changing both the temperature difference and the rotating speed on the heat transfer coefficient.

(3) Concerning the on-farm evaporation system, which requires a compact evaporator with high efficiency and minimal damage to milk, a logical development from this research is to use a rotating surface with an angle close to 90°, which means a disk type evaporator. It should provide a better heat transfer coefficient and is worth exploring

(4) It is suggested that a detailed investigation on whey fouling should be carried out with a close look at different whey solution components. Analysis of the composition and structure of deposited material could provide the further understanding of the fouling process. New techniques, such as X-ray photoelectron spectroscopy (XPS), should be employed in the further study. A thorough understanding of the mechanism of fouling should lead to methods to minimise fouling problem.

References

Al-Roubale, S. M. & Burton, H., 1979, Effect of free fatty acids on the amount of deposit formed from milk on heated surfaces, *Journal of Dairy Research,* **46**, 463-471.

Al-Zubaidi, A. A. J., 1987, Sea water desalination in Kuwait - A report on 33 years experience, *Desalination,* **63**, 1-55, Cited by Mackereth (1993).

Andrews, A. T., 1983, Proteinases in normal bovine milk and their action on caseins, *Journal of Dairy Research,* **50**, 45-55.

Angeletti, S. & Moresi, M., 1983, Modelling of multiple-effect falling-film evaporators, *Journal of Food Technology,* **18**, 539-563.

Anon, 1992, *Centrifugal-Flow Thin-Film Vacuum Evaporator, Evapor,* Enprotech Corp, New York.

Anon, 1990, Centrifugal, thin-film, vacuum evaporator, *The Chemical Engineer,* **25**(10), 21.

Armerding, G. D., 1966, Evaporation methods as applied to the food industry, *Advances in Food Research,* (Edited by Chichester, O. C.), **15,** pp. 303-358, Academic Press, New York and London,

Ashton, T. R., 1966, *Dairy Industries,* **31**, 480, Cited by Burton (1988).

Baier, R. B., 1981, Modification of surfaces to reduce fouling and/or improve cleaning, *Fundamentals and Applications of Surface Phenomena Associated*

with Fouling and Cleaning in Food Processing, (Edited by Hallström, B., Trägårdh, C., & Lund, D. B.), pp. 168-189, University of Lund, Sweden, Cited by Fryer *et al.* (1995).

Barton, K. P., Chapman, T. W. & Lund, D. B., 1985, Rate of precipitation of calcium phosphate on heated surfaces, *Biotechnology Progress,* **1**, 39-45, Cited by Fryer *et al.* (1995).

Bell, K. J., 1982, Heat exchangers with phase change, *Heat Exchangers Theory and Practice,* (Edited by Taborek, J. *et al.*), pp. 3-18, Hemisphere Publishing Co. New York.

Bell, K. J. & Sanders, C. F., 1944, Prevention of milkstone formation in a high-temperature-short-time heater by preheating milk, skim milk and whey, *Journal of Dairy Science,* **27**, 499-504.

Belmar-Beiny, M. T. & Fryer, P. J., 1994, *Fouling and Cleaning in Food Processing,* University of Cambridge, Jesus College, Cambridge, UK.

Belmar-Beiny, M. T. & Fryer, P. J., 1993, Preliminary stages of fouling from whey protein solutions, *Journal of Dairy Research,* **60**, 467-483.

Belmar-Beiny, M. T., Gotham, S. M., Paterson, W. R., Fryer, P. J. & Pritchard, A. M., 1993, The effect of Reynolds number and fluid temperature in whey protein fouling, *Journal of Food Engineering,* **19**, 119-139.

Benjamin, T. B., 1957, *Journal of Fluid Mechanics,* **2**, 254, Cited by Fulford (1965).

Bennet, R., 1996, *Personal Communication,* Food Technology Department, Massey University, New Zealand.

Bergles, A. Z. & Rohsenow, W. M., 1964, The determination of forced-convection surface-boiling heat transfer, *Journal of Heat Transfer,* **86**, 805-815.

Billet, R., 1989, *Evaporation technology: principles, applications, economics,* VCH Ellis Horwood Ltd, Chichester, England and Germany.

Blass, E., 1979, Gas/film flow in tubes, *International Chemical Engineering,* **12**(2), 183-195.

Bott, T. R., 1995, *Fouling of Heat Exchangers*, Elsevier Science B.V., Amsterdam, The Netherlands.

Bott, T. R., 1989, Fouling of heat exchangers: A review, *Process Engineering in the Food Industry - Developments and Opportunities,* (Edited by Field, R. W., & Howell, J. A.), pp. 97-109, Elsevier Applied Science, London and New York.

Bott, T. R., 1988, General fouling problems, *Fouling Science and Technology,* (Edited by Melo, L. F., Bott, T. R., & Bernardo, C. A.), pp. 3-14, Kluwer Academic Publishers, Dordrecht, The Netherlands.

Bouman, S. & Waalewijn, R., 1994a, Concentration of dairy products with rotating evaporators. 1. Theory and experimental methods, *Milchwissenschaft,* **49**(4), 190-193.

Bouman, S. & Waalewijn, R., 1994b, Concentration of dairy products with rotating evaporators. 2. Results and conclusions, *Milchwissenschaft,* **49**(5), 253-256.

Bouman, S., Waalewijn, R., de Jong, P. & Van Der Linden, H. J. L. J., 1993, Design of falling-film evaporators in the dairy industry, *Journal of the Society of Dairy Technology,* **46**(3), 100-106.

Bradley, S. E. & Fryer, P. J., 1992, A comparison of two fouling-resistant heat exchangers, *Biofouling,* **5**, 295-314, Cited by Fryer *et al.* (1995).

Brauer, H., 1956, *Chem.-Ing.-Tech.,* **32**, 719, Cited by Blass (1979).

Briggs, D. C., 1959, Heat transfer in rotating turbulent pipe flow, *Technic Report No. 45*, Department of Mechanical Engineering, Stanford University, Stanford, California, USA, Cited by Kreith (1968).

Britten, M., Green, M. L., Boulet, M. & Paquin, P., 1988, Deposit formation on heated surfaces: effect of interface energetics, *Journal of Dairy Research,* **55**, 551-562.

Brodov, Y. M., Savel'yev, R. Z., Permyakov, V. A., Kuptsov, V. K. & Gal'perin, A. G., 1977, The effect of vibration on heat transfer and flow of condensing steam on a single tube, *Heat Transfer-Sov. Res.,* **9**(No.1), 15-156, Cited by Carey (1992).

Burton, H., 1988, Chapter 10 Fouling of heat exchangers, *Ultra-High-Temperature Processing of Milk and Milk Products,* pp. 292-309, Elsevier Applied Science, London and New York.

Burton, H., 1972, Changes throughout lactation in the amount of deposit formation from milk of individual cows, *Journal of Dairy Research,* **39**, 183-187.

Burton, H., 1968, Reviews of the progress of dairy science: Section G. Deposits from whole milk heat treatment plant--a review and discussion, *Journal of Dairy Research,* **35**, 317-330.

Burton, H., 1967, Seasonal variation in deposit formation from whole milk on a heated surface, *Journal of Dairy Research,* **34**, 137-143.

Burton, H., 1966, A comparison between a hot-wire laboratory apparatus and plate heat exchanger for determining the sensitivity of milk to deposit formation, *Journal of Dairy Research,* **33**, 317-324.

Campanella, O. H., 1991, Empirical equation for the viscosity of sucrose solutions, An unpublished paper, Personal Communication.

Cannon, J. N. & Kays, W. M., 1969, Heat transfer to a fluid flowing inside a pipe rotating about its longitudinal axis, *Journal of Heat Transfer, Transactions of the ASME,* (2), 135-139.

Carey, V. P., 1992, *Liquid-Vapour Phase-Change Phenomena. An Introduction to the Thermophysics of Vaporization and Condensation Processes in Heat Transer Equipment,* Hemisphere Publishing Corporation, Washington, Philodelphia, London.

Carić, M. 1994, *Concentrated and Dried Dairy Products*, VCH Publishers, New York.

Chavarria, V. M., 1983, *Experimental Analysis of a Single Multi-Tube Absorption Driven Evaporator*, Ph.D. Dissertation, University of Massachusetts, Amherst, US, Cited by Schwartzberg (1988).

Chen, H., 1992, *Factors Affecting Heat Transfer in the Falling Film Evaporator*, Masterate Thesis, Massey University, Palmerston North, New Zealand.

Chen, H. & Jebson, R. S., 1992, Factors affecting heat transfer in a laboratory falling film evaporator, *Proceeding of IPENZ 1992 Annual Conference,* **1,** pp. 441-446, Christchurch, New Zealand.

Chen, H., Jebson, R. S. & Campanella, O. H., 1993, Factors affecting heat transfer in the Centritherm evaporator, *Proceeding of APCChE/CHEMECA 1993 Conference*, pp. 455-462, Melbourne, Australia.

Chen, S. L., Huang, K. M. and Hong, J. T. 1990, General solution of film condensation on a rotating cone, *Journal of the Chinese Institute of Chemical Engineering*, 21(1), 37-44.

Chun, K. R. & Seban, R. A., 1971, Heat transfer to evaporating liquid films, *Journal of Heat Transfer, Transactions of the ASME,* **93**(4), 391-396.

Chun, M. H. & Kim, K.T., 1990, Assessment of the new and existing correlations for laminar and turbulent flow film condensation on a vertical surface, *International Communications in Heat and Mass Transfer,* **17**, 431-441, Cited by Machereth (1993).

Clark, A. H., Judge, F. J., Richards, J. B., Stubbs, J. M. & Suggett, A., 1981, Electron microscopy of network structure in thermally-induced globular protein gels, *International Journal of Peptide and Protein Research,* **17**, 380-392.

Collier, J. G., 1981a, Heat transfer in condensation, *Two-Phase Flow and Heat Transfer in the Power and Processing Industries,* (Edited by Bergles, A. E. *et al.*), pp. 330-365, Hemisphere Publishing Company, New York and London.

Collier, J. G., 1981b, *Convective Boiling and Condensation,* 2nd edition, McGraw-Hill, New York.

Creamer, L. K., Parry, D. A. D. & Malcolm, G. N., 1983, Secondary structure of bovine ß-lactoglobulin B, *Archives of Biochemistry and Biophysics,* **227**, 98-105, Cited by Jelen & Rattray (1995).

Crittenden, B. D., Kolaczkowski, S. T. & Downey, I. L., 1992, Fouling of crude oil preheat exchangers, *Trans IChemE,* Part A, **70**, 547-557, Cited by Fryer *et al.* (1995).

Daufin, G., Labbe', J. P., Uuemerals, A., Brule', G., Michel, F., Roignant, M. & Priol, M., 1987, Fouling of a heat exchange surface by whey, milk and model fluids. An analytical study, *Lait,* **67**(3), 339-364.

Davis, E. J. & Anderson, G. H., 1966, The incipience of nucleate boiling in forced convection flow, *AIChEJ (Am. Inst. Chem. Eng. J.),* **12**, 774-80.

de Jong, P., Waalewijn, R. & Van Der Linden, H. J. L. J., 1993, Validity of a kinetic fouling model for heat-treatment of whole milk, *Lait,* **73**, 293-302.

de Jong, P., Bouman, S. & Van Der Linden, H. J. L. J., 1992, Fouling of heat treatment equipment in relation to the denaturation of ß-lactoglobulin, *Journal of the Society of Dairy Technology,* **45**(1), 3-8.

Delsing, B. M. A. & Hiddink, J., 1983, Fouling of heat transfer surfaces by dairy fluids, *Netherland Milk and Dairy Journal,* **37**, 139-148.

Dengler, C. E. & Addoms, J. N., 1956, Heat transfer mechanism for vaporization of water in a vertical tube, *Chemical Engineering Progress Symposium Series,* **52**(18), 95-103.

Deplace, F., Leuliet, J. C. & Tissier, J. P., 1994, Fouling experiments of a plate heat exchanger by whey proteins solutions, *Fouling and Cleaning in Food*

Processing, (Edited by Belmer-Beiny, M. T. & Fryer, P. J.), pp. 1-8, University of Cambridge.

Dickey, L. C. & Craig, J. C., 1993, Freeze concentration of liquid foods, *Physical Chemistry of Food Process: Volume 2, Advanced Techniques, Structures and Applications,* (Edited by Baianu, I. C., Pessen, H. & Kumosinski, T. F.), pp. 542-553, Van Nostrand Reihold, New York.

Donovan, M. & Mulvihill, D. M., 1987, Thermal denaturation and aggregation of whey proteins, *Irish Journal Food Science Technology,* **11**, 87-100.

Dukler, A. E., 1960, Fluid mechanics and heat transfer in vertical falling film system, *Chemical Engineering Progress Symposium Series,* **56**(30), 1-10, Cited by Fulford (1964).

Dukler, A. E. & Bergelin, O. P., 1952, Characteristics of flow in falling liquid films, *Chemical Engineering Progress,* **48**(11), 557-563.

Dupeyrat, M., Labbe', J. P., Michel, F., Billoudet, F. & Daufin, G., 1987, Wettability and solid-liquid interaction during fouling of several materials by whey and milk, *Lait,* **67**, 465-486.

Eigel, W. N., Butler, J. E., Ernstrom, C. A., Farrell, H. M. Jr., Harwalkar, V. R., Jenness, R. & Whitney, R. M., 1984, Nomenclature of proteins of cow's milk: fifth revision, *Journal of Dairy Science,* **67**, 1599-1631.

Elsaadi, M. S., 1992, *Heat Transfer to Thin Film Liquids on Closed Rotating Discs Systems*, Masterate Thesis, University of Newcastle, Upon Tyne, U.K, Cited by Jachuck and Ramshaw (1994).

Eucken, A., 1937, *Naturwissenschaten,* **25**, 209, Cited by Carey (1992).

Ferell, H., Fitch, E. C. & Boggs, J. H., 1957, An investigation of pressure drop through a rotating pipe, *Am. Inst. Chem. Engrs. Paper 57-PET-9,* Cited by Kreith (1968).

Fergusson, P. H., 1989, Developments in the evaporation and drying of dairy products, *Journal of the Society of Dairy Technology,* **42**(4), 94-101.

Fluck, A. A. J., 1988, Priciples of unit operations: Evaporation, *Journal of the Society of Dairy Technology,* **41**(4), 94.

Foster, C. L., Britten, M. & Green, M. L., 1989, A model heat-exchange apparatus for the investigation of fouling of stainless steel surfaces by milk. I. Deposit formation at 100°C, *Journal of Dairy Research,* **56**, 201-209.

Foster, C. L. & Green, M. L., 1990, A model heat exchange apparatus for the investigation of fouling of stainless steel surfaces by milk. II. Deposition of fouling material at 140°C, its adhesion and depth profiling, *Journal of Dairy Research,* **57**, 339-348.

Fox, P. F., 1989, The milk protein system, *Developments in Dairy Chemistry. 4. Functional Milk Proteins,* (Edited by Fox, P. F.), pp. 1-53, Elsevier Applied Science Publishers, London.

Frost, W. & Dzakowic, A. S., 1967, An extension of the methods of predicting incipient boiling on commercially finished surfaces, ASME paper 67-HT-61, presented at the *1967 National Heat Trasfer Conference*, Seattle, Washington.

Fryer, P. J., 1995, Chapter 9 Clean technology in the food industry, *Clean Technology and the Environment,* (Edited by Kirkwood, R. C., & Longley, A. J.), Blackie Academic & Professional, London.

Fryer, P. J., 1989, The uses of fouling models in the design of food process plant, *Journal of the Society of Dairy Technology,* **42**(1), 23-29.

Fryer, P. J., 1986, *Modelling Heat Exchanger Fouling*, Ph.D. Thesis, University of Cambridge, UK, Cited by Fryer *et al.* (1995).

Fryer, P. J., Belmar-Beiny, M. T. & Schreler, P. J. R., 1995, Fouling and cleaning in milk processing, *Heat-Induced Changes in Milk,* (Edited by Fox, P.F.), 2nd Edition, International Dairy Federation, Belgium.

Fryer, P. J. & Gotham, S. M., 1988, Fouling and cleaning in food processing, *Fouling and Cleaning in Process Plant,* pp. 167-181, St. Catherine's College, Oxford.

Fryer, P. J., Gotham, S. M. & Paterson, W. R., 1992, The concentration dependence of fouling from whey protein concentrates, *Proc. 20th Austr. Chemical Engineering Conference (CHEMCA 92),* **1,** pp. 368-375, Canberra, Australia.

Fulford, G. D., 1964, The flow of liquids in thin films, *Advances in Chemical Engineering,* (Edited by Drew, T. B., Hoopes, J. W., Vermenlen, T. & Cokelet, G. R.), **5,** pp. 151-236, Academic Press, New York and London.

Fulford, G. D., 1962, *Gas-Liquid Flow in an Inclined Channel*, Ph.D. Thesis, University of Birmingham, England, Cited by Fulford (1964).

Garrett-Price, B. A., 1985, *Fouling of Heat Exchangers, Characteristics, Costs, Prevention, Control, Removal.* Noyes Publications, New Jersey, Cited by Bott (1995).

Gimbutis, G. J., Drobacivius, A. J. & Sinkunas, S. S., 1978, Heat transfer of a turbulent water film at different initial flow conditions and high temperature gradients, *Proc. 6th Int. Heat Transfer Conf.*, Vol. 1, pp. 321-326, Toronto, Canada,

Gordon, K. P., Hankinson, D. J. & Carver, C. E., 1968, Deposition of milk solids on heated surfaces, *Journal of Dairy Science,* **51**(4), 520-526.

Gotham, S. M., 1990, *Mechanisms of Protein Fouling of Heat Exchangers*, Ph.D. Dissertation, University of Cambridge, UK, Cited by Fryer *et al.* (1995).

Gotham, S. M., Fryer, P. J. & Pritchard, A. M., 1989, Model studies of food fouling, *Fouling and Cleaning in Food Processing,* (Edited by Kessler, H. G. & Lund, D. B.), pp. 1-13, Prien, Bavarie, Germany.

Gotham, S. M., Fryer, P. J. & Pritchard, A. M., 1992, ß-lactoglobulin denaturation and aggregation reactions and fouling deposit formation: a DSC study, *International Journal of Food Science and Technology,* **27**, 313-327.

Grandison, A. S., 1988a, Ultra-high-temperature processing of milk: seasonal variation in deposit formation in heat exchangers, *Journal of the Society of Dairy Technology,* **41**, 43-49.

Grandison, A. S., 1988b, Effects of natural (or seasonal) variation in concentration of components of milk and addition of divalent cations on ultra-high-temperature

processing characteristics, *Journal of the Society of Dairy Technology,* **41**, 117-119.

Grandison, A. S., 1988c, *Fouling in Process Plant,* (Edited by Pritchard, A. M.), pp. 197-214, Institute of Corrosion, Science & Technology, London, Cited by Fryer *et al.* (1995).

Gray, R. M., 1981, Technology of skim milk evaporation, *Journal of the Society of Dairy Technology,* **34**(2), 53-57.

Green, M. L., Foster, C. L. & Britten, M., 1988, Formation and adhesion of deposit to heated surfaces in contact with milk, *Fouling in Processing Plant,* (Edited by Pritchard, A. M.), pp. 183-196, Institute of Corrosion, Science and Technology, London, Cited by Fryer *et al.* (1995).

Grønlund, M., 1984, Optimising evaporator and spray dryer performance in food processing, *Profitability of Food Processing,* pp. 397-408, Pergamon press, EFCE Publication Series No.36, The Institution of Chemical Engineers.

Gynning, K., Thome, K. E. & Samuelsson, E. G., 1958, Das Anbrennen in Plattenerhitzern, *Milchwissenschaft,* **13**, 62-70, Cited by Fryer *et al.* (1995).

Hahn, G., 1985, Evaporator design, *Concentration and Drying of Food,* (Edited by. MacCarthy, D.), pp. 113-131, University College, Cork, Republic of Ireland.

Hall, C. W. & Hedrick, T. I., *Drying of Milk and Milk Products*, AVI Publishing Company Inc., Westport Connecticut, Cited by Mackereth (1993).

Hallström, B., 1988a, Heat transfer and liquid foods, *Heat Transfer and Food Products,* (Edited by Hallström, B., Skjöldebrand, C. & Trägårdh, C.), pp. 140-143, London and New York.

Hallström, B., 1988b, Preconcentration: new developments, *Preconcentration and Drying of Food Materials,* (Edited by Bruin, S.), pp. 37-49, Elsevier Science Publishers, Amsterdam, The Netherlands.

Hallström, B., 1985, Heat exchange, *Evaporation, Membrane Filtration and Spray Drying in Milk Powder Cheese Production,* (Edited by Hansen, R.), pp. 25-43, North European Dairy Journal, Denmark.

Hallström, B., 1977, Evaporators with rotating conical heating surfaces, *Verfahrenstechnik,* **11**(8), 448, 450, 452, 454.

Hallström, B., 1969, Chapter 1 The use of Centri-therm, expanding-flow and forced-circulation plant evaporators, *The Use of Centri-Therm, Expanding-flow and Forced-circulation Plant Evaporators in the Food and Biochemical Industries,* pp. 3-13, United Nations Publication, Vienna and New York.

Hege, W. U. & Kessler, H. G., 1986a, Deposit formation of protein containing dairy liquids, *Milchwissenschaft,* **41**(6), 356-359.

Hege, W. U. & Kessler, H. G., 1986b, Die Ansatzbildung beim Erhitzen von Milch und Molke, *Int. Z. Lebensmittel-Technol. Verfahrenstechnik,* **37**, 92-100, Cited by Fryer *et al.* (1995).

Hegg, P. O., Castberg, H. B. & Lundh, G., 1985, Fouling of whey proteins on stainless steel at different temperatures, *Journal of Dairy Research,* **52**, 213-218.

Hegg, P. O. & Larsson, K., 1981, Ellipsometry studies of adsorbed lipids and milk proteins on metal surfaces, *Fundamentals and Application of Surface Phenomena Associated With Fouling and Cleaning in Food Processing,*

(Edited by Hallström, B., Lund, D. B. & Trägårdh, C.), pp. 250-255, Reprocentralen, Lund.

Holden, K. M., Wanniarachchi, A. S., Marto, P. J., Boone, P. J. & Rose, J. W., 1987, The use of organic coatings to promote dropwise condensation of steam, *Journal of Heat Transfer,* **109**, 768-744.

Honig, P., 1963, *Principles of Sugar Technology*, Elsevier Science Publishers, Amsterdam, The Netherlands.

Hiddink, J., Lalande, M. & Streuper, A., 1986, Heat treatment of whipping cream. I. Fouling of the pasteurization equipment, *Milchwissenschaft,* **41**(9), 542-546.

Houšová, J., 1970, Prestup tepla pri varu v odparkách se stékajícím filmem, *Prúmysl Polravin,* **21**(1), 7-12, Cited by Mackereth (1995).

Ito, R. & Nakanishi, T., 1967, Formation of milk deposits on heat exchange surfaces in UHT pasteurising plants, *Japanese Journal of Dairy Science,* **15A**, 78-88, Cited by Fryer *et al.* (1995).

Jachuck, R. J. J. & Ramshaw, C., 1994, Process intensification: heat transfer characteristics of tailored rotating surfaces, *Heat Recovery System & CHP,* **14**(5), 475-491.

Jackson, M. L., 1955, *AIChEJ (Am. Inst. Chem. Eng. J.)*, **1**, 231, Cited by Fulford (1964).

Jakob, M., 1936, *Mech. Eng.*, **58**, 729, Cited by Carey (1992).

Jebson, R. S., 1989, Chapter 2 The performances of falling film evaporator, *Evaporation and Spray Drying in the New Zealand Dairy Industry,* (Edited by

Jebson, R. S.), pp. 14-32, Food Technology Department, Massey University, Palmerston North, New Zealand.

Jebson, R. S., 1988, The performances of falling film evaporators, *Proceeding of IPENZ (The Institution of Professional Engineers of New Zealand) Conference*, Palmerston North, **2**, 195-204.

Jebson, R. S., Huston, T., Janata, W. & Murray, G., 1993, *Proposal for the Utilisation of LPG As a Source of Energy on Dairy Farms in General and Specifically for the on Farm Site Dewatering of Milk,* Energy Transfer Developments Group, Massey University, Palmerston North.

Jebson, R. S. & Iyer, M., 1991, Performances of falling film evaporator, *Journal of Dairy Research,* **58**, 29-38.

Jelen, P., 1981, Experience with direct and indirect UHT processing of milk-a Canadian viewpoint, Presented at 68th Annual meeting of IAMFES, Spokane, WA, USA, Cited by Swartzel (1983).

Jelen, P. & Rattray, W., 1995, Thermal denaturation of whey proteins, *Heat-Induced Changes in Milk,* (Edited by Fox, P. F.), 2nd Edition, pp. 66-85, International Dairy Federation, Belgeiun.

Jeurnink, T. J. M., 1991, Effect of proteolysis in milk on fouling in heat exchangers, *Netherland Milk and Dairy Journal,* **45**, 23-32.

Jeurnink, T. J. M., 1995a, Fouling of heat exchangers by fresh and reconstituted milk and the influence of air bubbles, *Milchwissenschaft,* **50**(4), 189-192.

Incropera, F. P. & DeWitt, D. P., 1990, Fundamentals of Heat Transfer and Mass Transfer, (3rd Edition), John Wiley & Sons, New York.

Jeurnink, T. J. M., 1995b, Relation between the denaturation and fouling behaviour of ß-lactoglobulin, *Heat Treatments and Alternative Methods,* p. 1.7, International Dairy Federation, Vienna, Austria.

Jeurnink, T. J. M. & Brinkman, D. W., 1994, The cleaning of heat exchangers and evaporators after processing milk or whey, *International Dairy Journal,* **4**, 347-368.

Jeurnink, T. J. M. & de Kruif, C. G., 1995, Calcium concentration in milk in relation to heat stability and fouling, *Netherland Milk and Dairy Journal,* **49**, 151-165.

Jeurnink, T. J. M., Walstra, P. & de Kruif, C. G., 1996, Mechanism of fouling in dairy processing, *Netherland Milk and Dairy Journal,* **50**, 407-426.

Johnson, J. J. & Roland, C. T., 1940a, Study of dairy cleaning problems. I. Films and deposits on hot milk equipment, *Journal of Dairy Science,* **23**, 457-461.

Johnson, J. J. & Roland, C. T., 1940b, Study of dairy cleaning problems. II. Effectiveness of alkalies in removing heat-deposited milk solids and butterfat films, *Journal of Dairy Science,* **23**, 463-469.

Kapitsa, P. L., 1948, Zh. Eksperim. i Teor. Fiz., 183, Cited by Fulford (1965).

Kast, W., 1963, Heat transfer during dropwise condensation (in German), *Chem.-Ing. Tech.,* **35**, 163-168, Cited by Carey (1992).

Kastanas, P., Jewis, M. J. & Grandison, A. S., 1995, Design and development of a miniature UHT plant for fouling studies and its evaluation using milk adjusted to different pH values, goat's milk and milk permeate, *Trans IChemE,* **73**, Part C, 67-75.

Kern, D. Q. & Karakus, H. J., 1958, Mechanically aided heat transfer, *AIChEJ. (Am. Inst. Chem. Eng.),* Preprint No. 17, New York, Cited by Reay (1991).

Kessler, H. G., 1989, Multistage evaporation and water vapour recompression with special emphasis on high dry matter content, product losses, cleaning and energy savings, *Dairy Industries,* 545-558.

Kessler, H. G., 1985, Energy aspects of food preconcentration, *Concentration and Drying of Food,* (Edited by MacCarthy, D.), pp. 147-163, Elsevier Applied Science, London and New York.

Kessler, H. G., Fiedler, J. & Hege, W. U., 1986, Formation of deposits from liquid foods on heated surfaces during heating and evaporation in UHT pasteurising plants, *Chem. Ing. Tech.,* **58**, 475-485, Cited by Fryer *et al.* (1995).

Kessler, H. G. & Lund, D. B., 1989, *Fouling and Cleaning in Food Processing,* University of Munich, Prien, Bavaria, Germany.

Kreith, F., 1968, Convection heat transfer in rotating systems, *Advances in Heat Transfer,* **5**, 129-251.

Kroll, J. F. & McCutchan, J. W., 1968, Heat transfer in an LTV falling film evaporator: A theoretical and experimental analysis, *Journal of Heat Transfer, Transactions of the ASME,* **58**(3), 201-210.

Kuo, C. Y., Lida, H. T., Tayler, J. H. & Kreith, F., 1960, *Journal of Heat Transfer,* **82**, 139, Cited by Kreith (1968).

Lalande, M. & Corrieu, G., 1981, Fouling of a plate heat exchanger by milk, *Fundamentals and Applications of Surface Phenomena Associated With Fouling and Cleaning in Food Processing,* (Edited by Hallström, B.,

Trägårdh, C. & Lund, D. B.), pp. 279-288, University of Lund, Sweden, Cited by Fryer *et al.* (1995).

Lalande, M., Tissier, J. P. & Corrieu, G., 1985, Fouling of heat transfer surfaces related to ß-lactoglobulin denaturation during heat processing of milk, *Biotechnology Progress,* **1**, 131-139, Cited by Fryer *et al.* (1995).

Lalande, M., Tissier, J. P. & Corrieu, G., 1984, Fouling of a plate heat exchanger used in ultra-high-temperature sterilization of milk, *Journal of Dairy Research,* **51**, 557-568.

Langton, M. & Hermansson, A., 1992, Fine-stranded and particulate gels of ß-lactoglobulin and whey protein at varying pH, *Food Hydrocolloids,* **5**(6), 523-539, Cited by Nørbøge (1994).

Leniger, H. A., 1986, Concentration by evaporation, *Preconcentrtion and Drying of Food Materials*, (Edited by Bruin, S.), pp 54-76, Elsevier Science Publishers B.V., Amsterdam, The Netherlands.

Levich, V. G., 1962, *Physiochemical Hydrodynamics,* Prentice-Hall, Englewood Cliffs. NJ., USA.

Lewicki, P. P. & Kowalczyk, R., 1979, Heat transfer in the Centri-Therm CT-1B evaporator, *International Union of Food Science and Technology, Food Engineering Symposium,* Warsaw Agriculture University, Warsaw, Poland.

Lim, S. T., 1980, *Hydrodynamics and Mass Transfer Processes Associated With the Absorption of Oxygen in Liquid Films Flowing Across a Rotating Disc*, Ph.D. Dissertation, University of Newcastle, Upon Tyne, U.K, Cited by Jachuck and Ramshaw (1994).

Lyle, O., 1947, *The Efficient Use of Steam,* His Majesty's Stationary Office, London. 276-286, Cited by Mackereth (1993).

Lyster, R. L. J., 1970, The denaturation of α-lactalbumin and β-lactoglobulin in heated milk, *Journal of Dairy Research,* **37**, 233-243.

Lyster, R. L. J., 1965, The composition of milk deposits in an ultra-high-temperature plant, *Journal of Dairy Research,* **32**, 203-208.

Maas, R., Lalande, M. & Hiddink, J., 1985, Fouling of a plate heat exchanger by whipping cream, *Fouling and Cleaning in Food Processing,* (Edited by Lund, D. B., Plett, E. A. & Sandu, C.), pp. 217-225, University of Wisconsin, Cited by Fryer *et al.* (1995).

Mackereth, A. R., 1995, Chapter 9 Evaporation, *Milk Powder Technology Principles & Process Applications,* (Edited by Tuoc Trinh), New Zealand Dairy Research Institute, Palmerston North,

Mackereth, A. R., 1993, *Thermal and Hydraulic Aspects of Falling Film Evaporation,* Ph.D. Thesis, University of Canterbury, Christchurch, New Zealand.

Mai, K. L., 1958, *Chem.Egn.Progr.Symp,* **54**, 57, Cited by Kreith (1968).

Mälkki, Y. & Veldstra, J., 1967, Flavour retention and heat transfer during concentration of liquid in a centritherm film evaporator, *Food Technology,* **21**, 1179-1184.

Mannheim, C. H. & Passy, N., 1974, Non-membrane concentration, *Advances in Preconcentration and Dehydration of Foods,* (Edited by Spicer, A.), pp. 152-193, Applied Science Publishers Ltd, London, UK.

Marrs, W. M. & Lewis, D. F., 1986, *Fouling of Heated Surfaces by Proteinaceous Fluids*, No.569, The British Food Manufacturing Industries Research Association, London, UK.

Martynov, Y. V., 1984, Flow of a Liquid film over the inner surface of a rotating cylinder, *Journal of Applied Mechanics Technical Physics,* **23**(3), 400-407.

McCabe, W. L. & Smith, J. C., 1965, *Unit Operations of Chemical Engineering. (2nd Edition),* Mcgraw-Hill Book Company, New York and London. New York and London.

Melo, L. F., Bott, T. R. & Bernardo, C. A., 1988, *Fouling Science and Technology,* Kluwer Academic Publishers, Dordrecht, The Netherlands.

Mincowycz, W. J. & Sparrow, E. M., 1966, Condensation heat transfer in the presence of non-condensables, interfacial resistance, superheating, variable properties, and diffusion, *International Journal of Heat and Mass Transfer,* **9**, 1125-1144.

Minton, P. E., 1986, *Handbook of Evaporation Technology,* Noyes Pulications, Park Ridge, New jersey, USA

Moresi, M., 1985, Design and optimisation of falling-film evaporators, *Developments in Food Preservation-3,* (Edited by Thorne, S.), pp. 183-244, Elsevier Applied Science Publishers, London and New York.

Muir, D. D. & Sweetsur, A. W. M., 1976, The influence of naturally occurring levels of urea on the heat stability of bulk milk, *Journal of Dairy Research,* **43**, 495-499.

Müller-Steinhagen, H., 1989, Heat Transfer and Heat Exchanger Design, *Continuing Education Seminar Notes*, Chemical and Materials Engineering Department, University of Auckland, New Zealand, Cited by Machereth (1995).

Mulvihill, D. M. & Donovan, M., 1987, Whey proteins and their thermal denaturation. A review., *Irish Journal Food Science Technology,* **11**, 43-75.

Nikolaev, V. S., Vachagin, K. D. & Baryshev, Y. N., 1967, Film flow of viscous liquids over surfaces of rapidly rotating conical discs, *International Chemical Engineering,* **7**(4), 595-598.

Nikuradse, J., 1933, Forschungsheft, **361**, 1, Cited by Dukler and Bergelin (1952).

Nocol, A. A. & Gacesa, M., 1970, Condensation of steam on a rotating vertical cylinder, *Journal of Heat Transfer,* **92**, 144-152.

Nong, T. C., 1969, Factors affecting the degree of concentration of apple juice in a centrifugal evaporator, *Przemysl-Spozywczy,* **23**(10), 438-440, (in Polish).

Nørbøge, L., 1994, *Whey Protein Gelation and Denaturation at Different pH and Calcium Chloride Concentrations*, Masterate Thesis, Massey University, Palmerston North, New Zealand.

Nukiyama, S., 1934, The maximum and minimum values of heat Q transmitted from metal to boiling water under atmospheric pressure, *Japan Soc. Mech. Eng.*, **37**, 367-374, English translation in *International Journal of Heat and Mass Transfer,* **9**, 1419-1433, (1966).

Nusselt, W., 1916, Die Oberflachenkondensation des Wasserdampfes, *Ver. Deut. Ingr. Z.,* **60**, 541-546, 569-575, Cited by Baumann (1990).

O'Connor, G. E. & Russell, T. W. F., 1978, Heat transfer in tubular fluid-fluid systems, *Advances in Chemical Engineering,* (Edited by Drew, T. B. *et al.*), **10,** pp. 1-53, Academic Press, New York and London.

Oliver-Daumen, B., 1986, Optimizing the operating parameters for alcohol reduction with the Centri-therm, *Monatsschrift-Fuer-Brauwissenschaft,* **39**(4), 132-142. (in German).

Oliver-Daumen, B., 1982, Practical experience with use of Centri-Therm equipment for reduction of the alcohol content of beer, *Monatsschrift-Fuer-Brauwissenschaft,* **35**(3), 101-106, (in German).

O'Neill, G. A. & Westwater, J. W., 1984, Dropwise condensation of steam on electroplated silver surfaces, *International Journal of Heat and Mass Transfer,* **27**, 1539-1549.

Pajunen, E., Vanhatalo, I., Linko, M. & Pessa, E., 1974, Concentration of yeast extract with a centrifugal film evaporator, *Proc. Int. Congress Food Science and Technology,* **4**, 390-396.

Parker, M. E. & Johnson, A. H., 1930, Cleaning of deposits on hot milk equipment, *Proceeding of the International Association of Milk Dealers 23rd Annual Convention,* Cited by Fryer *et al.* (1995).

Pattenden, R. F., 1964, *Journal of Mechanic Engineering and Science,* **6**, 144, Cited by Kreith (1968).

Peters, T. Jr., 1985, Serum albumin, *Advances in Protein Chemistry,* **37**, 161-245.

Pritchard, A. M., 1988, The economics of fouling, *Fouling Science and Technology,* (Edited by Melo, L. F., Bott, T. R. & Bernardo, C. A.), pp. 31-45, Kluwer Academic Publishers, Dordrecht, The Netherlands.

Pritchard, A. M., 1979, Heater exchanger fouling in British industry, *Fouling prevention research digest,* Vol. 1, pp. 4-6, Cited by Pritchard (1988).

Reay, D. A., 1991, Heat transfer enhancement-A review of techniques and their possible impact on energy efficiency in the UK, *Heat Recovery Systems & CHP,* **11**(1), 1-40.

Reed, R. G., Feldhoff, R. C., Clute, O. L. & Peters, T. Jr., 1975, Fragments of bovine serum albumin produced by limited proteolysis. Conformation and ligand binding, *Biochemistry,* **14** , 4578-4583.

Reed, R. G., Putnam, F. W. & Peters, T. Jr., 1980, Sequence of residues 400-403 of bovine serum albumin, *Biochemical Journal,* **191**, 867-868.

Robbins, R. M. & Holmes, L. G., 1970, Circular dichroism spectra of a-lactalbumin, *Archives of Biochemistry and Biophysics,* **221**, 234, Cited by Nørbøge (1994).

Robertson, N. M. & Dixon, A., 1969, The nitrogen fractions and the heat stability of bovine milk, *Agroanimalia,* **1**, 141-144, Cited by Fryer *et al.* (1995).

Robertson, P. S., 1987, Developments in dairy processing, *Milk-The Vital Force, Proceeding of the XXII International Dairy Congress,* The Hague, Supplement.

Rogers, G. F. C. & Mayhew, Y. R., 1984, *Thermodynamic and Transport Properties of Fliuds - SI Units,* 3rd edtion, Basil Blackwell, Oxford, London.

Roscoe, S. G. & Fuller K. L., 1994, Fouling of model surface: adsorption and removal of whole unpasteurized milk, *Food Research International,* **27**, 363-369.

Sandu, C. & Lund, D. B., 1982, Fouling of heat treatment equipment by food fluids: computational models, *Food Processing Engineering,* (Edited by Schwartzberg, H. G., Lund, D. B. & Bomben, J. L.), **78,** pp. 12-30, AIChE Symposium Series, No. 218, American Institute of Chemical Engineer, New York.

Sandu, G., 1989, Chemical reaction fouling due to milk: defects-growth model, *Fouling and Cleaning in Food Processing,* (Edited by Kessler, H. G., & Lund, D. B.), Prien, Baravia, Germany.

Sato, T. & Matsumura, H., 1961, Bull, *Japan. Soc. Mech. Eng.,* **7**, 392, Cited by Carey (1992).

Schlichting, H., 1968, *Boundary Layer Theory,* McGrew-Hill Book Company, New York.

Schwartzberg, H. G., 1988, Food property effects in evaporation, *Food Properties and Computer-Aided Engineering of Food Processing Systems,* (Edited by Singh, R. P. & Medina, A. G.), pp. 443-470, Kluwer Academic Publishers, Dordrecht, The Netherlands.

Semenov, P. A., 1944, *Zhurn. Tekh. Fiz.,* **14**, 7-8, Cited by Zhivaikin (1962).

Shinn, B. E., 1971, The Centri-therm evaporator and its application to heat sensitive foods, *Journal of Applied Chemical Biotechnology,* **21**(12), 366-371.

Silver, R. S., 1964, An approach to a general theory of surface condensers, *Proc. Inst. Mech. Eng.*, **178**, 339-376, Cited by Carey (1992).

Sinek, J. R. & Young, E. H., 1960, Heat transfer in falling film long tube vertical evaporators, *Chemical Engineering Progress,* **58**(12), 74-80.

Skudder, P. J., Brooker, B. E., Bonsey, A. D. & Alvarez-Guerrero, N. R., 1986, Effect of pH on the formation of deposit from milk on heated surfaces during UHT processing, *Journal of Dairy Research,* **53**, 75-87.

Skudder, P. J., Thomas, E. L., Pavey, J. A. & Perkin, A. G., 1981, Effect of adding potassium iodate to milk before UHT treatment, *Journal of Dairy Research,* **48**, 99-113.

Sparrow, E. M., Minkowycz, W. J. & Saddy, M., 1967, Forced convection condensation in the presence of non-condensables and interfacial resistance, *International Journal of Heat and Mass Transfer,* **10**, 1829-1845.

Sparrow, E. M. & Hartnett, J. P., 1961, Condensation on a rotating cone, *Journal of Heat Transfer, Transactions of the ASME, Series C,* **2**, 101-102.

Sparrow, E. M. & Gregg, J. L., 1959, A theory of rotating condensation, *Journal of Heat Transfer,* **81**, 113.

Steinhagen, R., Mller-Steinhagen, H. & Maani, K., 1990, *Heat Exchanger Applications, Fouling Problems and Fouling Costs in New Zealand Industries*, RD8829, Published by Market Information and Analysis Group, Energy and Resources Division, Ministry of Commerce, Wellington, New Zealand,

Stephan, K., 1992, *Heat Transfer in Condensation and Boiling,* Springer-Verlag, Berlin.

Sugawara, S. & Katusuta, K., 1966, Fundamental study on dropwise condensation, *Proc. 3rd Int. Heat Transfer Conf.,* **2**, 354-361, Cited by Carey (1992).

Swartzel, K. R., 1983, Tubular heat exchanger fouling by milk during ultra-high-temperature process, *Journal of Food Science,* **48**, 1507-1511.

Taborek, J., Aoki, T., Ritter, R. B., Palen, J. W. & Knudsen, J. G., 1972, Fouling: The major unresolved problem in heat transfer, *Chemical Engineering Progress,* **68**(2), 59-67.

Tanaka, H., 1981, Effect of Knudsen number on dropwise condensation, *Journal of Heat Transfer,* **103**, 606-607.

Tanaka, H., 1979, Further developments of dropwise condensation theory, *Journal of Heat Transfer,* **101**, 603-611.

Tanaka, H., 1975, A theoretical study of dropwise condensation, *Journal of Heat Transfer,* **97**, 72-78.

Taylor, D. C., 1982, The history of evaporation, 1750 to 1900, *The Chemical Engineer,* **5**, 187-190.

Thome, J. R., 1990, *Enhanced Boiling Heat Transfer,* Hemisphere Publishing Corporation, New York, Washington, Philadelphia and London.

Timasheff, S. N., Susi, H. & Stevens, L., 1967, Infrared spectra and protein conformation in aqueous solutions, *Journal of Biological Chemistry,* **242**, 5467-5473, Cited by Jelen & Rattray (1995).

Timasheff, S. N., Townend, R. & Meschanti, L., 1966, The optical rotary dispersion of the ß-lactoglobulin, *Journal of Biological Chemistry,* **241**, 1863-1870, Cited by Jelen & Rattray (1995).

Tissier, J. P. & Lalande, M., 1986, Experimental device and methods for studying milk deposit formation on heat exchange surfaces, *Biotechnology Progress,* **2**(4), 218-229.

Tissier, J. P., Lalande, M. & Corrieu, G., 1984, A study of milk deposit on a heat exchange surface during ultra-high-temperature treatment, *Engineering and Food. Vol 1. Engineering Sciences in the Food Industry,* (Edited by McKenna, B. M.), pp. 59-68, Applied Science Publishers, London, Cited by Fryer *et al.* (1995).

Traegardh, C., 1974, Production of leaf protein concentrate for human consumption by isopropanol treatment. A comparison between untreated raw juice and raw juice concentrated by evaporation and ultra-filtration, *Lebensmittel-Wissenschaft-Technoloie,* **7**(4), 199-201, (in Swedish).

Ueda, T. & Tanaka, H., 1975, Measurements of velocity, temperature and velocity fluctuation distributions in falling liquid films, *International Journal of Multiphase Flow,* **2**, 261-272.

Umur, A. & Griffith, P., 1965, Mechanism of dropwise condensation, *Journal of Heat Transfer,* **87**, 275-282.

Van Stralen, S. J. D. & Cole, R., 1979, *Boiling Phenomena,* Vols. 1 and 2 Hemisphere, Washington.

Vasiliev, L. L. & Khrolenok.V.V., 1993, Heat transfer enhancement with condensation by surface rotation, *Heat Recovery System & CHP,* **13**(6), 547-563.

Visser, J., 1988, Adhesion and removal of particles I, *Fouling and Cleaning in Process Plant,* pp. 83-100, St. Catherine's college, Oxford, United Kingdom.

Visser, J., Lindell, A. & Paulsson, M. A., 1995, Heat induced depositions of milk components onto a rotating disk, *Heat Treatments and Alternative Methods,* p. 1.8, International Dairy Conference, Vienna, Austria.

Visser, J., Minihan, A., Smits, P., Tjan, S. B. & Heertje, I., 1986, Effects of pH and temperature on the milk salt system, *Netherland Milk and Dairy Journal,* **40**, 351-368.

Walstra, P. & Jenness, R., 1984, *Dairy Chemistry and Physics,* John Wiley & Sons Inc., New York.

Welch, J. F. & Westwater, J. W., 1961, Microscopic study of dropwise condensation, *International Developments in Heat Transfer. Proc. Int. Heat Transfer Conf. ASME.,* **Part II**, 302-309, Cited by Carey (1992).

Westergard, V., 1983, *Milk Powder Technology Evaporation and Spray Drying (3rd and Revised Edition)*, A/S NIRO Atomizer, Copenhagen, Denmark.

Whalley, P. B., 1992, Fouling -still the major unresolved problem in heat transfer, *Trans IChemE,* **70**, Part A, 545.

Wiegand, B., 1985, Chapter 6 Evaporation, *Evaporation, Membrane Filtration and Spray Drying in Milk Powder Cheese Production,* (Edited by Hansen, R.), pp. 91-178, North European Dairy Journal, Denmark.

Wiegand, B., 1978, Multiple effect evaporation and the DRS tube and the noise problem., *Lecture Handout in November, 1977* at various places in New Zealand.

Wilke, W., 1962, Wärmeübergang an reiselfilme, *Ver. Dent.Ingr. Forschungsh,* 490, Cited by Chun & Seban (1971).

Wood, P. W., 1982, *Physical Properties of Dairy Products*, Technical Report, ISSN 0110-8948, Ministry of Agriculture and Fisheries, Hamilton, New Zealand,

Xiong, Y. L., 1992, Influence of pH and ionic environment on thermal aggregation of whey proteins, *Journal of Agricultural and Food Chemistry,* **40**, 380-384.

Xu, X., 1996, *The Investigation of the Quality of Milk Pre-Concentrated by an On-Farm Evaporation System*, Masterate Thesis, Massey University, Palmerston North, New Zealand.

Yanniotis, S. & Kolokotsa, D., 1996, Boiling on the surface of a rotating dise, *Journal of Food Engineering,* **30**, 313-325.

Yanniotis, S., 1983, *Thermal Characteristics of Absorption-Driven and Steam-Heated Long Tube Vertical Falling Film Evaporators*, Ph.D. Dissertation, University of Massachusetts, Amberst, USA, Cited by Schwartzberg (1988).

Yoon, J. & Lund, D. B., 1989, Effect of operating conditions, surface coatings and pretreatment on milk fouling in a plate heat exchanger, *Fouling and Cleaning in Food Processing,* (Edited by Kessler, H. G. & Lund, D. B.), pp. 59-80, University of Munich, Germany.

Zhivaikin, L. Ya., 1962, Liquid film thickness in film-type units, *International Chemical Engineering,* **2**(3), 337-341.

Zhivaikin, L. Ya. & Volgin, B. V., 1964, Hydraulic resistance in descending two-phase flow in film-type equipment, *International Chemical Engineering,* **4**(1), 80-84.

APPENDICES

Appendix I

Experimental results of heat transfer in evaporators

2.1 The results of 4^2 experiment in the Centritherm evaporator with water

TRIALS (Times)	ST (°C)	EV (°C)	ΔT (K)	FF ($\times10^{-3}m^3/s$)	RS (rad/s)	W_{exp} ($\times10^{-3}m^3/s$)	H_{cal} (kW/m^2K)	Ave-H_{cal} (kW/m^2K)
1-1	70	60	10	0.0167	104.720	0.0030	7.86	8.01
1-2	70	60	10	0.0167	104.720	0.0031	8.08	
1-3	70	60	10	0.0167	104.720	0.0031	8.08	
2-1	70	60	10	0.0500	104.720	0.0031	8.19	8.11
2-2	70	60	10	0.0500	104.720	0.0031	8.19	
2-3	70	60	10	0.0500	104.720	0.0030	7.97	
3-1	80	70	10	0.0167	104.720	0.0034	8.86	8.79
3-2	80	70	10	0.0167	104.720	0.0035	9.08	
3-3	80	70	10	0.0167	104.720	0.0033	8.43	
4-1	80	70	10	0.0500	104.720	0.0034	8.86	8.68
4-2	80	70	10	0.0500	104.720	0.0034	8.75	
4-3	80	70	10	0.0500	104.720	0.0033	8.43	
5-1	70	60	10	0.0167	186.401	0.0031	8.08	8.08
5-2	70	60	10	0.0167	186.401	0.0032	8.30	
5-3	70	60	10	0.0167	186.401	0.0030	7.86	
6-1	70	60	10	0.0500	186.401	0.0032	8.30	8.15
6-2	70	60	10	0.0500	186.401	0.0031	8.08	
6-3	70	60	10	0.0500	186.401	0.0031	8.08	
7-1	80	70	10	0.0167	186.401	0.0038	9.73	9.54
7-2	80	70	10	0.0167	186.401	0.0036	9.40	
7-3	80	70	10	0.0167	186.401	0.0037	9.51	
8-1	80	70	10	0.0500	186.401	0.0036	9.29	9.33
8-2	80	70	10	0.0500	186.401	0.0035	9.08	
8-3	80	70	10	0.0500	186.401	0.0037	9.62	
9-1	80	60	20	0.0167	104.720	0.0066	8.65	8.52
9-2	80	60	20	0.0167	104.720	0.0064	8.41	
9-3	80	60	20	0.0167	104.720	0.0065	8.52	
10-1	80	60	20	0.0500	104.720	0.0064	8.41	8.44
10-2	80	60	20	0.0500	104.720	0.0065	8.52	
10-3	80	60	20	0.0500	104.720	0.0064	8.41	
11-1	90	70	20	0.0167	104.720	0.0073	9.40	9.35
11-2	90	70	20	0.0167	104.720	0.0073	9.40	
11-3	90	70	20	0.0167	104.720	0.0071	9.24	
12-1	90	70	20	0.0500	104.720	0.0074	9.56	9.53
12-2	90	70	20	0.0500	104.720	0.0074	9.62	
12-3	90	70	20	0.0500	104.720	0.0073	9.42	
13-1	80	60	20	0.0167	186.401	0.0068	8.95	8.84
13-2	80	60	20	0.0167	186.401	0.0068	8.84	
13-3	80	60	20	0.0167	186.401	0.0067	8.73	
14-1	80	60	20	0.0500	186.401	0.0069	9.06	8.81
14-2	80	60	20	0.0500	186.401	0.0067	8.73	
14-3	80	60	20	0.0500	186.401	0.0066	8.62	
15-1	90	70	20	0.0167	186.401	0.0076	9.85	9.80

15-2	90	70	20	0.0167	186.401	0.0075	9.73	
15-3	90	70	20	0.0167	186.401	0.0076	9.83	
16-1	90	70	20	0.0500	186.401	0.0076	9.90	9.86
16-2	90	70	20	0.0500	186.401	0.0076	9.83	
16-3	90	70	20	0.0500	186.401	0.0076	9.85	
17-1	80	65	15	0.0333	146.608	0.0048	8.40	8.33
17-2	80	65	15	0.0333	146.608	0.0048	8.25	
17-3	80	65	15	0.0333	146.608	0.0048	8.33	
18-1	80	65	15	0.0333	146.608	0.0048	8.33	8.46
18-2	80	65	15	0.0333	146.608	0.0049	8.47	
18-3	80	65	15	0.0333	146.608	0.0049	8.57	

2.2 The experimental results obtained in the Centritherm evaporator with water

Hcal-ΔT								
TRIALS	ST (°C)	EV (°C)	ΔT (K)	FF ($\times10^{-3}m^3/s$)	RS (rad/s)	W_{exp} ($\times10^{-3}m^3/s$)	H_{cal} (kW/m^2K)	Ave-H_{cal} (kW/m^2K)
1-1	65	60	5	0.0500	186.401	0.0014	7.34	7.57
1-2	65	60	5	0.0500	186.401	0.0014	7.51	
1-3	65	60	5	0.0500	186.401	0.0015	7.86	
2-1	70	60	10	0.0500	186.401	0.0032	8.41	8.17
2-2	70	60	10	0.0500	186.401	0.0031	8.12	
2-3	70	60	10	0.0500	186.401	0.0030	7.97	
3-1	75	60	15	0.0500	186.401	0.0048	8.44	8.59
3-2	75	60	15	0.0500	186.401	0.0049	8.52	
3-3	75	60	15	0.0500	186.401	0.0050	8.81	
4-1	80	60	20	0.0500	186.401	0.0068	8.84	8.81
4-2	80	60	20	0.0500	186.401	0.0065	8.57	
4-3	80	60	20	0.0500	186.401	0.0069	9.01	
5-1	85	60	25	0.0500	186.401	0.0088	9.21	9.11
5-2	85	60	25	0.0500	186.401	0.0086	9.04	
5-3	85	60	25	0.0500	186.401	0.0087	9.08	
6-1	90	60	30	0.0500	186.401	0.0107	9.32	9.30
6-2	90	60	30	0.0500	186.401	0.0108	9.39	
6-3	90	60	30	0.0500	186.401	0.0105	9.21	
7-1	95	60	35	0.0500	186.401	0.0123	9.23	9.21
7-2	95	60	35	0.0500	186.401	0.0123	9.17	
7-3	95	60	35	0.0500	186.401	0.0123	9.23	
8-1	100	60	40	0.0500	186.401	0.0141	9.22	9.13
8-2	100	60	40	0.0500	186.401	0.0139	9.09	
8-3	100	60	40	0.0500	186.401	0.0139	9.09	
9-1	105	60	45	0.0500	186.401	0.0152	8.85	8.89
9-2	105	60	45	0.0500	186.401	0.0153	8.88	
9-3	105	60	45	0.0500	186.401	0.0153	8.93	
10-1	110	60	50	0.0500	186.401	0.0154	8.08	8.17
10-2	110	60	50	0.0500	186.401	0.0158	8.25	
10-3	110	60	50	0.0500	186.401	0.0156	8.19	

H_{cal}-RS								
TRIALS	ST (°C)	EV (°C)	ΔT (K)	FF ($\times10^{-3}m^3/s$)	RS (rad/s)	W_{exp} ($\times10^{-3}m^3/s$)	H_{cal} (kW/m^2K)	Ave-H_{cal} (kW/m^2K)
1-1	80	70	10	0.0500	41.888	0.0026	6.81	6.77
1-2	80	70	10	0.0500	41.888	0.0027	6.92	
1-3	80	70	10	0.0500	41.888	0.0025	6.59	
2-1	80	70	10	0.0500	73.304	0.0032	8.21	8.18
2-2	80	70	10	0.0500	73.304	0.0031	8.10	
2-3	80	70	10	0.0500	73.304	0.0032	8.21	
3-1	80	70	10	0.0500	104.720	0.0034	8.86	8.68
3-2	80	70	10	0.0500	104.720	0.0034	8.75	
3-3	80	70	10	0.0500	104.720	0.0033	8.43	
4-1	80	70	10	0.0500	146.608	0.0036	9.29	9.04
4-2	80	70	10	0.0500	146.608	0.0034	8.75	
4-3	80	70	10	0.0500	146.608	0.0035	9.08	
5-1	80	70	10	0.0500	178.024	0.0035	9.08	9.33
5-2	80	70	10	0.0500	178.024	0.0037	9.51	
5-3	80	70	10	0.0500	178.024	0.0036	9.40	
H_{cal}-FF								
TRIALS	ST (°C)	EV (°C)	ΔT (K)	FF ($\times10^{-3}m^3/s$)	RS (rad/s)	W_{exp} ($\times10^{-3}m^3/s$)	H_{cal} (kW/m^2K)	Ave-H_{cal} (kW/m^2K)
1-1	70	60	10	0.0133	146.608	0.0034	8.95	8.95
1-2	70	60	10	0.0133	146.608	0.0035	9.06	
1-3	70	60	10	0.0133	146.608	0.0034	8.84	
2-1	70	60	10	0.0250	146.608	0.0034	8.95	8.94
2-2	70	60	10	0.0250	146.608	0.0034	9.02	
2-3	70	60	10	0.0250	146.608	0.0034	8.84	
3-1	70	60	10	0.0333	146.608	0.0035	9.06	9.08
3-2	70	60	10	0.0333	146.608	0.0034	9.00	
3-3	70	60	10	0.0333	146.608	0.0035	9.17	
4-1	70	60	10	0.0417	146.608	0.0035	9.17	9.15
4-2	70	60	10	0.0417	146.608	0.0035	9.21	
4-3	70	60	10	0.0417	146.608	0.0035	9.06	
5-1	70	60	10	0.0500	146.608	0.0035	9.28	9.17
5-2	70	60	10	0.0500	146.608	0.0035	9.06	
5-3	70	60	10	0.0500	146.608	0.0035	9.17	
6-1	70	60	10	0.0617	146.608	0.0035	9.28	9.37
6-2	70	60	10	0.0617	146.608	0.0036	9.50	
6-3	70	60	10	0.0617	146.608	0.0036	9.34	
H_{cal}-FF-RS								
TRIALS	ST (°C)	EV (°C)	ΔT (K)	FF ($\times10^{-3}m^3/s$)	RS (rad/s)	W_{exp} ($\times10^{-3}m^3/s$)	H_{cal} (kW/m^2K)	Ave-H_{cal} (kW/m^2K)
1-1	80	70	10	0.0167	52.360	0.0029	7.48	7.56
1-2	80	70	10	0.0167	52.360	0.0029	7.56	
1-3	80	70	10	0.0167	52.360	0.0030	7.65	
2-1	80	70	10	0.0417	52.360	0.0029	7.48	7.58
2-2	80	70	10	0.0417	52.360	0.0029	7.56	
2-3	80	70	10	0.0417	52.360	0.0030	7.69	
3-1	80	70	10	0.0667	52.360	0.0029	7.56	7.90
3-2	80	70	10	0.0667	52.360	0.0031	8.00	

3-3	80	70	10	0.0667	52.360	0.0031	8.13	
4-1	80	70	10	0.0167	104.720	0.0034	8.86	9.08
4-2	80	70	10	0.0167	104.720	0.0035	9.08	
4-3	80	70	10	0.0167	104.720	0.0036	9.29	
5-1	80	70	10	0.0417	104.720	0.0034	8.77	9.00
5-2	80	70	10	0.0417	104.720	0.0035	9.08	
5-3	80	70	10	0.0417	104.720	0.0035	9.16	
6-1	80	70	10	0.0667	104.720	0.0035	9.08	9.29
6-2	80	70	10	0.0667	104.720	0.0036	9.29	
6-3	80	70	10	0.0667	104.720	0.0037	9.51	
7-1	80	70	10	0.0167	157.080	0.0036	9.21	9.48
7-2	80	70	10	0.0167	157.080	0.0037	9.51	
7-3	80	70	10	0.0167	157.080	0.0038	9.73	
8-1	80	70	10	0.0417	157.080	0.0035	9.08	9.35
8-2	80	70	10	0.0417	157.080	0.0036	9.42	
8-3	80	70	10	0.0417	157.080	0.0037	9.55	
9-1	80	70	10	0.0667	157.080	0.0036	9.29	9.58
9-2	80	70	10	0.0667	157.080	0.0038	9.73	
9-3	80	70	10	0.0667	157.080	0.0038	9.73	
H_{cal}-FF-RS-ΔT								
TRIALS	ST (°C)	EV (°C)	ΔT (K)	FF ($\times10^{-3}m^3/s$)	RS (rad/s)	W_{exp} ($\times10^{-3}m^3/s$)	H_{cal} (kW/m^2K)	Ave-H_{cal} (kW/m^2K)
1-1	80	70	10	0.0067	186.401	0.0039	10.16	10.09
1-2	80	70	10	0.0067	186.401	0.0038	9.94	
1-3	80	70	10	0.0067	186.401	0.0039	10.16	
2-1	80	70	10	0.0100	186.401	0.0038	9.73	9.65
2-2	80	70	10	0.0100	186.401	0.0037	9.51	
2-3	80	70	10	0.0100	186.401	0.0038	9.73	
3-1	80	70	10	0.0133	186.401	0.0037	9.51	9.57
3-2	80	70	10	0.0133	186.401	0.0037	9.62	
3-3	80	70	10	0.0133	186.401	0.0037	9.60	
4-1	80	70	10	0.0250	186.401	0.0036	9.29	9.29
4-2	80	70	10	0.0250	186.401	0.0035	9.08	
4-3	80	70	10	0.0250	186.401	0.0037	9.51	
5-1	80	70	10	0.0333	186.401	0.0036	9.42	9.22
5-2	80	70	10	0.0333	186.401	0.0035	9.08	
5-3	80	70	10	0.0333	186.401	0.0035	9.16	
6-1	80	70	10	0.0417	186.401	0.0036	9.29	9.36
6-2	80	70	10	0.0417	186.401	0.0036	9.29	
6-3	80	70	10	0.0417	186.401	0.0037	9.51	
7-1	80	70	10	0.0500	186.401	0.0035	9.18	9.15
7-2	80	70	10	0.0500	186.401	0.0035	9.08	
7-3	80	70	10	0.0500	186.401	0.0035	9.18	
8-1	80	70	10	0.0617	186.401	0.0035	9.08	9.19
8-2	80	70	10	0.0617	186.401	0.0036	9.42	
8-3	80	70	10	0.0617	186.401	0.0035	9.08	
1-1	100	70	30	0.0100	41.888	0.0077	6.63	6.70
1-2	100	70	30	0.0100	41.888	0.0078	6.70	
1-3	100	70	30	0.0100	41.888	0.0078	6.77	
2-1	100	70	30	0.0133	41.888	0.0080	6.92	6.95

2-2	100	70	30	0.0133	41.888	0.0081	6.99	
2-3	100	70	30	0.0133	41.888	0.0080	6.95	
3-1	100	70	30	0.0250	41.888	0.0083	7.13	7.11
3-2	100	70	30	0.0250	41.888	0.0083	7.20	
3-3	100	70	30	0.0250	41.888	0.0081	6.99	
4-1	100	70	30	0.0333	41.888	0.0085	7.35	7.35
4-2	100	70	30	0.0333	41.888	0.0085	7.35	
4-3	100	70	30	0.0333	41.888	0.0085	7.35	
5-1	100	70	30	0.0417	41.888	0.0086	7.42	7.35
5-2	100	70	30	0.0417	41.888	0.0085	7.35	
5-3	100	70	30	0.0417	41.888	0.0084	7.28	
6-1	100	70	30	0.0500	41.888	0.0084	7.28	7.32
6-2	100	70	30	0.0500	41.888	0.0085	7.35	
6-3	100	70	30	0.0500	41.888	0.0085	7.35	
7-1	100	70	30	0.0617	41.888	0.0085	7.35	7.37
7-2	100	70	30	0.0617	41.888	0.0086	7.42	
7-3	100	70	30	0.0617	41.888	0.0085	7.35	
	H_{cal}-FF-RS-ΔT							
TRIALS	ST (°C)	EV (°C)	ΔT (K)	FF ($\times 10^{-3} m^3/s$)	RS (rad/s)	W_{exp} ($\times 10^{-3} m^3/s$)	H_{cal} (kW/m^2K)	Ave-H_{cal} (kW/m^2K)
1-1	60	40	20	0.0500	186.401	0.0057	7.63	7.74
1-2	60	40	20	0.0500	186.401	0.0059	7.91	
1-3	60	40	20	0.0500	186.401	0.0058	7.69	
2-1	70	50	20	0.0500	186.401	0.0062	8.22	8.15
2-2	70	50	20	0.0500	186.401	0.0061	8.05	
2-3	70	50	20	0.0500	186.401	0.0062	8.16	
3-1	80	60	20	0.0500	186.401	0.0067	8.73	8.84
3-2	80	60	20	0.0500	186.401	0.0067	8.79	
3-3	80	60	20	0.0500	186.401	0.0069	9.01	
4-1	90	70	20	0.0500	186.401	0.0076	9.88	9.83
4-2	90	70	20	0.0500	186.401	0.0076	9.93	
4-3	90	70	20	0.0500	186.401	0.0074	9.67	

2.3 The experimental results obtained in Centritherm with sugar solutions

For 20% sugar solution								
H_{cal}-ΔT								
TRIALS	ST (°C)	EV (°C)	ΔT (K)	FF ($\times 10^{-3} m^3/s$)	RS (rad/s)	W_{exp} ($\times 10^{-3} m^3/s$)	H_{cal} (kW/m^2K)	Ave-H_{cal} (kW/m^2K)
1-1	65	60	5	0.0500	186.401	0.0013	6.99	7.13
1-2	65	60	5	0.0500	186.401	0.0014	7.42	
1-3	65	60	5	0.0500	186.401	0.0013	6.99	
2-1	70	60	10	0.0500	186.401	0.0028	7.42	7.71
2-2	70	60	10	0.0500	186.401	0.0030	7.75	
2-3	70	60	10	0.0500	186.401	0.0030	7.97	
3-1	75	60	15	0.0500	186.401	0.0047	8.22	8.03
3-2	75	60	15	0.0500	186.401	0.0046	8.01	
3-3	75	60	15	0.0500	186.401	0.0045	7.86	
4-1	80	60	20	0.0500	186.401	0.0063	8.24	8.24

4-2	80	60	20	0.0500	186.401	0.0063	8.19	
4-3	80	60	20	0.0500	186.401	0.0063	8.30	
5-1	85	60	25	0.0500	186.401	0.0078	8.21	8.38
5-2	85	60	25	0.0500	186.401	0.0082	8.56	
5-3	85	60	25	0.0500	186.401	0.0080	8.38	
6-1	90	60	30	0.0500	186.401	0.0096	8.41	8.42
6-2	90	60	30	0.0500	186.401	0.0097	8.48	
6-3	90	60	30	0.0500	186.401	0.0096	8.37	
7-1	95	60	35	0.0500	186.401	0.0103	7.74	7.80
7-2	95	60	35	0.0500	186.401	0.0105	7.86	
8-1	105	60	45	0.0500	186.401	0.0130	7.59	7.73
8-2	105	60	45	0.0500	186.401	0.0135	7.88	
9-1	110	60	50	0.0500	186.401	0.0144	7.53	7.45
9-2	110	60	50	0.0500	186.401	0.0141	7.38	
H_{cal}-RS								
TRIALS	ST (°C)	EV (°C)	ΔT (K)	FF ($\times10^{-3}m^3/s$)	RS (rad/s)	W_{exp} ($\times10^{-3}m^3/s$)	H_{cal} (kW/m^2K)	Ave-H_{cal} (kW/m^2K)
1-1	80	70	10	0.0500	41.888	0.0025	6.48	6.56
1-2	80	70	10	0.0500	41.888	0.0025	6.59	
1-3	80	70	10	0.0500	41.888	0.0025	6.59	
2-1	80	70	10	0.0500	73.304	0.0029	7.56	7.31
2-2	80	70	10	0.0500	73.304	0.0029	7.46	
2-3	80	70	10	0.0500	73.304	0.0027	6.92	
3-1	80	70	10	0.0500	104.720	0.0030	7.78	7.92
3-2	80	70	10	0.0500	104.720	0.0030	7.78	
3-3	80	70	10	0.0500	104.720	0.0032	8.21	
4-1	80	70	10	0.0500	146.608	0.0033	8.43	8.39
4-2	80	70	10	0.0500	146.608	0.0033	8.54	
4-3	80	70	10	0.0500	146.608	0.0032	8.21	
5-1	80	70	10	0.0500	178.024	0.0033	8.54	8.82
5-2	80	70	10	0.0500	178.024	0.0034	8.86	
5-3	80	70	10	0.0500	178.024	0.0035	9.08	
H_{cal}-FF (Fig1.3.1)								
TRIALS	ST (°C)	EV (°C)	ΔT (K)	FF ($\times10^{-3}m^3/s$)	RS (rad/s)	W ($\times10^{-3}m^3/s$)	H_{cal} (kW/m^2K)	Ave-H_{cal} (kW/m^2K)
1-1	70	60	10	0.0133	146.608	0.0030	7.73	7.96
1-2	70	60	10	0.0133	146.608	0.0030	7.97	
1-3	70	60	10	0.0133	146.608	0.0031	8.19	
2-1	70	60	10	0.0250	146.608	0.0031	8.19	7.97
2-2	70	60	10	0.0250	146.608	0.0030	7.86	
2-3	70	60	10	0.0250	146.608	0.0030	7.86	
3-1	70	60	10	0.0333	146.608	0.0032	8.30	8.12
3-2	70	60	10	0.0333	146.608	0.0031	8.21	
3-3	70	60	10	0.0333	146.608	0.0030	7.86	
4-1	70	60	10	0.0417	146.608	0.0032	8.30	8.26
4-2	70	60	10	0.0417	146.608	0.0031	8.08	
4-3	70	60	10	0.0417	146.608	0.0032	8.41	
5-1	70	60	10	0.0500	146.608	0.0031	8.19	8.26
5-2	70	60	10	0.0500	146.608	0.0032	8.30	
5-3	70	60	10	0.0500	146.608	0.0032	8.30	

6-1	70	60	10	0.0617	146.608	0.0031	8.08	8.37
6-2	70	60	10	0.0617	146.608	0.0032	8.41	
6-3	70	60	10	0.0617	146.608	0.0033	8.62	
For 30-60% sogar solutions								
H_{cal}-ΔT-TS								
TRIALS	ST (°C)	EV (°C)	ΔT (K)	FF ($\times10^{-3}m^3/s$)	RS (rad/s)	W_{exp} ($\times10^{-3}m^3/s$)	H_{cal} (kW/m^2K)	Ave-H_{cal} (kW/m^2K)
30%								
1-1	75	70	5	0.0417	186.401	0.0013	7.86	7.53
1-2	75	70	5	0.0417	186.401	0.0013	7.37	
1-3	75	70	5	0.0417	186.401	0.0013	7.37	
2-1	80	70	10	0.0417	186.401	0.0030	8.28	8.23
2-2	80	70	10	0.0417	186.401	0.0030	8.28	
2-3	80	70	10	0.0417	186.401	0.0030	8.14	
3-1	85	70	15	0.0417	186.401	0.0045	8.18	8.13
3-2	85	70	15	0.0417	186.401	0.0044	7.95	
3-3	85	70	15	0.0417	186.401	0.0046	8.25	
4-1	90	70	20	0.0417	186.401	0.0060	8.08	8.00
4-2	90	70	20	0.0417	186.401	0.0060	8.02	
4-3	90	70	20	0.0417	186.401	0.0059	7.91	
5-1	95	70	25	0.0417	186.401	0.0078	8.24	8.19
5-2	95	70	25	0.0417	186.401	0.0077	8.15	
5-3	95	70	25	0.0417	186.401	0.0077	8.19	
40%								
1-1	75	70	5	0.0417	186.401	0.0010	6.27	6.23
1-2	75	70	5	0.0417	186.401	0.0010	6.48	
1-3	75	70	5	0.0417	186.401	0.0009	5.94	
2-1	80	70	10	0.0417	186.401	0.0024	6.92	6.87
2-2	80	70	10	0.0417	186.401	0.0024	6.96	
2-3	80	70	10	0.0417	186.401	0.0023	6.72	
3-1	85	70	15	0.0417	186.401	0.0038	7.04	6.98
3-2	85	70	15	0.0417	186.401	0.0037	6.79	
3-3	85	70	15	0.0417	186.401	0.0038	7.10	
4-1	90	70	20	0.0417	186.401	0.0053	7.21	7.16
4-2	90	70	20	0.0417	186.401	0.0052	7.05	
4-3	90	70	20	0.0417	186.401	0.0053	7.21	
5-1	95	70	25	0.0417	186.401	0.0069	7.40	7.36
5-2	95	70	25	0.0417	186.401	0.0068	7.29	
5-3	95	70	25	0.0417	186.401	0.0068	7.38	
50%								
1-1	75	70	5	0.0417	186.401	0.0007	5.24	5.20
1-2	75	70	5	0.0417	186.401	0.0006	4.98	
1-3	75	70	5	0.0417	186.401	0.0007	5.37	
2-1	80	70	10	0.0417	186.401	0.0019	5.99	5.99
2-2	80	70	10	0.0417	186.401	0.0020	6.25	
2-3	80	70	10	0.0417	186.401	0.0018	5.73	
3-1	85	70	15	0.0417	186.401	0.0032	6.26	6.22
3-2	85	70	15	0.0417	186.401	0.0031	6.08	
3-3	85	70	15	0.0417	186.401	0.0033	6.34	
4-1	90	70	20	0.0417	186.401	0.0045	6.32	6.26

4-2	90	70	20	0.0417	186.401	0.0043	6.02	
4-3	90	70	20	0.0417	186.401	0.0045	6.42	
5-1	95	70	25	0.0417	186.401	0.0059	6.54	6.51
5-2	95	70	25	0.0417	186.401	0.0058	6.40	
5-3	95	70	25	0.0417	186.401	0.0059	6.59	
60%								
1-1	75	70	5	0.0417	186.401	0.0002	1.85	1.70
1-2	75	70	5	0.0417	186.401	0.0001	1.54	
1-3	75	70	5	0.0417	186.401	0.0001	1.70	
2-1	80	70	10	0.0417	186.401	0.0011	3.96	3.96
2-2	80	70	10	0.0417	186.401	0.0012	4.26	
2-3	80	70	10	0.0417	186.401	0.0010	3.65	
3-1	85	70	15	0.0417	186.401	0.0023	5.00	4.91
3-2	85	70	15	0.0417	186.401	0.0023	4.91	
3-3	85	70	15	0.0417	186.401	0.0023	4.82	
4-1	90	70	20	0.0417	186.401	0.0033	4.93	4.89
4-2	90	70	20	0.0417	186.401	0.0033	4.93	
4-3	90	70	20	0.0417	186.401	0.0032	4.80	
5-1	95	70	25	0.0417	186.401	0.0042	4.89	4.97
5-2	95	70	25	0.0417	186.401	0.0043	5.08	
5-3	95	70	25	0.0417	186.401	0.0042	4.94	
H_{cal}-RS-TS								
TRIALS	ST (°C)	EV (°C)	ΔT (K)	FF ($\times10^{-3}m^3/s$)	RS (rad/s)	W_{exp} ($\times10^{-3}m^3/s$)	H_{cal} (kW/m^2K)	Ave-H_{cal} (kW/m^2K)
30%								
1-1	80	70	10	0.0417	52.360	0.0024	6.67	6.64
1-2	80	70	10	0.0417	52.360	0.0023	6.44	
1-3	80	70	10	0.0417	52.360	0.0025	6.81	
2-1	80	70	10	0.0417	83.776	0.0026	7.13	7.09
2-2	80	70	10	0.0417	83.776	0.0027	7.36	
2-3	80	70	10	0.0417	83.776	0.0025	6.78	
3-1	80	70	10	0.0417	104.720	0.0028	7.82	7.78
3-2	80	70	10	0.0417	104.720	0.0027	7.36	
3-3	80	70	10	0.0417	104.720	0.0030	8.16	
4-1	80	70	10	0.0417	157.080	0.0029	7.93	8.01
4-2	80	70	10	0.0417	157.080	0.0030	8.28	
4-3	80	70	10	0.0417	157.080	0.0028	7.82	
5-1	80	70	10	0.0417	186.401	0.0030	8.28	8.23
5-2	80	70	10	0.0417	186.401	0.0030	8.28	
5-3	80	70	10	0.0417	186.401	0.0030	8.14	
40%								
1-1	80	70	10	0.0417	52.360	0.0018	5.28	5.25
1-2	80	70	10	0.0417	52.360	0.0019	5.52	
1-3	80	70	10	0.0417	52.360	0.0017	4.95	
2-1	80	70	10	0.0417	83.776	0.0020	5.67	5.61
2-2	80	70	10	0.0417	83.776	0.0019	5.40	
2-3	80	70	10	0.0417	83.776	0.0020	5.76	
3-1	80	70	10	0.0417	104.720	0.0021	6.00	6.00
3-2	80	70	10	0.0417	104.720	0.0022	6.24	
3-3	80	70	10	0.0417	104.720	0.0020	5.76	

4-1	80	70	10	0.0417	157.080	0.0023	6.72	6.68
4-2	80	70	10	0.0417	157.080	0.0024	6.82	
4-3	80	70	10	0.0417	157.080	0.0023	6.48	
5-1	80	70	10	0.0417	186.401	0.0024	6.92	6.87
5-2	80	70	10	0.0417	186.401	0.0024	6.96	
5-3	80	70	10	0.0417	186.401	0.0023	6.72	
50%								
1-1	80	70	10	0.0417	52.360	0.0013	4.17	4.17
1-2	80	70	10	0.0417	52.360	0.0013	3.96	
1-3	80	70	10	0.0417	52.360	0.0014	4.37	
2-1	80	70	10	0.0417	83.776	0.0014	4.48	4.44
2-2	80	70	10	0.0417	83.776	0.0014	4.37	
2-3	80	70	10	0.0417	83.776	0.0014	4.48	
3-1	80	70	10	0.0417	104.720	0.0016	4.84	4.81
3-2	80	70	10	0.0417	104.720	0.0015	4.63	
3-3	80	70	10	0.0417	104.720	0.0016	4.95	
4-1	80	70	10	0.0417	157.080	0.0018	5.73	5.55
4-2	80	70	10	0.0417	157.080	0.0018	5.47	
4-3	80	70	10	0.0417	157.080	0.0018	5.47	
5-1	80	70	10	0.0417	186.401	0.0019	5.99	5.99
5-2	80	70	10	0.0417	186.401	0.0020	6.25	
5-3	80	70	10	0.0417	186.401	0.0018	5.73	
60%								
1-1	80	70	10	0.0417	52.360	0.0007	2.44	2.42
1-2	80	70	10	0.0417	52.360	0.0007	2.56	
1-3	80	70	10	0.0417	52.360	0.0006	2.28	
2-1	80	70	10	0.0417	83.776	0.0008	2.92	2.90
2-2	80	70	10	0.0417	83.776	0.0008	3.04	
2-3	80	70	10	0.0417	83.776	0.0008	2.74	
3-1	80	70	10	0.0417	104.720	0.0010	3.47	3.49
3-2	80	70	10	0.0417	104.720	0.0010	3.65	
3-3	80	70	10	0.0417	104.720	0.0009	3.35	
4-1	80	70	10	0.0417	157.080	0.0010	3.53	3.61
4-2	80	70	10	0.0417	157.080	0.0010	3.65	
4-3	80	70	10	0.0417	157.080	0.0010	3.65	
5-1	80	70	10	0.0417	186.401	0.0011	3.96	3.96
5-2	80	70	10	0.0417	186.401	0.0012	4.26	
5-3	80	70	10	0.0417	186.401	0.0010	3.65	
Sugar 20 and 68%								
	H_{cal}-TS							
TRIALS	ST (°C)	EV (°C)	ΔT (K)	FF ($\times10^{-3}m^3/s$)	RS (rad/s)	W_{exp} ($\times10^{-3}m^3/s$)	H_{cal} (kW/m^2K)	Ave-H_{cal} (kW/m^2K)
1-1	75	70	10	0.0417	186.401	0.0035	9.15	9.25
1-2	75	70	10	0.0417	186.401	0.0035	9.22	
1-3	75	70	10	0.0417	186.401	0.0035	9.37	
6-1	80	70	10	0.0417	186.401	0.0003	1.22	1.09
6-2	80	70	10	0.0417	186.401	0.0002	0.97	
6-3	80	70	10	0.0417	186.401	0.0003	1.08	

2.4 The experimental results obtained in Centritherm with skim milk (11% total solids)

H_{cal}-ΔT								
TRIALS	ST (°C)	EV (°C)	ΔT (K)	FF ($\times10^{-3}m^3/s$)	RS (rad/s)	W_{exp} ($\times10^{-3}m^3/s$)	H_{cal} (kW/m^2K)	Ave-H_{cal} (kW/m^2K)
1-1	65	60	5	0.0500	186.401	0.0013	6.55	6.88
1-2	65	60	5	0.0500	186.401	0.0013	6.77	
1-3	65	60	5	0.0500	186.401	0.0014	7.34	
2-1	70	60	10	0.0500	186.401	0.0030	7.86	7.60
2-2	70	60	10	0.0500	186.401	0.0029	7.60	
2-3	70	60	10	0.0500	186.401	0.0028	7.34	
3-1	75	60	15	0.0500	186.401	0.0045	7.86	7.87
3-2	75	60	15	0.0500	186.401	0.0046	8.01	
3-3	75	60	15	0.0500	186.401	0.0044	7.74	
4-1	80	60	20	0.0500	186.401	0.0063	8.19	8.11
4-2	80	60	20	0.0500	186.401	0.0062	8.08	
4-3	80	60	20	0.0500	186.401	0.0062	8.08	
5-1	85	60	25	0.0500	186.401	0.0078	8.21	8.27
5-2	85	60	25	0.0500	186.401	0.0078	8.21	
5-3	85	60	25	0.0500	186.401	0.0080	8.38	
6-1	90	60	30	0.0500	186.401	0.0096	8.41	8.31
6-2	90	60	30	0.0500	186.401	0.0096	8.37	
6-3	90	60	30	0.0500	186.401	0.0093	8.15	
H_{cal}-RS								
TRIALS	ST (°C)	EV (°C)	ΔT (K)	FF ($\times10^{-3}m^3/s$)	RS (rad/s)	W_{exp} ($\times10^{-3}m^3/s$)	H_{cal} (kW/m^2K)	Ave-H_{cal} (kW/m^2K)
1-1	80	70	10	0.0500	41.888	0.0025	6.48	6.56
1-2	80	70	10	0.0500	41.888	0.0025	6.59	
1-3	80	70	10	0.0500	41.888	0.0025	6.59	
2-1	80	70	10	0.0500	73.304	0.0029	7.56	7.31
2-2	80	70	10	0.0500	73.304	0.0029	7.46	
2-3	80	70	10	0.0500	73.304	0.0027	6.92	
3-1	80	70	10	0.0500	104.720	0.0030	7.78	7.92
3-2	80	70	10	0.0500	104.720	0.0030	7.78	
3-3	80	70	10	0.0500	104.720	0.0032	8.21	
4-1	80	70	10	0.0500	146.608	0.0033	8.43	8.39
4-2	80	70	10	0.0500	146.608	0.0033	8.54	
4-3	80	70	10	0.0500	146.608	0.0032	8.21	
5-1	80	70	10	0.0500	178.024	0.0033	8.54	8.82
5-2	80	70	10	0.0500	178.024	0.0034	8.86	
5-3	80	70	10	0.0500	178.024	0.0035	9.08	
H_{cal}-FF								
TRIALS	ST (°C)	EV (°C)	ΔT (K)	FF ($\times10^{-3}m^3/s$)	RS (rad/s)	W_{exp} ($\times10^{-3}m^3/s$)	H_{cal} (kW/m^2K)	Ave-H_{cal} (kW/m^2K)
1-1	70	60	10	0.0133	146.608	0.0030	7.75	7.50
1-2	70	60	10	0.0133	146.608	0.0028	7.21	
1-3	70	60	10	0.0133	146.608	0.0029	7.53	
2-1	70	60	10	0.0250	146.608	0.0029	7.53	7.71
2-2	70	60	10	0.0250	146.608	0.0030	7.86	
2-3	70	60	10	0.0250	146.608	0.0030	7.75	
3-1	70	60	10	0.0333	146.608	0.0030	7.86	7.86

3-2	70	60	10	0.0333	146.608	0.0029	7.64	
3-3	70	60	10	0.0333	146.608	0.0031	8.08	
4-1	70	60	10	0.0417	146.608	0.0031	8.12	7.98
4-2	70	60	10	0.0417	146.608	0.0031	8.08	
4-3	70	60	10	0.0417	146.608	0.0030	7.75	
5-1	70	60	10	0.0500	146.608	0.0031	8.03	8.03
5-2	70	60	10	0.0500	146.608	0.0031	8.19	
5-3	70	60	10	0.0500	146.608	0.0030	7.86	
6-1	70	60	10	0.0617	146.608	0.0031	8.19	8.19
6-2	70	60	10	0.0617	146.608	0.0031	8.08	
6-3	70	60	10	0.0617	146.608	0.0032	8.30	

Appendix II
Calculation of surfaces areas on the cone

The overall heat transfer rate (Q) from the heating medium to evaporating liquid across the wall of the cone and the liquid films can be described by the following equation:

$$Q = h_s A_s (T_s - T_{ws}) = A_m \frac{k_w}{\delta_w} (T_{ws} - T_{wl}) = h_l A_l (T_{wl} - T_l)$$

So, the temperature differences can be calculated as follows:

$$T_s - T_{ws} = \frac{Q}{h_s A_s}$$

$$T_{ws} - T_{wl} = \frac{Q\delta_w}{k_w}$$

$$T_{wl} - T_i = \frac{Q}{h_l A_l}$$

$$T_s - T_l = Q\left(\frac{1}{h_s A_s} + \frac{\delta_w}{k_w A_m} + \frac{1}{h_s A_l}\right)$$

The overall heat transfer equation based on inner surface of the cone can be written as follows:

$$\frac{1}{H_{cal}} = \frac{A_s}{h_s A_s} + \frac{\delta_w A_s}{k_s A_m} + \frac{1}{h_l A_l}$$

The surface areas on the cone:

$$A_s = \pi\ l\left(\frac{D_o + d_o}{2}\right) = \pi \sqrt{(R_i - r_i)^2 + S^2}\,(R_i + r_i + 2\delta_w)$$

$$A_l = \pi\ l\,(R_i - r_i) = \pi \sqrt{(R_i - r_i)^2 + S^2}\,(R_i + r_i)$$

$$A_m = \frac{A_s - A_l}{\ln\left(\frac{A_s}{A_l}\right)} = \left(\frac{\pi \sqrt{(R_i - r_i)^2 + S^2}\,2\delta_w}{\ln\left(1 + \frac{2\delta_w}{R_i + r_i}\right)}\right)$$

Appendix III

Correlations of the physical properties for water, sugar solution and skim milk

3. 1 Water physical properties

The data of physical properties for water were taken from Thermophysical Properties of Water Substance by Rogers and Mayhew (1982). A computer programm of Fig.P (Fig.P Software Corporation, Ver.6.0, 1992) was used to fit the data and generate the correlations. These correlations could be used for the temperature range of 40 to110°C.

3.1.1 Water density

Water density as a function of temperature was determined by the following correlation in the units of kg/m^3:

$$\rho = 1.0167x\,10^3 - 0.9143T + 1.0929x\,10^2$$
$$-8.675x\,10^{-5}T^{-3} + 1.01x10\text{-}11T^{-6}$$

(R^2 = 99.95%, df =10)

3.1.2 Water kinematic viscosity

Water dynamic viscosity as a function of temperature was determined by the following correlation in the units of m^3/s:

$$\nu = 1.407 \times 10^{-7} \exp\left(\frac{73.87}{T}\right)$$

(R^2 = 99.1%, df = 16)

3.1.3 Water thermal capacity

Water thermal capacity as a function of temperature was determined by the following correlation in the units of J/kg.K:

$$C_p = 4.1828 \times 10^3 - 0.4457\,T + 7.959 \times 10^{-3}\,T^2$$

(R^2 = 99.9%, df = 16)

3.1.4 Water thermal conductivity

Water thermal conductivity as a function of temperature was determined by the following correlation in the units of W/m.K:

$$k = 0.5682 + 1.85 \times 10^{-3} T - 7.273 \times 10^{-6} T^2$$
$$(R^2 = 99.9\%, \text{df} = 16)$$

3.1.5 Latent heat of vaporisation

Latent heat of vapourization as a function of evaporation temperature was determined by the following correlation in the units of J/kg:

$$h_{fg} = 2.5132 \times 10^6 - 2.565 \times 10^3 T_{evp}$$
$$(R^2 = 99.9\%, \text{df} = 16)$$

3.2 Sugar solution physical properties

3.2.1 Sugar solution density

Sugar solution density as a function of temperature and total solids was determined by the following correlation in the units of kg/m^3 (MacKereth, 1993):

$$\rho_{ss} = (0.9831 - 9.667 \times 10^{-3} T \cdot C_1 + 6.187 \times 10^{-4} C_1 \cdot C_2 - 6.2268 \times 10^{-5} C_1^2 + 4.095 \times 10^{-4} C_2) D_{20}$$

Where:

$$D_{20} = 1183.2 + 216.147 C_3 + 30.9247 C_3^2 + 0.27466 C_3^3$$

$$C_1 = \frac{T - 60}{20}, \qquad C_2 = \frac{TS - 50}{20}, \qquad C_3 = \frac{TS - 41.5}{41.5}$$

The total solids is in the range of 30 to 70% and the temperature is in the range of 40 to 80°C.

3.2.2 Sugar solution dynamic viscosity

The correlation was proposed by Campanella (1992) and the application ranges are of 0 to60% total solids and 0-95°C temperature. The unit of viscosity is in centipoise.

$$\mu_{ss} = 8.194 \times 10^{-2} \exp\left(9.176 \times 10^{-2} (1 + TS)^{4.9029}\right) \exp\left(\frac{2.5027 \times 10^7 + 4.4433 (1 + TS)^{4.9029}}{T^{2.8774}}\right)$$

3.2.3 Sugar solution thermal conductivity

Sugar solution thermal conductivity as a function of temperature and total solids was determined by the following correlation, which fitted to 9 data points from Honig (1963) using Fig.P programm. The units of thermal conductivity are W/mK:

$$k_{ss} = 0.596 + 9.31 \times 10^{-4} T - 3.49 \times 10^{-3} TS$$
$$(R^2 = 99.7\%)$$

The temperature is in the range of 50 to 70°C and total solids are in the range of 40 to 60%.

3.2.4 Sugar solution boiling point elevation

The boiling point of skim milk as a function of total solids was determined by the following correlations in the unit of degree centigrade (Mechereth, 1993):

$$BPE_{ss} = \exp\left(-9.013 \times 10^{-2} - 3.33 \times 10^{-2} TS + 8.095 \times 10^{-4} TS^2\right)$$

3.3 Skim milk physical properties

3.3.1 Skim milk density

Skim milk density as a function of temperature and total solids was determined by the following correlation in the units of kg/m^3 (Hall and Hedrick, 1966):

$$\rho_{skim} = \left[\frac{(2K_6 Ts - K_4 T - K_5)^2 - (K_4 T - K_5)^2 + 4K_6 (K_1 - K_2 T + K_3 T^2)}{\frac{4}{K_6}} \right]$$

Where: $K_1 = 989$; $K_2 = 0.064$; $K_3 = 0.0024$; $K_4 = 0.0076$; $K_5 = 3.75$; $K_6 = 0.00166$

The temperatures are in the range of 0 to 10°C and total solids are in the range of 9 to 50%.

3.3.2 Skim milk dynamic viscosity

The correlation fitted to 6 data point from Wood (1982) using Fig.P programm. The dynamic viscosity was in the unit of centipoise. The temperature is in the range of 30-70°C.

$$\mu_{skim} = 14.6899 \exp(-0.0949T) + 0.7286$$

$$(R^2 = 98.6\%)$$

3.3.3 Skim milk thermal conductivity

The correlation fitted to 6 data point from Wood (1982) using Fig.P programm.
The thermal conductivity was in the units of W/m.K. The temperature is in the range of 40 to 90°C.

$$k_{skim} = 0.54 + 2.0 \times 10^{-3} T - 1.07 \times 10^{-5} T^2$$
$$(R^2 = 99.7\%)$$

3.3.4 Skim milk boiling point elevation

The boiling point of skim milk as a function of total solids was determined by the following correlations in the unit of degree centigrade (Mackereth, 1993):

$$BPE_{skim} = 2.78 \times 10^{-3} TS + 2.94 \times 10^{-4} TS^2 - 4.65 \times 10^{-3}$$
$$(R^2 = 98.5\%)$$

Appendix IV

Results of numerical calculation

4.1 The theoretical results of the model

X^*		100	500	1000	5000	10000
T_i (°C)		70	70	70	70	70
FF ($x10^{-5}$ m^3/s)		5.0	5.0	5.0	5.0	5.0
RS(rad/s)		157	157	157	157	157
δ^*	β=10°	48.24	23.84	16.54	6.28	4.02
	β=20°	33.34	13.84	9.03	3.18	2.04
	β=30°	24.78	9.43	6.03	2.09	1.32
	β=40°	19.13	6.96	4.42	1.52	0.96
	β=50°	15.04	5.33	3.38	1.16	0.73

X^*		100	500	1000	5000	10000
T_i (°C)		70	70	70	70	70
β		40°	40°	40°	40°	40°
RS(rad/s)		157	157	157	157	157
δ^*	FF=$6.7x10^{-5}$ (m^3/s)	21.09	7.67	4.87	1.68	1.06
	FF=$6.7x10^{-5}$ (m^3/s)	19.13	6.96	4.42	1.52	0.96
	FF=$6.7x10^{-5}$ (m^3/s)	16.66	6.06	3.85	1.33	0.84
	FF=$6.7x10^{-5}$ (m^3/s)	13.35	4.85	3.08	1.06	0.67

X^* ($x10^3$)		5.57	5.57	5.57	5.57	5.57	5.57
T_i (°C)		70	70	70	70	70	70
FF ($x10^{-5}$ m^3/s)		5.0	5.0	5.0	5.0	5.0	5.0
R_o		$4x10^{-5}$	$4x10^{-4}$	$4x10^{-3}$	$4x10^{-2}$	$4x10^{-1}$	4
δ^*	β=10°	12.54	9.07	4.70	2.20	1.00	0.48
	β=20°	10.00	7.20	3.70	1.75	0.80	0.37
	β=30°	8.69	6.30	3.25	1.53	0.71	0.33
	β=40°	7.88	5.70	2.95	1.39	0.65	0.30
	β=50°	7.29	5.27	2.73	1.28	0.60	0.28

X^* ($x10^3$)		5.57	5.57	5.57	5.57	5.57	5.57
T_l (°C)		70	70	70	70	70	70
FF ($x10^{-5}$ m^3/s)		5.0	5.0	5.0	5.0	5.0	5.0
RS(rad/s)		52	105	157	210	262	314
Nu	β=10°	0.097	0.135	0.171	0.204	0.235	0.265
	β=20°	0.171	0.260	0.337	0.407	0.472	0.532
	β=30°	0.253	0.394	0.514	0.622	0.721	0.814
	β=40°	0.344	0.540	0.706	0.855	0.991	1.119
	β=50°	0.449	0.708	0.927	1.122	1.302	1.470

X (m)	0.093	0.124	0.155	0.186	0.217
ET (°C)	70	70	70	70	70
ΔT (K)	10	10	10	10	10
FF ($x10^{-5}m^3/s$)	5.0	5.0	5.0	5.0	5.0
RS(rad/s)	157	157	157	157	157
k_w/d_w ($kw/m^2.K$)	28.13	28.13	28.13	28.13	28.13
h_l^c($kW/m^2.K$)	13.72	16.61	19.27	21.76	24.12
h_s ($kW/m^2.K$)	60.91	59.14	57.88	56.66	55.80
H_{cal} ($kW/m^2.K$)	7.96	8.83	9.50	10.03	10.48

X (m)	0.093	0.124	0.155	0.186	0.217
ET (°C)	70	70	70	70	70
ΔT (K)	10	10	10	10	10
FF ($x10^{-5}m^3/s$)	5.0	5.0	5.0	5.0	5.0
RS(rad/s)	186	186	186	186	186
T_{wl} (°C)	75.83	75.34	74.96	74.64	74.37
T_{ws} (°C)	78.68	78.51	78.38	78.23	78.12
δ ($x10^{-5}$)(m)	4.38	3.70	3.25	2.91	2.65
Re	345	257	205	170	146

4.2. The calculated heat transfer coefficients in the Centritherm evaporator

4.2.1 For water

ET (°C)	60	70	70	70	70
ΔT (K)	50	10	10	10	10
FF (m^3/s)	$5.0x10^{-5}$	$0.7x10^{-5}$	$1.0x10^{-5}$	$1.3x10^{-5}$	$2.5x10^{-5}$
RS(rad/s)	186	186	186	186	186
T_{wl} (°C)	81.5	72.7	73.1	73.5	74.2
T_{ws} (°C)	98.0	77.4	77.4	77.7	78.0
h_l '($x10^4$) ($W/m^2.K$)	2.21	4.90	3.88	3.40	2.50
h_s ($x10^4$) ($W/m^2.K$)	3.85	5.10	5.10	5.30	5.50
H_{cal}($x10^3$) ($W/m^2.K$)	9.18	13.22	12.33	11.89	10.68

ET (°C)	70	70	70	70	70
ΔT (K)	10	10	10	10	30
FF (m^3/s)	$3.3x10^{-5}$	$4.2x10^{-5}$	$5.0x10^{-5}$	$6.2x10^{-5}$	$1.0x10^{-5}$
RS(rad/s)	186	186	186	186	42
T_{wl} (°C)	74.5	74.7	74.9	75.0	81.6
T_{ws} (°C)	78.1	78.2	78.3	78.2	88.6
h_l'($x10^4$) ($W/m^2.K$)	2.28	2.08	1.95	1.80	1.70
h_s ($x10^4$) ($W/m^2.K$)	5.6	5.62	5.72	5.65	1.78
H_{cal}($x10^3$) ($W/m^2.K$)	10.22	9.81	9.54	9.15	6.64

ET (°C)	70	70	70	70	70
ΔT (K)	30	30	30	30	30
FF (m^3/s)	$1.3x10^{-5}$	$2.5x10^{-5}$	$3.3x10^{-5}$	$4.2x10^{-5}$	$5.0x10^{-5}$
RS(rad/s)	42	42	42	42	42
T_{wl} (°C)	83.1	85.7	86.8	87.6	88.1
T_{ws} (°C)	89.8	91.4	97.2	92.8	93.1
$h_l'(x10^4)$ ($W/m^2.K$)	1.40	1.00	0.90	0.80	0.77
h_s ($x10^4$) ($W/m^2.K$)	1.80	1.90	1.96	1.99	2.0
$H_{cal}(x10^3)$ ($W/m^2.K$)	6.23	5.36	5.06	4.81	4.63

ET (°C)	70	60	60	60	60
ΔT (K)	10	10	10	10	10
FF (m^3/s)	$6.2x10^{-5}$	$1.3x10^{-5}$	$2.5x10^{-5}$	$3.3x10^{-5}$	$4.2x10^{-5}$
RS(rad/s)	42	147	147	147	147
T_{wl} (°C)	88.7	64.0	64.5	65.0	65.1
T_{ws} (°C)	93.4	67.8	68.0	68.2	68.1
$h_l'(x10^4)$ ($W/m^2.K$)	0.71	2.67	2.00	1.81	1.65
h_s ($x10^4$) ($W/m^2.K$)	2.00	4.57	4.53	4.82	4.75
$H_{cal}(x10^3)$ ($W/m^2.K$)	4.43	10.49	9.25	8.91	8.49

ET (°C)	60	60
ΔT (K)	10	10
FF (m^3/s)	$5.0x10^{-5}$	$6.2x10^{-5}$
RS(rad/s)	147	147
T_{wl} (°C)	65.2	65.5
T_{ws} (°C)	68.1	68.3
$h_l'(x10^4)$ ($W/m^2.k$)	1.55	1.44
h_s ($x10^4$) ($W/m^2.K$)	4.73	4.89
$H_{cal}(x10^3)$ ($W/m^2.K$)	8.20	7.92

4.2.2 For sugar solutions

TS (%)	20	20	20	20	20
ET (°C)	60	60	60	60	60
ΔT (K)	10	10	10	10	10
FF (m^3/s)	$1.3x10^{-5}$	$2.5x10^{-5}$	$3.3x10^{-5}$	$4.2x10^{-5}$	$5.0x10^{-5}$
RS(rad/s)	147	147	147	147	147
T_{wl} (°C)	64.5	65.1	65.4	65.6	65.7
T_{ws} (°C)	68.0	68.1	68.3	68.4	68.3
$h_l'(x10^4)$ ($W/m^2.K$)	2.20	1.60	1.50	1.40	1.30
h_s ($x10^4$) ($W/m^2.K$)	4.75	4.79	4.89	4.93	4.90
$H_{cal}(x10^3)$ ($W/m^2.K$)	9.81	8.60	8.17	7.85	7.50

TS (%)	20	20	20	20	20
ET (°C)	60	70	70	70	70
ΔT (K)	10	5	10	15	20
FF (m^3/s)	$6.2x10^{-5}$	$4.2x10^{-5}$	$4.2x10^{-5}$	$4.2x10^{-5}$	$4.2x10^{-5}$
RS(rad/s)	147	186	186	186	186
T_{wi} (°C)	65.9	73.0	75.5	77.9	80.2
T_{ws} (°C)	68.4	74.4	78.5	82.5	86.4
$h_i'(x10^4)$ ($W/m^2.K$)	1.20	1.70	1.75	1.79	1.83
h_s ($x10^4$) ($W/m^2.K$)	4.99	7.38	5.92	5.29	4.90
$H_{cal}(x10^3)$ ($W/m^2.K$)	7.19	9.24	9.07	9.02	9.10

TS (%)	20	20	30	30	30
ET (°C)	70	70	70	70	70
ΔT (K)	25	30	5	10	15
FF (m^3/s)	$4.2x10^{-5}$	$4.2x10^{-5}$	$4.2x10^{-5}$	$4.2x10^{-5}$	$4.2x10^{-5}$
RS(rad/s)	186	186	186	186	186
T_{wi} (°C)	82.4	84.5	73.0	75.8	78.3
T_{ws} (°C)	90.0	94.0	74.2	78.6	82.6
$h_i'(x10^4)$ ($W/m^2.K$)	1.88	1.92	1.51	1.55	1.58
h_s ($x10^4$) ($W/m^2.K$)	4.60	4.40	6.80	6.00	5.30
$H_{cal}(x10^3)$ ($W/m^2.K$)	9.00	9.01	8.54	8.51	8.46

TS (%)	30	30	30	40	40
ET (°C)	70	70	70	70	70
ΔT (K)	20	25	30	5	10
FF (m^3/s)	$4.2x10^{-5}$	$4.2x10^{-5}$	$4.2x10^{-5}$	$4.2x10^{-5}$	$4.2x10^{-5}$
RS(rad/s)	186	186	186	186	186
T_{wi} (°C)	80.8	83.0	85.4	73.3	76.2
T_{ws} (°C)	86.6	90.3	94.3	74.4	78.6
h_i´$9x10^4$) ($W/m^2.K$)	1.62	1.66	1.70	1.28	1.31
h_s ($x10^4$) ($W/m^2.K$)	4.97	4.62	4.46	7.29	6.1
H_{cal}($x10^3$) ($W/m^2.K$)	8.48	8.46	8.52	7.80	7.75

TS (%)	40	40	40	40	50
ET (°C)	70	70	70	70	70
ΔT (K)	15	20	25	30	5
FF (m^3/s)	$4.2x10^{-5}$	$4.2x10^{-5}$	$4.2x10^{-5}$	$4.2x10^{-5}$	$4.2x10^{-5}$
RS(rad/s)	186	186	186	186	186
T_{wi} (°C)	79.0	81.7	84.3	86.7	73.7
T_{ws} (°C)	82.9	87.0	91.0	94.8	74.5
h_i´($x10^4$) ($W/m^2.K$)	1.34	1.38	1.41	1.44	1.03
h_s ($x10^4$) ($W/m^2.K$)	5.50	5.12	4.83	4.57	7.95
H_{cal}($x10^3$) ($W/m^2.K$)	7.76	7.79	7.82	7.85	6.80

TS (%)	50	50	50	50	50
ET (°C)	70	70	70	70	70
ΔT (K)	10	15	20	25	30
FF (m^3/s)	$4.2x10^{-5}$	$4.2x10^{-5}$	$4.2x10^{-5}$	$4.2x10^{-5}$	$4.2x10^{-5}$
RS(rad/s)	186	186	186	186	186
T_{wi} (°C)	77.0	80.0	82.8	85.7	88.5
T_{ws} (°C)	79.1	83.3	87.3	91.5	95.7
$h_i'(x10^4)$ ($W/m^2.K$)	1.06	1.09	1.11	1.14	1.17
h_s ($x10^4$) ($W/m^2.K$)	6.79	5.86	5.28	5.00	4.77
$H_{cal}(x10^3)$ ($W/m^2.K$)	6.86	6.86	6.88	6.94	7.00

TS (%)	60	60	60	60	60
ET (°C)	70	70	70	70	70
ΔT (K)	5	10	15	20	25
FF (m^3/s)	$4.2x10^{-5}$	$4.2x10^{-5}$	$4.2x10^{-5}$	$4.2x10^{-5}$	$4.2x10^{-5}$
RS(rad/s)	186	186	186	186	186
T_{wi} (°C)	74.2	77.7	81.1	84.3	87.5
T_{ws} (°C)	74.7	79.2	83.6	87.9	92.2
$h_i'(x10^4)$ ($W/m^2.K$)	7.79	8.00	8.20	8.50	8.70
h_s ($x10^4$) ($W/m^2.K$)	8.92	7.00	6.20	5.60	5.30
$H_{cal}(x10^3)$ ($W/m^2.K$)	5.67	5.69	5.74	5.80	5.86

TS (%)	60	68	20	20	20
ET (°C)	70	70	70	70	70
ΔT (K)	30	10	5	10	15
FF (m^3/s)	$4.2x10^{-5}$	$4.2x10^{-5}$	$4.2x10^{-5}$	$4.2x10^{-5}$	$4.2x10^{-5}$
RS(rad/s)	186	186	147	147	147
T_{wi} (°C)	90.7	78.6	73.1	75.5	78.2
T_{ws} (°C)	96.6	79.6	74.4	78.0	82.3
$h_i'(x10^4)$ ($W/m^2.K$)	8.90	6.14	1.46	1.48	1.52
h_s ($x10^4$) ($W/m^2.K$)	5.10	8.23	6.38	4.90	4.5
$H_{cal}(x10^3)$ ($W/m^2.K$)	5.94	4.72	8.23	8.07	8.08

TS (%)	20	20	20	30	30
ET (°C)	70	70	70	70	70
ΔT (K)	20	25	30	5	10
FF (m^3/s)	$4.2x10^{-5}$	$4.2x10^{-5}$	$4.2x10^{-5}$	$4.2x10^{-5}$	$4.2x10^{-5}$
RS(rad/s)	147	147	147	147	147
T_{wi} (°C)	80.7	83.1	85.3	73.2	76.0
T_{ws} (°C)	86.3	90.1	93.7	74.3	78.4
$h_i'(x10^4)$ ($W/m^2.K$)	1.55	1.59	1.62	1.28	1.30
h_s ($x10^4$) ($W/m^2.K$)	4.30	4.07	3.87	6.33	5.22
$H_{cal}(x10^3)$ ($W/m^2.K$)	8.08	8.09	8.09	7.70	7.60

TS (%)	30	40	40	50	50
ET (°C)	70	70	70	70	70
ΔT (K)	30	10	30	10	30
FF (m^3/s)	$4.2x10^{-5}$	$4.2x10^{-5}$	$4.2x10^{-5}$	$4.2x10^{-5}$	$4.2x10^{-5}$
RS(rad/s)	147	147	147	147	147
T_{wl} (°C)	86.3	76.6	87.6	77.1	89.5
T_{ws} (°C)	94.3	78.9	94.9	79.0	95.9
$h_l'(x10^4)$ ($W/m^2.K$)	1.44	1.12	1.14	0.90	0.99
h_s ($x10^4$) ($W/m^2.K$)	3.96	5.62	1.22	5.70	4.30
$H_{cal}(x10^3)$ ($W/m^2.K$)	7.64	6.96	7.02	6.05	6.24

4.2.3 For skim milk

ET (°C)	60	60	60	60	60	70
ΔT (K)	10	10	10	10	10	10
FF ($x10^{-5}$ m^3/s)	1.3	2.5	3.3	4.2	5.0	4.2
RS(rad/s)	147	147	147	147	147	147
T_{wl} (°C)	64.5	65.3	65.5	65.7	65.9	66
T_{ws} (°C)	67.8	68.3	68.3	68.4	68.5	68.4
$h_l'(x10^4)$ ($W/m^2.K$)	2.10	1.60	1.44	1.30	1.24	1.15
h_s ($x10^4$) ($W/m^2.K$)	4.60	4.90	4.89	4.93	5.00	4.99
$H_{cal}(x10^3)$ ($W/m^2.K$)	9.52	8.40	7.91	7.55	7.29	6.96

4.3 The calculated heat transfer coefficients in the cone evaporator

ET (°C)	70	70	70	70	70
ΔT (K)	10	10	10	10	10
FF (m^3/s)	$5x10^{-5}$	$5x10^{-5}$	$5x10^{-5}$	$5x10^{-5}$	$5x10^{-5}$
RS(rad/s)	52	84	105	157	186
T_{wl} (°C)	76.5	76.2	76.0	75.6	75.5
T_{ws} (°C)	77.7	77.7	77.6	77.6	77.7
$h_l'(x10^4)$ ($W/m^2.K$)	0.51	0.68	0.78	1.02	1.12
h_s ($x10^4$) ($W/m^2.K$)	1.46	1.80	2.10	2.50	2.67
$H_{cal}(x10^3)$ ($W/m^2.K$)	3.33	4.20	4.70	5.75	6.13

ET (°C)	70	70	60	60	60
ΔT (K)	10	10	10	10	10
FF (m^3/s)	$5x10^{-5}$	$5x10^{-5}$	$5x10^{-5}$	$5x10^{-5}$	$5x10^{-5}$
RS(rad/s)	209	230	52	84	105
T_{wl} (°C)	75.3	75.2	66.6	66.3	76.0
T_{ws} (°C)	77.6	77.6	67.7	67.7	67.6
$h_l'(x10^4)$ ($W/m^2.K$)	1.24	1.33	0.48	0.64	0.73
h_s ($x10^4$) ($W/m^2.K$)	2.91	3.05	1.40	1.78	1.96
$H_{cal}(x10^3)$ ($W/m^2.K$)	6.61	6.92	3.17	4.00	4.46

ET (°C)	60	60	60	60	70
ΔT (K)	10	10	10	10	4
FF (m^3/s)	$5x10^{-5}$	$5x10^{-5}$	$5x10^{-5}$	$5x10^{-5}$	$4.2x10^{-5}$
RS(rad/s)	157	186	209	230	230
T_{wi} (°C)	65.7	65.6	65.4	65.3	72.7
T_{ws} (°C)	67.6	67.8	67.6	67.6	73.2
$h_i'(x10^4)$ ($W/m^2.K$)	0.96	1.04	1.17	1.24	1.30
h_s ($x10^4$) ($W/m^2.K$)	2.40	2.59	2.79	2.93	3.90
$H_{cal}(x10^3)$ ($W/m^2.K$)	5.49	5.85	6.32	6.62	7.40

ET (°C)	70	70	60	60	60
ΔT (K)	10	15	10	10	10
FF (m^3/s)	$4.2x10^{-5}$	$4.2x10^{-5}$	$1.7x10^{-5}$	$4.2x10^{-5}$	$6.7x10^{-5}$
RS(rad/s)	230	230	230	230	230
T_{wi} (°C)	75.1	77.2	64.0	65.0	65.7
T_{ws} (°C)	76.7	81.0	66.9	67.4	68.0
$h_i'(x10^4)$ ($W/m^2.K$)	1.40	1.50	2.10	1.33	1.11
h_s ($x10^4$) ($W/m^2.K$)	3.10	2.70	2.80	2.85	3.04
$H_{cal}(x10^3)$ ($W/m^2.K$)	7.20	7.14	8.26	6.82	6.27

ET (°C)	50	50	50
ΔT (K)	10	10	10
FF (m^3/s)	$5x10^{-5}$	$5x10^{-5}$	$5x10^{-5}$
RS(rad/s)	157	157	157
T_{wi} (°C)	55.9	65.7	75.6
T_{ws} (°C)	57.7	67.6	77.6
$h_i'(x10^4)$ ($W/m^2.K$)	8.70	0.96	1.02
h_s ($x10^4$) ($W/m^2.K$)	2.30	2.40	2.50
$H_{cal}(x10^3)$ ($W/m^2.K$)	5.16	5.49	5.75

Appendix V

An example of determining the uncertainty for overall heat transfer coefficient

The measured overall heat transfer coefficient can be calculated using following equation:

$$H_{exp} = \frac{W_{exp}\, h_{fg}}{A\, \Delta T}$$

If the evaporating temperature was 70°C ±0.5°C and the steam temperature was 80°C ±0.5 °C, then the temperature difference and its uncertainty can determined as follows:

$$\Delta T = (80 - 70) \pm (0.5^2 + 0.5^2)^{1/2} = 10 \pm 0.71 \ ^\circ C$$

Therefore, 95% confidence interval in percentage terms as follows:

$$P1 = (0.71/10) \times 100 = 7.1$$

The condensate flow rate was measured in a typical run as 175, 185, 188 ml/min, so its mean and uncertainty were 182.67 ± 11 ml/min [Standard deviation (s) = 2.55, t = 4.3, 95% confidence interval (B) = $s \cdot t = 2.55 \times 4.3 = 10.965$].

Therefore:

$$P2 = (10.965/182.67) \times 100 = 6.0$$

$$Pr = (P1^2 + P2^2)^{1/2} = (7.1^2 + 6.0^2)^{1/2}$$

$$= (50.4 + 36)^{1/2} = 9.3$$

The overall heat transfer coefficient was calculated as follows:

$$H_{cal} = \frac{182.67 \times 2360}{0.09 \times 10} = 7.06 \quad (kW / m^2 K)$$

The uncertainty of overall heat transfer coefficient can be calculated as follows:

$H_{cal} = 7.06 \pm 7.06 \times 9.3 / 100 = 7.06 \pm 0.66$ kW/m^{2}K (or 7.06 kW/m^{2}K ±10%)

So the 95% confident interval of measured overall heat transfer coefficient was about 10%.

Appendix VI

Polyacrylamide gel electrophoresis (PAGE)

Polyacrylamide gel electrophoresis (PAGE) is regarded as a standard method to identify the undenatured whey proteins in milk. The Bio-Rad Mini Protean II equipment (Bio-Rad Laboratories, Richmond, CA 94804, USA) was used to perform PAGE. The prepared whey protein solutions were diluted (1:7.5, 1:22.5, 1:45 or 1:85 for 10, 30, 60, or 120g/kg WP solutions respectively) with the appropriate sample buffer and analyzed using native-PAGE as described by Andrews (1983). 10 µl of each sample was applied to the gel. The gels were run at 200 V for about 45 minutes until the dye disappeared from the bottom of the gel. Afterwards the gels were stained for one hour, with Coomassie Blue dye solution in a closed container with continuous vibrations. This was followed by two destaining steps of one hour and nineteen hours, in destaining solution. Finished gels were kept in distilled water until scanning. A 35 mm camera fitted with both a green (XI) and an orange (G) Hoya filter (to minimize the stray light) was used to photograph the gels on a 100ASA Kodak T-max film.

The gels were scanned using an Ultrascan XL laser densitometer and the results were analyzed using an LKB 2400 GelScanXL software program (LKB Produkter AB, Stockholm-Bromma 1, Sweden) to obtain quantitative results. The protein bands on the resultant gels were identified by concurrent electrophoresis of samples of BSA, α-lactalbumin, β-lactoglobulin A, β-lactoglobulin B. The peak area of each protein band was reported as a percentage of the corresponding band in the unheated control whey protein solution samples.

Appendix VII

Experimental results of fouling in the Centritherm evaporators

Time (hr)	ST (°C)	ET (°C)	FT (°C)	FF ($\times10^{-3}$ m^3/s)	W_{exp} ($\times10^{-3}$ m^3/s)	RS (rad/s)	H_{cal} (kW/m^2K)	Ave-H_{cal} (kW/m^2K)	R_f (m^2K/kW)
0	80	60	61	0.0417	0.0067	186.4	8.73	8.59	0.000
	80	60	59	0.0417	0.0064	186.4	8.41		
	80	60	60	0.0417	0.0066	186.4	8.62		
0.5	80	60	61	0.0417	0.0066	186.4	8.62	8.55	0.000
	80	60	63	0.0417	0.0067	186.4	8.73		
	80	60	59	0.0417	0.0063	186.4	8.30		
1 3	80	60	58	0.0417	0.0063	186.4	8.30	8.44	0.002
	80	60	62	0.0417	0.0066	186.4	8.62		
	80	60	61	0.0417	0.0064	186.4	8.41		
1.5	80	60	62	0.0417	0.0062	186.4	8.08	7.82	0.011
	80	60	60	0.0417	0.0059	186.4	7.75		
	80	60	59	0.0417	0.0058	186.4	7.64		
2	80	60	59	0.0417	0.0055	186.4	7.21	7.42	0.018
	80	60	59	0.0417	0.0055	186.4	7.21		
	80	60	62.5	0.0417	0.0060	186.4	7.86		
2.5	80	60	59	0.0417	0.0055	186.4	7.21	7.08	0.025
	80	60	59	0.0417	0.0054	186.4	7.05		
	80	60	58	0.0417	0.0053	186.4	6.99		
3	80	60	58	0.0417	0.0053	186.4	6.92	7.18	0.023
	80	60	61	0.0417	0.0056	186.4	7.27		
	80	60	62	0.0417	0.0056	186.4	7.36		
3.5	80	60	62	0.0417	0.0056	186.4	7.31	7.05	0.025
	80	60	59	0.0417	0.0053	186.4	6.92		
	80	60	59	0.0417	0.0053	186.4	6.92		
4	80	60	58	0.0417	0.0051	186.4	6.66	6.70	0.033
	80	60	58	0.0417	0.0050	186.4	6.55		
	80	60	60	0.0417	0.0053	186.4	6.88		
4.5	80	60	62	0.0417	0.0053	186.4	6.99	6.73	0.032
	80	60	60	0.0417	0.0051	186.4	6.66		
	80	60	59	0.0417	0.0050	186.4	6.55		
5	80	60	60	0.0417	0.0052	186.4	6.77	6.67	0.034
	80	60	61	0.0417	0.0052	186.4	6.83		
	80	60	59	0.0417	0.0049	186.4	6.40		
5.5	80	60	61	0.0417	0.0053	186.4	6.90	6.85	0.030
	80	60	59	0.0417	0.0050	186.4	6.55		
	80	60	62	0.0417	0.0054	186.4	7.10		
6	80	60	62	0.0417	0.0053	186.4	6.88	6.69	0.033

	80	60	60	0.0417	0.0051	186.4	6.64		
	80	60	60	0.0417	0.0050	186.4	6.55		
6.5	80	60	60	0.0417	0.0049	186.4	6.40	6.38	0.040
	80	60	59	0.0417	0.0049	186.4	6.38		
	80	60	59	0.0417	0.0049	186.4	6.38		
7	80	60	60	0.0417	0.0049	186.4	6.38	6.42	0.039
	80	60	59	0.0417	0.0048	186.4	6.33		
	80	60	60.5	0.0417	0.0050	186.4	6.55		

Time (hr)	ST (°C)	ET (°C)	FT (°C)	FF ($\times10^{-3}$ m^3/s)	W_{exp} ($\times10^{-3}$ m^3/s)	RS (rad/s)	H_{cal} (kW/m^2K)	Ave-H_{cal} (kW/m^2K)	R_f (m^2K/kW)
0	90	70	68	0.0417	0.0083	186.4	10.70	10.77	0.000
	90	70	70	0.0417	0.0083	186.4	10.81		
	90	70	71	0.0417	0.0083	186.4	10.81		
0.5	90	70	72	0.0417	0.0077	186.4	9.94	9.65	0.007
	90	70	71	0.0417	0.0075	186.4	9.73		
	90	70	69	0.0417	0.0072	186.4	9.29		
1	90	70	70	0.0417	0.0068	186.4	8.75	8.61	0.021
	90	70	68	0.0417	0.0064	186.4	8.32		
	90	70	71	0.0417	0.0068	186.4	8.75		
1.5	90	70	71	0.0417	0.0062	186.4	8.00	7.71	0.032
	90	70	68	0.0417	0.0058	186.4	7.56		
	90	70	68	0.0417	0.0058	186.4	7.56		
2	90	70	70	0.0417	0.0056	186.4	7.24	7.10	0.045
	90	70	68	0.0417	0.0053	186.4	6.92		
	90	70	70	0.0417	0.0055	186.4	7.13		
2.5	90	70	72	0.0417	0.0056	186.4	7.24	6.97	0.045
	90	70	69	0.0417	0.0053	186.4	6.92		
	90	70	68	0.0417	0.0052	186.4	6.76		
3	90	70	71	0.0417	0.0055	186.4	7.13	7.02	0.047
	90	70	70	0.0417	0.0054	186.4	7.02		
	90	70	69	0.0417	0.0053	186.4	6.92		
3.5	90	70	72	0.0417	0.0056	186.4	7.24	6.95	0.045
	90	70	69	0.0417	0.0053	186.4	6.81		
	90	70	69	0.0417	0.0053	186.4	6.81		
4	90	70	68	0.0417	0.0052	186.4	6.70	7.05	0.056
	90	70	72	0.0417	0.0056	186.4	7.24		
	90	70	72	0.0417	0.0056	186.4	7.20		
4.5	90	70	72	0.0417	0.0056	186.4	7.28	7.00	0.044
	90	70	70	0.0417	0.0054	186.4	7.02		
	90	70	68	0.0417	0.0052	186.4	6.70		

5	90	70	71	0.0417	0.0055	186.4	7.13	7.17	0.047
	90	70	72	0.0417	0.0058	186.4	7.46		
	90	70	70	0.0417	0.0053	186.4	6.92		
5.5	90	70	70	0.0417	0.0057	186.4	7.35	7.30	0.043
	90	70	71	0.0417	0.0057	186.4	7.35		
	90	70	70	0.0417	0.0056	186.4	7.20		
6	90	70	69	0.0417	0.0055	186.4	7.13	7.31	0.047
	90	70	70	0.0417	0.0056	186.4	7.24		
	90	70	73	0.0417	0.0058	186.4	7.56		

Time (hr)	ST (°C)	ET (°C)	FT (°C)	FF ($\times 10^{-3}$ m^3/s)	W_{exp} ($\times 10^{-3}$ m^3/s)	RS (rad/s)	H_{cal} (kW/m^2K)	Ave-H_{cal} (kW/m^2K)	R_f (m^2K/kW)
0	90	70	70	0.0417	0.0082	104.7	10.59	10.59	0.000
	90	70	70	0.0417	0.0083	104.7	10.70		
	90	70	70	0.0417	0.0081	104.7	10.48		
0.5	90	70	69.8	0.0417	0.0065	104.7	8.43	8.43	0.024
	90	70	68.5	0.0417	0.0063	104.7	8.21		
	90	70	69.9	0.0417	0.0067	104.7	8.64		
1	90	70	70.5	0.0417	0.0063	104.7	8.21	8.07	0.027
	90	70	69	0.0417	0.0059	104.7	7.67		
	90	70	72	0.0417	0.0064	104.7	8.32		
1.5	90	70	70.5	0.0417	0.0057	104.7	7.35	7.58	0.042
	90	70	72	0.0417	0.0060	104.7	7.78		
	90	70	72	0.0417	0.0059	104.7	7.61		
2	90	70	73	0.0417	0.0058	104.7	7.56	7.24	0.038
	90	70	70.5	0.0417	0.0056	104.7	7.24		
	90	70	69	0.0417	0.0053	104.7	6.92		
2.5	90	70	68	0.0417	0.0052	104.7	6.70	6.84	0.055
	90	70	69	0.0417	0.0052	104.7	6.70		
	90	70	70	0.0417	0.0055	104.7	7.13		
3	90	70	70	0.0417	0.0053	104.7	6.92	7.13	0.050
	90	70	72	0.0417	0.0057	104.7	7.35		
	90	70	71	0.0417	0.0055	104.7	7.13		
3.5	90	70	71	0.0417	0.0054	104.7	7.02	6.81	0.048
	90	70	68	0.0417	0.0052	104.7	6.70		
	90	70	68	0.0417	0.0052	104.7	6.70		
4	90	70	70	0.0417	0.0053	104.7	6.92	7.13	0.050
	90	70	71.5	0.0417	0.0055	104.7	7.13		
	90	70	72	0.0417	0.0057	104.7	7.35		
4.5	90	70	69	0.0417	0.0052	104.7	6.70	6.77	0.055
	90	70	68	0.0417	0.0050	104.7	6.48		

	90	70	71	0.0417	0.0055	104.7	7.13		
5	90	70	69	0.0417	0.0051	104.7	6.59	6.59	0.057
	90	70	68	0.0417	0.0050	104.7	6.48		
	90	70	69	0.0417	0.0052	104.7	6.70		
5.5	90	70	71	0.0417	0.0055	104.7	7.13	6.99	0.046
	90	70	72	0.0417	0.0055	104.7	7.13		
	90	70	70	0.0417	0.0052	104.7	6.70		
6	90	70	70	0.0417	0.0055	104.7	7.13	6.84	0.046
	90	70	70	0.0417	0.0052	104.7	6.70		
	90	70	70	0.0417	0.0052	104.7	6.70		

Time (hr)	ST (°C)	ET (°C)	FT (°C)	FF ($\times 10^{-3}$ m^3/s)	W_{exp} ($\times 10^{-3}$ m^3/s)	RS (rad/s)	H_{cal} (kW/m^2K)	Ave-H_{cal} (kW/m^2K)	R_f (m^2K/kW)
0	80	70	70	0.0167	0.0037	186.4	9.51	9.58	0.000
	80	70	70	0.0167	0.0037	186.4	9.51		
	80	70	73	0.0167	0.0038	186.4	9.73		
0.5	80	70	72	0.0167	0.0037	186.4	9.51	9.29	0.003
	80	70	69	0.0167	0.0036	186.4	9.29		
	80	70	69	0.0167	0.0035	186.4	9.08		
1	80	70	70	0.0167	0.0035	186.4	9.08	9.15	0.005
	80	70	72	0.0167	0.0036	186.4	9.29		
	80	70	71	0.0167	0.0035	186.4	9.08		
1.5	80	70	70	0.0167	0.0033	186.4	8.64	8.69	0.011
	80	70	73	0.0167	0.0034	186.4	8.86		
	80	70	72	0.0167	0.0033	186.4	8.56		
2	80	70	68	0.0167	0.0030	186.4	7.65	7.71	0.025
	80	70	71	0.0167	0.0031	186.4	7.91		
	80	70	68	0.0167	0.0029	186.4	7.56		
2.5	80	70	70	0.0167	0.0032	186.4	8.21	7.88	0.023
	80	70	70	0.0167	0.0030	186.4	7.65		
	80	70	68	0.0167	0.0030	186.4	7.78		
3	80	70	71	0.0167	0.0030	186.4	7.78	7.71	0.025
	80	70	70	0.0167	0.0030	186.4	7.78		
	80	70	68	0.0167	0.0029	186.4	7.56		
3.5	80	70	68	0.0167	0.0029	186.4	7.56	7.78	0.024
	80	70	70	0.0167	0.0030	186.4	7.78		
	80	70	72	0.0167	0.0031	186.4	8.00		
4	80	70	70	0.0167	0.0031	186.4	8.08	7.87	0.023
	80	70	71	0.0167	0.0030	186.4	7.87		
	80	70	68	0.0167	0.0030	186.4	7.65		
4.5	80	70	70.5	0.0167	0.0030	186.4	7.78	7.58	0.028

	80	70	68	0.0167	0.0029	186.4	7.61		
	80	70	68	0.0167	0.0028	186.4	7.35		
5	80	70	70	0.0167	0.0031	186.4	8.00	7.78	0.024
	80	70	67	0.0167	0.0029	186.4	7.56		
	80	70	68	0.0167	0.0030	186.4	7.78		
5.5	80	70	70	0.0167	0.0030	186.4	7.65	7.66	0.026
	80	70	68	0.0167	0.0029	186.4	7.56		
	80	70	70	0.0167	0.0030	186.4	7.78		
6	80	70	70	0.0167	0.0030	186.4	7.65	7.66	0.026
	80	70	68	0.0167	0.0029	186.4	7.56		
	80	70	70	0.0167	0.0030	186.4	7.78		

Time (hr)	ST (°C)	ET (°C)	FT (°C)	FF ($\times 10^{-3}$ m^3/s)	W_{exp} ($\times 10^{-3}$ m^3/s)	RS (rad/s)	H_{cal} (kW/m^2K)	Ave-H_{cal} (kW/m^2K)	R_f (m^2K/kW)
0	80	65	67	0.0283	0.0058	146.6	10.14	9.75	0.000
	80	65	65	0.0283	0.0056	146.6	9.64		
	80	65	63.5	0.0283	0.0055	146.6	9.47		
0.5	80	65	67	0.0283	0.0054	146.6	9.41	9.27	0.005
	80	65	67	0.0283	0.0054	146.6	9.41		
	80	65	63	0.0283	0.0052	146.6	8.98		
1	80	65	65	0.0283	0.0050	146.6	8.69	8.62	0.013
	80	65	65.5	0.0283	0.0051	146.6	8.78		
	80	65	63	0.0283	0.0048	146.6	8.40		
1.5	80	65	64	0.0283	0.0045	146.6	7.82	7.79	0.026
	80	65	63	0.0283	0.0043	146.6	7.53		
	80	65	64.5	0.0283	0.0046	146.6	8.02		
2	80	65	65	0.0283	0.0045	146.6	7.82	7.70	0.027
	80	65	66	0.0283	0.0044	146.6	7.68		
	80	65	65	0.0283	0.0044	146.6	7.62		
2.5	80	65	63	0.0283	0.0040	146.6	6.95	7.22	0.036
	80	65	64	0.0283	0.0042	146.6	7.24		
	80	65	65	0.0283	0.0043	146.6	7.47		
3	80	65	65	0.0283	0.0042	146.6	7.24	7.29	0.035
	80	65	65.5	0.0283	0.0043	146.6	7.39		
	80	65	65	0.0283	0.0042	146.6	7.24		
3.5	80	65	65	0.0283	0.0042	146.6	7.24	7.10	0.038
	80	65	63	0.0283	0.0039	146.6	6.81		
	80	65	65	0.0283	0.0042	146.6	7.24		
4	80	65	65	0.0283	0.0042	146.6	7.24	7.24	0.036
	80	65	65	0.0283	0.0042	146.6	7.24		
	80	65	65	0.0283	0.0042	146.6	7.24		

Time (hr)	ST (°C)	ET (°C)	FT (°C)	FF ($\times10^{-3}$ m^3/s)	W_{exp} ($\times10^{-3}$ m^3/s)	RS (rad/s)	H_{cal} (kW/m^2K)	Ave-H_{cal} (kW/m^2K)	R_f (m^2K/kW)
0	80	60	60	0.0417	0.0066	104.7	8.62	8.57	0.000
	80	60	60	0.0417	0.0066	104.7	8.62		
	80	60	60	0.0417	0.0065	104.7	8.47		
0.5	80	60	62	0.0417	0.0066	104.7	8.69	8.54	0.000
	80	60	62	0.0417	0.0066	104.7	8.62		
	80	60	60	0.0417	0.0063	104.7	8.30		
1	80	60	60	0.0417	0.0063	104.7	8.30	8.19	0.005
	80	60	60	0.0417	0.0063	104.7	8.30		
	80	60	59	0.0417	0.0061	104.7	7.97		
1.5	80	60	60	0.0417	0.0058	104.7	7.64	7.63	0.014
	80	60	59	0.0417	0.0057	104.7	7.42		
	80	60	60	0.0417	0.0060	104.7	7.82		
2	80	60	60	0.0417	0.0057	104.7	7.47	7.23	0.022
	80	60	58	0.0417	0.0054	104.7	7.10		
	80	60	57.5	0.0417	0.0055	104.7	7.14		
2.5	80	60	59.5	0.0417	0.0054	104.7	7.05	7.15	0.023
	80	60	61	0.0417	0.0055	104.7	7.21		
	80	60	61	0.0417	0.0055	104.7	7.21		
3	80	60	60	0.0417	0.0053	104.7	6.88	6.94	0.028
	80	60	61	0.0417	0.0053	104.7	6.99		
	80	60	61	0.0417	0.0053	104.7	6.94		
3.5	80	60	57	0.0417	0.0048	104.7	6.33	6.49	0.037
	80	60	60	0.0417	0.0050	104.7	6.48		
	80	60	61.5	0.0417	0.0051	104.7	6.66		
4	80	60	60	0.0417	0.0049	104.7	6.44	6.24	0.044
	80	60	60.5	0.0417	0.0048	104.7	6.33		
	80	60	58.5	0.0417	0.0046	104.7	5.96		
`Fresh whey changed									
4.5	80	60	60	0.0417	0.0048	104.7	6.29	6.32	0.042
	80	60	60.5	0.0417	0.0048	104.7	6.33		
	80	60	61	0.0417	0.0048	104.7	6.33		
5	80	60	59	0.0417	0.0046	104.7	6.00	6.04	0.049
	80	60	60.5	0.0417	0.0047	104.7	6.11		
	80	60	60	0.0417	0.0046	104.7	6.00		
5.5	80	60	60	0.0417	0.0043	104.7	5.63	5.59	0.062
	80	60	58	0.0417	0.0042	104.7	5.46		
	80	60	60	0.0417	0.0043	104.7	5.68		
6	80	60	60	0.0417	0.0044	104.7	5.79	5.64	0.061
	80	60	61	0.0417	0.0043	104.7	5.68		
	80	60	59	0.0417	0.0042	104.7	5.46		

6.5	80	60	59	0.0417	0.0041	104.7	5.35	5.46	0.067
	80	60	60.5	0.0417	0.0042	104.7	5.46		
	80	60	61	0.0417	0.0043	104.7	5.57		
7	80	60	64	0.0417	0.0043	104.7	5.63	5.48	0.066
	80	60	62	0.0417	0.0042	104.7	5.46		
	80	60	61	0.0417	0.0041	104.7	5.35		
Fresh whey changed again									
7.5	80	60	60	0.0417	0.0040	104.7	5.24	5.09	0.080
	80	60	60	0.0417	0.0039	104.7	5.13		
	80	60	58	0.0417	0.0038	104.7	4.91		
8	80	60	60	0.0417	0.0038	104.7	4.91	4.91	0.087
	80	60	58	0.0417	0.0038	104.7	4.91		
	80	60	59	0.0417	0.0038	104.7	4.91		
8.5	80	60	62	0.0417	0.0038	104.7	4.91	4.81	0.091
	80	60	60.5	0.0417	0.0037	104.7	4.80		
	80	60	59	0.0417	0.0036	104.7	4.72		
9	80	60	58	0.0417	0.0035	104.7	4.59	4.72	0.095
	80	60	60	0.0417	0.0036	104.7	4.76		
	80	60	61	0.0417	0.0037	104.7	4.80		

Time (hr)	ST (°C)	ET (°C)	FT (°C)	FF ($\times 10^{-3}$ m^3/s)	W_{exp} ($\times 10^{-3}$ m^3/s)	RS (rad/s)	H_{cal} (kW/m^2K)	Ave-H_{cal} (kW/m^2K)	R_f (m^2K/kW)
0	70	60	58	0.0167	0.0032	104.7	8.38	8.69	-0.002
	70	60	60.5	0.0167	0.0034	104.7	8.95		
	70	60	60	0.0167	0.0033	104.7	8.73		
0.5	70	60	60	0.0167	0.0033	104.7	8.73	8.63	-0.001
	70	60	59	0.0167	0.0032	104.7	8.43		
	70	60	60	0.0167	0.0033	104.7	8.73		
1	70	60	60	0.0167	0.0033	104.7	8.52	8.66	-0.001
	70	60	60	0.0167	0.0033	104.7	8.52		
	70	60	61.5	0.0167	0.0034	104.7	8.95		
1.5	70	60	60	0.0167	0.0033	104.7	8.52	8.52	0.002
	70	60	59	0.0167	0.0033	104.7	8.52		
	70	60	58	0.0167	0.0033	104.7	8.52		
2	70	60	62	0.0167	0.0033	104.7	8.52	8.30	0.004
	70	60	60	0.0167	0.0032	104.7	8.30		
	70	60	59	0.0167	0.0031	104.7	8.08		
2.5	70	60	59.5	0.0167	0.0032	104.7	8.30	8.30	0.004
	70	60	60	0.0167	0.0032	104.7	8.30		
	70	60	61	0.0167	0.0032	104.7	8.30		
3	70	60	61.5	0.0167	0.0033	104.7	8.52	8.15	0.006

	70	60	59	0.0167	0.0031	104.7	8.08		
	70	60	57	0.0167	0.0030	104.7	7.86		
3.5	70	60	64	0.0167	0.0032	104.7	8.43	8.34	0.003
	70	60	61	0.0167	0.0032	104.7	8.30		
	70	60	60	0.0167	0.0032	104.7	8.30		
4	70	60	63	0.0167	0.0032	104.7	8.47	8.28	0.004
	70	60	60.5	0.0167	0.0032	104.7	8.30		
	70	60	60	0.0167	0.0031	104.7	8.08		
4.5	70	60	64	0.0167	0.0033	104.7	8.52	8.35	0.003
	70	60	60	0.0167	0.0032	104.7	8.25		
	70	60	61	0.0167	0.0032	104.7	8.30		
5	70	60	60	0.0167	0.0032	104.7	8.30	8.22	0.005
	70	60	61.5	0.0167	0.0032	104.7	8.30		
	70	60	60	0.0167	0.0031	104.7	8.08		
5.5	70	60	60	0.0167	0.0032	104.7	8.30	8.15	0.002
	70	60	59	0.0167	0.0031	104.7	8.08		
	70	60	59	0.0167	0.0031	104.7	8.08		
6	70	60	60	0.0167	0.0032	104.7	8.30	8.15	0.006
	70	60	59	0.0167	0.0031	104.7	8.08		
	70	60	59	0.0167	0.0031	104.7	8.08		

Time (hr)	ST (°C)	ET (°C)	FT (°C)	FF ($\times 10^{-3}$ m^3/s)	W_{exp} ($\times 10^{-3}$ m^3/s)	RS (rad/s)	H_{cal} (kW/m^2K)	Ave-H_{cal} (kW/m^2K)	R_f (m^2K/kW)
0	70	60	60	0.0417	0.0036	186.4	9.48	9.78	0.000
	70	60	62	0.0417	0.0038	186.4	9.83		
	70	60	63	0.0417	0.0038	186.4	10.04		
0.5	70	60	60	0.0417	0.0033	186.4	8.73	8.85	0.011
	70	60	61	0.0417	0.0035	186.4	9.08		
	70	60	60	0.0417	0.0033	186.4	8.73		
1	70	60	60.5	0.0417	0.0034	186.4	8.95	8.52	0.015
	70	60	57.5	0.0417	0.0030	186.4	7.86		
	70	60	60	0.0417	0.0033	186.4	8.73		
1.5	70	60	60.5	0.0417	0.0032	186.4	8.47	8.50	0.015
	70	60	58.5	0.0417	0.0031	186.4	8.08		
	70	60	61	0.0417	0.0034	186.4	8.95		
2	70	60	60	0.0417	0.0034	186.4	8.95	8.68	0.013
	70	60	60	0.0417	0.0033	186.4	8.56		
	70	60	60	0.0417	0.0033	186.4	8.52		
2.5	70	60	60	0.0417	0.0033	186.4	8.65	8.65	0.013
	70	60	60	0.0417	0.0033	186.4	8.65		
	70	60	60	0.0417	0.0033	186.4	8.65		

3	70	60	59	0.0417	0.0032	186.4	8.30	8.66	0.013
	70	60	60	0.0417	0.0033	186.4	8.52		
	70	60	62	0.0417	0.0035	186.4	9.17		

Time (hr)	ST (°C)	ET (°C)	FT (°C)	FF ($\times10^{-3}$ m^3/s)	W_{exp} ($\times10^{-3}$ m^3/s)	RS (rad/s)	H_{cal} (kW/m^2K)	Ave-H_{cal} (kW/m^2K)	R_f (m^2K/kW)
0	80	70	71	0.0417	0.0038	186.4	9.73	9.48	0.001
	80	70	71.5	0.0417	0.0037	186.4	9.64		
	80	70	68.5	0.0417	0.0035	186.4	9.08		
0.5	80	70	70	0.0417	0.0032	186.4	8.21	8.33	0.016
	80	70	71.5	0.0417	0.0034	186.4	8.77		
	80	70	69.8	0.0417	0.0031	186.4	8.00		
1	80	70	67.5	0.0417	0.0028	186.4	7.35	7.92	0.022
	80	70	71	0.0417	0.0031	186.4	8.00		
	80	70	72.5	0.0417	0.0033	186.4	8.43		
1.5	80	70	70	0.0417	0.0030	186.4	7.78	7.78	0.024
	80	70	70	0.0417	0.0030	186.4	7.78		
	80	70	70	0.0417	0.0030	186.4	7.78		
2	80	70	72	0.0417	0.0031	186.4	7.91	7.15	0.036
	80	70	70	0.0417	0.0027	186.4	6.92		
	80	70	68	0.0417	0.0026	186.4	6.61		
2.5	80	70	70	0.0417	0.0027	186.4	6.87	6.97	0.039
	80	70	72.5	0.0417	0.0029	186.4	7.56		
	80	70	67	0.0417	0.0025	186.4	6.48		
3	80	70	70	0.0417	0.0027	186.4	6.92	6.92	0.040
	80	70	70	0.0417	0.0027	186.4	6.92		
	80	70	70	0.0417	0.0027	186.4	6.92		
3.5	80	70	66	0.0417	0.0023	186.4	6.05	6.60	0.047
	80	70	69	0.0417	0.0026	186.4	6.83		
	80	70	70	0.0417	0.0027	186.4	6.92		

Time (hr)	ST (°C)	ET (°C)	FT (°C)	FF ($\times10^{-3}$ m^3/s)	W_{exp} ($\times10^{-3}$ m^3/s)	RS (rad/s)	H_{cal} (kW/m^2K)	Ave-H_{cal} (kW/m^2K)	R_f (m^2K/kW)
0	90	70	70	0.0167	0.0072	104.7	9.29	9.29	0.000
	90	70	70	0.0167	0.0072	104.7	9.29		
	90	70	70	0.0167	0.0072	104.7	9.29		
1	90	70	70	0.0167	0.0061	104.7	7.91	7.72	0.032
	90	70	70	0.0167	0.0059	104.7	7.67		
	90	70	70	0.0167	0.0058	104.7	7.56		

2	90	70	70	0.0167	0.0051	104.7	6.66	6.63	0.056
	90	70	70	0.0167	0.0051	104.7	6.59		
	90	70	72	0.0167	0.0051	104.7	6.66		
3	90	70	70	0.0167	0.0047	104.7	6.12	6.04	0.069
	90	70	70	0.0167	0.0046	104.7	5.94		
	90	70	70	0.0167	0.0047	104.7	6.05		
4	90	70	70	0.0167	0.0047	104.7	6.05	6.05	0.071
	90	70	70	0.0167	0.0047	104.7	6.05		
	90	70	70	0.0167	0.0047	104.7	6.05		
5	90	70	70	0.0167	0.0047	104.7	6.05	6.05	0.071
	90	70	70	0.0167	0.0047	104.7	6.05		
	90	70	70	0.0167	0.0047	104.7	6.05		

Time (hr)	ST (°C)	ET (°C)	FT (°C)	FF ($\times 10^{-3}$ m^3/s)	W_{exp} ($\times 10^{-3}$ m^3/s)	RS (rad/s)	H_{cal} (kW/m^2K)	Ave-H_{cal} (kW/m^2K)	R_f (m^2K/kW)
0	80	60	60	0.0167	0.0068	104.7	8.95	8.95	-0.005
	80	60	60	0.0167	0.0068	104.7	8.95		
	80	60	60	0.0167	0.0068	104.7	8.95		
1	80	60	60	0.0167	0.0067	104.7	8.73	8.72	-0.002
	80	60	60	0.0167	0.0066	104.7	8.69		
	80	60	60	0.0167	0.0067	104.7	8.73		
2	80	60	60	0.0167	0.0064	104.7	8.41	8.41	0.002
	80	60	60	0.0167	0.0065	104.7	8.52		
	80	60	60	0.0167	0.0063	104.7	8.30		
3	80	60	60	0.0167	0.0061	104.7	7.97	7.97	0.014
	80	60	60	0.0167	0.0061	104.7	7.97		
	80	60	60	0.0167	0.0061	104.7	7.97		
4	80	60	60	0.0167	0.0060	104.7	7.82	7.77	0.012
	80	60	60	0.0167	0.0059	104.7	7.75		
	80	60	60	0.0167	0.0059	104.7	7.75		
5	80	60	60	0.0167	0.0057	104.7	7.42	7.50	0.017
	80	60	60	0.0167	0.0058	104.7	7.53		
	80	60	60	0.0167	0.0058	104.7	7.53		

Time (hr)	ST (°C)	ET (°C)	FT (°C)	FF ($\times 10^{-3}$ m^3/s)	W_{exp} ($\times 10^{-3}$ m^3/s)	RS (rad/s)	H_{cal} (kW/m^2K)	Ave-H_{cal} (kW/m^2K)
5	70	65	66	0.0283	0.0013	146.6	6.69	6.37
	70	65	65.5	0.0283	0.0012	146.6	6.26	
	70	65	64.5	0.0283	0.0012	146.6	6.17	
10	75	65	65	0.0283	0.0026	146.6	6.73	6.66
	75	65	64	0.0283	0.0025	146.6	6.52	
	75	65	65	0.0283	0.0026	146.6	6.73	
20	85	65	65.5	0.0283	0.0056	146.6	7.34	7.37
	85	65	65.5	0.0283	0.0057	146.6	7.39	
	85	65	65	0.0283	0.0057	146.6	7.39	
25	90	65	65	0.0283	0.0072	146.6	7.52	7.63
	90	65	65	0.0283	0.0073	146.6	7.65	
	90	65	65	0.0283	0.0074	146.6	7.73	
30	95	65	66	0.0283	0.0090	146.6	7.82	7.84
	95	65	65	0.0283	0.0089	146.6	7.75	
	95	65	65	0.0283	0.0092	146.6	7.96	

Appendix VIII

A typical native-PAGE patterns of whey proteins